Université de Lille 1 Sciences et Technologies
École Doctorale Sciences Pour l'Ingénieur
Laboratoire Génie Civil et géo-Environnement

THÈSE

Pour l'obtention du grade de

DOCTEUR DE L'UNIVERSITÉ DE LILLE

Discipline: Génie Civil

Par

Elias FARAH

DETECTION OF WATER LEAKAGE USING INNOVATIVE SMART WATER SYSTEM – APPLICATION TO SUNRISE SMART CITY DEMONSTRATOR

Soutenue le 2 Novembre 2016 devant le jury composé de

SHAHROUR Isam	Professeur, Université de Lille 1	Directeur
HALWANI Jalal	Professeur, Université Libanaise	Rapporteur
HANI Azzedine	Professeur, Université Badji Mokhtar Annaba	Rapporteur
CHARRIER – EL BOUHTOURY Fatima	MCF - HDR, Université de Pau et des Pays de l'Adour	Examinateur
HAGE CHEHADE Fadi	Professeur, Université Libanaise	Examinateur
OUNAIES Sana	MCF, Université de Lille 1	Examinateur
SOULHI Aziz	Professeur, École Nationale Supérieure des Mines/Rabat	Examinateur

This PhD thesis is dedicated to my beloved parents who have been supporting my efforts. Thank you for all your sacrifices throughout my life. You are the reason of what I become today.

ACKNOWLEDGMENTS

I would like to take this opportunity to acknowledge all the people who contributed to the completion of this thesis. This work has been carried out at the Laboratory of Civil Engineering and geo-Environment (LGCgE), Polytech'Lille, University of Lille 1.

Foremost, I would like to express my sincere gratitude to my supervisor, Professor Isam SHAHROUR for his patience, encouragement, kindness, immense knowledge, precious advices and smart ideas. I have been extremely lucky to have a supervisor who taught me the passion for work and how to do a lot of things at one time. He taught me a differently.

I would like to thank my PhD committee for accepting to be a part of this achievement by reviewing and examining my work. Thanks to Prof. Jalal HALWANI, Prof. Azzedine HANI, Dr. Fatima CHARRIER EL-BOUHTOURY, Prof. Fadi HAGE CHEHADE, Dr. Sana OUNAIES and Prof. Aziz SOULHI.

I am very grateful to the partners who have contributed to this work by their experiences and supports. Thanks to Mr. Francis DROBSCZYNSKI, head of PC security and DUSVA of Lille 1 University, for his availability and his help in collecting the archived asset data. My sincere thankfulness goes to the company “Eaux Du Nord”. Thanks to Mr. Jérôme LEMAHIEU (Suez - Eau France, Lyonnaise des eaux) for his cooperation and his precious comments. I am also thankful to the company “Sainte-Lizaigne Groupe Claire”, the provider of the acoustic system. Many thanks go to Mr. Denis DARY and Mr. Pascal BEAUTOUR for their assistance and the following-up of the results. Thanks also to Mr. Hussein AL CHAER, head of the company BAT’Y, for his support in the technical and experimentation field.

I would like to extend my gratitude to Thames Water Utilities Limited and the Sheffield University in the United Kingdom who accepted to welcome me for a scientific visit of one month. Thanks to Mrs. Catalina PEDRAZA and the whole team in Reading and in Sheffield for your encouragements, advices and valuable comments.

I am thankful also to the KWR Watercycle Research Institute in the Netherlands where I spent three weeks and got the opportunity to exchange the knowledge with all the researchers there. Thanks to Dr. Peter VAN THIENEN and Dr. Mirjiam BLOKKER. Your valuable remarks and advices have helped me to improve the quality of my work.

I would like to acknowledge the Lebanese University, Faculty of Engineering, Branch I for the PhD scholarship giving me the opportunity to continue my studies. Many thanks go also to the Laboratory of Civil Engineering and geo-Environment (LGCgE), the Department of International Action (DAI) of the Doctoral College Lille Nord de France and the Franco-Dutch network for the financial support funding my scientific visits in UK and Netherlands.

My further thanks go to all my friends and colleagues in the LGCgE, with whom I have spent unforgettable moments. Thank you for all your confidence, concerns and motivations.

Last but not least, I would like to express my genuine gratitude to my beloved parents Daad and Adel for their unwavering support, love and sacrifices. They have been always a great motivation for me in every step in my life. As well, I would like to thank my two sisters and my brother for all their encouragements. Thank you.

ABSTRACT

This work concerns the use of the Smart Water Technology for the detection of water leakage. It is a part of SunRise project which aims at turning the Scientific Campus of the University of Lille into a large scale demonstrator site of the "Smart and Sustainable City". The campus is representative to a small town of 25000 inhabitants. This work is also a part of the European Project SmartWater4 Europe, which aims at developing 4 demonstrators of the Smart Water Technology.

This thesis includes five parts.

The first part includes a literature review concerning the technologies used in leakage detecting.

The second part presents the SunRise Smart City demonstrator, which is used as a basis for this thesis. The chapter details the instrumentation installed in the demo site as well as leak simulations tests to analyze the efficiency of an acoustic system of leakage detection.

The third part focuses on the analysis of the water consumption at different time scales. Analysis concerns both sub-meters and bulk meters. It is conducted using a developed platform for the aggregation and the interpretation of the data. The chapter presents also major leakage events in 2015.

The fourth part concerns leak detection using the water balance calculation based on the top down and bottom up approaches. It also presents the Active Leakage Control (ALC) strategy applied to the demo site in order to reduce the level of Non-Revenue Water (NRW).

The last part concerns the use of advanced methods for leak detection with application on the Campus data. These methods include the Comparison of Flow Pattern Distribution Method (CFPD), the Minimum Night Flow (MNF) method and two statistical approaches.

Keywords: smart water network, leak detection, consumption, water balance, minimum night flow, statistical approaches.

RÉSUMÉ

Le travail de thèse porte sur l'utilisation des réseaux d'eau potable intelligents pour la détection des fuites. Il s'inscrit dans le cadre du projet SunRise qui vise à transformer la Cité Scientifique de l'Université de Lille en une ville intelligente et durable. Le campus représente une petite ville de 25000 habitants. Ce travail fait également partie du projet européen SmartWater4Europe, qui vise à développer 4 démonstrateurs des réseaux d'eau intelligents.

Le travail comporte 5 parties.

La première partie comprend une étude bibliographique sur les technologies utilisées pour la détection des fuites.

La deuxième partie présente le démonstrateur SunRise Smart City, qui sert de support pour cette thèse. Cette partie détaille les instrumentations installées dans le site démonstrateur et les tests de simulation des fuites pour analyser l'efficacité d'un système acoustique de détection des fuites.

La troisième partie comporte une analyse de consommation d'eau à différentes échelles. L'analyse concerne les sous-compteurs installés dans les bâtiments et les compteurs généraux placés à l'entrée des secteurs. Cette analyse est menée à l'aide d'une plateforme développée pour faciliter l'agrégation et l'interprétation des données. Cette partie présente aussi les fuites majeures en 2015.

La quatrième partie concerne la détection des fuites en se basant sur le bilan d'eau avec les deux évaluations ascendantes et descendantes. Elle présente aussi la stratégie du Contrôle Actif des Fuites (CAF) appliquée sur le site démonstrateur afin de réduire le niveau de l'Eau Non-Vendue (ENV).

La dernière partie comporte l'application des méthodes avancées pour la détection des fuites. Ces méthodes comprennent l'approche CFPD 'Comparison of Flow Pattern Distribution', la méthode du Débit Nocturne Minimal (DNM) et deux approches statistiques développées.

Mots-clés: réseau d'eau intelligent, détection des fuites, consommation, bilan d'eau, débit nocturne minimal, approches statistiques.

Table of Contents

List of Figures

List of Tables

List of Abbreviations

ALC	Active Leakage Control
AMI	Automatic Meter Infrastructure
AMR	Automatic Meter Reader
ANN	Artificial Neural Network
CDF	Cumulative Distribution Function
CFPD	Comparison of Flow Pattern Distribution
CSV	Comma Separated Values
DMA	District Meter Area
EAR	Early Alarm Recording
FDR	False Discovery Rate
FN	False Negative
FNR	False Negative Rate
FP	False Positive
FPR	False Positive Rate
GIS	Geographic Information System
GPR	Ground Penetrating Radar
GPRS	General Packet Radio Service
GSM	Global System for Mobile communications
IWA	International Water Association
LCI	Linear Consumption Index
LLI	Linear Losses Index
LTE	Long Term Evolution
MA	Moving Average
MNF	Minimum Night Flow
MSD	Moving Standard Deviation
MSE	Mean Squared Error
NPV	Negative Predictive Value
NRW	Non-Revenue Water
PDF	Probability Density Function
PPV	Positive Predicted Value
ROC	Receiver Operating Characteristics
SCADA	Supervisory Control And Data Acquisition
STD	Standard Deviation
SUNRISE	Smart Urban Networks for Resilient Infrastructure and Sustainable Ecosystems
SVM	Support Vector Machine
SW4EU	Smart Water for Europe
SWN	Smart Water Network
TN	True Negative

TNR	True Negative Rate
TP	True Positive
TPR	True Positive Rate
TWCP	Threshold Water Consumption Profile
WDS	Water Distribution System
WSN	Wireless Sensor Network

Introduction

Water is a vital resource for all aspects of life. It is classified as a rare commodity essential for human health as well as for agriculture, industrial and hydropower productions. However, the fresh water represents only 2.5% of the water present on the Earth. The majority of this proportion is frozen leaving less than 1% for the human alimentation. The world population growth, rapid urbanization, migration, climate change, aging infrastructures and the weak policies increase the pressure on water resources. According to UN-Water, it is estimated that 1.8 billion people will be living in countries with absolute water scarcity by 2025, and almost two-thirds of the world population could be under conditions of water stress. Over 1.6 million people die every year from the consequences of water related diseases.

The water distribution systems suffer from a large percentage of water lost in transit from treatment plants to consumers. The World Bank estimates that the actual Non-Revenue Water (NRW) level in the developing countries is probably in the range of 40 to 50% of the water produced. In order to recover the lost water and to alleviate water shortages, some countries have developed new cost-intensive techniques such as the seawater desalination. This method costs up to eight times more than the average cost of urban water supplies. According to the Global Water Intelligence, the United Arab Emirates (UAE) is expecting to spend from 2016 around 3.22 billion dollars per year on building, operating and maintenance of desalination plants. Furthermore, the construction of new water treatment plants is getting nowadays more and more expensive. Therefore, the water utilities start to focus on managing the available water resources and the usable infrastructures.

Water leakage is a major concern in any water network. The largest proportion of unaccounted water is lost through leaks in supply lines. It can occur also in joints, valves and fire hydrants. Many factors can contribute to leaks: material, age, composition and joining methods. Environmental and external conditions such as the surrounding soil type, stress from traffic vibrations and frost loads can influence leaks occurrence. The water conditions are also considered a related factor including the velocity, pressure and temperature. Water losses lead to (i) economic impacts including the cost of reparation and the non-billing lost water, (ii) social effects represented by the consumer inconvenience due to low pressure and service interruptions in addition to health risks and (iii) ecological impacts characterized by the requirement of additional energy to extract water.

In order to save water and reduce economic loss, water networks operators rely on different methods of leak detection. The acoustic techniques detect the vibration or the noise emitted from the water jet escaping only from metal pipes. The tracer gas method is based on the injection of

non-toxic gas like helium or hydrogen into an isolated pipe section. The gas escapes through the leaks and reaches the surface. The water leaking from underground pipes change the thermal characteristics of the surrounding soil. The thermal anomalies can be detected using infrared handheld cameras or embedded in a vehicle or a plane. Another technique based on the ground penetrating radar has been used to localize the leak. The radar waves are reflected to the surface when they encounter underground voids created by the emission of water. These hardware-based methods are efficient to detect background leakage but they require expensive investments, skilled employees and they are expensive in terms of man-hour needed. Currently, the water utilities rely on the combination water balance calculation and the hardware-based techniques to detect the leaks in a District Metered Area (DMA). Measuring the quantity of water entering and leaving a sector created by closing appropriate valves allows the water companies to identify efficiently the high levels of leakage. However, the water audit approach depends on the estimation of several components like the night flows and the apparent losses and it is also highly influenced by the accuracy of the flow meters.

The new Information and Communication Technologies (ICT) applied in urban networks has generated the notion of a Smart City, where the infrastructure components become more intelligent, interconnected and efficient. Based on the latest development in the hydraulic sensor technology and online data acquisition systems, the traditional water networks turned to be smart. The Water Distribution Systems (WDSs) have started to be equipped by a set of flow and pressure sensors that communicate in quasi real-time the data collected. The water companies are then able to monitor carefully the distribution networks and detect any faults. The development for data analysis methodology stills a challenge to detect immediately the abnormal events. The most commonly used method is the Minimum Night Flow (MNF) that usually occurs between 2 am and 4 am. Accordingly, the MNF approach remains a manual process relying on a human interpretation of the results and lack of any thresholds representing the boundaries of the normal state.

This present work aims to develop and implement a smart water network in the Scientific Campus of Lille 1 University in order to detect leakage in real-time. It is a part of SunRise project which goals to make the Campus as a demonstrator site of the "Smart and Sustainable City". The site is representative to a small town of 25000 inhabitants and 150 buildings with variable usages: administration, teaching, research, students' residence, restaurant and sport. This work is also a part from Smart Water for Europe (SW4EU) project which aims to develop 4 well-scaled and real-life demonstration sites and integrate 12 innovative solutions in the domain of water quality management, leak management, energy optimization and customer interaction.

This thesis is divided into five chapters in addition to a main introduction and a general conclusion.

The first chapter includes a literature review. The review describes the available techniques for detecting the leakage in WDSs with their advantages and limitations. The described techniques range from the conventional manual sounding surveys to the implementation of the smart grid which allows the identification of the leakage in near real-time.

The second chapter presents a demo site of a large scale demonstrator of the smart water system: SunRise Smart Water. It also details the instrumentation installed in the demo site such as the smart meters, the pressure sensors and the acoustic hydrophone. This chapter also includes the leak simulations tests to analyze the response of the acoustic system to the leak.

The third chapter details the analysis of the water consumption in the demo site at different time scales. The analysis includes the sub-meters and the bulk meters that measure the water consumption in different sectors. A data transformation platform is also presented to facilitate the aggregation and the interpretation of the data. Three critical periods in 2015 corresponding to possible leaks are also reported in this chapter.

The chapter 4 is dedicated for the leak detection in the demo site using the water balance calculation based on the top down and bottom up approaches. This chapter also presents the Active Leakage Control (ALC) strategy applied to the demo site in order to reduce the level of NRW.

The chapter 5 presents novels methodologies for leak detection. The Comparison of Flow Pattern Distribution Method (CFPD) is tested on the data collected from the smart meters installed in the buildings and at the entry of the sectors. The MNF approach is developed in order to automate the detection process. Two statistical approaches are also presented in a way to improve the detection of the leakage in near real time. All these methods are evaluated according to their efficiency towards detecting the leaks identified and reported in the third chapter.

Chapter 1

Water Leak Detection - State of the Art

This chapter reviews the state-of-the-art of the leak detection technologies in water distribution systems (WDS). Failure in the transmission networks can lead to water loss. In order to avoid the economic, social and ecological impacts of water leak, the water utilities have developed different technologies to detect water leaks. First of all, they used manual sounding technique and then they have developed more sophisticated methods such as those based on smart technologies. This chapter presents the technologies used in the detection of water leaks as well as the advantages and limitations of each technology.

1.1. Water supply system

The main purpose of the water supply system is to deliver water from the source to the customer. The water distributed should be potable for domestic use and with sufficient pressure for fire protection (Misiūnas, 2005). The water sources can be wells, rivers, lakes, aquifers and reservoirs. An example for water supply system from the treatment plant to a distribution network is illustrated in Figure 1.1. The water network consists of reservoirs, pipes, fittings, valves, pumps and hydrants.

In general, the water distribution networks are composed of two types:

- Branched network, in which the water cannot return in the pipelines; it is similar to the branching of a tree (Figure 1.2.a). It is economical but any accident in the main line will cause water interruption for customers in the downstream.
- Looped network, in which the water can reach any point from more than one path (Figure 1.2.b). Its installation is more expensive than that of a branched network. When a failure occurs, loops allow consumers to continue receiving water. Looped systems coupled with sufficient valves divide the networks into district zones, which are easy to be monitored and thus providing additional level of reliability (Martínez-Rodríguez et al., 2011).

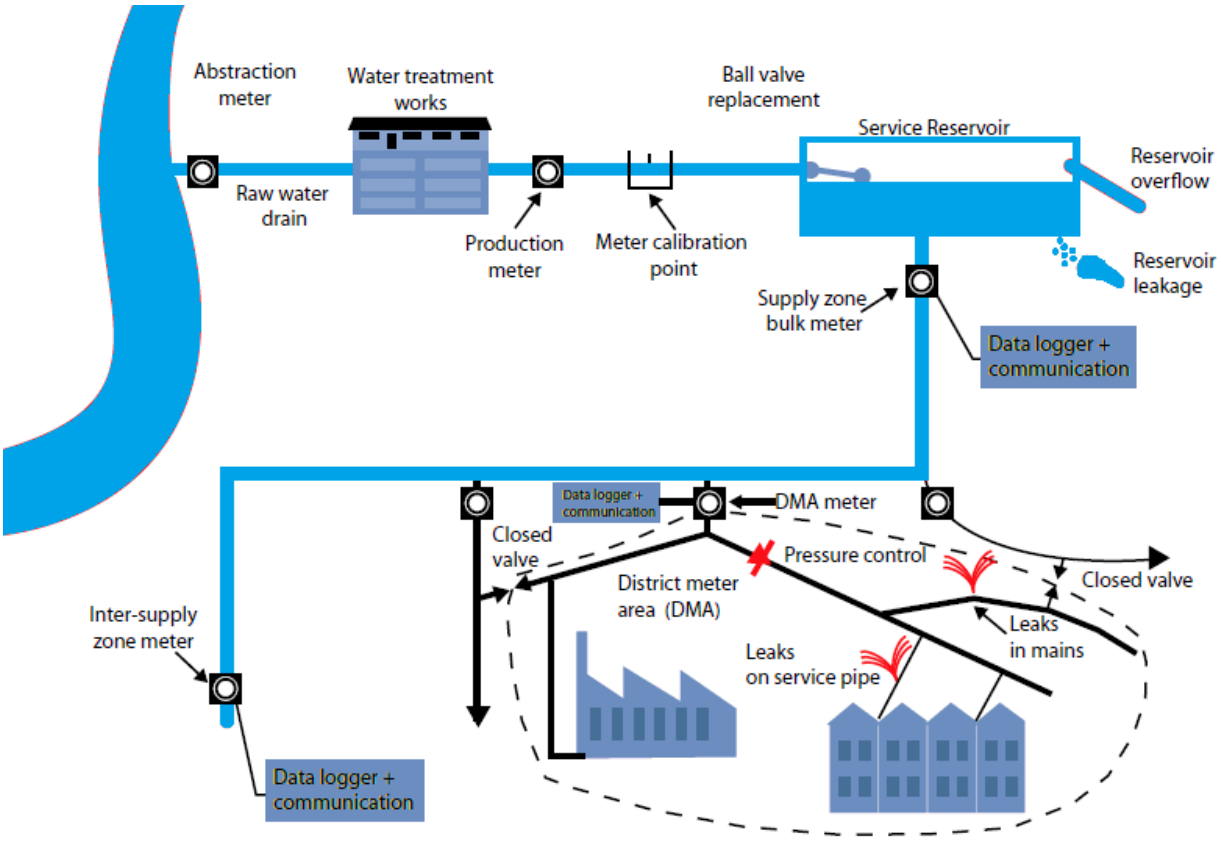

Figure 1.1: Typical water distribution network (Farley et al., 2008)

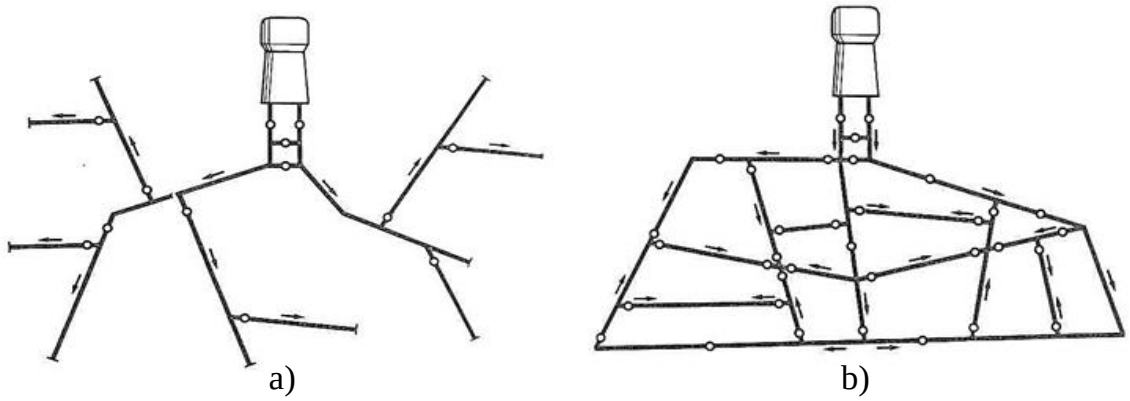

Figure 1.2: a) Branched network, b) Looped network (Blindu, 2004)

1.2. Water Leaks

The main role of a water distribution network is to deliver continuously water to consumers in prescribed quantity and quality (Yazdani et al., 2011). However, this function that seems simple requires a nonstop monitoring of the network due to degradations that can occur over time. These deteriorations could concern the pipelines or the hydraulic control elements (valves, tanks, pumps, joints). The water pipes representing the largest part of the network must ensure:

- Water transmission with a sufficient pressure and flow.
- Water supply with a standard quality.
- Continuity of the distribution.

These functions could be altered with time and cause water losses. The International Water Association (IWA) classifies water losses or the Non-Revenue Water (NRW) into two categories (Lambert et al., 2002):

- Real losses, which correspond to physical escape of water from transmission and distribution mains through joints, fittings or bursts up to the customer metering point. It also includes leakage from reservoirs and storage overflows.
- Apparent losses, which correspond to non-physical losses caused by an unauthorized consumption (illegal use, theft), customer meter inaccuracies and data handling errors in billing systems.

Globally, according to the World Bank, it is estimated that the actual Non-Revenue Water NRW level in the developing countries ranges from 40 to 50% of the clean water produced and pumped into the distribution systems (Kingdom et al., 2006). Figure 1.3 illustrates the NRW rates by country.

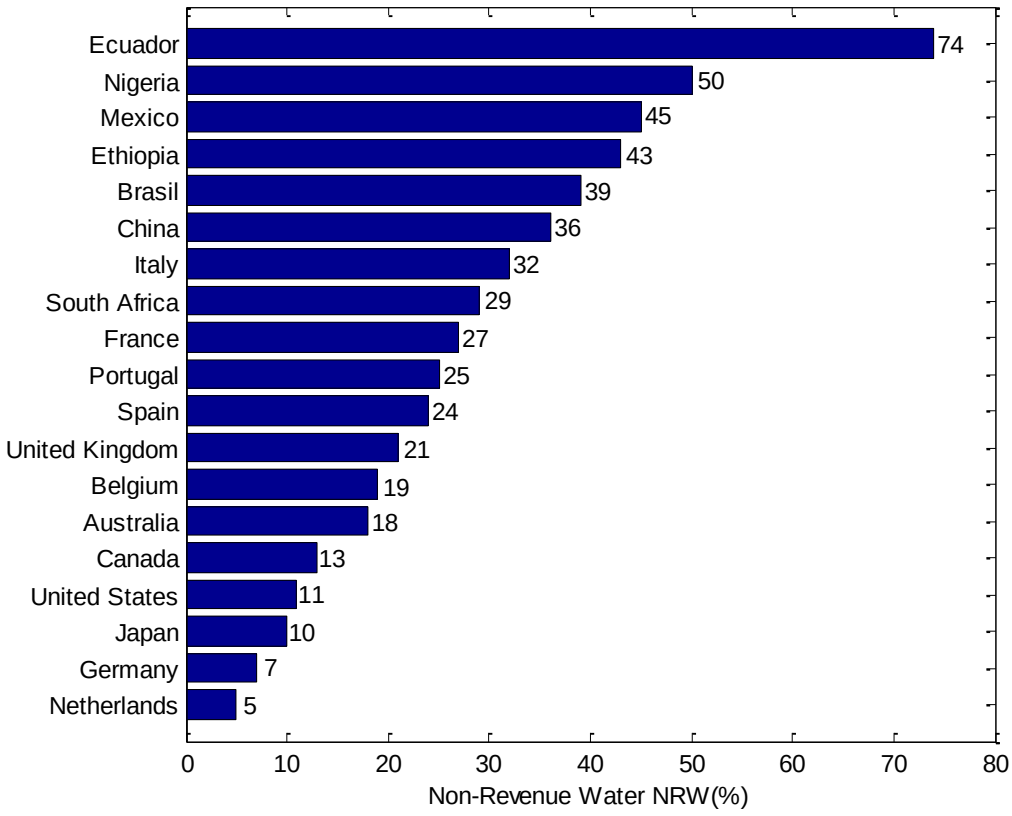

Figure 1.3: Non-Revenue Water NRW rates by country (GrowingBlue, 2011)

1.2.1. Real losses

The physical losses in water distribution system reflect a good indicator of the efficiency of a water supplier. Real losses can be subdivided into three components (GIZ, 2011):

- Reported or visible leaks: They generally have high flow rates and derive from sudden bursts in pipes or joints. They are located easily by visual survey. They induce a pressure drop and a supply interruption among the customers.
- Unreported or hidden leaks: They have moderate flow rates (250 l/h at 50 m pressure), which could not be reported from the ground. They can be identified using acoustic and non-acoustic methods.
- Background leakage: They have low flow rates (less than 250 l/h at 50 m pressure), which could result from leakage at the air valves, hydrants or taps. Generally, they are not detected. The background leaks characterized by their long runtimes could be reduced by replacing the infrastructure or through pressure management.

1.2.2. Causes of real losses

Real losses exist in the majority of water distribution networks. They can never be totally eliminated, and even recent sections could be subjected to some inevitable volume of water lost. Among the most common causes of physical losses, we distinguish:

- *Corrosion*: It is the gradual destruction of materials produced by a chemical reaction between the pipe wall and its environment (soil or water). All metallic pipes are exposed to internal and external corrosion characterized by a wall thickness reduction (Rajani et al., 2013). The internal corrosion is dependent on water chemistry (pH, dissolved oxygen rate, carbonate balance, chlorine concentration) and flow characteristics such as water velocity (Yaminighaeshi, 2009). It leads to a decrease in the internal pipe diameter. The external corrosion occurs in pipes buried in corrosive soils in the form of spots or pits that expand with time. Many factors can accelerate corrosion of metallic pipes like stray electrical current and soil characteristics such as moisture and microbiological content (Rajani et al., 2001).
- *Material and age:* Pipes used in water distribution networks vary from gray cast iron, plastic and reinforced concrete materials. The absence of corrosion protection on steel pipes eases their damage by the presence of graphitization in the case of gray cast iron conducts (Makar et al., 2001). Plastic pipe materials are also subjected to chemical degradation. High sulfate alteration with water affects concrete pipes especially those with poor reinforcement cover. In addition to the pipe material, the age of the pipe is one of important factor causing leaks.
- *Joints:* The lack of professionalism in handling of pipe joints is an additional cause of leakage. Welded steel pipes often lack proper internal and external corrosion protection along the weld seam. Leakage can also occur when socket pipes exceeds the maximum

allowed angular bending or if water hammer and high pressure affect joints that are not locked.

- *Pressure:* The increase in pressure results in a higher flow rate from existing leaks and contribute to the appearance of new bursts. Conversely, low pressure complicates the leak detection efforts, because the water is less likely to reach the surface. The significant variations in pressure within the network can also promote leaks in plastic pipes. Similarly, water hammer mainly developed from inappropriate control mechanisms causes pipe breaks, joints disconnection and damages valves leading to water loss.
- *Soil and bedding:* The water leaking into cohesive soils such as clay or silt has the capability to appear at the surface while leaks into non-cohesive like sand or gravel have the ability to drain below the ground making it difficult to be detected. Insufficient backfill and compaction of the pipe trench may cause subsidence. Plastic pipes are subjected to longitudinal and spiral cracks as a result of stony bedding materials. Coarse or rocky bedding materials spoil external coatings on steel or cast iron pipes and support corrosion.
- *Excessive forces:* The traffic, climate and soil-pipe interaction are additional sources, which cause pipes' failure (Rajani et al., 2004). The mechanical stresses leading to a pipe break was classified into three main categories (Rajani et al., 2001):
  - Circumferential breaks, which are due to longitudinal stresses caused by thermal contraction (due to low temperature of the water inside and outside the pipe), bending stress due to soil differential movement or large voids in the bedding near the pipe, and third-party influence such as excavations.
  - Longitudinal breaks, which are due to transverse stress caused by hoop stress due to the pipe pressure, ring stress due to live loading like traffic and increase in ring loads by the expansion of the freezing moisture in the ground.
  - Split bell caused by transverse stress on the pipe joint.

Figure 1.4 shows the failure modes of buried pipelines: direct-tension, bending or flexural failure and hoop stress.

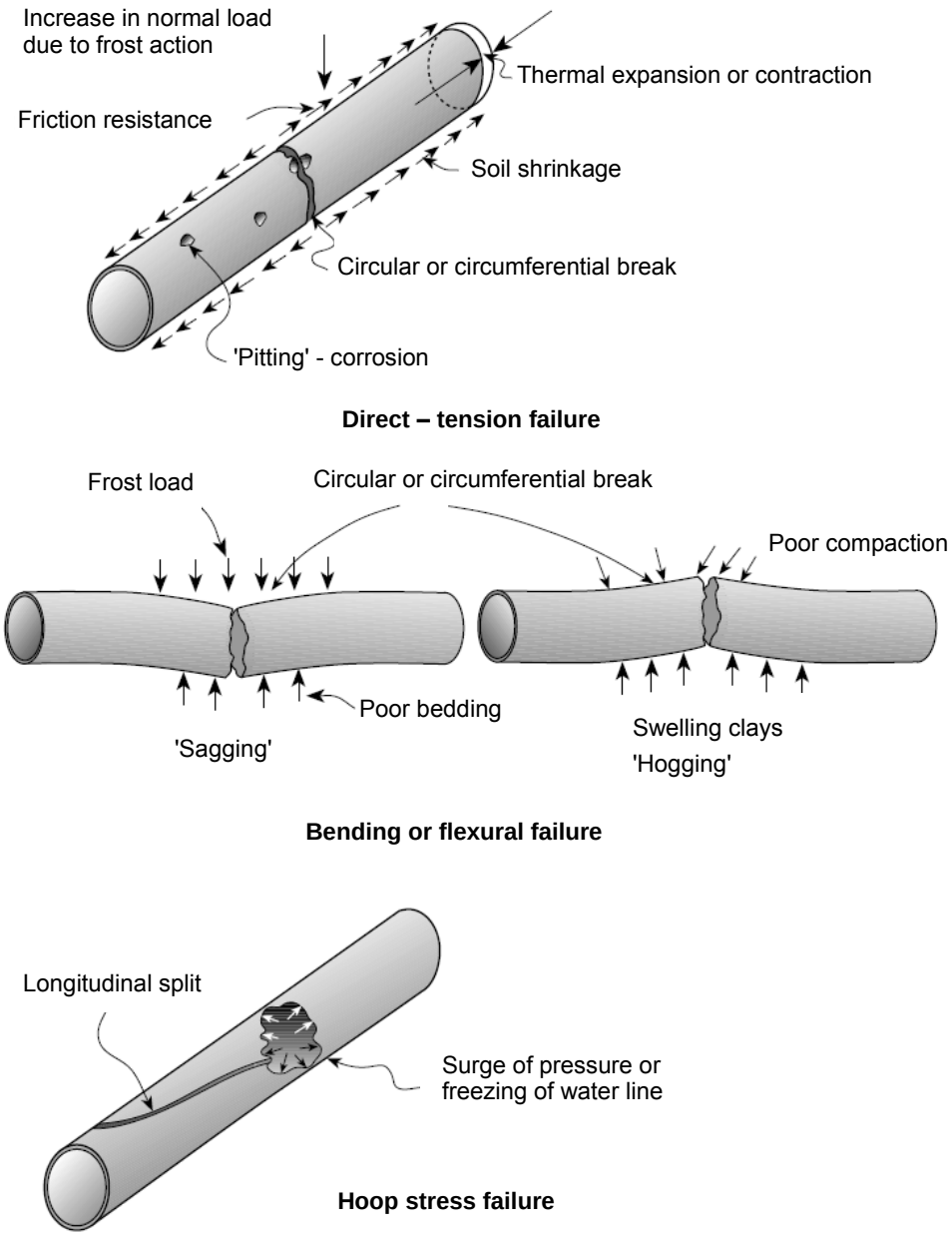

Figure 1.4: Failure modes for buried pipes (Rajani et al., 2001)

1.2.3. Pipes failure description

The pipes failure process begins when the corrosion is developed internally and externally after the buried pipes have been operated for some time. Figure 1.5 illustrates the pipe failure development described as a multi-step process.

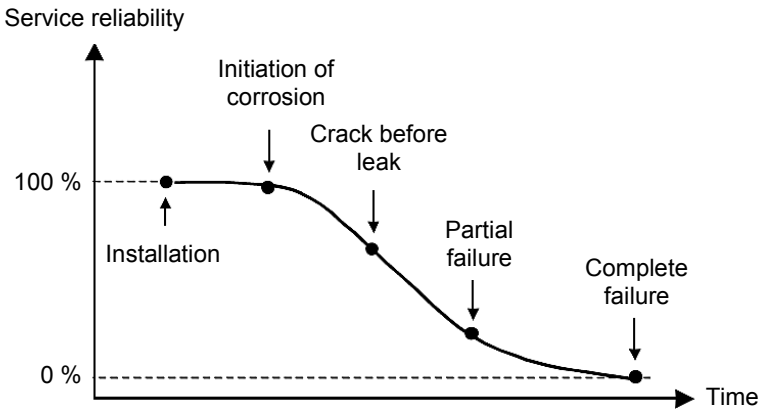

Figure 1.5: Pipe failure development (Misiūnas, 2005)

During the failure process, pipes are subjected to different mechanical stresses as shown in Figure 1.6.

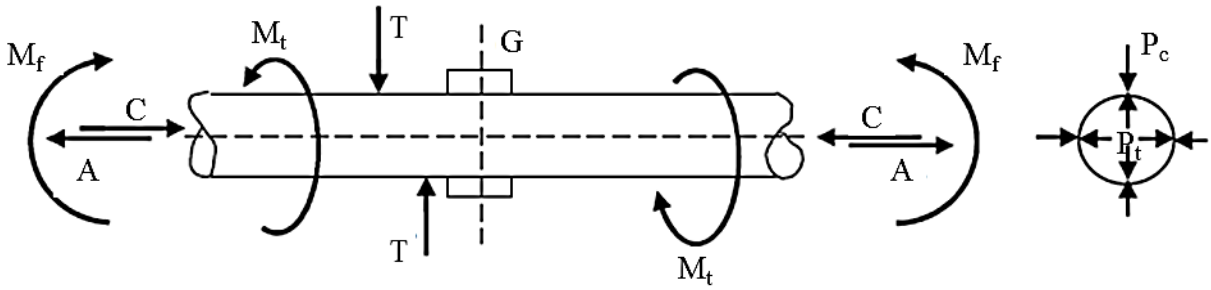

Figure 1.6: Stresses acting on a pipe (Blindu, 2004)

These stresses are as follows:

- Flexure moment (M_f).
- Torsional moment (M_t).
- Shear stress (T).
- Axial tensile stress (A).
- Axial compression stress (C).
- Internal overpressure (P_t) that may cause the pipe burst.
- External overpressure (P_c) that may cause the pipe crush.

A failure or leakage corresponds to a weakening of the pipe, either by the decrease of the wall thickness at an accurate point (pitting) or not (crack) combined with an increase of stresses

on the pipe, or by a seal lack at joints. They may also correspond to a burst following a violent action (water hammer, ground movement ...). Three main breaks can occur along the pipes: transversal ruptures caused by the mechanical actions, longitudinal ruptures developed by the internal overpressure and holes formed due to corrosion. Figure 1.7 shows the failures percentages in function of the diameter and break type. The transversal ruptures mainly occur in small pipes' diameters whereas those of large diameters suffer from longitudinal breaks and holes.

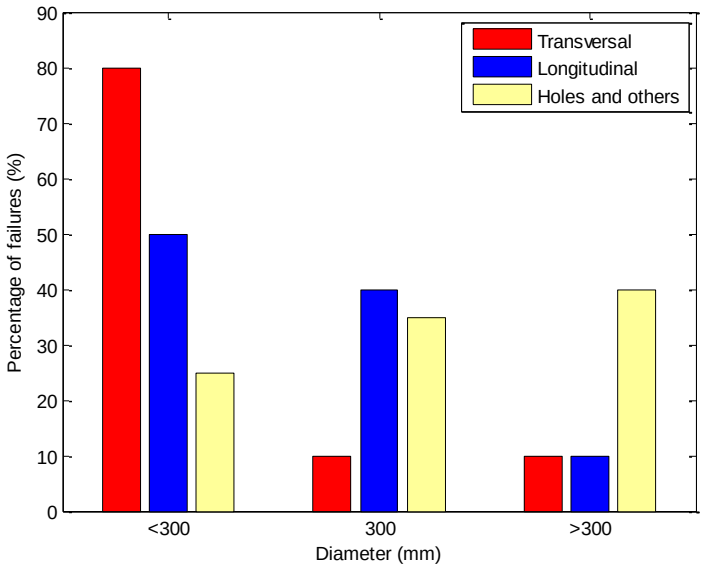

Figure 1.7: Frequency of rupture types in function of diameter (Blindu, 2004)

Similarly, leaks along pipes occur mostly in small diameters whereas large pipes' diameters have leaks at joints (see Figure 1.8).

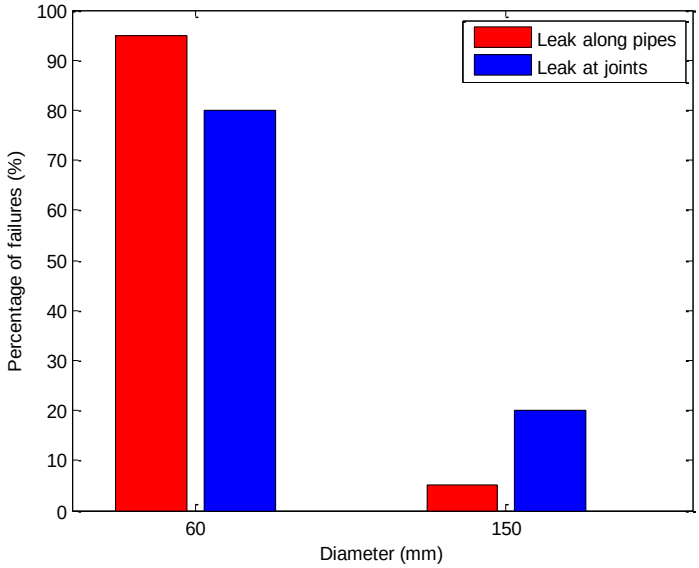

Figure 1.8: Leaks distribution in pipes and in joints according to the diameter (Blindu, 2004)

1.3. Apparent losses

The non-physical losses include the amount of water actually delivered to the costumer without being measured and recorded accurately. Apparent water losses are caused by:

- Water meter inaccuracies.
- Data handling errors (reading and billing systems).
- Unauthorized consumption related to water theft and illegal connections.

The economic impact of apparent losses is greater than real ones. Thus, apparent losses are valued at the retail cost of water charged to customers, while the baseline cost of real losses is generally attributed to the production cost (power, chemicals) (Thornton et al., 2008).

1.4. Consequences of leakage

Several factors are associated with leakage such as the soil saturation, water velocity variation, vibrations, difference in water pressure at both side of the leak and the variation in soil temperature. Economical, technical, social and environmental impacts of water loss and can lead to:

- Excessive costs, not only for reparation work but also for the production (if leakage is 50% of the production, the energy and the treatment costs will be doubled).
- Infrastructure damage due to voids created by leaks that can lead to the collapse of roads and buildings.
- Air intruding into the pipes that cause water hammer, damage to water meters and measurement errors.
- Customer dissatisfaction due to the pressure reduction at taps, showers and garden irrigation systems.
- Polluted water causing risk of bacterial infection spreading contagious diseases.
- Additional stress on superficial and subterranean water to compensate water loss.
- Excessive energy required for long-distance pumping or introducing complex treatment technologies like desalination or wastewater reuse.

1.5. Leak detection technologies

Leak detection is a major factor in managing the water distribution system and increasing their efficiency. A large number of leak detection techniques have been developed. They can be classified into 2 main categories: hardware and software-based methods.

1.5.1. Hardware-based methods

In order to detect the water loss using the hardware-based methods, some equipment are required. The hardware-based methods can be divided into three main categories: i) non-acoustic methods that include the visual survey, gas injection, thermography, ground penetrating radar and negative pressure waves, ii) acoustic techniques such as the manual listening sticks, the leak noise correlation and leak noise loggers and iii) in-line detection methods that include the tethered systems (Sahara), the free-swimming systems (SmartBall), fiber optics and robotic devices.

1.5.1.1. Visual survey

The visual observation is the traditional way to detect leaks. It consists in walking along a pipeline, searching for wet spots developed due to leaks, or suspicious green growth patches above the water line in the case of very dry regions (Thornton et al., 2008). The performance of this method depends on the surveyor's experience and the inspection frequency. Trained dogs can be helpful by smelling substances that may be released from a leak (Zhang, 1997).

1.5.1.2. Gas injection

This tracing technique consists in injecting a non-toxic, water-insoluble and lighter-then-air gas into an isolated segment of water pipe (Hunaidi, 2000). The most common gases used are helium and hydrogen. The sulfur hexafluoride (SF6) and industrial hydrogen (95% nitrogen, 5% hydrogen) can also be injected into buried and ducted cables and pipelines (Farley, 2001). The gas escaping from the leaks permeates to the surface through the soil and pavements. The leak can be detected by scanning the ground surface over the pipe using highly-sensitive gas detectors. The gas injection method detects water leakage in all pipe materials from 75 mm to 1000 mm in diameter (Hamilton et al., 2013). The tracer gas methodology combined with spectrometer leak detectors can also be applied for industrial applications (Calcatelli et al., 2007). It is characterized by a speed tracing, but the high cost reduces the use of this method for leak inspections in pipelines.

1.5.1.3. Thermography

The infrared thermography method has been used in water supply systems, gas pipelines and machinery (Ge et al., 2008; Fahmy et al., 2009). The water leaking from a buried pipe changes the thermal characteristics of the adjacent soil which become a more effective heat sink than the dry soil. The thermal anomalies above pipes are detected with hand-held or vehicle or aircraft-mounted infrared cameras (Burn et al., 1999). This technique can cover large areas without any excavation but its performance can be affected by several factors: solar radiations, cloud over, wind speed, ambient temperatures, ground's moisture and surface conditions of the test area (Ghazali, 2012).

1.5.1.4. Ground penetrating radar

The Ground Penetrating Radar (GPR) is a non-destructive geophysical method, which is used during the last few years for leak detection (Charlton et al., 2001; Crocco et al., 2009; Ayala–Cabrera et al., 2013). The electromagnetic waves generated by the radar propagate to the ground and then reflected back to the surface when they encounter an anomaly in dielectric properties such as a void or a pipe. The reflected waves are received using an antenna and stored in a digital control unit. The depth of the reflecting object is evaluated by the time lag between transmitted and reflected waves. The scanning ground surface gives an idea about the size and the shape of the buried objects. The water leak can be detected in two ways: i) identifying soil voids developed by the leak, or ii) detecting sections of pipe which appear deeper than they actually are due to the increase of the dielectric properties of the surrounding saturated soil (Hunaidi et al., 1998). Figure 1.9 shows an example of GPR profiles for five different scans: soil without pipe, only pipe without water leakage and with leakage under/beside/above the pipe (Dong et al., 2011). The GPR technology can be used for metallic or plastic pipes but it is expensive and quite time-consuming. It is also difficult to choose the right radio frequency due to the different response of variant types of soil. Moreover, a false alarm can be reported when the reflected waves come possibly from anomalies like metal objects in the ground (Ghazali, 2012).

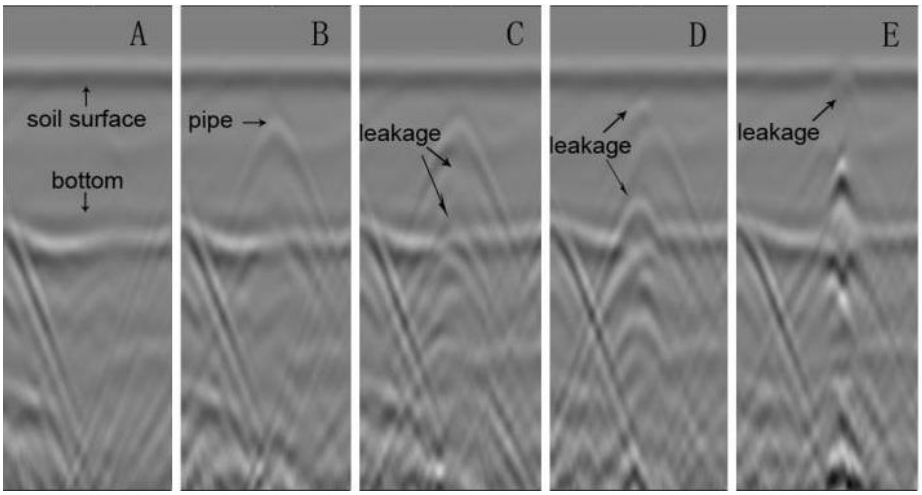

Figure 1.9: GRP profiles: (A) without pipe (B) only pipe without leakage (C) leakage under pipe (D) leakage beside pipe (E) leakage above pipe (Dong et al., 2011)

1.5.1.5. Negative pressure waves

Any singularities in the system such as leaks, blockage or roughness transition reflect the wave propagated from an incoming transient signal (Colombo et al., 2009; Meniconi et al., 2010). A leak affects the transient signal by increasing its damping rate, or creating reflected signals in the pressure trace (Colombo et al., 2009). Water hammer is one of the most common methods to generate hydraulic transient waves (Gong et al., 2012). A sudden pipe break creates a negative pressure wave that travels in both directions to be reflected at the pipelines boundaries (Misiūnas

et al., 2005). The arrival time of this negative known-speed wave at each pressure transducer determines the leak location. The break size is estimated using the magnitude of the transient wave. The transient-based approach has the advantage of being non-invasive, cost-effectively, and with a large operational range (Torres, 2014). The existing transient-based leak detection can be divided into two categories: the time-domain techniques (Misiūnas et al., 2007) and the frequency-domain methods that can be deduced from the time domain using the Fast Fourier transforms (Ferrante et al., 2003a), or the wavelet transform (Ferrante et al., 2003b; Brunone et al., 2004).

1.5.1.6. Manual listening sticks

The listening stick or the stethoscope is one of the traditional leak detection instruments that have been used since 1850s (Pilcher, 2003). The mechanical listening stick could be metal, wooden or plastic. It is applied to listen to leaks on fittings, hydrants or service connections and to localize the leak. The water escaping from a leak under high pressure causes vibrations that are transmitted along the pipe as a structure-borne noise (GIZ, 2011). This sound is transferred through the steel shaft and then heard at the earpiece (Thornton et al., 2008). This technique suits the metallic pipelines between 75 mm and 250 mm under a pressure above 10 m (Hamilton et al., 2013). Listening sticks have been developed in the mid-1960s. They are equipped by a battery sound amplifier to enhance the leak, which were called ground microphones or geophones (Pilcher, 2003). This electronic device works on the same principle of the mechanical stick. It is used to pinpoint the surrounding underground noise from the surface in areas with few fittings. The geophones have the ability to detect leakage in plastic pipes, in areas of low pressure and where there may be high noise interference from the passing traffic, water use, ground movement and wind (De Silva et al., 2011). This process is time consuming and its performance depends on the experience of the user (Hunaidi et al., 2006).

1.5.1.7. Leak noise correlation

The leak noise correlation method is based on the comparison of the noise detected at two different measurement points in the buried pipelines. Considering a consistent pipe material and diameter, the noise travels from the both directions of the leak at a constant velocity. The measured leak signals are transmitted wirelessly from the sensors to the correlator that pinpoints leaks using the cross-correlation method. In fact, the two sensors detect the noise at the same time if the leak is equidistant from them. However, in most cases, the leak is located asymmetrically between measured points and consequently there is a time shift measured by the correlation process (Hunaidi et al., 2006). Figure 1.10 illustrates this principle.

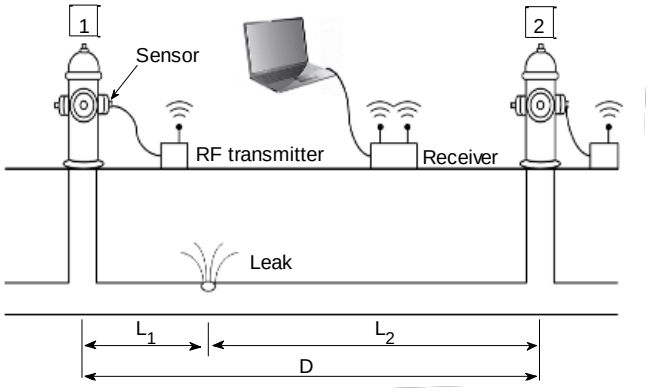

Figure 1.10: Schematic representation of the cross-correlation method for locating a leak (Brennan et al., 2007)

The sensors are located on convenient access points for underground pipes, i.e. fire hydrants or valves. The time lag between the two signals is given by the following equation:

$$\Delta T = T_2 - T_1 = \frac{L_2 - L_1}{V} \tag{1.1}$$

T_1 and T_2 are the arrival time of signal 1 and 2 respectively, L_1 and L_2 represents the distance from the leak to the sensors 1 and 2 respectively and V is the sound propagation velocity in the pipe. Substituting L_2=L-L_1 in Equation (1.1) and rearranging it, we can find the distance from the nearer logger to the leak site:

$$L_1 = \frac{L - V\Delta T}{2} \tag{1.2}$$

Leak noise correlation requires a noise signal that can be generated using accelerometers and hydrophones. On the first hand, the accelerometers that sense the acceleration of vibration induced by leak signals can be installed directly to the pipe, or attached to fire hydrants or underground valves. These sensors are more responsive at high frequencies and work well in case of metallic pipes (Hunaidi et al., 2006). On the other hand, the hydrophones that sense the sound induced by leak noise in the water core of the pipe are placed at fire hydrants or air release valves by using special fittings. These devices are more effective than accelerometers for low-frequency leak signals encountered in the case of plastic pipes and larger diameter mains (Hamilton et al., 2013). They are used to locate small leaks, e.g. joint leak at 6 l/min (Hunaidi, 1999).

The leak noise correlation technique is effective in detecting leaks in metal pipe; its performance is influenced by the distance between the sensors. However, this method presents several limitations in pinpointing leaks in plastic pipelines. The sound waves become weaker as they travel along the plastic pipes, which absorb sound energy due to their viscoelastic properties (Ghazali et al., 2012). Consequently, Hunaidi et al. (2004) found that the distance between two sensors to locate leaks in plastic pipes should be lower than 100 m. Hunaidi et al. (1999) studied

the acoustical characteristics of leaks signals in plastic pipes using both accelerometers and hydrophones. It has been concluded that the amplitude of leak signals diminished rapidly with distance, at a rate of 0.25 dB/m. In addition, the propagation velocity of leak signals is identical for both hydrophone and accelerometer-measured signals. The cross-correlation method was found to be accurate within 30 to 60 cm, but proved too expensive, time-consuming with a short range (Fuchs et al., 1991).

1.5.1.8. Leak noise loggers

The noise loggers are compact units composed of an acoustic sensor coupled with a programmable data logger and a communication module (Hunaidi et al., 2006). The associated acoustic device can be divided into two categories: i) noise sensors with a magnetic base to enable their installation on hydrants or valves and ii) hydrophones placed into the pipes to get efficient acoustic waves propagation in the water. These loggers are arranged in a group of six or more at adjacent pipe, typically 200 to 500 m apart in metallic networks, while this range may decrease to 80 m in plastic pipes. They are programmed to automatically turn on at night to monitor system noise and transform the acoustic vibrations caused by pipe leaks into actionable information on the location of leaks. These units collect noise data usually between 2 and 4 am to minimize the interference from other noise sources, such as roads traffic or high daytime water consumption sound. In case of the temporary emplacement, the noise loggers store the data to be downloaded to a computer before they are deployed at the next location. Recent models of acoustic noise loggers can be placed permanently and the stored result is transmitted wirelessly to a receiver. A geographic information system (GIS) for the water system network facilitates the leak detection by comparing the latest leak sound levels introduced in the map with the previously saved ones. A total of 216 leaks were identified during the acoustic noise mapping survey of 1100 km water distribution network in Halifax Regional Water Commission (Brothers et al., 2001).

1.5.1.9. Tethered systems (Sahara)

The tethered systems or the pipeline pigging methods have been developed to meet various demands in oil and gas industry like inspection, cleaning, leakage detection and reporting the geometric information relating to the pipelines (Licciardi, 1998; Russell, 2005; Jones et al., 2006; Beuker et al., 2009). The Sahara System represents an application, developed by the Water Research in the UK, of this in-line leak detection technology in water transmission mains (Chastain-Howley, 2005). The Sahara System, illustrated in Figure 1.11, operates by deploying a highly sensitive acoustic sensor (hydrophone) through a tapping of 50 mm or larger while the pipeline remains under pressure between 0.3 and 13.8 bar (Mergelas et al., 2005). The hydrophone is connected to a signal processing and display unit via an umbilical cable. A small drag chute uses the flow of water (the flow rate must be greater than 0.3 m/s) to draw the sensor through the pipeline. As the acoustic detector passes any leakage on the pipeline, it detects the noise generated by the escaping water and gives an indication about the leak position to be

marked on the surface. This method is able to detect leak as small as 1 L/hour without being influenced by the pipe material neither the soil type. It is also possible to survey up to 1.5 km per insertion. However, this technology is relatively expensive and different factors can block the tether cable's path such as drag, friction at bends and the presence of in-line valves (Chapman, 2012).

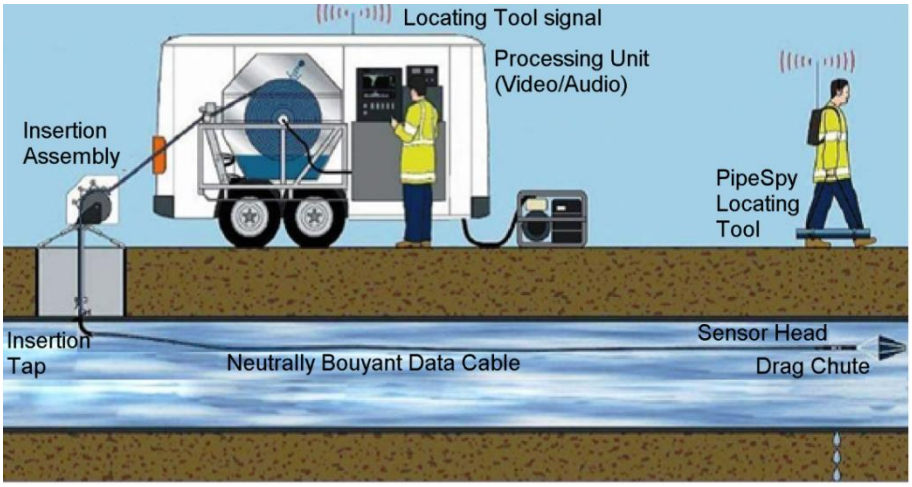

Figure 1.11: Schematic representation of Sahara system (Mergelas et al., 2005)

1.5.1.10. Free-swimming systems (SmartBall)

The main purpose of the free swimming systems is to detect and localize leakage at early stage in pressurized pipelines (Noran et al., 2010). SmartBall is an innovated combination of free-swimming system with an untethered leak detection device. It was invented by Pure Technologies in Canada in 2005 for water transmission pipelines. SmartBall is composed of aluminum alloy core that contains a power source, electronic components and instrumentation (acoustic sensor, accelerometer, magnetometer, GPS synchronized ultrasonic transmitter, and temperature sensor) as shown in Figure 1.12. In order to reduce the effective density of the ball allowing it to be propelled by the water flow, the core is encapsulated inside a protective outer foam shell which creates an additional surface area (Ariaratnam et al., 2010).

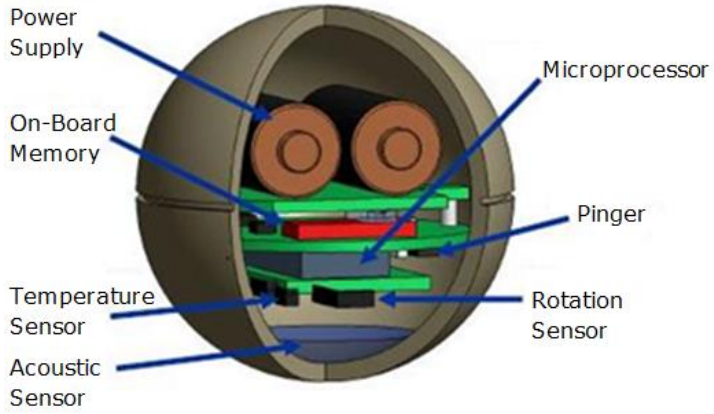

Figure 1.12: SmartBall internal components (Ariaratnam et al., 2010)

The spherical shape eliminates the noise produced by the device as it passes along the pipe, and thus permitting the sensitive acoustic sensor to operate free of external interference (Oliveira et al., 2011). The SmartBall is introduced into the pipeline through an available 90 mm open port valve and retrieved at an extraction point downstream with the same parameter using a specialized material. As the device travels along the pipeline using the water flow, it records the acoustic environment and save all the data. It can traverse around tight bends and through inline valves. Once the SmartBall is captured, the acoustic data is analyzed to identify the leak location using it GPS component (Pure-Technologies, 2011). Figure 1.13 illustrates a schematic representation of the system deployment during a survey.

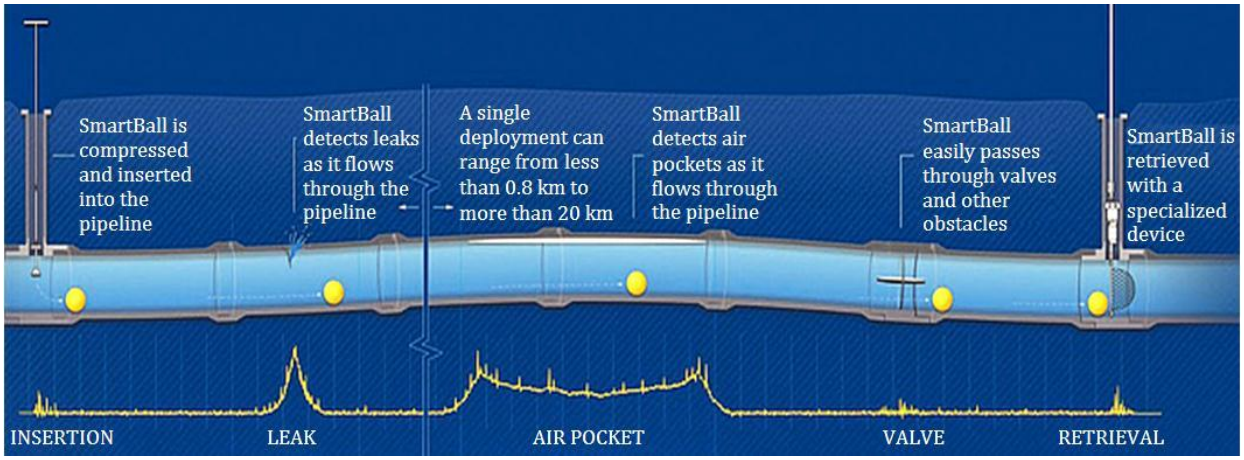

Figure 1.13: Overview of a typical SmartBall survey (Chapman, 2012)

The maximum length of pipeline that can be surveyed depends on the flow rate of the pipeline and the battery life of the device. For a flow rate of 1 m/s and a maximum operating life of 12 hours, the system can survey 43 km for a single insertion point (Hamilton et al., 2013). The SmartBall can be used to detect leaks on large diameter pipe (>300 mm in diameter) without being affected by the pipeline material. It can detect also the pockets of trapped gas in pressurized pipes. Due to its optimum acoustic sensitivity, this device can detect leaks smaller than 0.15 gallons per hour (Pure-Technologies, 2011). However, a false alarm can be generated from acoustic characteristic similar to leaks on pressurized pipelines. This technology has been tested in many case studies. The Birmingham Water Works Board (BWWB) used in 2012, SmartBall leak detection for the inspections of 12 km of 1000 mm reinforced concrete pipe. The survey was successful in locating 26 leaks of varying size with close location accuracy and preventing consequently a long-term water loss (Rothwell, 2013).

1.5.1.11. Fiber optic

The fiber optic sensor systems require the installation of a fiber optic cable alongside the entire length of the pressurized pipelines (Geiger, 2006). This method is used to detect and localize leakage in liquid and gas pipes based on a real-time monitoring. Any liquid escape changes the thermal characteristics of the surrounding soil that can be detected by the fiber optic sensors

(Nikles et al., 2004). These devices are able to measure temperatures and strains along the cable. The continuous monitoring helps in preventing the failure, detecting in time the problem and repairing the fault (Frings et al., 2010). In some cases, the existing fiber optic telecommunication lines can be used for temperature monitoring and detecting leakage that can be localized with an accuracy of 1 or 2 meters (Inaudi et al., 2008).

1.5.1.12. Robotic devices

Robotics could be used to inspect virtually any pipeline from 300 mm diameter or larger; consequently they can help in detection of water leakage. PureRobotics, developed by Pure Technologies, has the capability to traverse up to 5 kilometers from a single access and through radius bends (Figure 1.14). It provides the online monitoring by performing multi-sensor inspections in dry or submerged pipelines where the access can be limited. This device is a vehicle tethered by copper or a fiber optic cable. It includes the following instruments (Mueller, 2013):

- High definition digital pan-tilt-zoom closed circuit television (CCTV).
- High speed profiling SONAR designed specifically for pipeline inspection.
- Laser profiling with 3D reporting capabilities.
- P-Wave electromagnetic sensors for assessing the structural integrity of prestressed concrete cylinder pipe.

Figure 1.14: Pipeline inspection using PureRobotics (Mueller, 2013)

1.5.2. Software-based methods

The software-based methods depend on the flow, pressure and temperature data measured at different points through the water distribution network. They can be classified into five categories: flow change, pressure point analysis, water balance, hydraulic modeling, statistical analysis and artificial intelligence and pattern recognition.

1.5.2.1. Flow change

This method relies on the assumption that a high rate of change of flow at the inlet or outlet indicates the occurrence of a leak. A leak alarm is generated if the flow rate of change is higher than a predefined figure within a specific time period.

Van Thienen (2013) presented a method based on the Comparison of Flow Pattern Distributions (CFPD) to identify and quantify the changes in the amounts of water supplied for two different periods. Anomalies are identified by plotting one set against the other, the best linear fit with slope *a* and intercept *b* indicated respectively consistent (changing in weather or population size) and inconsistent changes (due to increased leakage). This method allowed to: i) detect the leakage in WDS of different sizes and characteristics and ii) check archived data for abnormalities in flow datasets (Van Thienen et al., 2013; 2014; Irons et al., 2015). In order to detect in real-time new leakage or to identify unregistered changes in valve status, Van Thienen et al. (2016) developed Cuboid for automated feature recognition in CFPD analyses of supply area flow data.

1.5.2.2. Pressure Point Analysis (PPA)

The pressure point analysis (PPA) is based on the pressure drop when a leak occurs in a pipeline. The leak can be identified through the pressure by three different ways: i) monitoring of pressure change rate, ii) detecting abnormal low pressures, or iii) comparing the current pressure measurements against a running statistical analysis built from previous data (Stafford et al., 1996). The pressure is measured using sensors that are installed into the pipeline and can vary from a single measurement point to a number of pressure transducers distributed along the pipeline (Oven, 2014). If the pressure decrease exceeds a predefined level, a leak alarm is generated. The relation between leak rate and pressure drop is given by (Winncy et al., 2008):

$$Leak\ rate\,(cm^3/s) = \frac{Total\ Test\ Volume\,(cm^3) \times Pressure\ Decay\,(mbar/s)}{Atmospheric\ Pressure\,(mbar)} \qquad (1.3)$$

The PPA method is applied to pressurized pipelines from 75 to 1000 mm in diameter without being affected by the pipe material or liquid properties. This method is interesting for low complexity and cost, but it can only detect major leaks. Furthermore, the leak is not the unique event that causes pressure drop, consequently the PPA technique could yield false alarm.

1.5.2.3. Water balance

Water balance, mass balance or water audit is the most widespread technique currently in use to quantify the total water losses in a network. It relies on the principle of conservation of mass: the fluid that enters the pipe section either remains or leaves the pipe section (Stafford et al., 1996). A leak is identified if the difference between the amount of water put into the distribution and the sum of the components of water consumed or used exceeds an established tolerance (Farley, 2001). Assuming that under steady conditions mass and energy are conserved (Sturman et al., 2004), the entire pipeline networks are pressurized and there is no storage within the pipes, the water balance can be calculated basically using the following formula:

$$W_L = W_I - W_C \tag{1.4}$$

W_L is the water leakage; W_I is the water supply system input and W_C is the water consumption.

In order to standardize this method and to include all the components that contribute for the water loss, the International Water Association (IWA) produced a standard approach for water audit calculations with a common terminology as shown in Table 1.1.

The efficiency of the mass balance depends on the accurate measurement of the mass entering and exiting the water network (Newell et al., 2006). The main disadvantage of the water audit technique is the assumption of steady state. According to this hypothesis, the volumes balance have to be calculated over a longer time interval to prevent false alarms (Misiūnas, 2005). The water balance method is also limited face pinpointing the leaks in the network and need consequently to be associated with other active leakage methods.

Table 1.1: IWA Standard International Water Balance and Terminology

<table>
<tr><td rowspan="8">System Input Volume</td><td rowspan="3">Authorized Consumption</td><td rowspan="2">Billed Authorized Consumption</td><td>Billed Metered Consumption (including water exported)</td><td rowspan="2">Revenue Water</td></tr>
<tr><td>Billed Unmetered Consumption</td></tr>
<tr><td rowspan="2">Unbilled Authorized Consumption</td><td>Unbilled Metered Consumption</td><td rowspan="6">Non-Revenue Water (NRW)</td></tr>
<tr><td>Unbilled Unmetered Consumption</td></tr>
<tr><td rowspan="5">Water Losses</td><td rowspan="2">Apparent Losses</td><td>Unauthorized Consumption</td></tr>
<tr><td>Metering Inaccuracies</td></tr>
<tr><td rowspan="3">Real Losses</td><td>Leakage on Transmission and/or Distribution Mains</td></tr>
<tr><td>Leakage and Overflows at Utility's Storage Tanks</td></tr>
<tr><td>Leakage on Service Connections up to point of Customer metering</td></tr>
</table>

1.5.2.4. Hydraulic modeling

In the last three decades, the hydraulic modeling has been well developed as a tool for monitoring the operations of a network in present and in the future (AWWA, 2005). It is used to operate and manage water supply systems, anticipate problems in planned networks and design effective interventions. The model based systems describe mathematically the fluid flow using the conservation of mass, conservation of momentum and conservation of energy equations as well as the equations of state for the fluid (Zhang, 1997). The hydraulic modeling consists in organizing the data in a hierarchical structure and calibrating the model until it reflects the reality as close as possible. However, the model calibration remains a challenging issue (Savic et al., 2009). The calibration describes the process of minimizing the differences between the real or measured values and the model simulated results by adjusting the hydraulic parameters of the model. The calibration process involves the roughness, water consumption and water losses (Ormsbee et al., 1997; Lansey et al., 2001). The genetic algorithm is used to calibrate the hydraulic model (Vítkovský et al., 2000; Z. Y. Wu et al., 2002; Nikjoofar et al., 2013). It is essential to note that the development of the model could be affected by several error sources:

- Database (topography, diameter and length pipe).
- Uncertainty about the valves status.
- Accuracy of measurement systems (sensors, data loggers).

Once the model is calibrated, it is used to describe the real behavior of the system and estimate the hydraulic characteristics of the network at any time and location.

The hydraulic model can estimate the leakage within the areas by minimizing the difference between the measured and the numerical estimated pressure and flow rates (Adachi et al., 2014). It can also be used for leakage management, including leakage modeling as pressure dependent demand (Giustolisi et al., 2008; Tabesh et al., 2008; Z. Wu et al., 2009) and pressure management planning for leakage control (Burrows et al., 2000).

1.5.2.5. Statistical leak detection analysis

The statistical leak detection technique is based on the analysis of the flow rate, pressure and temperature measurements of pipeline.

ATMOS Pipe, developed in Shell, is the original statistical leak detection technology used to detect changes in the relationship between flow and pressure data collected from a SCADA system (Zhang, 1997). A sequential probability ratio test (SPRT) is applied to detect the discrepancy between the inlet and the outlet flow and pressure (Zhang et al., 2000). A leak will cause a pressure drop in the pipeline associated with a difference between the receipt and delivery flow-rate. The total mass entering and leaving a network must be balanced by the inventory variation inside the network. That balance cannot be maintained if a leak occurs in a network (Zhang et al., 1998). These patterns are detected by ATMOS Pipe that compares two statistical hypotheses: leak versus no-leak system. Once the comparison yields a confidence level

of 99%, a leak alarm is signaled. This methodology led to reduce false alarms to a low rate. ATMOS Pipe has been successfully applied to the following pipelines: crude oil, refined products, natural gas and other materials such as ammonia, chlorine gas and carbon monoxide. It is suitable for real-time application and can detect even small leaks under transient conditions.

Buchberger et al. (2004) proposed a statistical method to detect the magnitude of leaks in small residential service zones. The method relies on computing the sample mean and variance from the set of measured flow rates as the set is truncated progressively from below. In the case of unsteady network leakage, the method will estimate the maximum and minimum rates of leakage, instead of a single average rate. The proposed method provides a way to prioritize zones in the network where loss controls are most urgently needed. This approach has not been tested in a real case study.

1.5.2.6. Artificial intelligence and pattern recognition

The Artificial Neural Networks (ANN) is also used to detect and localize the leakage (Mounce et al., 2003; 2006; 2009; 2014). Neural Networks are computational systems that model the operation of the human nervous system. They include a collection of nodes linked by connections. Each connection is associated with a real number referred to as its weight. Neural Networks define a mapping between input patterns and output patterns. They are trained on a collection of training cases called a training set. The input data characterizes the states of the fluid network under normal and abnormal (with leaks) operating conditions. Then it acts as a classifier in order to estimate the actual system status and pinpoint leaks, based on available information (De Silva et al., 2011). During training, the weights are adjusted to minimize the mean square error between the predicted output and the actual output pattern, a procedure referred to "back-propagation" (Caputo et al., 2002).

The ANN method developed by Mounce et al. (2010) based on flow and pressure data was verified on a real case study of 144 zones in the United Kingdom. It has been found that this method is effective to detect bursts.

The artificial neural network model can be integrated in geographic information system (GIS) to assess water leakage and to prioritize pipeline replacement (Ho et al., 2010). The input factors of ANN was the pipe diameter, pipe material and number of magnitude-3^{+} earthquakes, while the number of monthly breaks was used for the prediction output.

Jafar et al. (2010) used 14-years data to predict using ANN the pipe failures in the water supply system of Wattrelos City in France. The model determinates also the optimal time for the renovation of pipes in the system.

The multi-class SVM advanced pattern recognizer was recently used to detect the leakage (De Silva et al., 2011; Mashford et al., 2012). The multi-class support vector machine (SVM) advanced pattern recognizer was successfully applied to detect and classify the different stages of pipelines leaks and breaks (Mamo et al., 2014).

1.5.3. Comparison of leak detection methods

The leak detection methods have advantages and limitations. In order to compare the presented method, five evaluation criteria are used (Table 1.2):

- Leak sensitivity: the ability to detect small leaks.
- Leak location: the capability to pinpoint the leak.
- Real time monitoring: the possibility to monitor continuously the WDS.
- False alarm: the frequency of generating false alarm when leaks do not exist.
- Cost.

Table 1.2: Comparison of leak detection methods

Methods		**Leak Sensitivity**	**Leak Location**	**Real time monitoring**	**False alarms**	**Cost**
Non-acoustic	Visual survey	High	Yes	No	Low	High
	Gas injection	High	Yes	No	Low	High
	Thermography	High	Yes	No	Medium	High
	Ground penetrating radar	High	Yes	No	Medium	High
	Negative pressure waves	High	Yes	No	High	Medium
Acoustic	Manual listening sticks	High	Yes	No	Medium	High
	Leak noise correlation	Medium	Yes	Yes	Medium	High
	Leak noise loggers	Medium	Yes	Yes	Medium	High
In-line	Tethered systems Sahara	High	Yes	No	Low	High
	SmartBall	High	Yes	No	Low	High
	Fiber optic	High	Yes	Yes	Low	High
	Robotic devices	High	Yes	No	Low	High
Software based	Flow change	Medium	No	Yes	Low	Low
	Pressure Point Analysis	Low	No	Yes	Medium	Medium
	Water Balance	Medium	No	Yes	Low	Low
	Hydraulic modeling	Medium	Yes	Yes	High	Medium
	Statistical Analysis	Medium	No	Yes	High	Low
	Artificial intelligence	Medium	Yes	Yes	High	Low

1.6. Smart Water Networks (SWNs)

The application of the Information and Communication Technologies to urban networks resulted in the development of the Smart City Concept, where the infrastructure components become more intelligent, interconnected and efficient (Chourabi et al., 2012). The successful results of the smart grid implementation in the electrical field (Fang et al., 2012) encouraged water utilities to apply the smart approach to the WDSs. The smart water networks concept is based on the process of equipping the pipes with sensors that provide a complete monitoring system of the pipe condition and performance (Liu et al., 2013). The main objective of a smart water network is to build a complete monitoring system, integrating sensors technology, data acquisition, data interpretation, and decision for real-time management of water network assets (Boulos et al., 2013). Figure 1.15 illustrates the concept and the architecture of a smart water network.

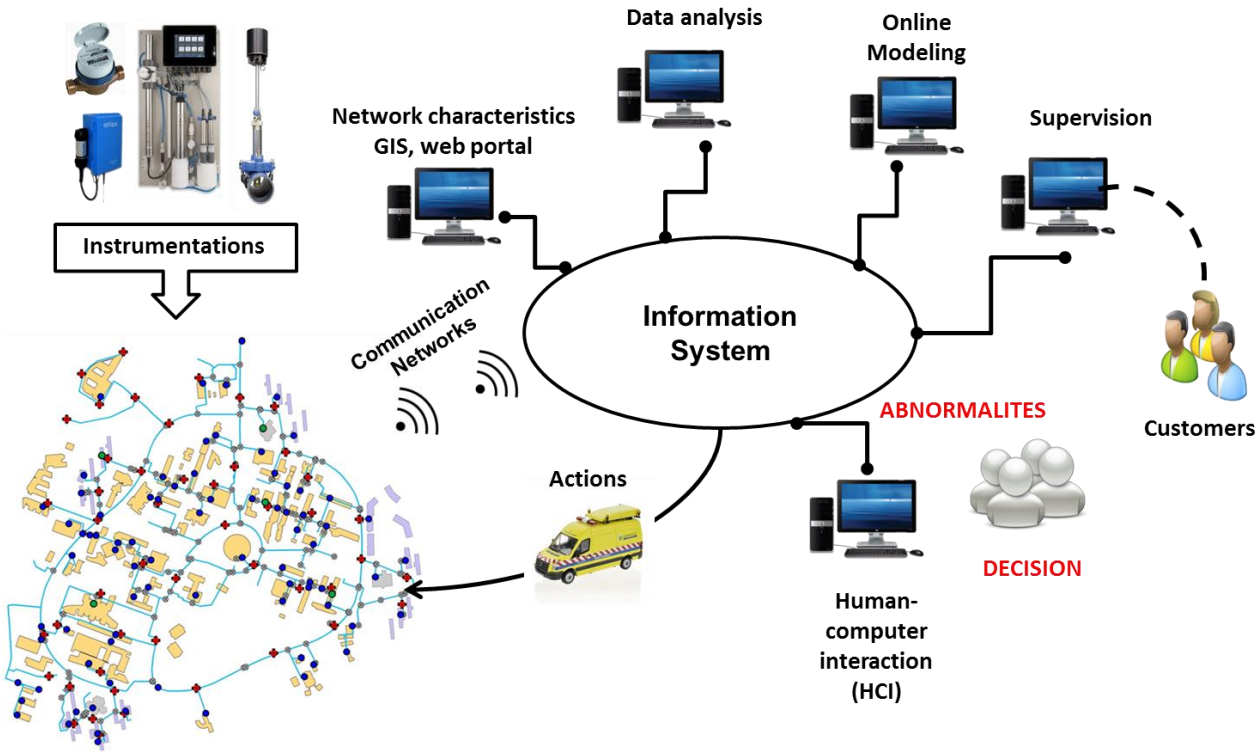

Figure 1.15: The concept of a smart water network

The process of a smart water network (Figure 1.15) includes five principal layers (Cahn, 2013):

- Physical layer: all the characteristics of the physical components of a WDS such as pipes, valves, reservoirs, pumps, etc.
- Sensing and control: measure water parameters such as flow, pressure, quality and other critical characteristics.
- Collection and Communication: collect automatically and continuously the measured data.

- Data management and display: build a database platform to organize the collected data, present it through visualization tools like GIS and set up a customer information system.
- Data fusion and analysis: study the different responses in the network via modeling software and apply predictive analytics for event detection, leak detection and localization, decision support, etc. The network is therefore remotely and automatically managed through the communication channels.

Günther et al. (2015) applied these layers to build a smart water network based on an experimental water distribution system (EWDS-TUG) that includes artificial customers, sensors and control magnetic valves.

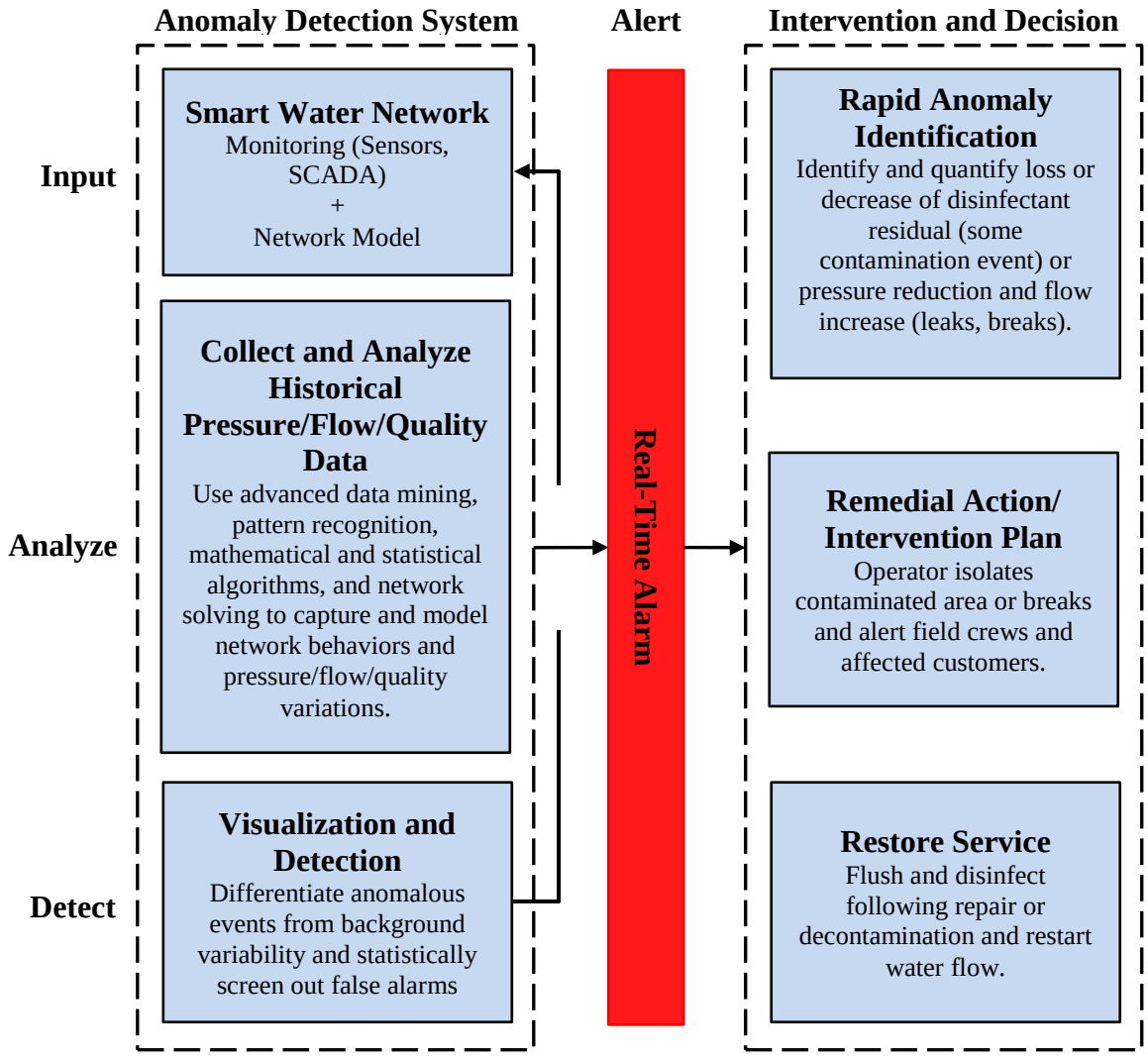

Figure 1.16: Smart Water Network process (Boulos et al., 2013)

Thanks to the smart grid concept, water utilities can reduce water loss through reliable and consistent visibility of water distribution networks. The real-time monitoring of water distribution networks present major benefits (Figure 1.17):

- Water savings.
- Energy savings.
- Operational network visibility.
- Improved basis for decision making.
- Early detection of network inefficiencies.
- Decreased need for on-site inspection.

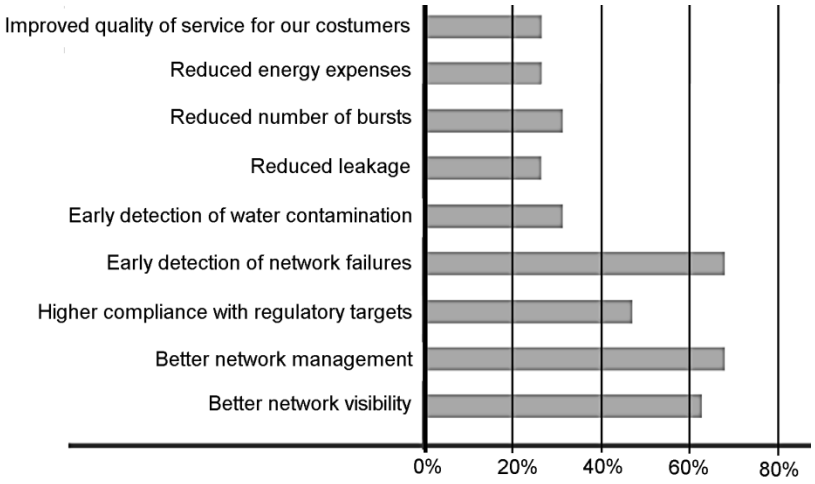

Figure 1.17: Benefits of online monitoring (SWAN, 2012)

1.7. Automatic Meter Reading - Smart metering

The most traditional method to obtain the meter data was the Manual Meter Reading (MMR). An operator visits each customer's supply points in a pre-determined time sequence (monthly, three or six-monthly), reads the value and transcribes it manually the reading on a paper. This acquisition technique works well. It is still used by many water providers for billing purposes. However, it meets some difficulties. The manual water meter reading is a tedious, expensive and highly labor-intensive job (Depuru et al., 2011). The development of the communication technologies enables households and water utilities to get the water usage data through smart water meters or automatic meter readings (AMRs). These smart meters are able to collect and communicate in real time the recorded data. The AMR systems can be walk-by, drive-by, or fixed network and the communication with the meter is one-way. Conversely, the Automatic Meter Infrastructure (AMI) allows a two-way communication between the meter and the water utility. The meter talks to the meter-reading device and the device can send back commands to the meter. The AMR and AMI are components of the Intelligent Urban Water Network (IUWN). An IUWN is defined as ‘a network management system that exploits new technologies to monitor performance, remotely sense asset condition, assess water availability and monitor real

time water use and water quality to improve delivery of water, wastewater and stromwater service for the benefits of all stakeholders' (Boyle et al., 2013). The relationship between the AMR, AMI and IUWN is illustrated in Figure 1.18.

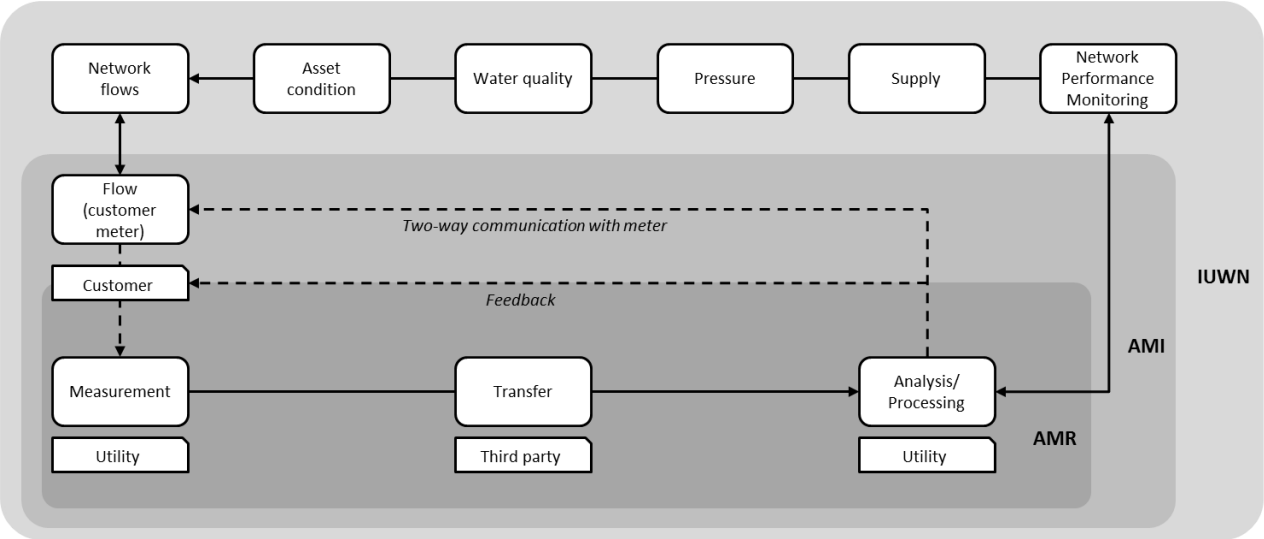

Figure 1.18: Relationship between Automatic Meter Reading (AMR), Automatic Meter Infrastructure (AMI) and within an Intelligent Urban Water Network (IUWN) (Boyle et al., 2013)

1.7.1. Walk-by

The walk-by meter reading was the first step forward from the traditional manual metering. In this AMR generation, an operator carrying a handheld computer with a wireless or wired connection collects the readings as he/she walks from meter to meter. Using a 2G/3G connection, the recorded data in the handheld unit are directly transferred to a billing or data collection system, eliminating any manual entry errors. In newer houses, the individual meters are linked together using twisted pair lines and a local network. The operator plugs the handheld device into an exterior port (probe) located in the metered building and collect then all the data without the need to access to each customer property. This technology improved the accuracy and efficiency of the meter reading, but it remains a labor-cost process and the operator stills need to step along the designated meter route. The meter readers are able to collect from 600 to 1000 reads per day using a radio-equipped handheld computer (Sehgal, 2005).

1.7.2. Drive-by

The Drive-by method uses a vehicle equipped with communication devices to read meters values without physical access the customer properties. The vehicle includes a roof-top mounted antenna, Radio Frequency (RF) receiver/transceiver and a laptop with appropriate software. As the patrol car drives slowly through the service area, the transceiver sends a radio wake-up signal to all AMR devices and then receives the meter readings. A GPS mapping software is integrated in the drive-by system allowing the operators to control the data collection process and check

any missed readings before leaving the route. The mobile data collection system is applied in high population density areas and where the access to the meters is difficult or risky. A large number of meter reads can be achieved, reaching about 20000 meters per day (Christodoulou et al., 2012).

1.7.3. Fixed Network Data collection system

The third generation of AMR communication system refers to the Fixed Network. A permanently infrastructure of established antennas is installed to collect meter readings and to transfer these data to a central computer. Fixed Networks use cable and wireless fixed communication networks publicly or privately. The AMR signals are transmitted via the network, directly if close enough or to repeaters and then sent to the central receiving station at the programmed times (McNabb, 2012). Even if the construction and the installation costs of the fixed network systems are much higher than "Walk-by" and "Drive-by", this third generation is a worthy method due to its benefits. In fact, installing a fixed network reduces the need of the staff costs and problems in the field. Moreover, this system provides the meter reading at any frequency interval (hourly or even shorter periods) and at any time of the day (Christodoulou et al., 2012). These systems can be incorporated with water provider SCADA (Supervisory Control and Data Acquisition) management systems. In order to avoid the cost of the fixed communication infrastructure, the water utilities use commercially available wireless and mobile communications networks like GSM-GPRS, WiFi (L. Li et al., 2009), Zigbee-3G (Han et al., 2010) and 4G Long Term Evolution (LTE) (Yaacoub, 2014).

1.8. Smart Water projects

- **WaterWise@SG**

The Wireless Water Sentinel project in Singapore (WaterWise@SG) is based on the WSN process. It uses hardware and software platform that manages continuously the hydraulic, acoustic and water quality parameters. WaterWise supports also some applications including predictions of water demand and hydraulic state, online detection of events such as pipe bursts, and data mining for identification of longer-term trends (Allen et al., 2011). WaterWise has a step farther than PipeNet by facilitating in-situ experimentation. The sensor nodes used currently in Singapore cover an area of 60 km^2. The sensor is packaged in a clear plastic acrylic tube, with PVC caps at each end. This device supports the simultaneous attachment of three types of sensors: a pressure sensor, a hydrophone and a flow meter. The pipe burst is detected and located by analyzing pressure, flow and acoustic signals. Figure 1.19 describes the operational flow between the components of the WaterWise@SG software and middleware architecture.

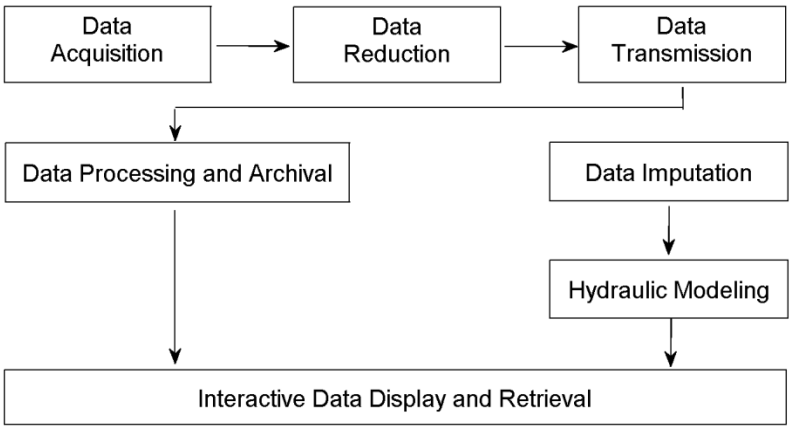

Figure 1.19: Software and Middleware Architecture (Whittle et al., 2013)

For a wireless communication, a USB 3G modem and a USB Wi-Fi radio are connected to the main processing board (Whittle et al., 2010). The WaterWise communication system is illustrated in Figure 1.20. The nodes collect real-time sensor measurements, log system diagnostic data, and transmit the collected data to the backend server infrastructure. The server archives the data, performs data processing, interfaces with hydraulic, modeling tools, and hosts a web portal providing various services for data access and visualization.

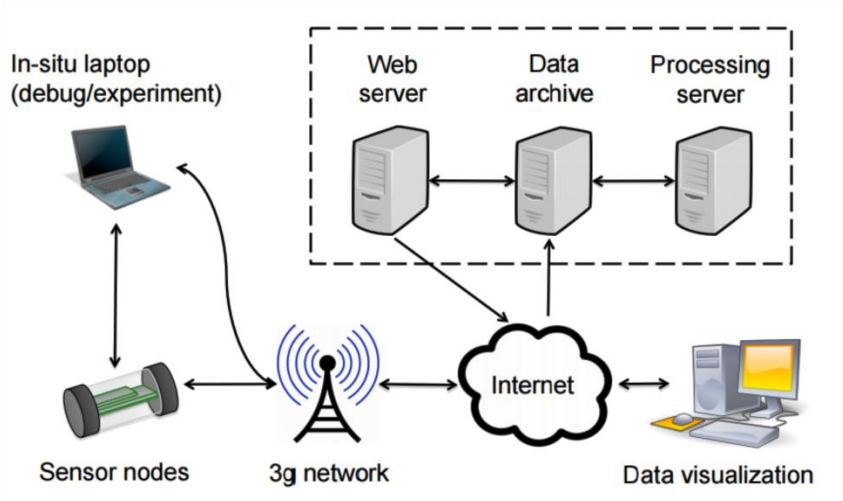

Figure 1.20: WaterWise communication system (Whittle et al., 2010)

- **Wireless Sensor Network (WSN)**

The wireless sensor network (WSN) is composed of small interconnected wireless nodes with sensing, computing and wireless communication capabilities, with power supply requirements. A pipeline-monitoring WSN is made of sensor nodes that collaborate to collect data and transmit it to a base station (Owojaiye et al., 2013). Some issues concerning the smart pipe should be taken into consideration such as the radio propagation channel, power and memory constraints and efficient routing protocols (Lin et al., 2008).

PipeNet is an example of a system based on wireless sensor networks, which aims to detect, localize and quantify bursts and leaks in water transmission pipelines (Stoianov et al., 2007). The development process of PipeNet is divided into three stages. The first one requires a field validation of a small-scale prototype deployment to evaluate the preliminary design in terms of durability of sensors. The second stage consists in testing and validating some of the more advanced data acquisition and analysis techniques including time synchronized data collection and acoustic leak detection in a laboratory setting. The final one assembles the two previous stages to build a complete real-time monitoring solution.

Sadeghioon et al. (2014) used smart wireless sensor network to measure the pressure and the temperature in plastic pipes. The sensors nodes consumed a low power (2.2 µW) and collect datz every 6 hours. Analysis showed that the temperature data combined with the pressure changes is necessary to differentiate leaks from other pressure changes in the system.

- **ICeWater project**

The ICT Solutions for Efficient Water Resources Management (ICeWater) aimed at increasing the stability of freshwater supply using the smart-grid integration (Fantozzi et al., 2014). The ICeWater system is composed of three layers: i) sensors, data loggers and smart meters, ii) data treatment such as filtering, normalization, aggregation and storage, iii) online or offline interaction with users. The IceWater project was tested in the water distribution systems in Milan (Italy) and Timisoara (Romania). The water loss is predicted using statistical and machine learning methods. The data collected from Milan demo site was classified to identify typical urban water demand and provide short term forecasts for each hour of the day (Candelieri et al., 2014).

- **iWIDGET project**

The Improved Water efficiency through ICT for integrated supply-Demand side management (iWIDGET) project aims at providing a web-based platform for the integrated management of urban water. The iWIDGET platform offers for both households and water utilities a near real-time about water consumption and a decision-support tool to promote water and related energy efficient use behaviors (Barry et al., 2014). The iWIDGET system focused on the last two processes of the intelligent metering systems: “processing and analysis” and “feedback of water use data”, as illustrated in Figure 1.21.

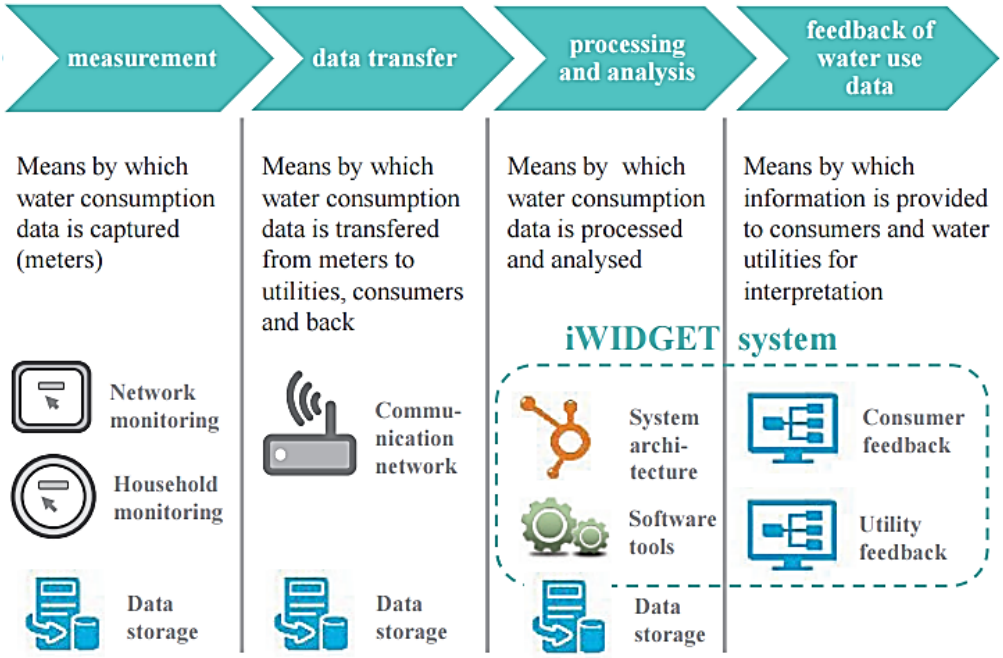

Figure 1.21: Integration of iWIDGET system in the intelligent water metering system process (Ribeiro et al., 2015)

The data used in the iWIDGET project is collected from Greece, Portugal and the United Kingdom. The collected information used for developing a water pricing system and forecasting the demand (Walker et al., 2015).

1.9. Leakage monitoring – The DMA concept

A District Metered Area (DMA) is created via subdividing the water distribution network into discrete zones using valves (Figure 1.22). The water flowing into and out of the DMA is periodically analyzed in order to monitor the level of leakage and reduce the actual losses to an economic level. The concept of DMA was firstly introduced to the UK water industry in the early 1980s (Morrison, 2010). The size of an individual DMA depends on (Farley, 2001):

- The required economic level of leakage.
- Geographic/demographic factors (urban or rural, industrial areas) and the number of properties.
- Previous leakage control technique.
- Hydraulic conditions (limitations of closing valves).

In order to collect data, flow and pressure sensors are placed on the DMA boundaries. This monitoring allows the investigation of leakage. It also used by utilities to prioritize the maintenance of the water network.

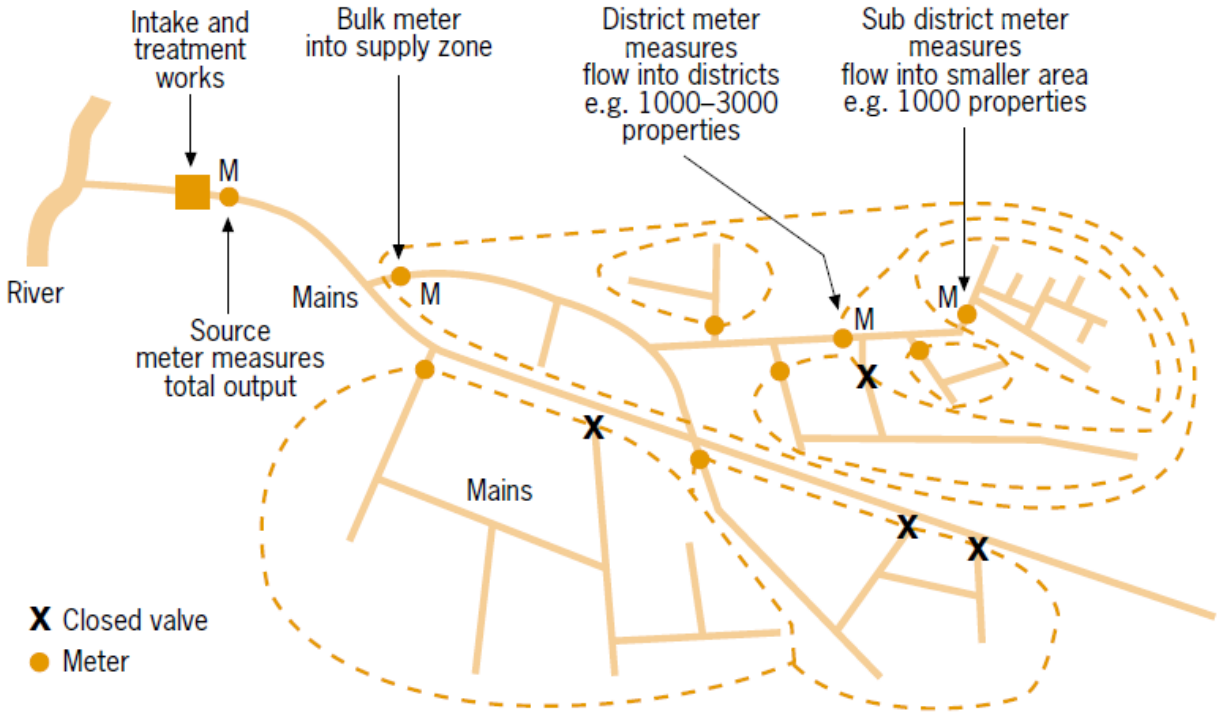

Figure 1.22: Typical DMA layout (Farley et al., 2008)

The first step of creating a DMA consists in planning: each DMA has to be separated from adjacent DMA to ensure a net calculation of the input and the output volume. Therefore, a meter is installed or a valve is closed where the DMA boundary crosses a main. Large distribution mains (higher than 300 mm) should be excluded from DMAs to avoid costly meter installations and to improve the accuracy of flow information (Fanner et al., 2007). Once the DMA is planned, testing is necessary to check that the pressures are maintained up to the standards. All the stages in design and installation of a DMA are described in Figure 1.22.

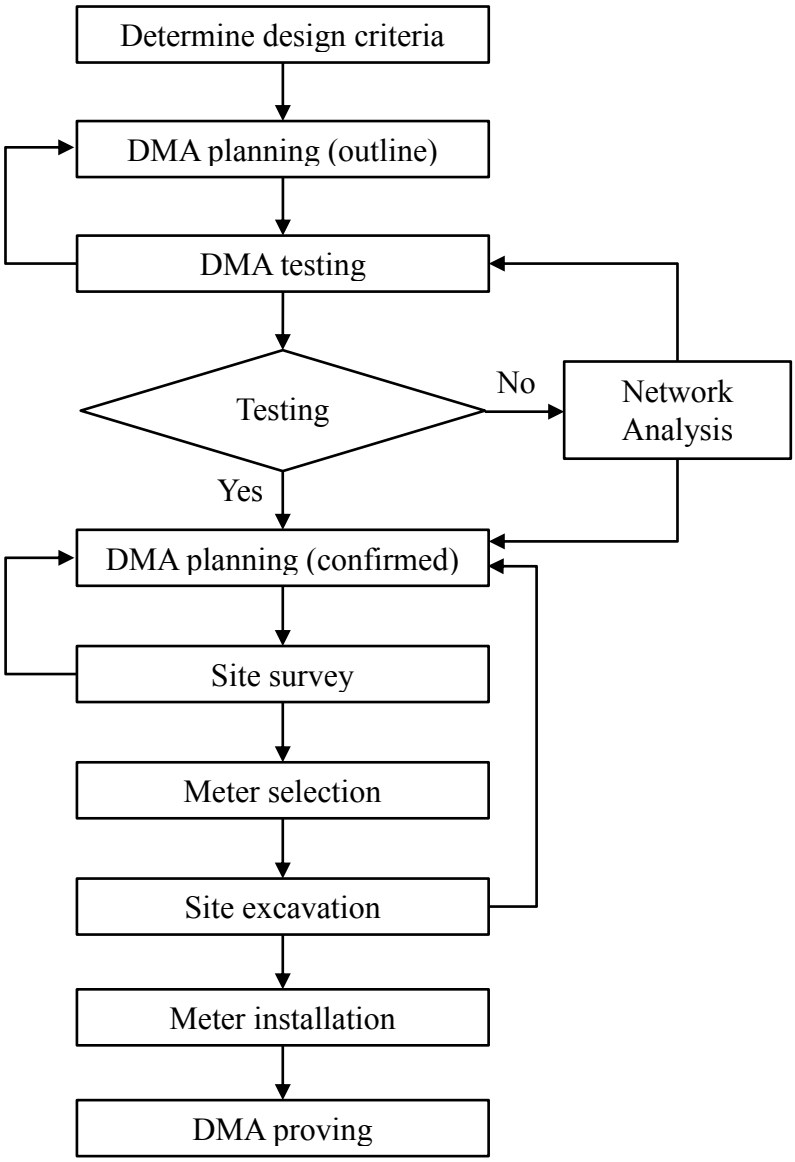

Figure 1.23: Stages in DMA design and installation (Farley, 2001)

1.9.1. Minimum Night Flow (MNF)

The most common method of determining the level of leakage in a DMA is the analysis of the minimum night flow (MNF), which occurs between midnight and 4 a.m. The MNF is measured between 2 a.m. and 4 a.m. when customer demand is least, network pressures are high and leakage is dominant in a District Metered Area (DMA) (Thornton et al., 2008). A leak alarm is generated when the MNF in a DMA exceeds a threshold set by water utility companies, which depends on the age and the length of the pipes, the number of connections and the pressure (Alkasseh et al., 2013). As shown in Figure 1.24, the leakage is calculated as the difference between the legitimate night consumption and the minimum night flow. The legitimate night consumption includes the household and non-household night uses. From one hand, the household customers use water during the night for toilet flushing, automatic washing machine,

and outdoor irrigation. On the other hand, the non-household night usage includes the water used by the machines programmed to remain turned on also at night.

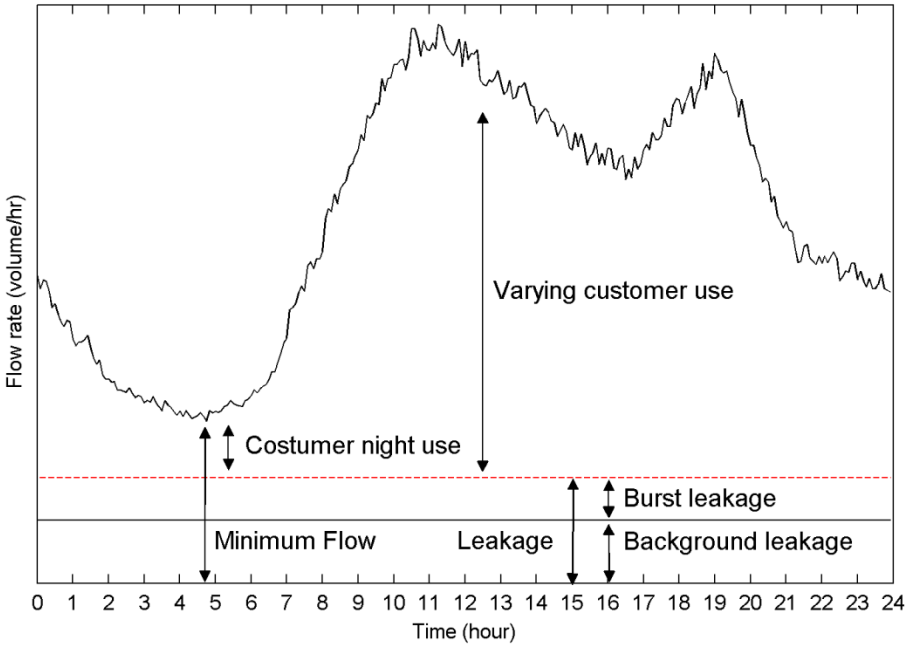

Figure 1.24: Typical 24-hour flow profile (Farley et al., 2008)

Once the leakage flow rate $Q_L(t_{MNF})$ at minimum night-time flow t_{MNF} has been extracted, the leakage flow rate $Q_L(t)$ at a time t can be calculated using the FAVAD principle developed by May (1994):

$$Q_L(t) = Q_L(t_{MNF}) \times \left(\frac{P_{AZT}(t)}{P_{AZT}(t_{MNF})} \right)^{\alpha} \tag{1.5}$$

$P_{AZT}(t)$ and $P_{AZT}(t_{MNF})$ are the average zone pressure at time t and at MNF hour respectively, and α is the leakage exponent. According to Thornton et al. (2008), α is estimated at 0.5 for fixed areas leaks that occurs in rigid pipes (cast, steel). For variable areas leaks at joints or flexible plastic pipes, α is estimated to 1.5 if the cracks where the length changes with pressure and 2.5 if the cracks where the length and width change simultaneously with pressure.

1.9.2. Case studies

- **Halifax, North America**

The Halifax Regional Water Commission in North America serves a population of 320000 residents through 1300 km of pipes aging approximately 50 years old. The water network is divided into 60 DMAs including: 2500 customer connections or 30 km of water main, 150 – 200 hydrants and more than 100 meters sites monitored by a SCADA system to collect the flow data between 3 am and 4 am. The MNF values found are compared to references of economical level

of leakage for each DMA to detect the leak. Consequently, the performance indicator has been reduced from 9 to 3.8 (MacDonald et al., 2005).

- **Napoli Est, Italy**

A subdivision analysis of the water distribution network in Napoli Est was conducted by Giugni et al. (2008) in order to reduce the water loss percentage, which was estimated at 40%. The total surface area of the zone is 920 hectares. It includes between 65000 and 70000 residences. The water network is supplied by 5 tanks for a total storage volume of 30000 m^3. Pipes are in reinforced concrete, grey cast iron, steel and ductile cast iron, with a diameter ranging from 40 to 1000 mm. An electromagnetic flow meter is installed along the reservoir exit pipe. The flow results show a MNF never below than 220 l/s whereas the peak flow varies between 440 to 450 l/s. It follows that the Napoli Est network presents a large percentage of leakage since the zone is characterized by small night use of water. Therefore, six DMAs were designed and simulated by installing 14 intercepting valves and 9 pressure reducing valves. Consequently, the water saved following this subdivision was equal to 34% of the physical losses.

- **Beijing, China**

W. Li et al. (2011) described an integrated system for the detection, early warning, and control of pipeline leakage in Beijing. The total pipeline length is about 8120 km serving an area of 665 km^2. The water network is divided into DMAs covered by 2644 locations identified as the optimal sites for the leakage monitoring meters. The leakage status can be detected through discerning the acoustic signature of leaks; data information is transmitted in real time to the control unit. A probabilistic method is used to predict the leak in the pipelines and to facilitate the inspection and maintenance decisions. In addition, the principle characteristics of the network (pipe age, diameter, length) and related information (time leak occurred, leak type, intensity of leak) were used in a genetic programming to forecast leakage. This project led to detect 102 non-obvious leakages (i.e. 14.2% of the total detected in Beijing) over 1 year, which saved 2,385,000 m^3 of water.

1.10. Conclusion

Water loss is one of the major problems for many cities. The detection and localization of the leaks constitute a priority in the management of drinking water systems. Leak detection methods have been developed over years from the conventional manual sounding technique to the smart management. In this chapter, a literature review of the leak detection techniques has been presented. Two main categories have been discussed: hardware-based and software-based techniques. The hardware-based methods have included acoustic techniques, visual survey, gas injection, thermography, ground penetrating radar, negative pressure waves and inline technologies. The software-based techniques have comprised the flow change, pressure point analysis, water balance, hydraulic modeling, statistical analysis and artificial intelligence. The principle of each method is described and its main advantages and limitations have been identified. The performance of the described methods have been classified according to: i) the ability to detect small leaks and pinpoint the bursts, ii) the possibility of a continuous monitoring, iii) the frequency of generating alarms and iv) the cost.

None of the existing leak detection techniques can be used on its own and needs consequently to be combined with another method. Currently, the water companies have started to implement the smart grid in the water distribution systems to detect immediately the water loss and minimize the runtime of the leaks. Thanks to the development of the hydraulic sensors and the data acquisition systems, the smart water networks help the water companies to optimize operations and save money while improving customer services. The leakage detection solution in smart water networks prevent water loss and large bursts that interrupt services and cause property damages. In parallel, the pressure management control network water pressure to reduce burst frequency and extend infrastructure lifetime. Furthermore, the water quality monitoring lets the water companies to manage and avoid quality issues before customers are impacted. Such capabilities enhance a water utility's ability to deliver clean, constant and affordable water.

The real time monitoring of the smart water networks requires data analysis methods to detect immediately and automatically unusual events. Currently, the most commonly applied method to detect the leakage in the smart water networks is the Minimum Night Flow (MNF) approach. The MNF method is based on the monitoring of the night flow in a District Meter Area (DMA). The MNF approach stills depend on a human interpretation of the data and the definition of a threshold remains the challenge for the researchers.

In the light of the above, a large scale demonstrator of the smart water system is presented in the following chapters. This demo site is implemented in the Scientific City of Lille University in North of France. The analysis of the water consumption will be detailed in order to understand the behavior of the buildings in terms of water usage. The Scientific City water system suffers from real and apparent water losses. The real-time monitoring of the flow allows the verification of the water balance and the determination of the water losses. In order to identify the leakage in near real time, advanced leak detection methods are developed. In particular, a development of the minimum night approach will be discussed and new statistical approaches will be presented in the next chapters.

Chapter 2

SunRise Smart Water Demo Site

This chapter describes the SunRise Smart Water demo site: a large scale demonstrator of the smart water system. The demo site concerns the water distribution network of the Scientific Campus of the University of Lille. The physical components of the water network are integrated into multiple layers in a georeferenced map. The demo site is monitored by a set of hydraulic sensors that measure the water consumption and pressure as well as the noise level through the pipeline. This chapter presents the characteristics of the sensors with some examples of measurements. It presents also a set of leak simulations experiments using the hydrants in order to analyze the response of the acoustic system to leak.

2.1. Introduction

The water distribution network of the Scientific Campus suffers from significant from significant losses due to: i) aging infrastructures and leaks due to soil movement (freeze-thaw cycles, works in proximity), ii) unauthorized consumption related to water theft from the fire hydrants and iii) unmetered water volumes consumed for specific needs to clean the network or used by constructing companies. In order to monitor and reduce the leakage rate, the water distribution network of the campus should be transformed from passive to active. It is nowadays a large scale demonstrator of the smart water systems.

The first step of transformation was to build a Geographic Information System (GIS) model of the water network. A GIS is a computer-based tool that collects and combines all type of information based on geographic location in order to provide a new spatial framework. GIS is widely used in various fields such as urban planning, environment and management of different networks. In general, a GIS model includes four subsystems:

- Geographic data (pipe environment, soil characteristics, geology…).
- Database-management system for archiving, organization and access of data.
- Spatial analysis for processing and exploitation of geographical data subsystem.
- A system for reporting the results either as a graphic map display or as lists and tables.

GIS allows a fine representation of water distribution networks. The water network is represented by a map consisting of lines corresponding to pipes and nodes matching either the water supply points or the connections between the pipelines and the hydraulic elements or the water meters (Khomsi et al., 1996)

The second step is to instrument the water network by smart sensors. The water consumption, the pressures and flows values can be transferred through the communication channels to the GIS system.

GIS networks are used to illustrate the main operations data such as leaks, repairs and inspections for a decision-making, a future assessing pipe/facility conditions and prioritizing capital improvement projects (Grise et al., 2001).

2.2. Built assets

The Scientific Campus was inaugurated in 1967. It is located in Villeneuve d'Ascq in the suburbs of Lille, and covers an area of 1.1 km^2. Nowadays, the campus includes 150 buildings aged from 1 to 50 years with a total construction area of 325000 m^2. They are divided into 10 domains:

- University of Lille: 95 buildings including scientific faculties, engineering schools, administrative, service buildings and the institute IUT.
- CROUS ('Centre Régional des Œuvres Universitaires et Scolaires'): 35 buildings.
- ECL ('Ecole Centrale de Lille): 15 buildings including 6 buildings for the residence Leonardo De Vinci
- ENSCL ('Ecole Nationale Supérieure de Chimie de Lille'): 1 building.
- Meteo France: 1 building.
- CNED ('Centre National d'Enseignement à Distance'): 1 building.
- Telecom Lille: 2 buildings.

In addition to these 8 domains, the company "BONDUELLE" and the polyclinic "4Cantons" are located in the campus.

Figure 2.1 illustrates the GIS map of the campus. Buildings are regrouped by their appropriate domains.

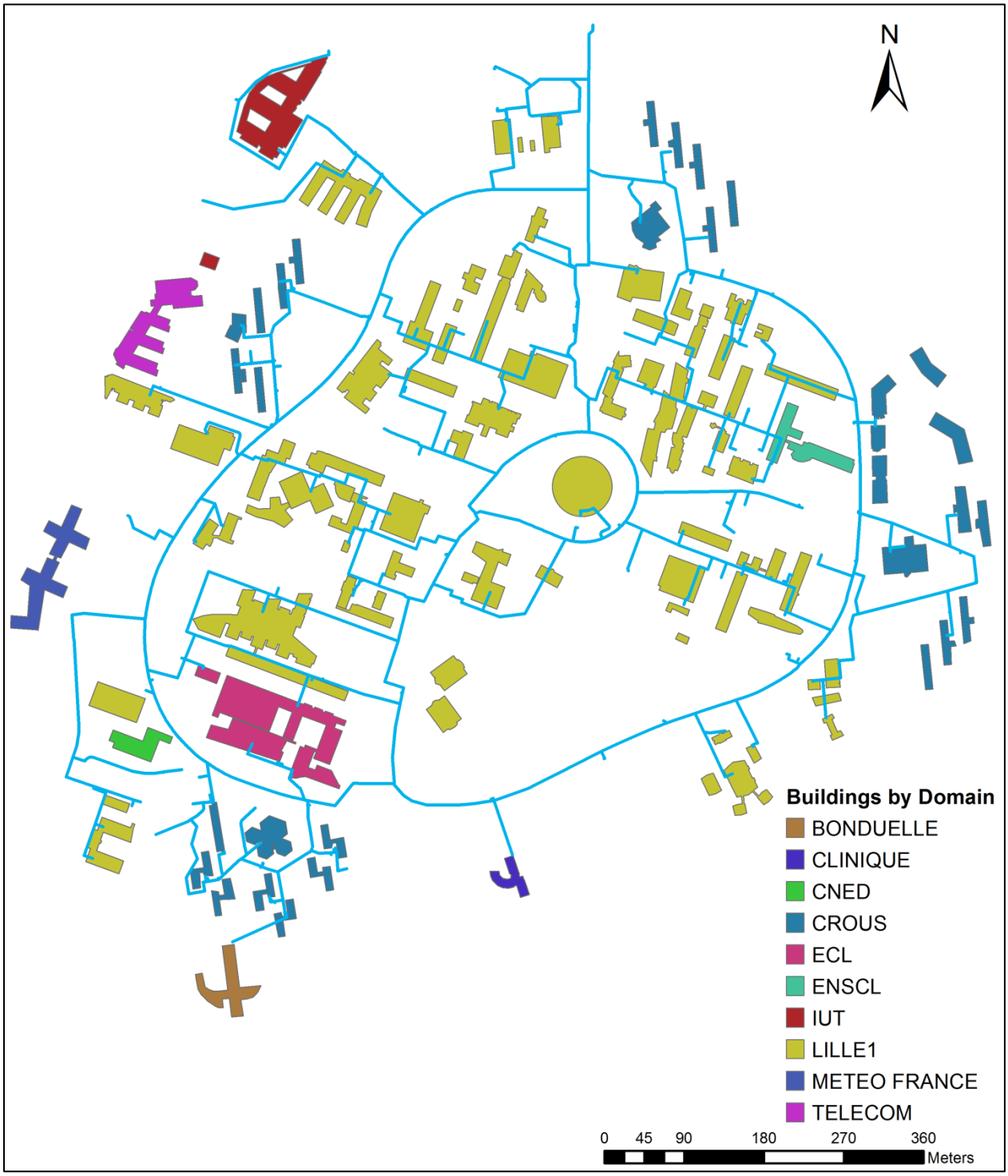

Figure 2.1: Geographic distribution of the demo site buildings according their domains

2.3. Water network

2.3.1. Pipes

The pipes of the water network are in majority made in gray cast iron (see Table 2.1). The pipes diameter varies from 20 to 300 mm as shown in Figure 2.2. The pipes with large diameters are in ductile iron. The length of the water network is equal to approximately 15 km divided into 13.5 km for the Campus (private sector) and 1.5 km for the public sector (owner Eaux Du Nord) as shown in Figure 2.3. The pipes are defined in the GIS model by the length, diameter, material, roughness and the emplacement zones. The pipes are buried under the roads or under vegetated lands. A part of the pipeline network is located in technical galleries that link some buildings in the campus. A significant portion of the water network is old (around 60 years old). Pipes are weakened by the corrosion that leads to bursts and unwanted leakage. The leak incidents that occurred previously in the demo site are referenced in the GIS model by the date and localization as shown in Figure 2.5.

Table 2.1: Pipes material

Material	**Length (m)**	**Percentage (%)**
Cast Iron	13344.640	90.2
Ductile	1160.340	7.9
PVC	283.650	1.9
Total	**14788.630**	**100**

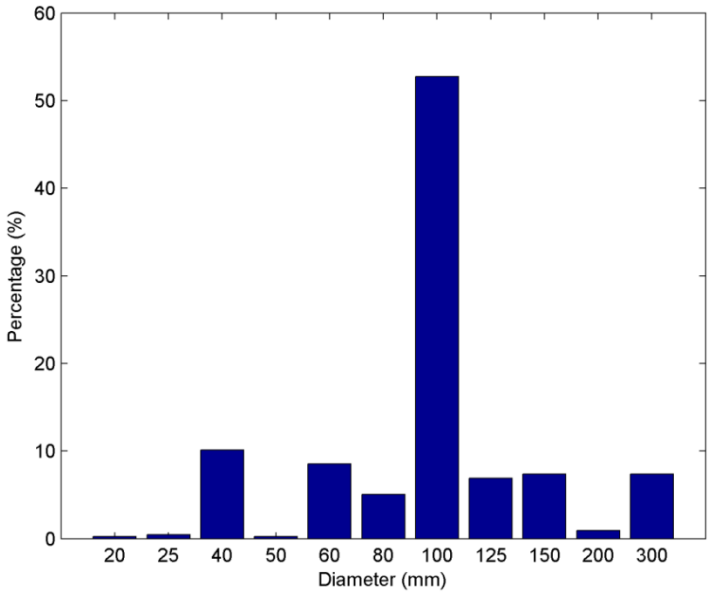

Figure 2.2: Pipes distribution in function of the diameter

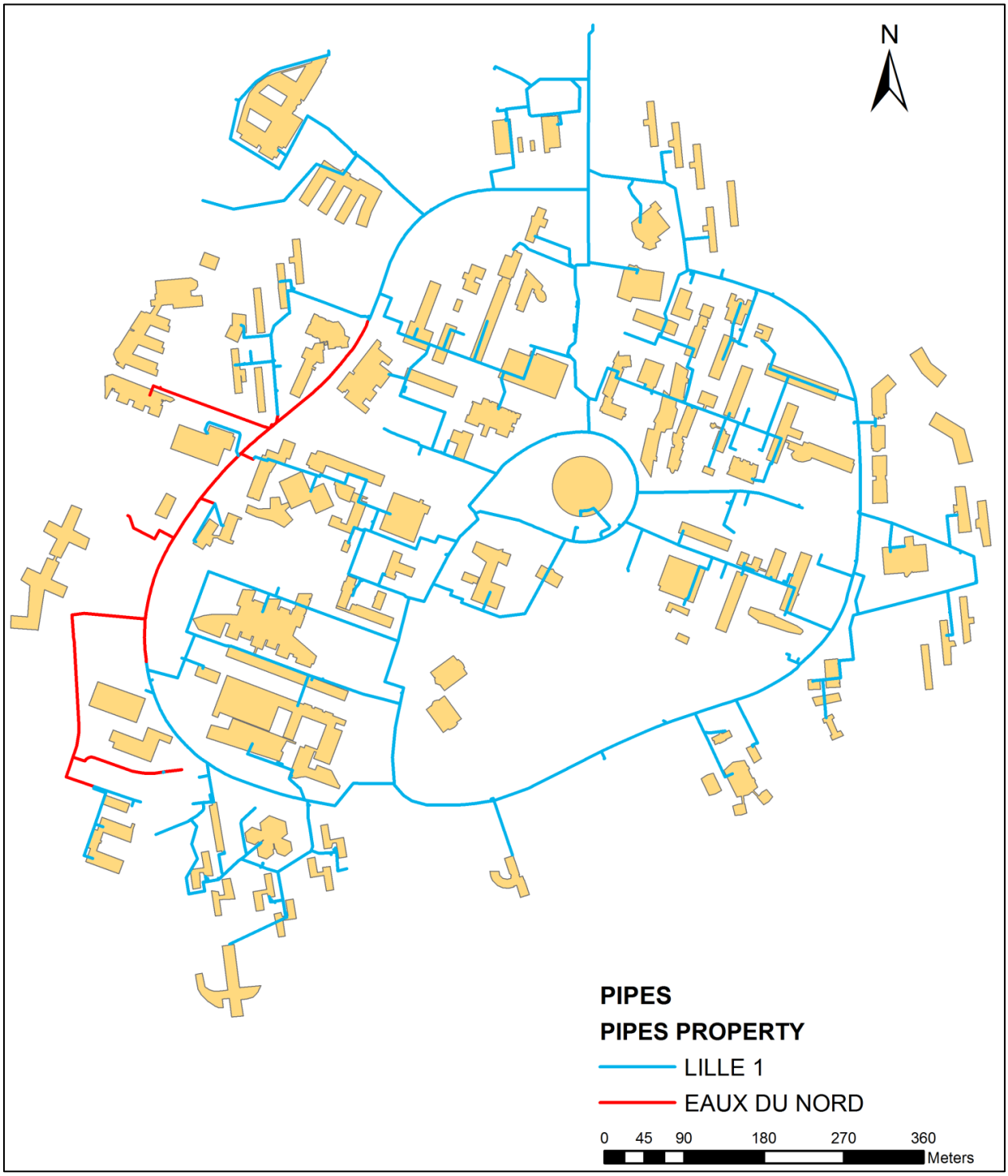

Figure 2.3: Pipes distribution according to their properties

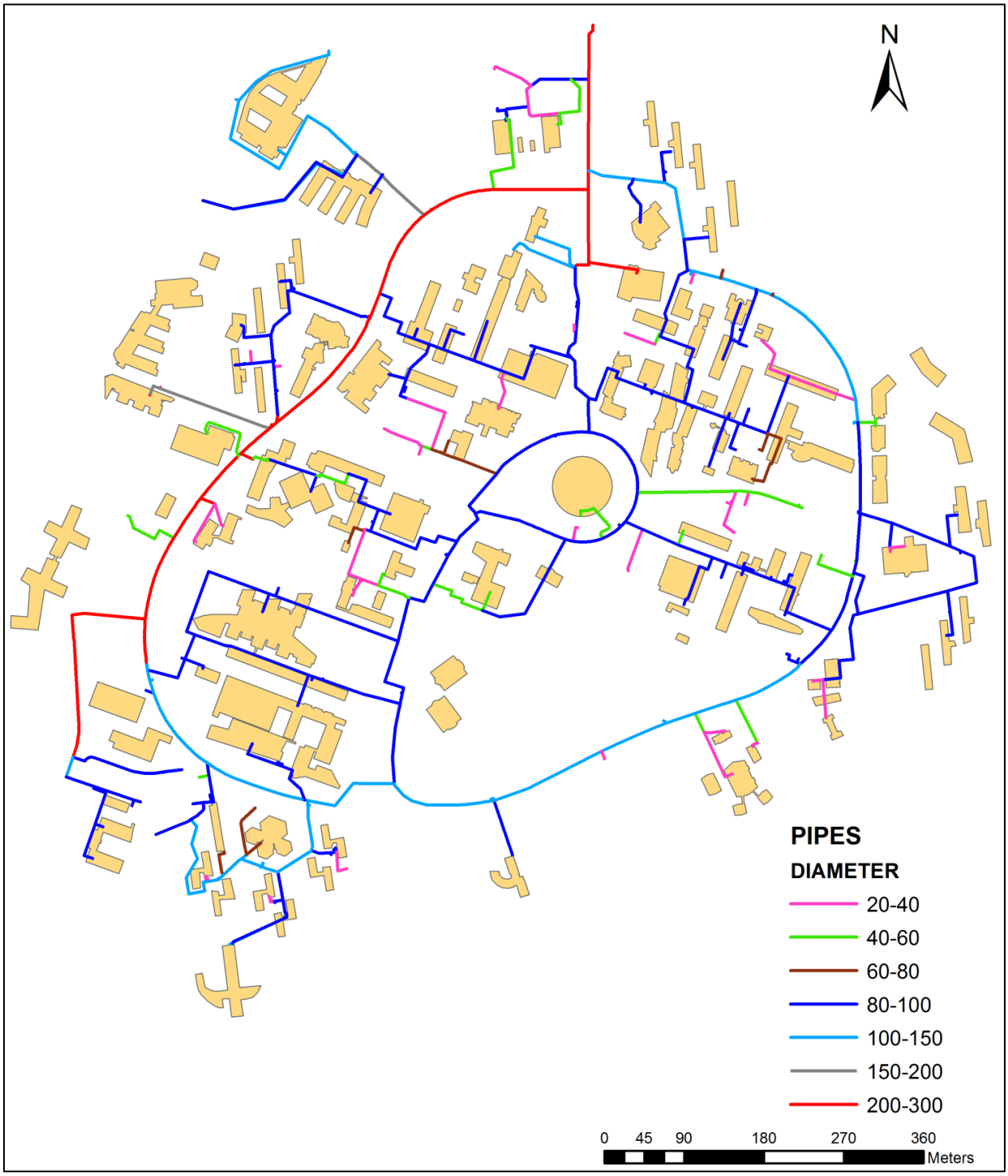

Figure 2.4: Pipes distribution according to the diameter

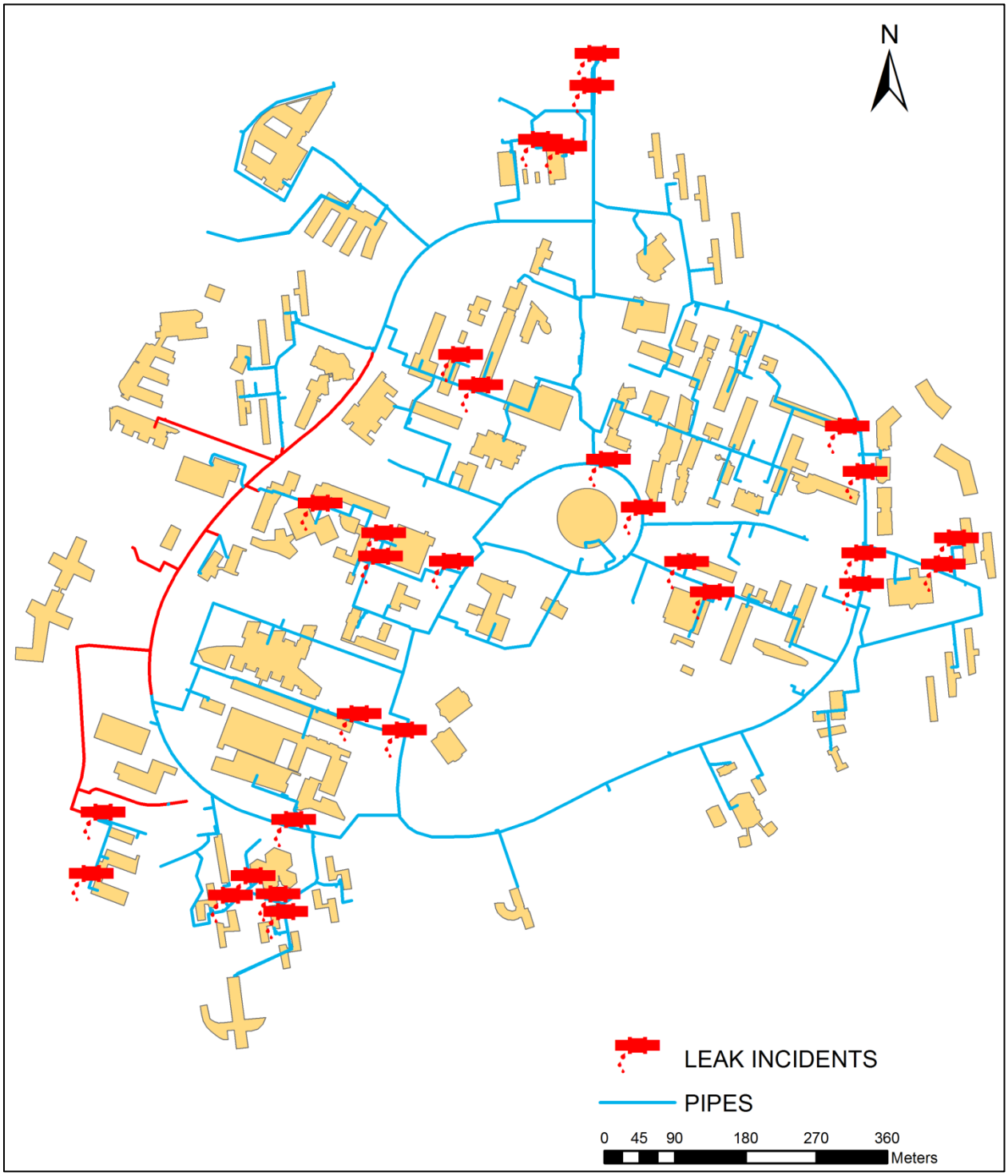

Figure 2.5: Leaks incidents in the campus between 2011 and 2015

2.3.2. Hydrants

The demo site includes 49 hydrants. Each year, a set of flow-pressure tests are conducted to verify the compliance of the fire hydrants. According to the standard NF 61.213, the nominal flow at the level of the fire hydrants of 100 and 150 mm has to be equal or higher than 60 m^3/h under a pressure of 1 bar. The dynamic pressure must be equal or exceed 1 bar. The results of the tests from 2011 are tabulated and integrated in the GIS model. Each hydrant is linked to its appropriate test result as shown in Figure 2.6. The fire hydrants in the campus are successively renovated and placed underground offering a high level of safety and preventing the water theft (see Figure 2.7).

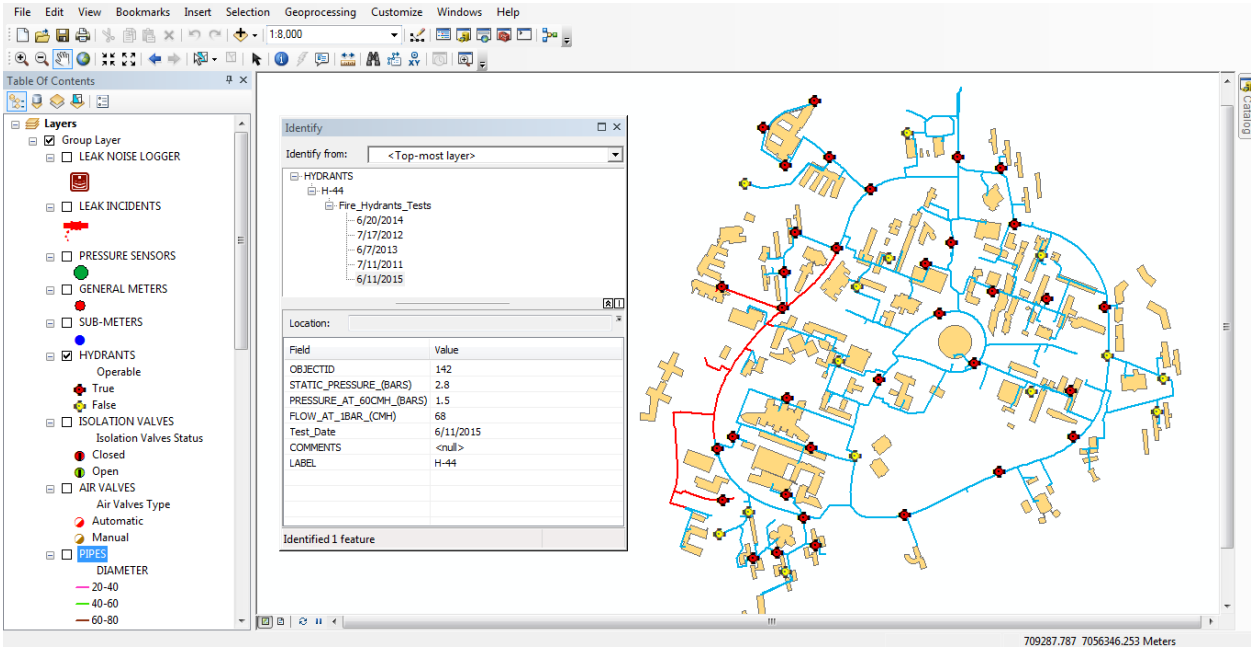

Figure 2.6: Attributes for hydrant H44 including the compliance tests results

Figure 2.7: Hydrant before and after replacement

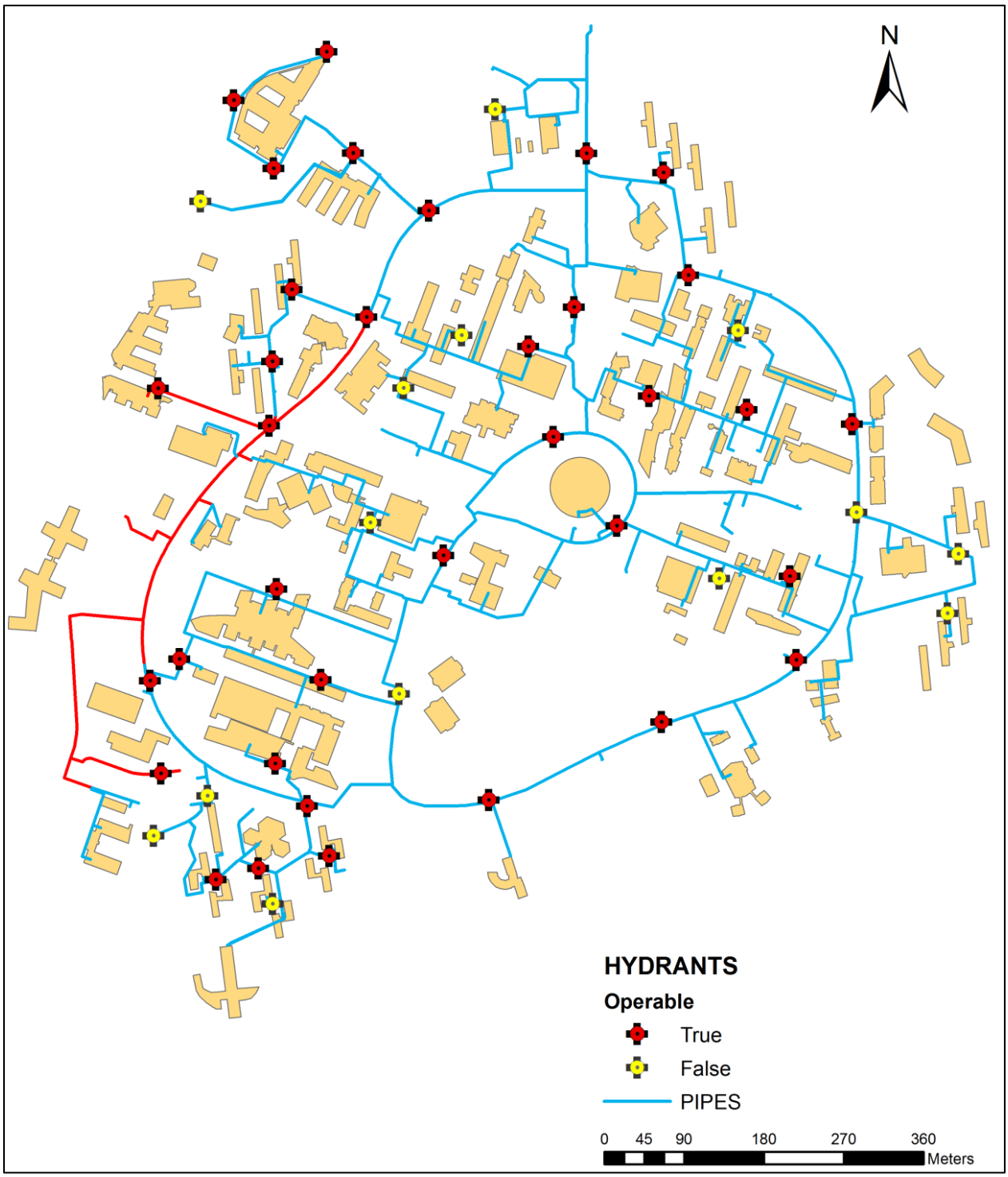

Figure 2.8: Hydrants distribution in the campus with the operation status in 2015

2.3.3. Valves

The water distribution network of the campus includes about 250 isolation valves. The majority of these valves are so old, corroded and some of them suffer from leaks. All the valves, with the collaboration of the "Eaux du Nord" water utility, have been checked during a procedure that took more than 6 months covering all the campus. The valves already closed for anonymous reasons were opened. Nowadays, some of the valves are renovated and pulled up to be at the level of the ground. Figure 2.9 shows an old corroded valve and another new renovated valve in the demo site. In addition to the isolation valves, the network includes a set of manual and automatic air valves, which allow the release of the accumulated air that comes out of solution within a pressurized pipeline or admit air into the system when the internal pressure of the pipeline drops below atmospheric pressures. The valves are integrated in the GIS model by the coordinates, diameter, the reference pipe and the status (open or closed). The distribution of the valves in the demo site is shown in Figure 2.10.

Figure 2.9: Valves in the demo site

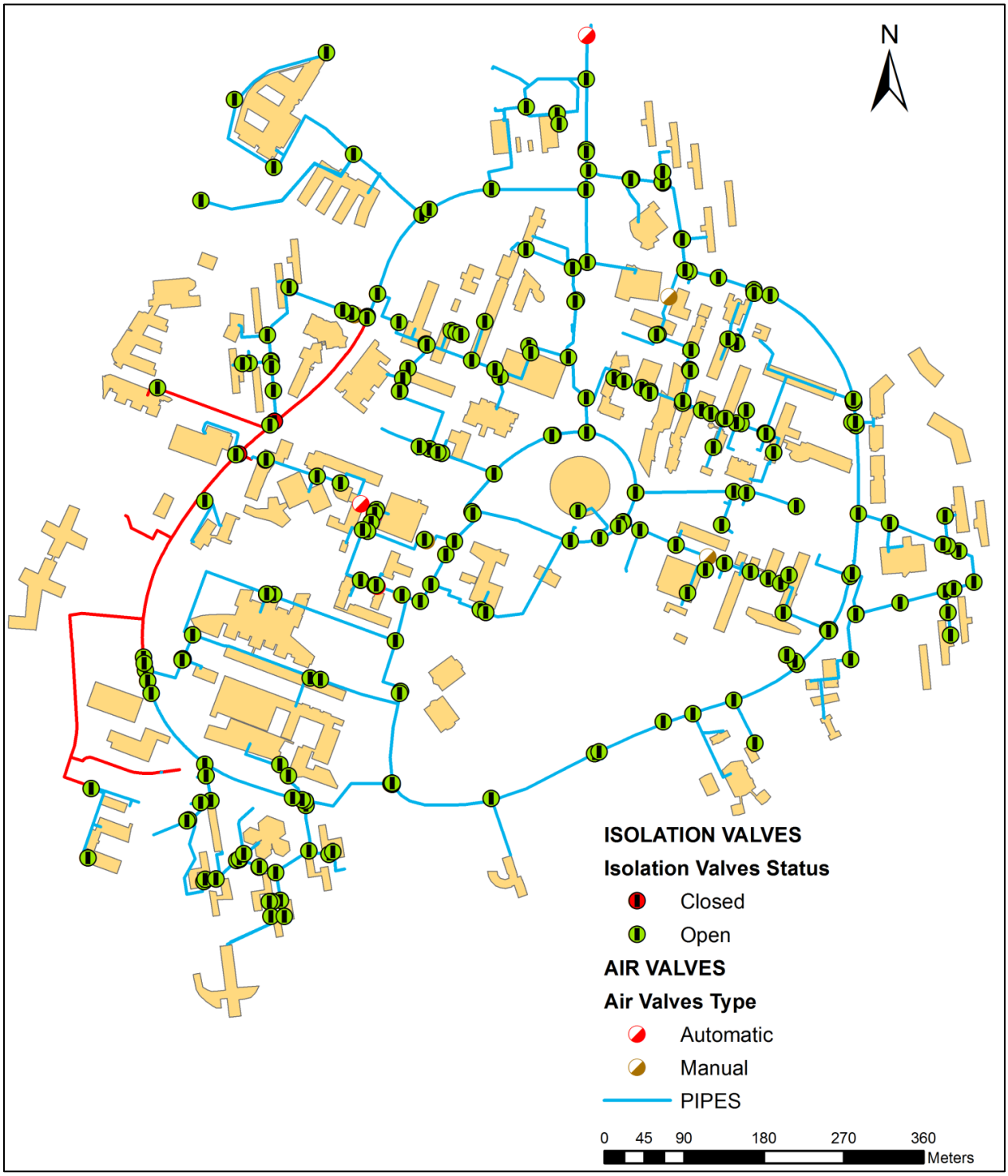

Figure 2.10: Distribution of isolation valves and air valves

2.4. Instrumentation

2.4.1. Automatic Meter Readers (AMRs)

The water distribution network is monitored by 93 Automatic Meters Readers (AMRs) to measure the water consumption hourly. They allow detecting abnormal consumption related to leakage or abnormal use.

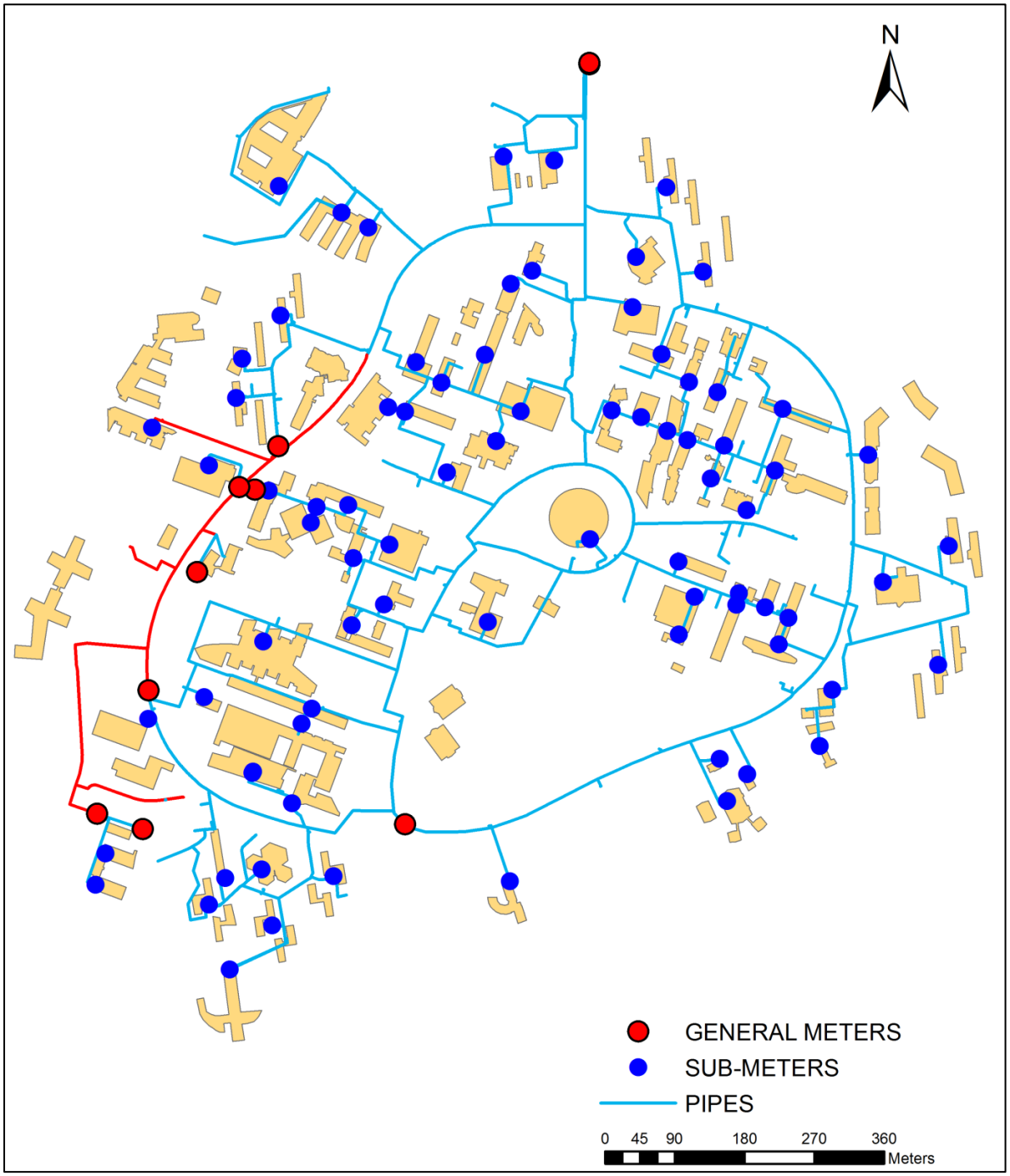

Figure 2.11: Distribution of the general and sub-meters in the demo site

The 93 AMRs are integrated in the GIS model (Figure 2.11) by their IDs, coordinates, meter number and associate sensor serial number and the building reference as well as a photo of the AMR (Appendix A).

The water supply of the campus is determined from 13 general meters regrouped as follows (Table 2.2):

- The first group includes 4 AMRs entitled 4CANTONS, ECL, BACHELARD, M5 and the regrouping of 5 AMRs CITE SCIENTIFIQUE: looped network.
- The second group comprises 4 AMRs entitled CUEEP, DELTEC_ICARE, HALL_VALLIN, and LML: branched network (disconnected part).

Table 2.2: General meters

Sites		**ID**	
General Meters	Looped network	CITE SCIENTIFIQUE	CITE_1
			CITE_2
			CITE_3
			CITE_4
			CITE_5
		BACHELARD	
		M5	
		ECL	
		4CANTONS	
	Branched	CUEEP	
		DELTEC_ICARE	
		HALL_VALLIN	
		LML (M6)	

The consumption of the main buildings is measured by 80 AMRs distributed as follows:

- University of Lille (55)
- Reeflex (2)
- CROUS (Centre régional des œuvres universitaires et scolaires) (14)
- "Ecole Nationale Supérieure de Chimie de Lille" (ENSCL) (1)
- "Ecole Centrale de Lille" (ECL) (6)
- "Bonduelle" company and the Clinic "4Cantons" (2)

Table 2.3 describes these AMRs with their IDs, the area of the associated building, the usage type and the year of construction of the building.

Table 2.3: Sub-meters IDs and distribution according to the sites and sectors

Sites and Sectors		ID		Area (m^2)	Usage type of the associated building	Year of construction
Lille 1	Mathematics	M1		6100	Research	1966
		M2		3629	Teaching and Research	1966/1994
		M3	M3	7029	Teaching and Research	1966/2004
			M3_LIFL			
		M4_CRI		2830	Service (Computer Center)	1966/2010
		M5		2973	Teaching	1993
	Physics	P1		9642	Teaching	1966
		P2		4447	Teaching and Research	1966
		P3		5860	Research	1966
		P4		3230	Teaching and Research	1966
		P5		9245	Research	1966/1999
		P5_BIS (CERLA)		1327	Research	1998
	Chemistry	C1		3308	Teaching	1966
		C3		2889	Research	1966
		C4		2396	Research	1966
		C5		3540	Teaching and Research	1966
		C6		5077	Teaching and Research	1966
		C8		2939	Teaching and Research	1966
		C9		4526	Research	1966/1995
		C11		1098	Research	1966/2000
		TP_C16		785	Teaching	1996
	Biology	SN1		8813	Teaching	1966
		SN1_SERRES		838	Research	1990
		SN2		4261	Research	1966
		SN3		5072	Research	1966
		SN4		2223	Research	1966
		SN5		5145	Teaching and Research	1966
		SN6		415	Research	1996
	Social Science	SH1		2392	Teaching	1988
		SH2		3917	Teaching and Research	1996
		SH3		7454	Teaching	2003
		UFR_GEOGRAPHIE		2677	Teaching and Research	1996
	Sport	COSEC		2375	Sport	1975
		COSEC_ADMIN		374	Administration	1975
		CLUBHOUSE		393	Sport	1994
		GREMEAUX		2410	Sport	1994

		V2		598	Sport	1975
		VALLIN		2589	Sport	1994
	Engineering Schools	Polytech	EPU_A_B_C	28092	Teaching and Research	1970/1997
			EPU_D			
			EPU_D_ECL			
	Institutes	IUT		19836	Teaching	1972/2004
		B5		3492	Teaching	1993
		B6		3492	Teaching	1993
		B8_CUEEP		3461	Teaching	1995
	Administration	A3		5835	Administration	1966/1992
		A7_PCET		1276	Administration	1996
		SUDES		1550	Administration	1996
		SUPSUAIO		6430	Administration and Teaching	2004
	Service	A1		1585	Service (Heating Center)	1966
		A2		928	Service	1966
		A10		751	Service (Health Center)	2000
		A16 (CAS 2)		312	Service	2006
		BU (Learning Center)		9009	Service (Library)	1966/2017
		ESPACE_CULTURE		1565	Service	2002
		MDE		650	Service	2007
Reeflex		REEFLEX		13644	Residence	2015
		CRECHE_REEFLEX		592	Service (Nursery)	2015
CROUS	Students' Residence	Bachelard	L	12751	Residence	1966
			N			
			PYTHAGORE			
		Boucher	G	12388	Residence	1996
			J			
		Camus	R	19065	Residence	1966/Under renovation
			S			
			U			
			W			
		Galois	A_B	12844	Residence	1966/Under renovation
			D_C			
	Restaurant	BARROIS		1827	Restaurant	2004
		PARISELLE		3784	Restaurant	1966
		SULLY		3497	Restaurant	1966

ENSCL		C7 (Chemistry)	8500	Teaching and Research	1964/2002
Ecole Centrale	Engineering Schools	ECL	ECL_C	17306	Teaching and Research	1966
			ECL_FOSSE			
			FONDERIE			
			INCENDIE			
		C_D_DEVINCI		5492	Students Residence (L.Devinci)	1996
Others		BONDUELLE		-	Service (Company)	-
		CLINIQUE		1053	Service (Health Center)	1966

2.4.2. Telemetry system

The Automatic Meter Reading technology is used for the remote reading of water consumption. This technology consists of collecting automatically consumption data and their transfer to a central server. The AMR system consists of low-power radio transmitters. Each water meter has an impulse sensor and a VHF radio transmitter. The index of the water consumption is read by the impulse sensor that converts it to an electronic index. The impulse counter is connected to a microcontroller unit to store the cumulative readings for transmission. The readings are then transmitted via a radio frequency (169 MHz) to the collectors or the base stations. The radio receivers are installed on 4 buildings: M1, P5, C7 and Residence Camus as shown in Figure 2.13. These receivers gather all the indexes transmitted within a maximum range of 300 meters in urban area. The base stations send data via the mobile network to a central information system with 4 signals per day of $1/10^{th}$ of a second. The telemetry principle of the AMRs is described in Figure 2.12.

Figure 2.12: Telemetry architecture to remote water meter readings

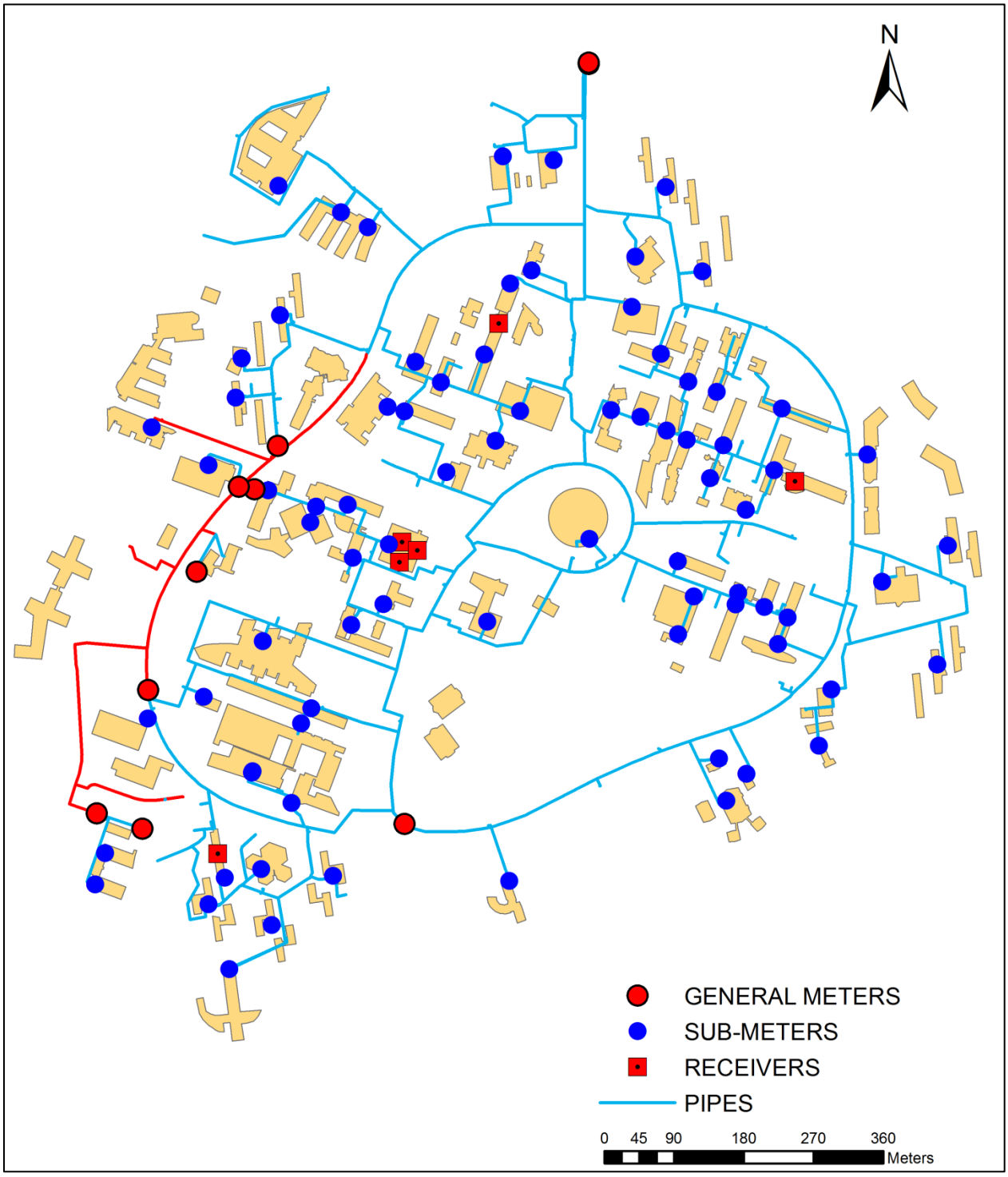

Figure 2.13: Distribution of the receivers in the campus

2.4.2.1. Transmitters

The water network of the Campus is equipped by two types of transmitters: compact transmitters and regular (deported) transmitters.

- Compact transmitters

Figure 2.14: Compact transmitter (Itron)

These transmitters include a built-in sensor (Cyble LRF VHF=169 MHz) to get the index of the water meter through a pulse output. The compact transmitters are reliable and are easily placed without any wires. Table 2.4 describes the radio frequency features for the compact transmitter, while Figure 2.15 shows a compact transmitter installed in the meter in the building C of the engineering school "Ecole Centrale de Lille".

Table 2.4: Technical characteristics for the compact VHF transmitter ITRON CYBLE LRF

Radio Frequency Features	
Protocol	Ondeo Systems (owner)
Modulation	Frequency Shift Keying (FSK)
Frequency carrier	169.44375 MHz (free frequency)
Transmission	1 way
Transmission frequency	2 to 4 times / 24 hours
Bandwidth	12.5 kHz
Radiated power	<100 mW, typical 50 mW

Figure 2.15: Compact transmitter installed on the water meter in the building C of the engineering school "Ecole Centrale de Lille"

- Deported transmitters

Deported transmitters as shown in Figure 2.16 are composed of a Cyble sensor V2 that is placed on a meter with a pulse output connected through a cable to a stand-alone transmitter to send the collected data to the base station. They are used in the basements where the radio signal is low. The sensor's electronic circuit includes 3 detector coils. Under flowing conditions, the target passes in front of each coil. The presence of the target is detected by a variation of the signal within the coil, due to an eddy current effect. The use of 3 coils ensures that the direction of rotation of the needle and therefore the forward and return directions of the water flow are identified. These transmitters have an internal battery life of 12 years.

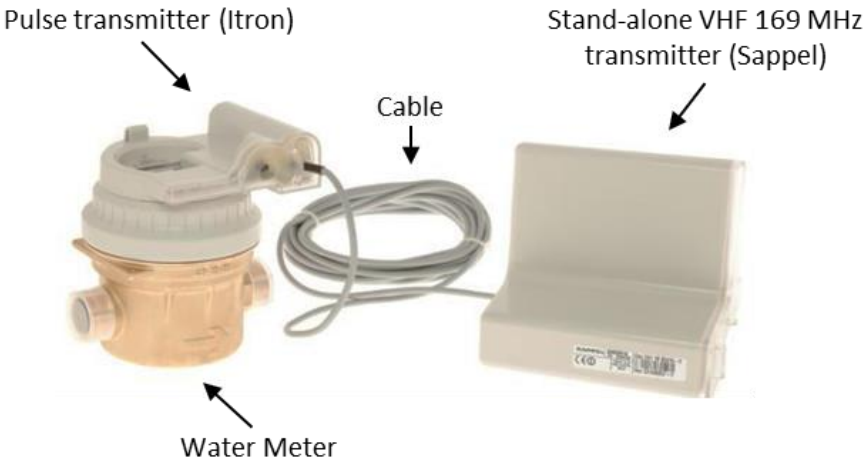

Figure 2.16: Deported transmitter

Table 2.5 describes the radio frequency features for the stand-alone VHF transmitter, while Figure 2.17 shows a deported transmitter installed in the building SN5.

Table 2.5: Technical characteristics for the stand-alone VHF transmitter 169 MHz (Sappel)

Radio Frequency Features	
Frequency carrier	169.44375 MHz (free frequency)
Bandwidth	12.5 kHz
Radiated power	100 mW
Transmission interval	120 ms

Figure 2.17: Deported transmitter installed in the SN5 building

2.4.2.2. Collectors (receivers)

Collectors are used to gather the data sent by the transmitters through at a radio frequency of 169 MHz. The receivers are placed on the roof of 4 buildings in order to cover all the campus. These buildings are: M1, P5, R (CAMUS) and C7. The technical characteristics of the VHF receivers installed in the campus are described in Table 2.6. Figure 2.18 shows the base station on the roof of building C7. It consists of an antenna, a VHF card and a collector.

Table 2.6: Technical characteristics for the VHF receiver 169 MHz

Frequency	169 MHz
Protocol	Ondeo Systems (owner)
Frequency modulation	Frequency Shift Keying (FSK)
Standard	EN 300 220
Operating temperature range	-15°C / +55°C
Storage temperature range	-30°C / +70°C
Protection rating	IP54
Diode	Diode indicating the reception of the bit frames

Figure 2.18: Base station on the roof of C7 building

2.4.2.3. Example of flow measurement

Figure 2.19 shows an example of water consumption over a week measured by the general meter 4 CANTONS. It shows that the water consumption decreases during the weekend; the minimum consumption occurs between 2 am and 4 am. We observe 2 peaks: at noon and at 8 pm.

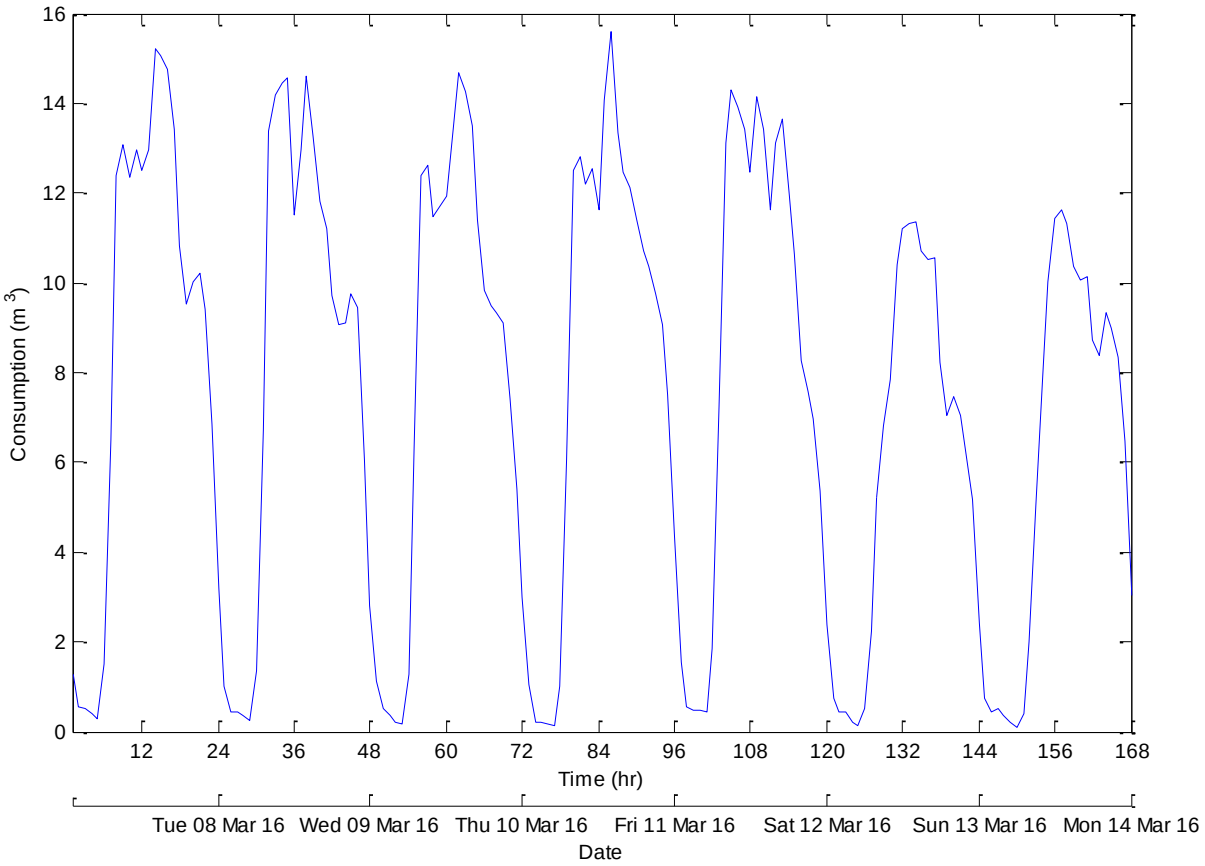

Figure 2.19: Water consumption profile over a week for a general meter (4CANTONS)

2.4.3. Pressure sensors

A set of 5 piezoresistive pressure sensors is installed in the campus covering the major campus zones. Each sensor measures the water pressure. It connects to a standard thread and delivers a signal proportional to the pressure in the pipe. The sensor is attached to a data logger used to remote the pressure values measured each 15 minutes. Based on a high-performance internal antenna, the data loggers send their gathered data via SMS at user-definable periods (every 8 hours in our case).

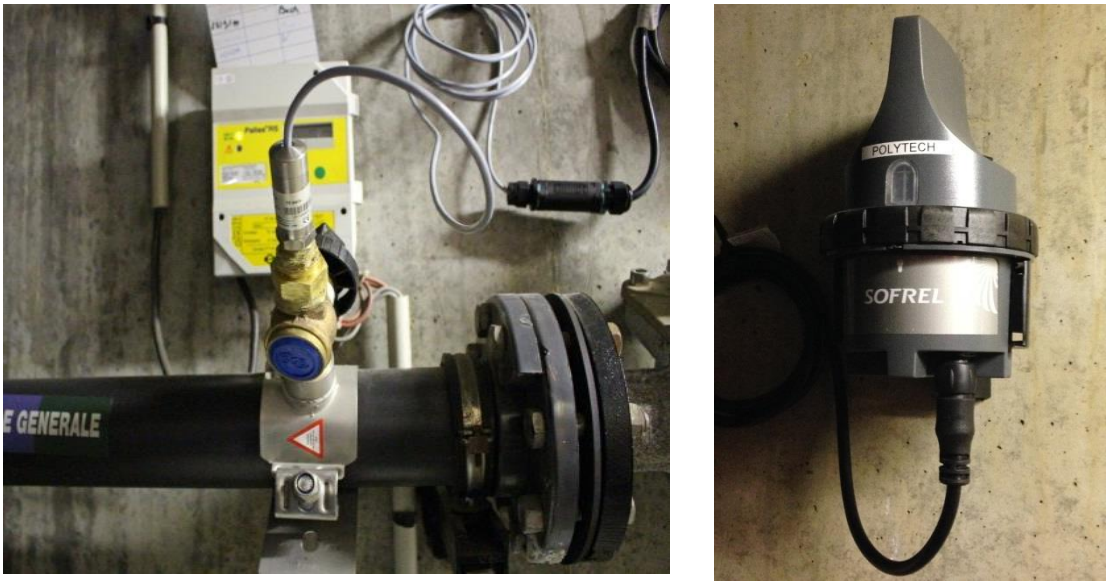

Figure 2.20: Pressure sensor installed in Polytech'Lille with its appropriate data logger

Table 2.7 and Table 2.8 describe the technical characteristics of the SOFREL pressure sensor and the LS42 data logger, respectively.

Table 2.7: Technical characteristics for the SOFREL CNP_R piezoresistive pressure sensor

Wiring	4-20 mA output 2 wires
Power supply	7 to 30 VDC
Temperature range	-25°C to +85°C
Protection	PVC cable with capillary tube, protected against water infiltration (IP68) - Integrated over-voltage protection
Precision	< +/-0.35% FSO according to IEC 60770
Pressure resistance	60 bars for the 16 bar model

Table 2.8: Technical characteristics of the data logger SOFFREL LS42

Presentation	IP68 water tightness
	LED-based operator dialog
	Connection cable with “military” grade connectors (2 m)
Power supply	User-changeable lithium battery (~5 years)
Communication	Built-in dual band antenna
	Built-in GSM/GPRS modem
	Transmission of alert SMS messages to a mobile phone
	On-site connection to logger via Bluetooth

The pressure sensors are integrated in the GIS model by their coordinated, associated building and a photo of the sensor. The map of the pressure sensors is illustrated in Figure 2.21.

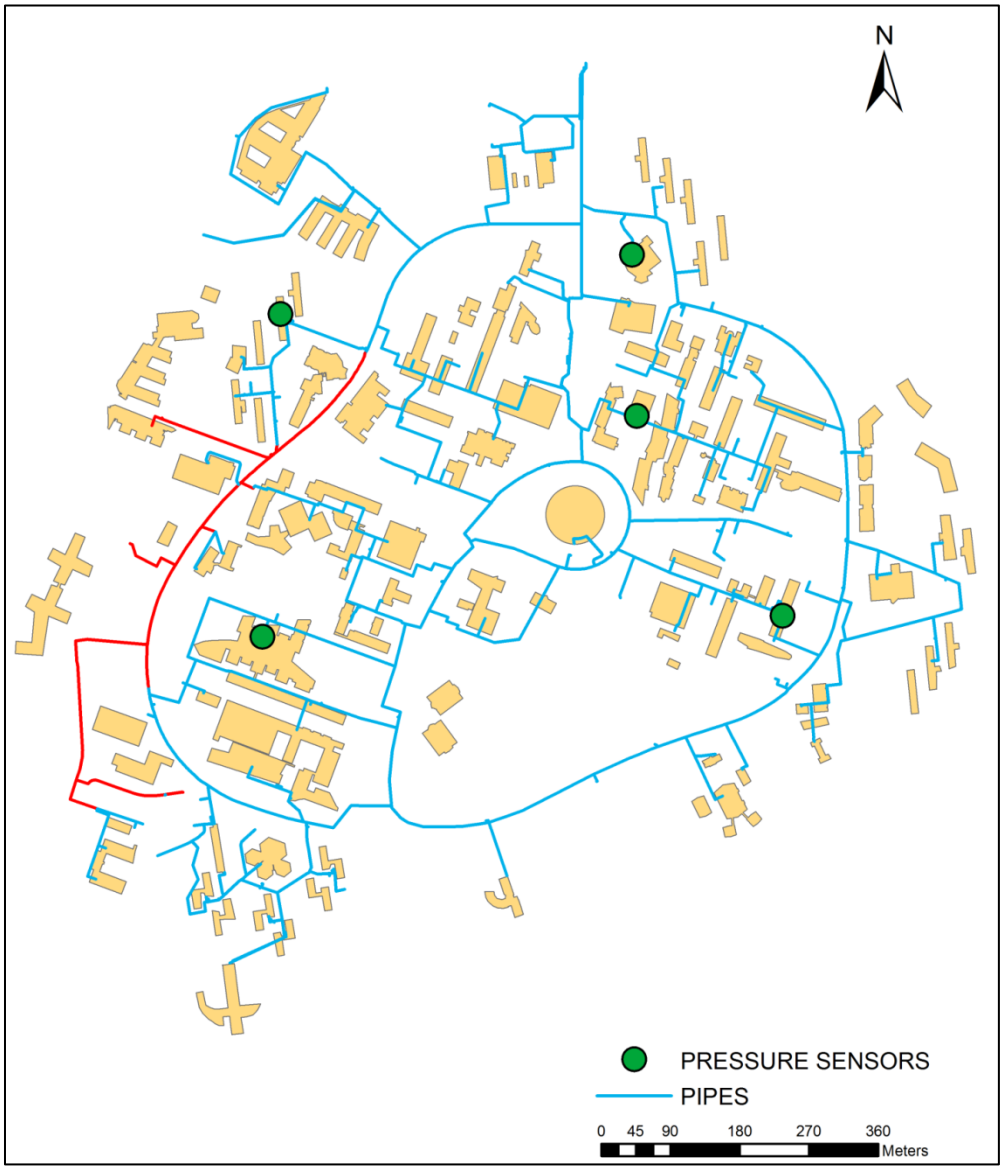

Figure 2.21: Distribution of the pressure sensors in the demo site

2.4.3.1. Example of pressure measurement

Figure 2.22 illustrates an example of measurement of the pressure in building C1. The pressure has an average value of 3 bars. A pressure drop of 0.4 bars occurs between 10 a.m. and 6 p.m. which can be explained by the significant water consumption during this period. It is also remarkable that the pressure increases in the weekend when the water consumption is low.

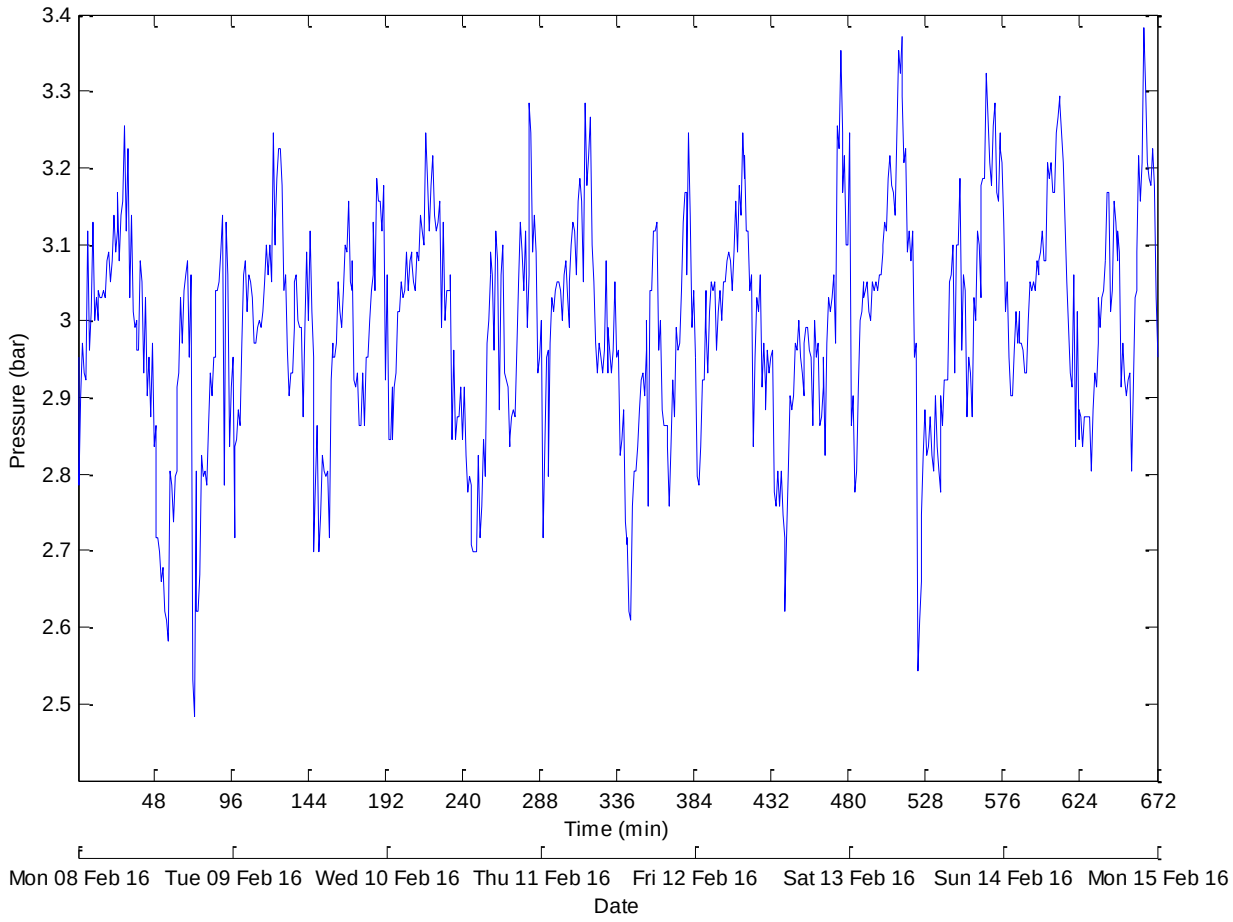

Figure 2.22: Pressure values measured each 15 min over a week in C1 building

2.4.4. Noise logger – EAR system

EAR (Early Alarm Recording) is a listening system enabling a permanent and reliable monitoring of the water network. The system, as shown in Figure 2.23 is composed of: i) hydrophone positioned into the fluid vein, which allows direct acquisition of noises in the pipe and ii) SEBA LOG HYDRO transmitter enabling the transmission of recorded data. The EAR system is installed on a 100 mm grey cast iron pipe, in a technical gallery in the Biology sector. The pipe is at a height of 220 cm from the ground.

The system is programmed to turn on between 2 am and 4 am and transform the acoustic vibrations into actionable information on the location of leaks. Data during the night aims at minimizing the interference with other noise sources, such as roads traffic or high daytime water

consumption sound. However, in the technical gallery, we detect the presence of a compressor that generates noise but we have verified that it is regularly cut when it reaches the nominal pressure in the reservoir.

The recorded values are collected between 2 pm and 5 pm using a computer equipped by a device that captures the radio signal (patrol mode).

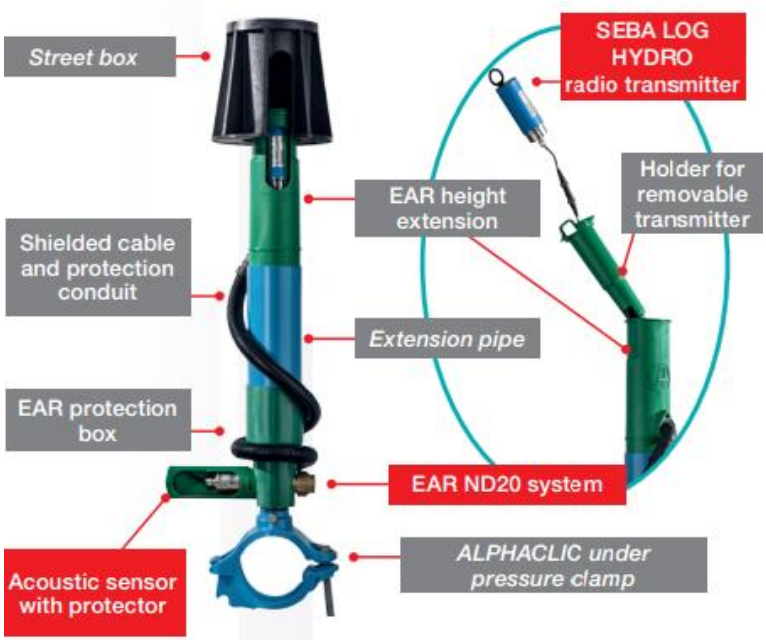

Figure 2.23: EAR system

Figure 2.24: Installation of EAR system in the demo site

2.4.4.1. Measurements

The noise level measured between 2 am and 4 am during Christmas holidays shows a minimum value of 36 dB with a frequency of 30 Hz (Table 2.9 and Appendix B). The minimum value of 36 dB is quite significant. It requires an investigation of the night water consumption in the buildings close to the EAR system located in the biology sector.

Table 2.9: Minimum noise level measured during Christmas holidays with the associated frequencies

Date	**Minimum noise level (dB)**	**Associated frequency (Hz)**
Wednesday 23/12/2015	36	30
Thursday 24/12/2015	37	40
Wednesday 25/12/2015	36	30
Saturday 26/12/2015	37	30
Sunday 27/12/2015	37	30
Monday 28/12/2015	37	40
Tuesday 29/12/2015	37	40
Wednesday 30/12/2015	37	30

The night water consumption between 2 am and 4 am of the biology sector is shown in Figure 2.25. Over these 2 hours, the water consumption is equal to 0.5 m^3 and reaches sometimes 1 m^3. This consumption is due to research facilities in the biology faculty.

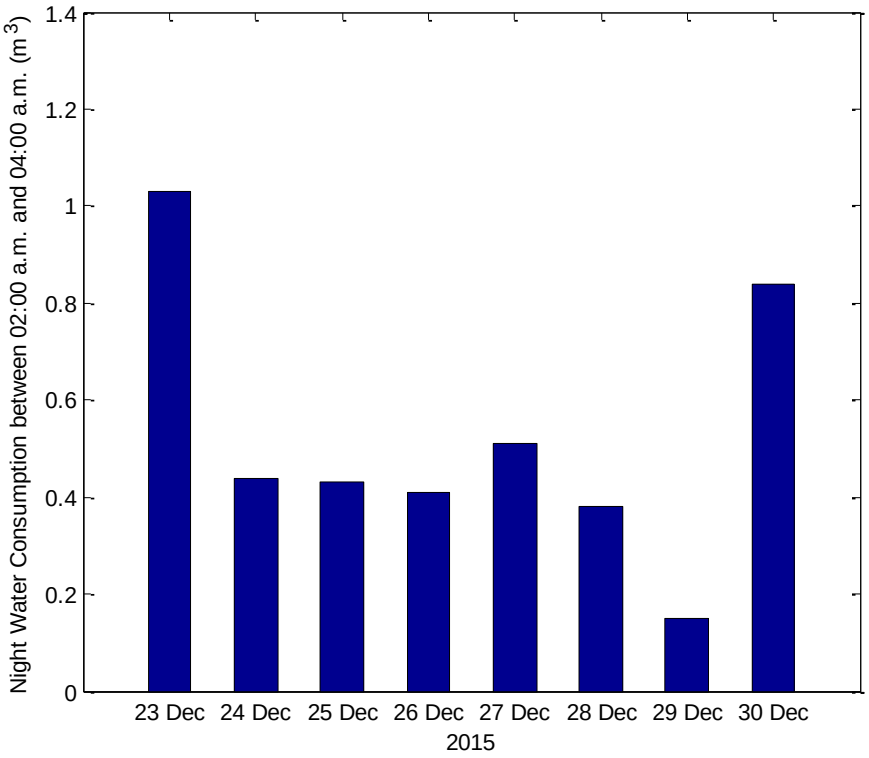

Figure 2.25: Night water consumption for the buildings in the biology sector

Figure 2.26 shows the measured noise levels registered December, 28, 2015 between 2 am and 4 am (minimum 37 dB), while Figure 2.27 shows the noise levels for the same at 2 pm (minimum 36 dB). The comparison between these two figures shows a clear difference in the frequency associated with the measured noise. Between 2 am and 4 am, the frequency of the

noise varies between 30 Hz and 40 Hz, while the frequency measured at 2:00 pm is equal to 50 Hz. However, there is not much difference between the noise levels measured during the day and during the early morning during this non-working day. It seems that the water consumption during the holidays does not influence as much the noise level. Therefore, in order to highlight the effect of the leakage on the noise level, a set of artificial leak simulations was conducted in the afternoon. Noting that, the surrounding noises from the traffic, which can affect the acoustic results, are limited during Christmas holidays.

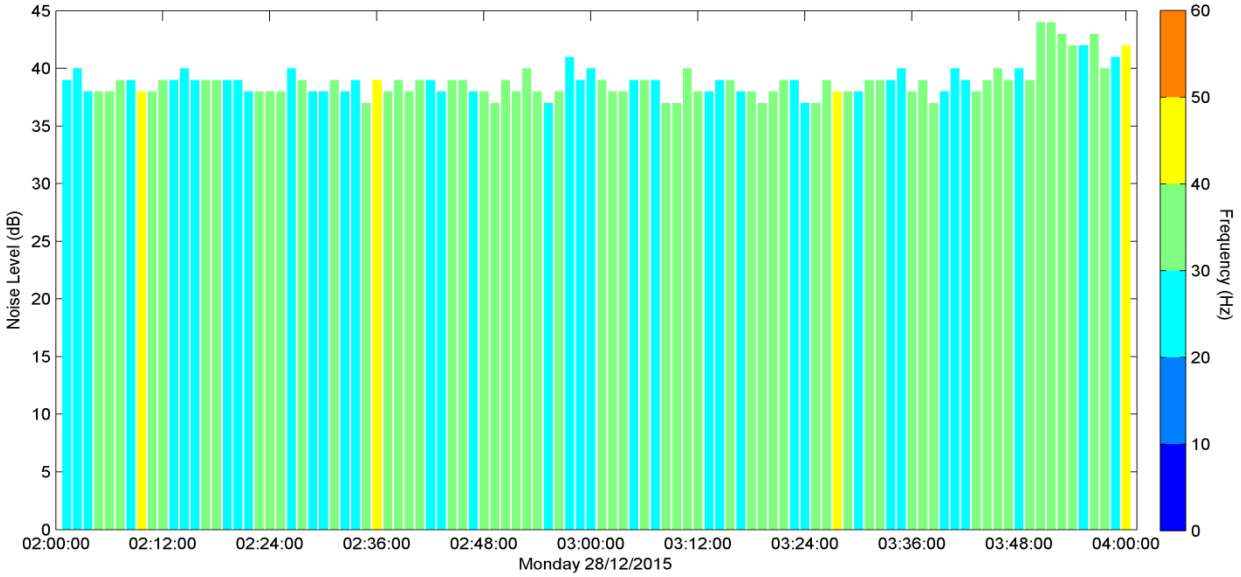

Figure 2.26: Noise level measured in the early morning of Monday 28/12/2015

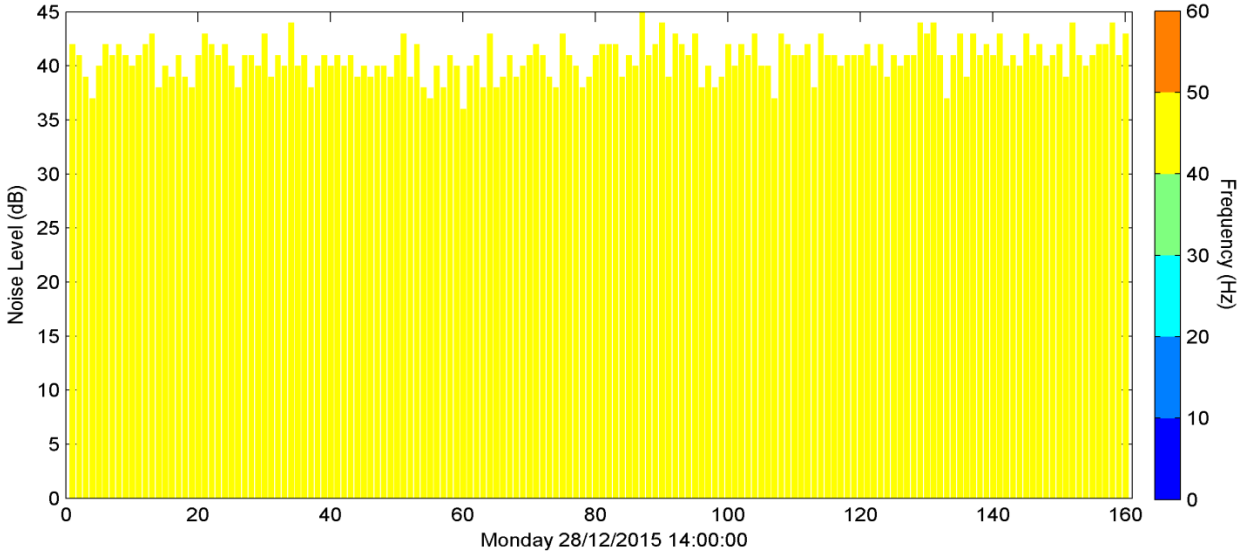

Figure 2.27: Noise level measured in real time starting from 2 p.m. on Monday 28/12/2015

2.4.4.2. Leak simulations

Several leaks were simulated using 4 hydrants. Figure 2.28 illustrates the position of the fire hydrants used to simulate a leak. The distance between hydrants and the acoustic device as well as the simulated leakage rates are described in Table 2.10.

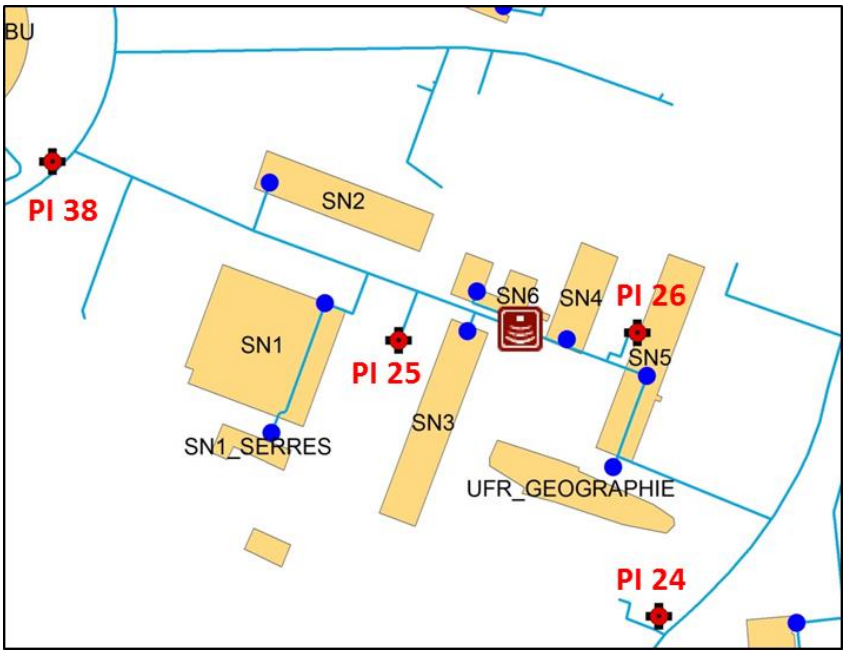

Figure 2.28: The position of the hydrants compared to the location of EAR system

Table 2.10: Distance between the fire hydrants and the EAR system and the rates of the simulated leaks

Hydrant N°	Distance from the EAR system (m)	Rates of simulated leaks (l/s)
26	56	0.30; 0.45; 0.80; 5
25	62	
38	190	
24	195	

Figure 2.29: Simulated leaks using the fire hydrants

2.4.4.3. Results

The results of the leaks' simulations for different flow rates are extracted point by point following a video recording of the signal obtained in real time. The acoustic results after the leak simulation on hydrant N°26 are depicted in Table 2.11 and Figure 2.30. A trickle of water generates a noise level from 43 to 48 dB with a frequency of 50 Hz. However, a huge burst has a significant noise level around 54 dB with an associated frequency that reaches 250 Hz.

Table 2.11: Results following the simulated leaks using hydrant N°26

Leak rate (l/s)	Noise level (dB)	Frequency (Hz)
0	37 to 41	50
0.30	43 to 48	50
0.45	50 to 52	50 – 100
0.80	51 to 53	50 – 100 – 250
5	54	100 – 150 – 250

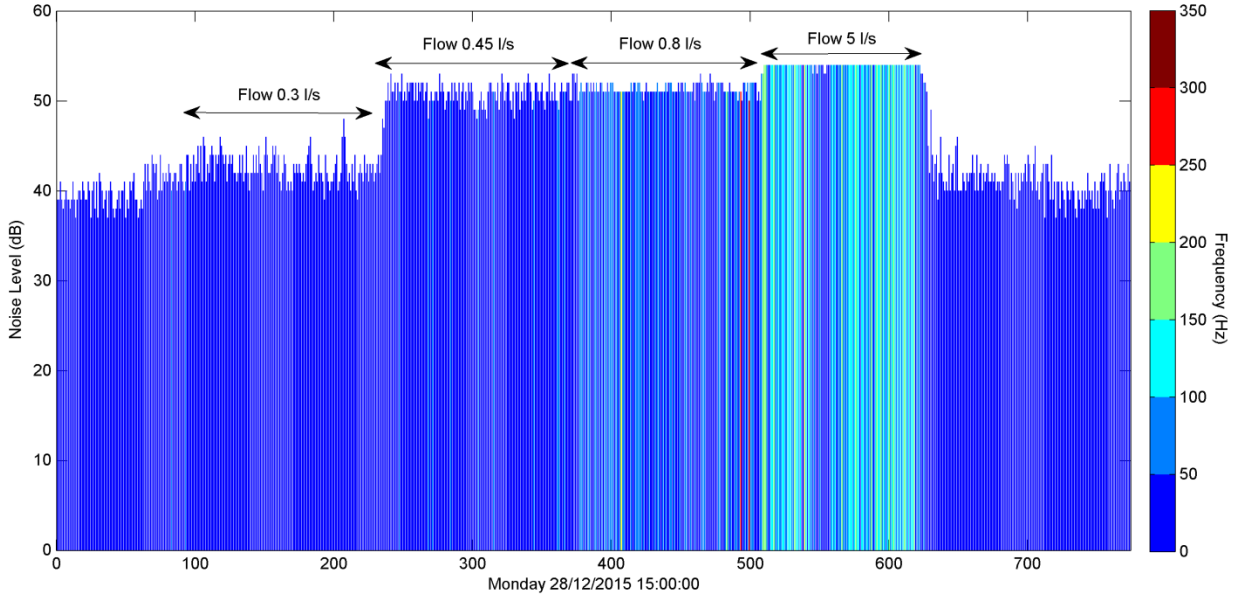

Figure 2.30: Leak noise levels following simulated leaks on hydrant N°26 (56 m distant from EAR)

For a fire hydrant a little bit further from the EAR system, the noise generated from a small leak of 0.3 l/s is damped by the baseline signal (Figure 2.31). Leaks with a flow rate of 0.45 l/s were able to be detected in this case where the hydrant is 62 m distant from the EAR system.

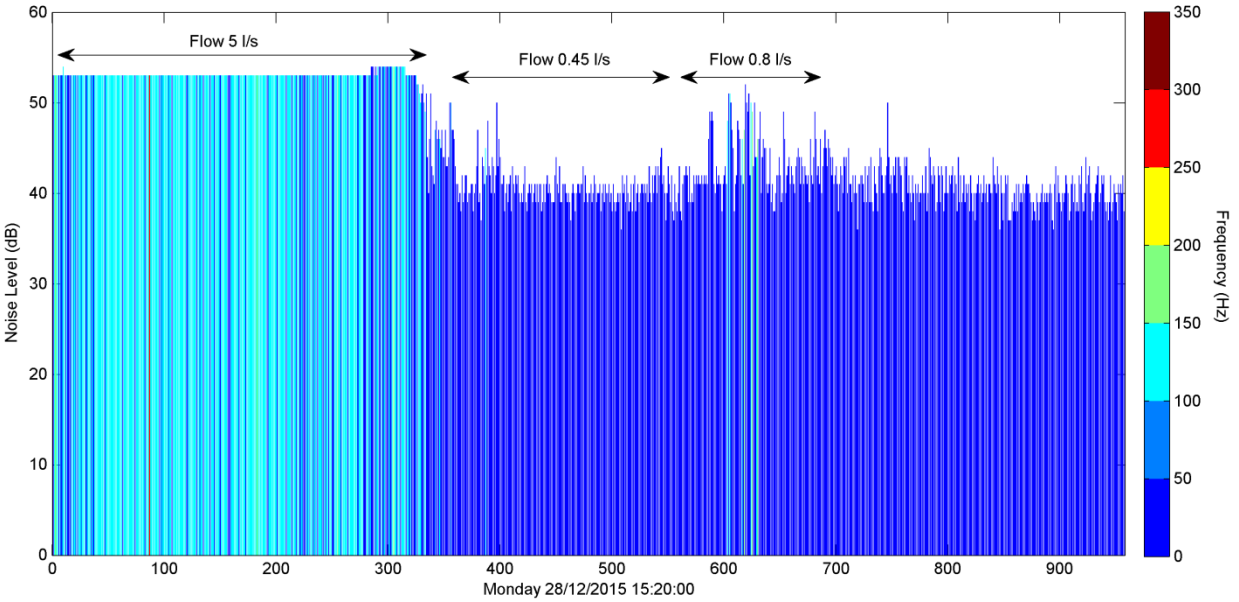

Figure 2.31: Leak noise levels following simulated leaks on hydrant N°25 (62 m distant from EAR)

For the hydrants at 190 m and 195 m from the EAR system, only the significant leaks with a flow rate up to 5 l/s were detected. These leaks are characterized by a noise level that reaches 50 dB with a frequency of 100 Hz.

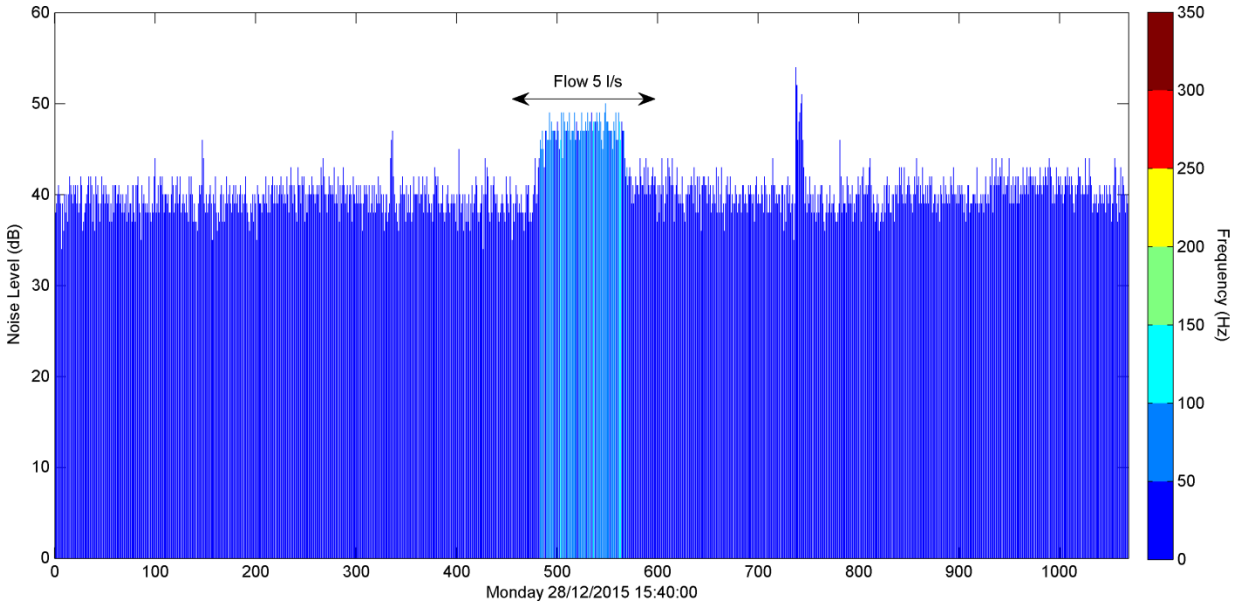

Figure 2.32: Leak noise levels following simulated leaks on hydrant N°38 (190 m distant from EAR)

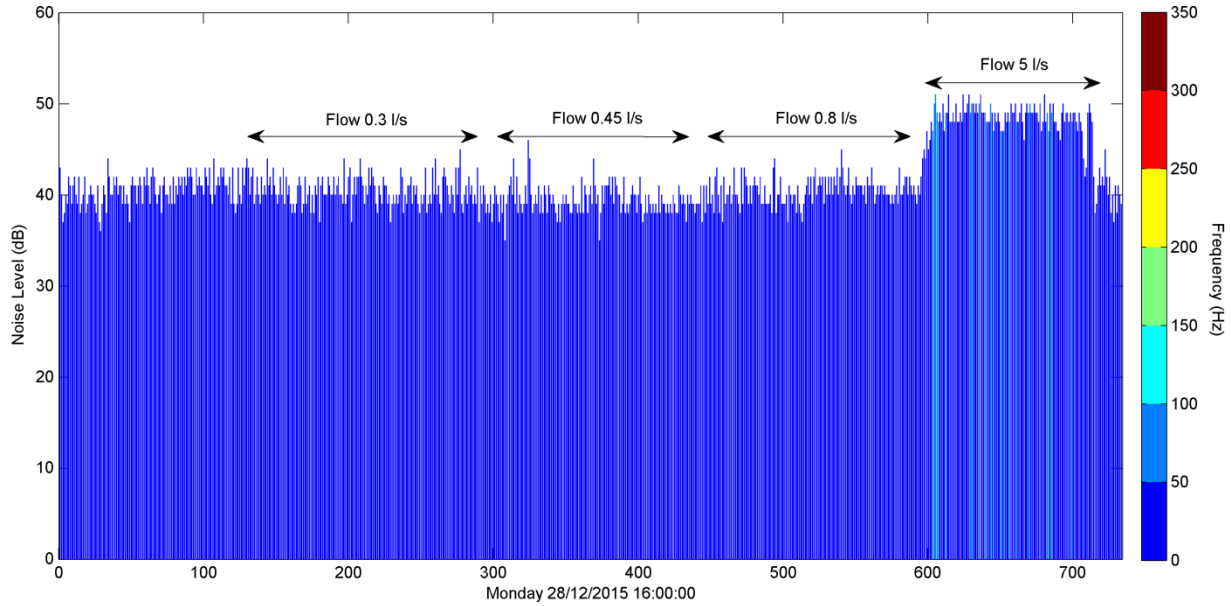

Figure 2.33: Leak noise levels following simulated leaks on hydrant N°24 (195 m distant from EAR)

2.4.4.4. Synthesis of acoustic tests

Acoustic tests show that a leak of 0.45 l/s occurring at a distance of 60 m from the acoustic device is detected following an increase of the noise level up to 50 dB and characterized by high frequencies of 100 Hz. The small leaks and the bursts occurring far from the EAR system generate noises that are damped into the original noise level of 37 dB.

2.5. Conclusion

This chapter presented a description of SunRise – Smart Water demo site: a large scale demonstrator of a smart water system. The physical components of the network and the hydraulic sensors were integrated in a Geographic Information System.

The water network is a highly meshed and old network, which suffers from significant water leakage.

The water network is monitored by 93 AMRs, 5 pressure sensors and an acoustic logger. The network instrumentation allows following both the water supply of the campus as well as the water consumption of buildings at hourly step. Thanks to this data, we can detect water leakage using different methods, which will be presented in the following chapters.

The data concerning the water pressure together with the data concerning water flow allow the calibration of hydraulic model for the campus, which could be useful for understanding the water flow in the water network.

The acoustic system allowed the detection of a leak of 0.45 l/s at a distance of 60 m from the acoustic system.

The data concerning the water flow, water pressure and the acoustic system is available for more than one year. It could be used for testing models developed for the smart management of water networks.

Chapter 3

Water Consumption Analysis

This chapter presents analysis of the water consumption in the demo site. The data transmitted via the communication channels are stored in a database. A platform has been developed to aggregate easily the water consumption at different time scales. The first step consists in analyzing of the consumption in 2015 of the general meters as well as the sub-meters according to the domains defined in the previous chapter. Using the correlation matrix, the weekly analysis of the water consumption of the campus allows: i) a classification of the meter IDs according to their consumption and ii) the identification of the sub-meters related to the appropriate general supply point. The hourly profile of the general meters reveals three critical periods in 2015 corresponding to "possible" leaks. The hourly profile of the sub-meters shows the behavior of each building in term of water usage. It also permits the classification of the minimum night flow as a background leakage or a night usage.

3.1. Smart meters data

The water consumption data collected using the communication channels are stored in a PostgreSQL database. The water data table is composed of 4 elements: Start Date, End Date as time-stamp, meter IDs and the consumption value. The dynamic table of the meter data is connected to the static table via the Meter ID. All the meters are defined in a static table that contains the coordinates of the meters, the serial number of the sensor, the meter number and the category of the building associated to the meter. The architecture of the water meter tables are illustrated in Figure 3.1.

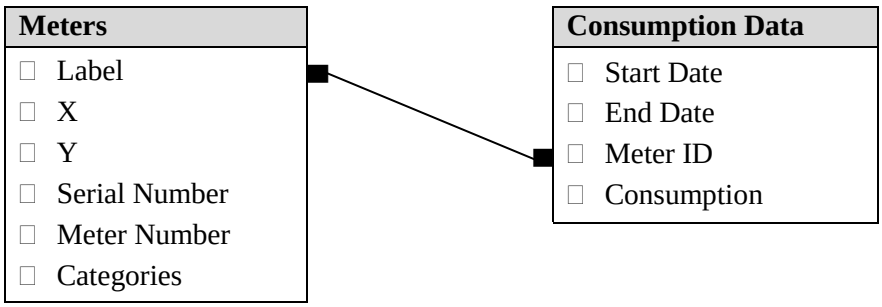

Figure 3.1: Architecture of water meter tables in PostgreSQL

Data analysis is performed using the open source KNIME platform to describe the water usage of each meter ID on different time scales: hourly, daily, weekly, yearly…(Silipo et al., 2013). Figure 3.2 shows the workflow developed for data reading and transformation. The input of this workflow is the PostgreSQL connector. The outcomes are:

- Aggregation of the water consumption values by hour, day, week, month, and year.
- Average water usage by day, week, month and year.
- Average and percentage values of used water on each week from Monday through Sunday.
- Average water used over business days (BD) and weekend (WE).
- Average and percentage values of the water consumed during five different day segments: early morning (7 am - 9 am), morning (9 am - 1 pm), early afternoon (1 pm – 6 pm), late afternoon (6 pm – 10 pm), night (10 pm – 7 am).
- Water loss by hour, day, month and year as well as the corresponding plot. The non-revenue water is the volume in difference between the input measured by the principal meters installed in the entrance of the campus and the consumed water recorded by the meters fixed in the buildings.
- Graphic representation of the aggregate values for each time scale according to a user-defined time window and meter ID.
- Minimum night flow between 2 am and 6 am per day and the monthly average value.
- CSV files summarizing all the results.

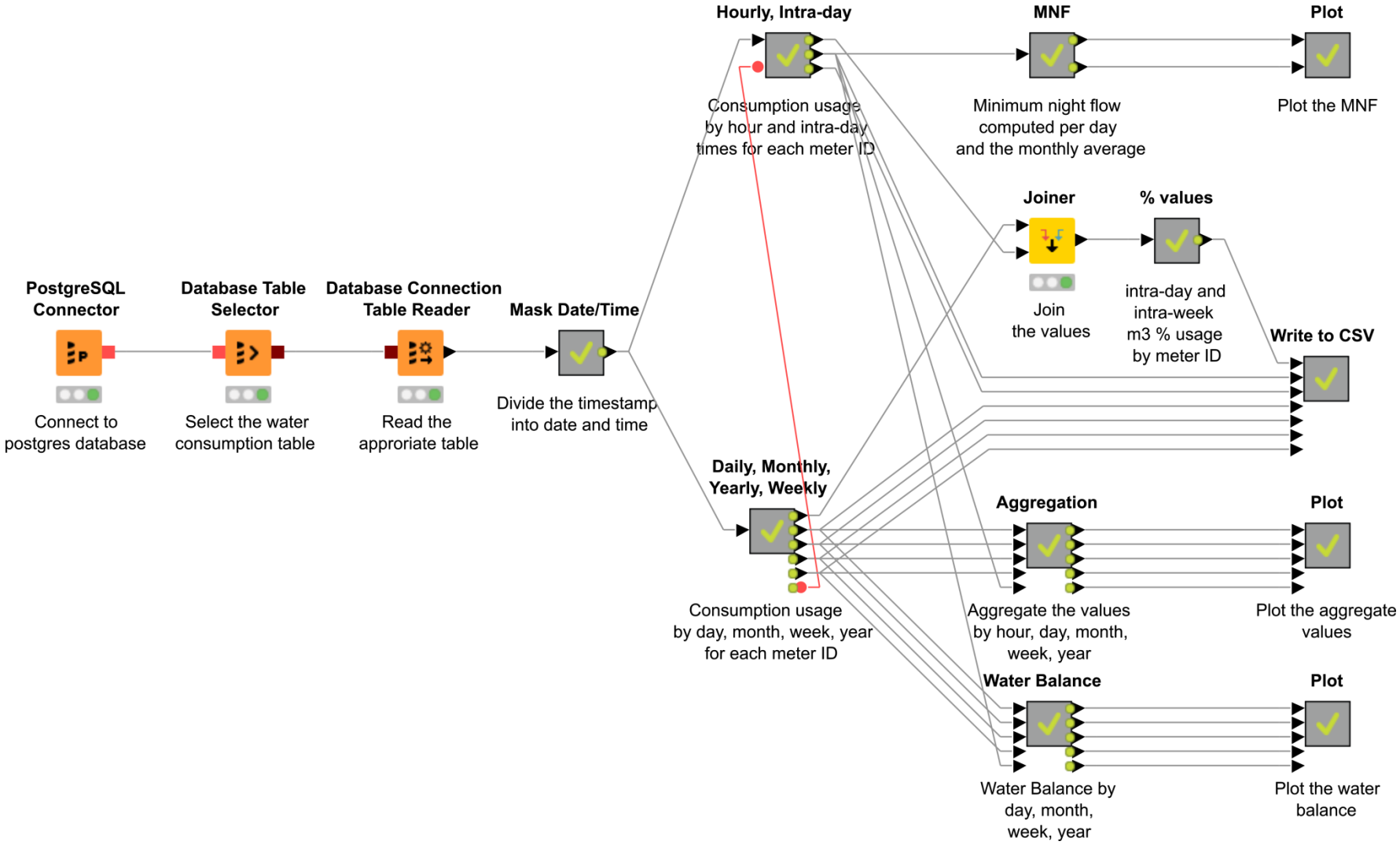

Figure 3.2: Workflow for data readings and transformations

3.2. Water consumption of the Campus (general meters)

The campus consumption (supply) is measured using 13 general or principal meters: CITE SCIENTIFIQUE (a group of 5 meters), 4CANTONS, BACHELARD, ECL, M5, CUUEP, DELTEC ICARE, LML and HALLE VALLIN. The total consumption of these principal meters from 2013 to 2015 is illustrated in Figure 3.3. It can be shown that the water consumption increases from 225 785 m^3 in 2013 to 362 862 m^3 in 2015. This can be explained by: i) the water loss due to leakage, ii) the water volumes consumed by the construction companies and iii) water consumption of new buildings. Between 2013 and 2015, two new buildings were built (REEFLEX, CISIT).

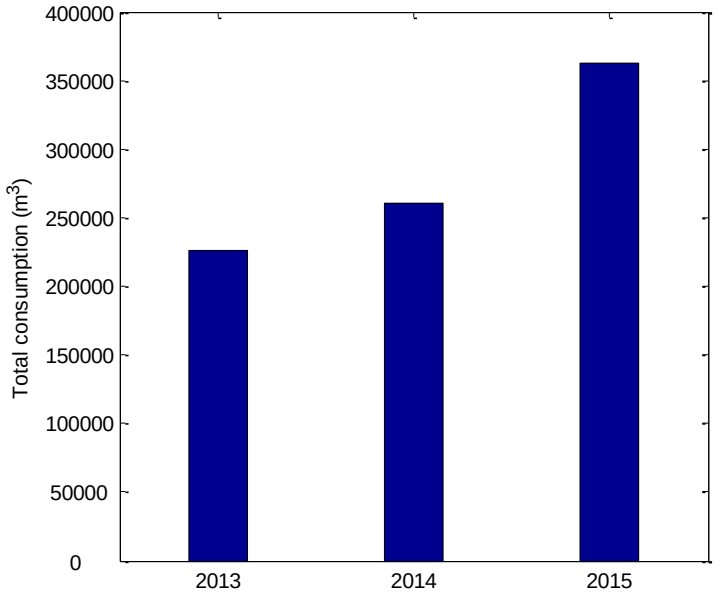

Figure 3.3: Total consumption of the general meters

The analysis of the water consumption volumes measured by the general meters in 2015 shows that 99.6% of the total consumption are distributed through the following measurement points in the looped network: the group of 5 meters CITE SCIENTIFIQUE: 44.4% (161003 m^3), ECL: 25.2% (91394 m^3), 4CANTONS: 19.8% (71818 m^3), BACHELARD: 8.6% (31126 m^3) and M5: 1.7% (6003 m^3).

The remaining 0.4% of water consumption concerns AMRs installed in: CUEEP (990 m^3), LML (305 m^3), HALLE VALLIN (115 m^3) and DELTEC ICARE (108 m^3).

The distribution of the water consumption over the general meters in 2015 is described in Figure 3.4.

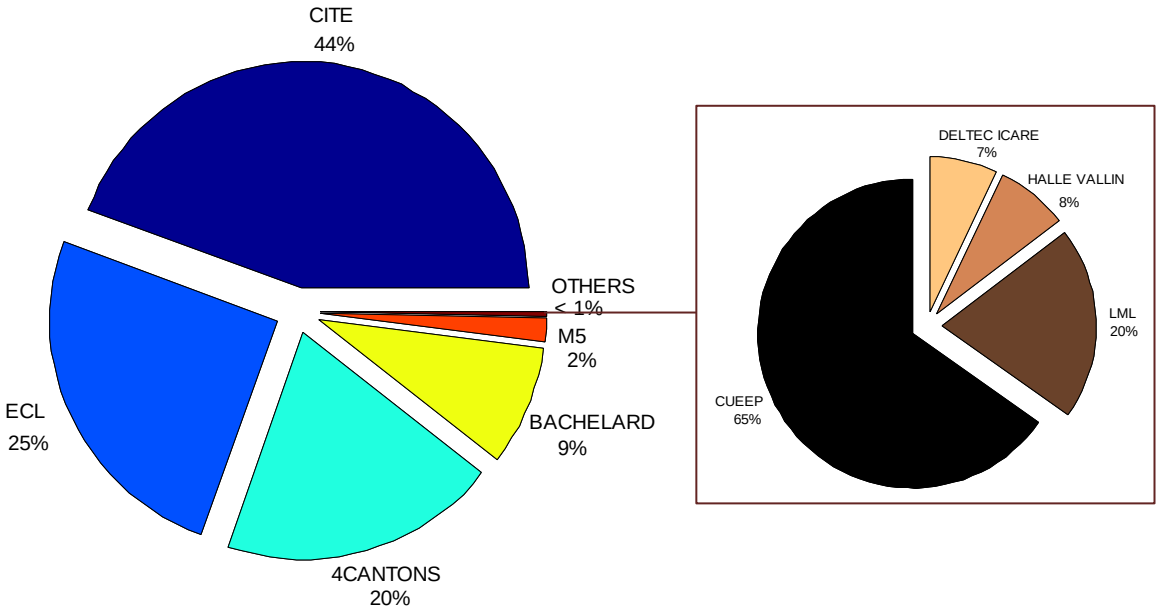

Figure 3.4: Distribution of the water consumption over the general meters in 2015

3.3. Building Water consumption (sub-meters)

The 80 AMRs installed in the buildings are regrouped in different domains as mentioned in Chapter 2. The distribution of the water consumption in 2015 is illustrated in Figure 3.5. The CROUS (104 015 m^3) and LILLE1 (58 303 m^3) consume 80% of the campus water supply.

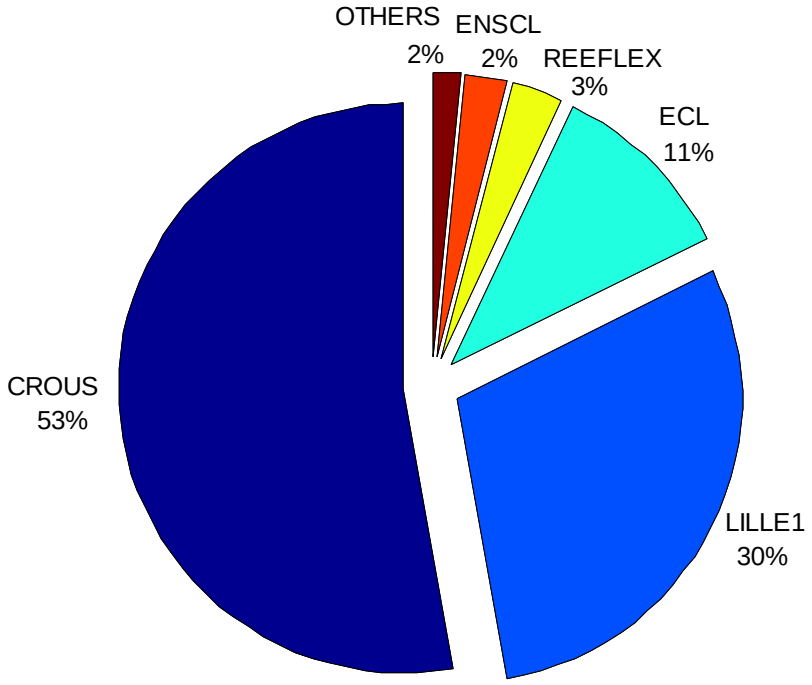

Figure 3.5: Distribution of the water consumption over the domains

3.3.1. CROUS buildings (53% of the total consumption)

The CROUS domain includes 4 students' residences and 3 restaurants. Figure 3.6 shows the water consumption of these buildings in 2015.

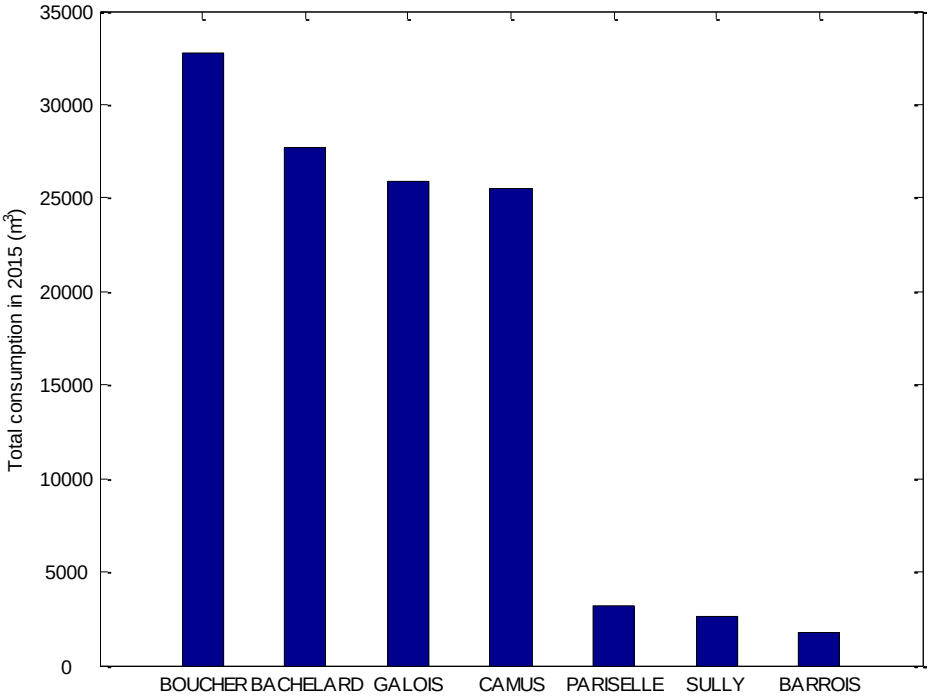

Figure 3.6: Water consumption for the CROUS domain

The water consumption of the residences exceeds 25 000 m^3:

- BOUCHER (32 746 m^3),
- BACHELARD (27 749 m^3),
- GALOIS (25 868 m^3),
- CAMUS (25 530 m^3).

The restaurants PARISELLE (3 231 m^3) consumes more than the two others (SULLY: 2 661 m^3 and BARROIS: 1 771 m^3) because welcomes more students.

3.3.2. LILLE 1 domain (30% of the total consumption)

The total consumption of LILLE 1 domain is measured by 55 AMRs. The consumption in 2015 is represented in Figure 3.7. Five buildings have high consumptions: higher than 4 000 m^3 for C6, IUT and the extension of P5 building (P5_BIS CERLA) and higher than 5 000 m^3 for P5 and POLYTECH. In addition to the teaching, these buildings host research facilities.

Three other buildings in the biology sector consume more than 2 000 m^3: SN1, SN1_SERRES and SN3. Eight other buildings consume higher than 1000 m^3: A3, C9, SUPSUAIO, SH3, C5, P3, C8, P1 and A1.

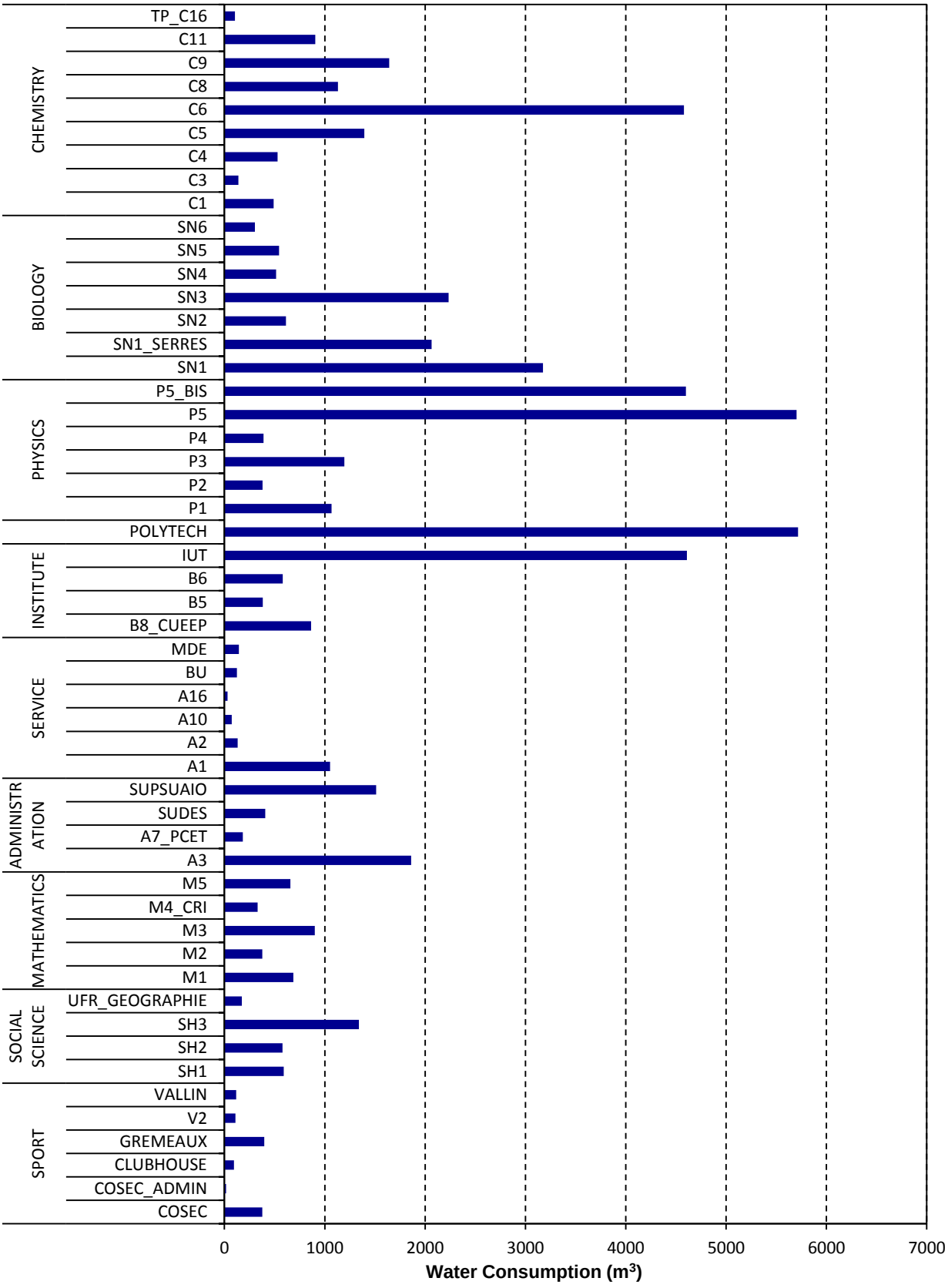

Figure 3.7: Consumption of LILLE1 buildings in 2015

The distribution of the water consumption of LILLE1 buildings according to their activities is shown in Figure 3.8. The three sectors: CHEMISTRY (15 770 m^3), PHYSICS (13 334 m^3) and BIOLOGY (9 450 m^3) consume 60% of this domain. This is due to the presence of research facilities, which have high water consumption. The sectors ADMINISTRATION, MATHEMATICS, SOCIAL SCIENCE, SERVICES and SPORT seem to use water for domestic usage like the sanitation.

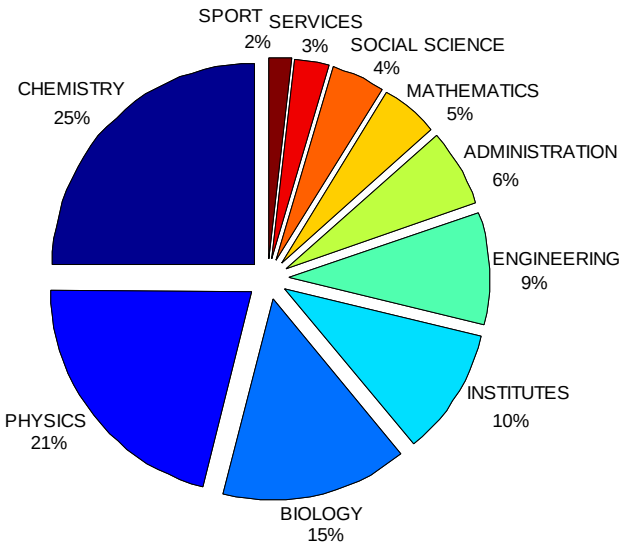

Figure 3.8: Distribution of the water consumption by activity domain – LILLE1 domain

3.3.3. ECL domain (11% of the total consumption)

The ECL domain includes 4 AMRs that measure engineering school consumption and 1 AMR for the 6 buildings of the residence L. DEVINCI. The student residence represents 80% of the total consumption of this domain. The engineering school consumed in 2015 of 4 131 m^3.

3.3.4. REEFLEX domain (3% of the total consumption)

REELEX is the new students' residence inaugurated in June 2015. It includes 4 buildings and a nursery. This domain comprises 2 AMRs: one at the main entry of the residence and the other (CRECHE_REEFLEX) measure the water consumption of the nursery.

3.3.5. ENSCL domain (2% of the total consumption)

The ENSCL domain includes the C7 building in the CHEMISTRY sector. This school consumed 4 853 m^3 in 2015. This building is used for teaching and research.

3.3.6. OTHER domain (2% of the total consumption)

The remaining two buildings in the demo site BONDUELLE and CLINIQUE consumed in 2015 1 251 m^3 (42%) and 1 746 m^3 (58%), respectively.

3.4. Weekly Water consumption - general meters

Figure 3.9 shows the weekly consumption of the campus. We observe a low consumption period (< 6 000 m^3/week) referring to the summer holidays from mid-July to the end of August (week 29 to 36). The period of winter holidays (week 9 to 10) and spring holidays (week 17 to 18) present consumption inferior to 7 000 m^3/week. The intensive consumption is observed in periods March to April (weeks 11 to 17, mean 7 900 m^3/week, max 8 190 m^3/week), May to June (weeks 21 to 27, mean 7 220 m^3/week, max 7 450), September to November (weeks 38 to 47, mean 8 400 m^3/week, max 10 140 m^3/week).

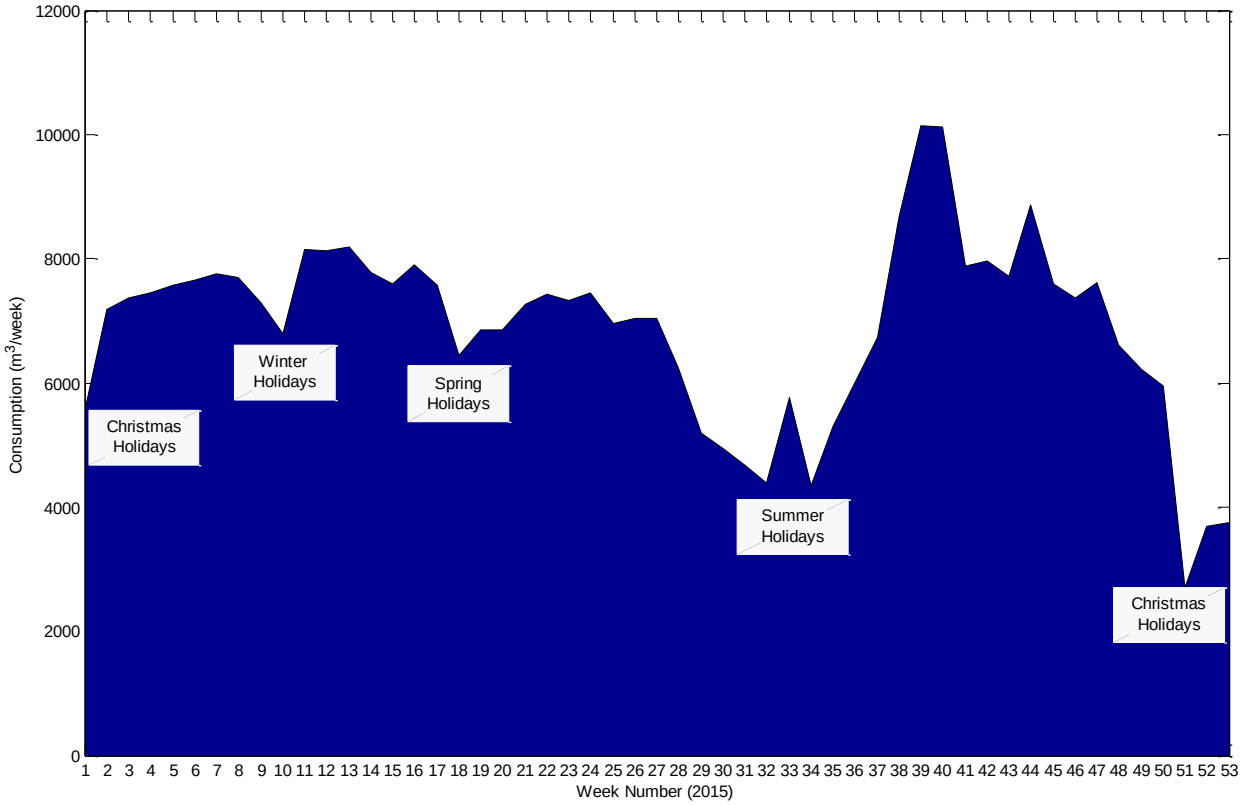

Figure 3.9: Weekly water consumption profile of the 13 general meters in 2015

The significant increase in the consumption observed in October could be attributed to the new students' residence REEFLEX. The abnormal consumption in the summer holidays (week 33) is probably due to a leak and will be investigated later. We observe also a decrease in the consumption during the New Year holidays (week 1) compared to Christmas Holidays (weeks 51 to 53). This is due to the reparation of leakages detected.

3.4.1. Weekly consumption - general meters in the looped network

The water consumption through the looped water network of the campus is measured by the regrouping the 5 AMRs CITE SCIENTIFIQUE and the AMRs: 4CANTONS, ECL, BACHELARD and M5. They represent 99.6% of the total consumption. The evolution of the water consumption of these meters over the 53 weeks in 2015 is illustrated in Figure 3.10. It can be shown that the 3 AMRs CITE SCIENTIFIQUE, ECL and 4CANTONS have the same profile.

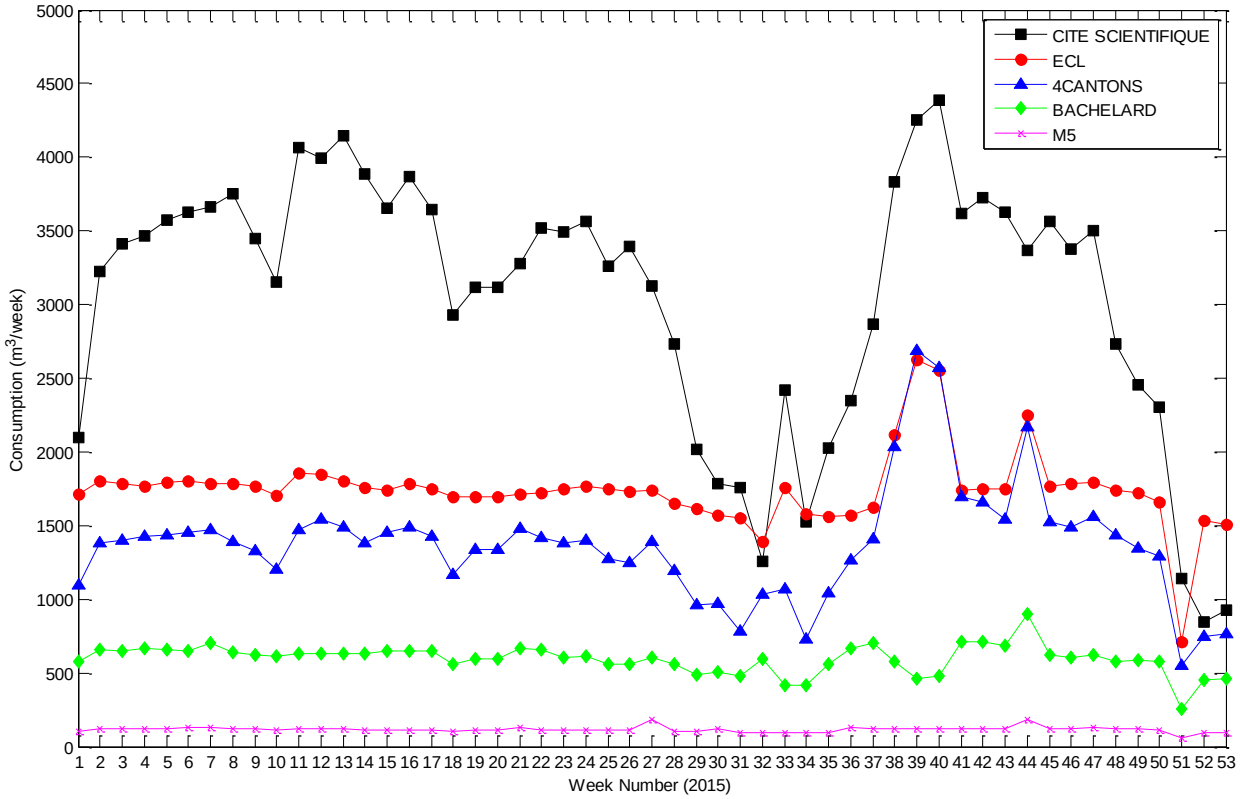

Figure 3.10: Weekly water consumption profile of the general meters connected to the looped network

In order to classify the general meters according to the measured consumption, the correlation matrix between the weekly consumption in 2015 has been established. The correlation matrix, calculated using the Pearson coefficient varying from 0 to 1, indicates the correlation between the variables. The variables that have similar tendency have a correlation factor close to 1. As shown in Figure 3.11, two groups can be distinguished:

- Group A: the 3 AMRs CITE SCINETIFIQUE, ECL and 4CANTONS with a correlation factor higher than 0.68.
- Group B: the 2 AMRs BACHELARD and M5 with a coefficient of 0.72. The correlation between these 2 AMRs and the group A is lower than 0.57.

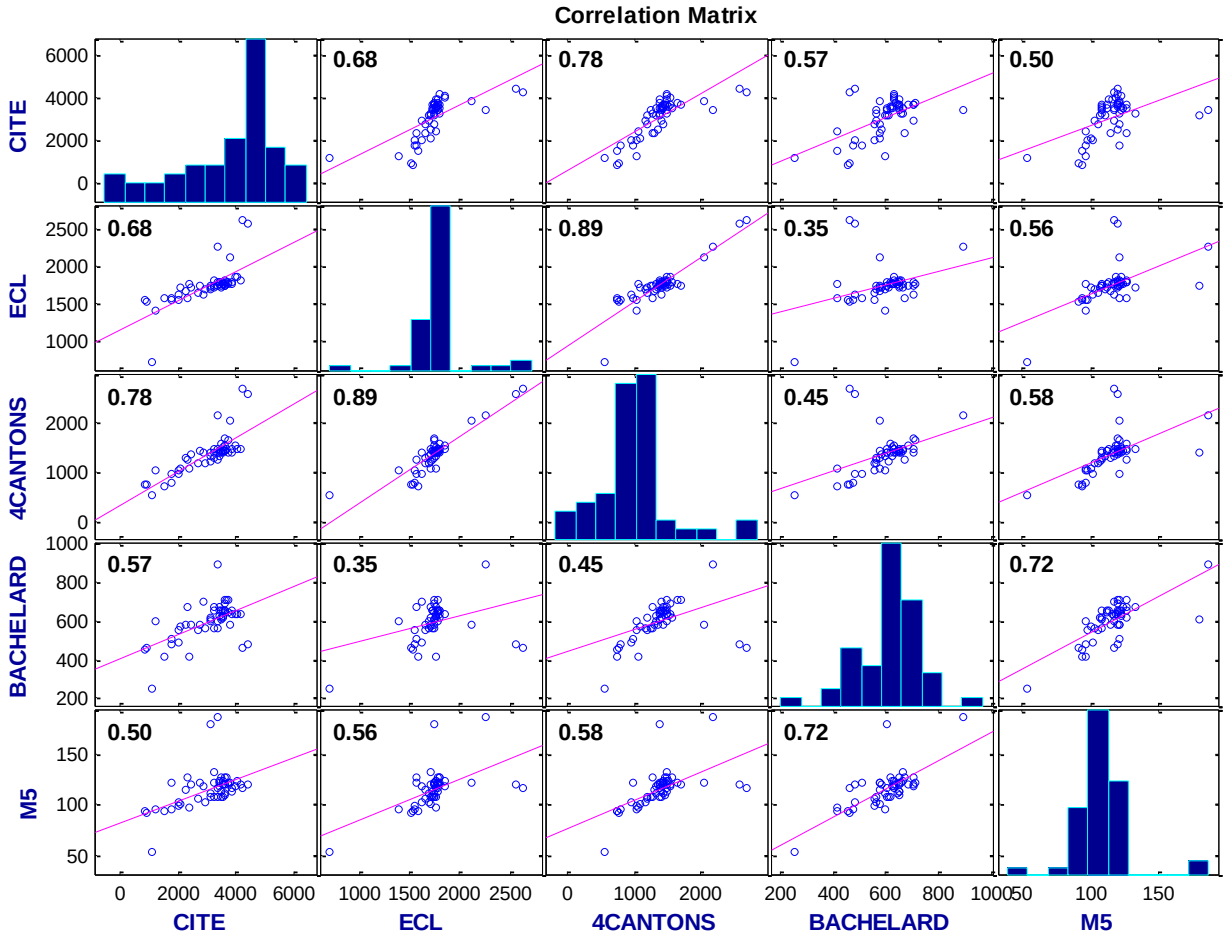

Figure 3.11: Correlation matrix between general meters over the 53 weeks in 2015 (Pearson coefficient)

3.4.1.1. Group A

The 3 AMRs of this group: CITE SCIENTIFIQUE, ECL and 4CANTONS present same behaviors. The water consumption decreases during winter, spring, summer and Christmas holidays. Two singularities can be extracted from the profile of this group. The first leak in week 33 is accounted through the 2 meters CITE SCIENTIFIQUE and ECL. Therefore, the detected leak is located in the North West side of the campus: the meter CITE SCIENTIFIQUE is located in the North of the campus, while the ECL meter is in the West. The leak in week 44 is measured by the meters ECL and 4CANTONS. It occurs consequently in the South West of the campus.

3.4.1.2. Group B

The AMRs (BACHELARD and M5) represent 11% of the campus consumption. The general meter BACHELARD seems to measure the consumption of BACHELARD residence that includes 3 AMRs (L, N and PYTHAGORE). The correlation matrix between the general meter BACHELARD and the supposed associated sub-meters is shown in Figure 3.12. We observe that the general meter correlates with the sub-meters L and N with a coefficient higher than 0.60.

However, the profile of the PYTHAGORE meter is different from the general meter BACHELARD.

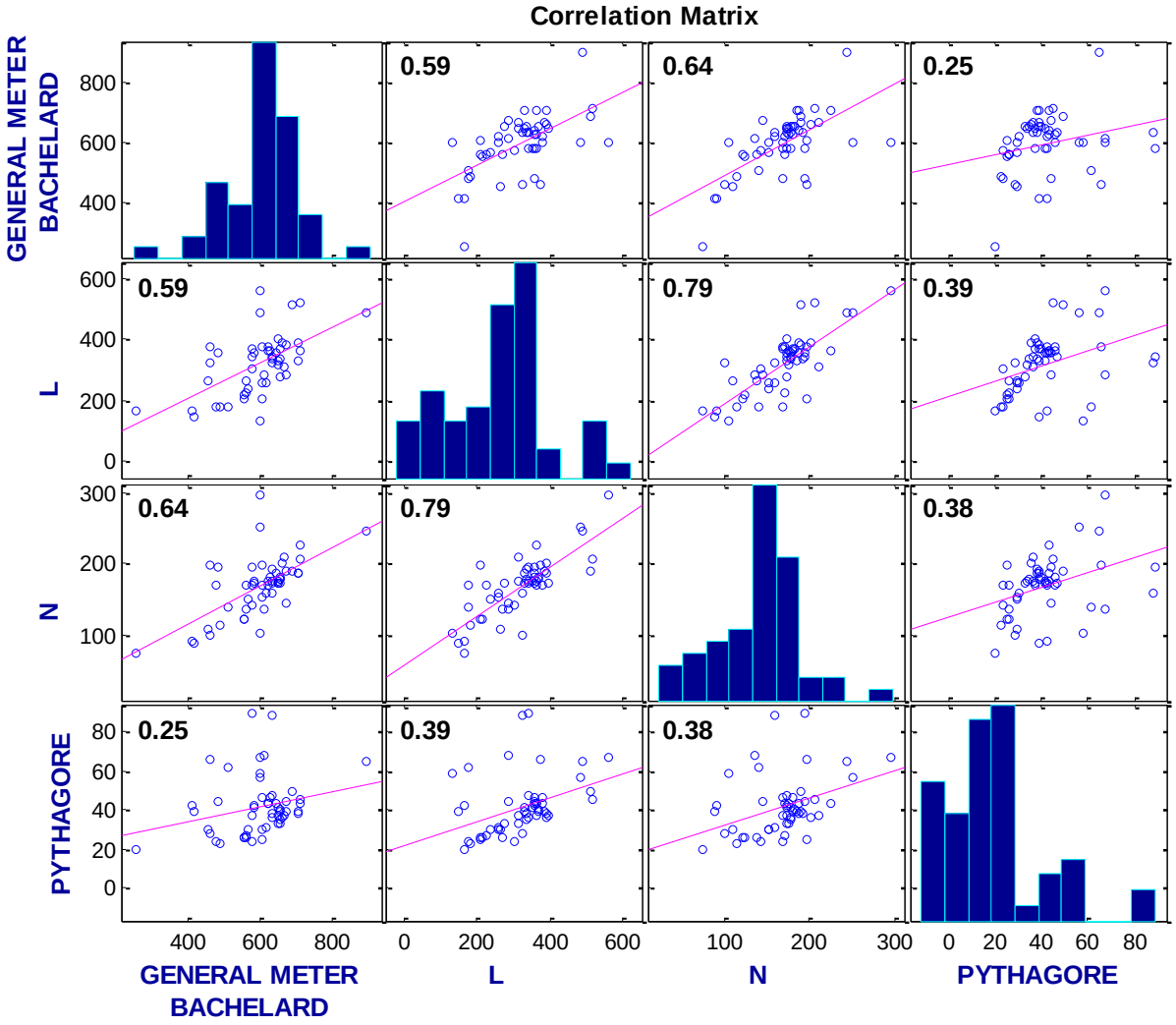

Figure 3.12: Correlation matrix between general meter BACHELARD and the associated sub-meters

The general meter BACHELARD is supposed to be the bulk water meter of the 3 sub-meters L, N and PHYTAGORE. However, as shown in Figure 3.13, the summation's profile of these 3 AMRs does not overlap with the profile of the principal meter BACHELARD. The correlation coefficient between BACHELARD meter and the 3 sub-meters (L, N and PHYTAGORE) is equal to 0.63. We observe that the two consumptions match better starting from the week 44 of 2015.

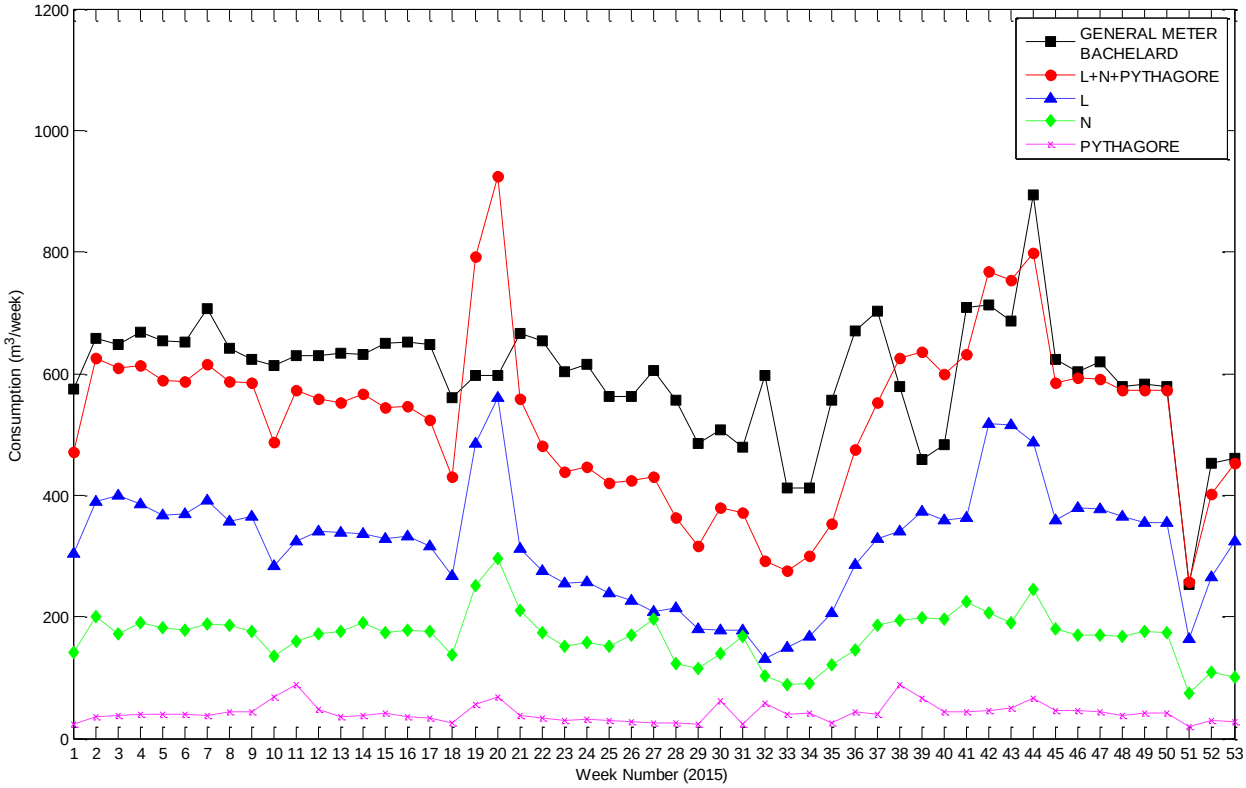

Figure 3.13: Weekly consumption profile of the general meter BACHELARD with the supposed associated sub-meters

The general meter M5 is installed at the entry of the mathematics sector of the campus. It is supposed to supply the mathematics buildings (M5, M4CRI, M3LIFL, M3, M2 and M1). The correlation matrix between the weekly consumption of the general meter M5 and that of building M1 shows a correlation factor of 0.02. Therefore, the building M1 seems to be supplied from another section.

The weekly consumption of the general meter M5 and the summation of the consumption of the sub-meters M5, M4CRI, M3LIFL, M3 and M2 are depicted in Figure 3.14. The two graphs show a difference of approximately 80 m^3/week. This can be explained by a leak of 0.5 m^3/h. This hypothesis will be confirmed by the analysis of the hourly profile of the general meter M5 (cf. section 3.5.1).

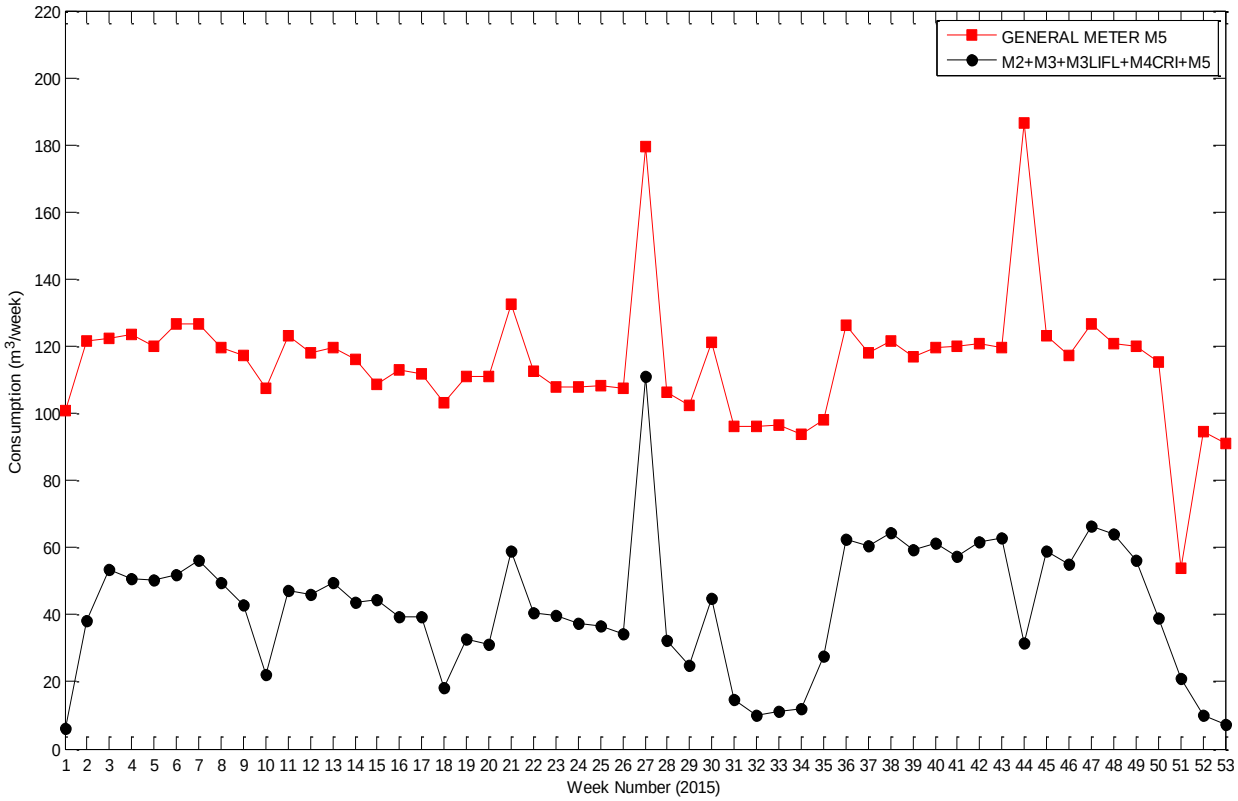

Figure 3.14: Weekly consumption profile of the general meter M5 with the sum of the supposed associated sub-meters

3.4.2. Weekly consumption - general meters in the disconnected part

The water consumption through disconnected part of the water network in the campus is measured by 4 AMRs: CUEEP, LML, HALLE VALLIN and DELTEC ICARE. They represent 0.4% of the total consumption. The water consumption of these meters in 2015 is illustrated in Figure 3.15.

The LML general meter measures the water consumption of the building M6 dedicated for research. The weekly profile of this meter shows a mean consumption of 6.17 m^3/week and a maximum of 10 m^3/week in the 2nd week of April 2015. The minimum consumption, occurring at the summer holidays (2.18 m^3/week in the 2nd week of August 2015).

The HALLE VALLIN meter concerns the water consumption of the hall of sport VALLIN. The mean consumption of this hall is 1.91 m^3/week. The maximum consumption is equal to 8.78 m^3/week; it occurs in the 3rd week of May 2015. During summer, the hall is closed and consequently the volume of water consumed is null as shown in Figure 3.15.

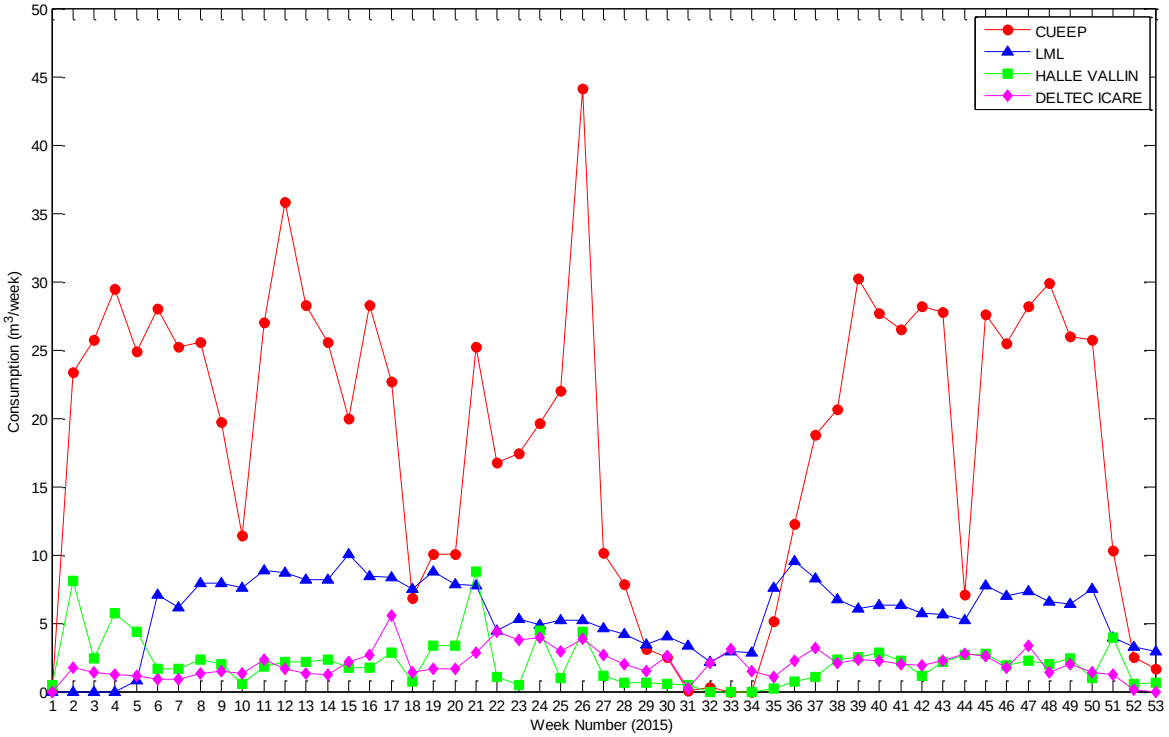

Figure 3.15: Weekly profile of the general meter BACHELARD with the supposed associated sub-meters

3.4.2.1. General meter CUEEP

The general meter CUEEP concerns buildings B5 and B6. The correlation between the weekly values of the CUEEP and B5 as well as B6 exceeds 0.90 as shown in Figure 3.16.

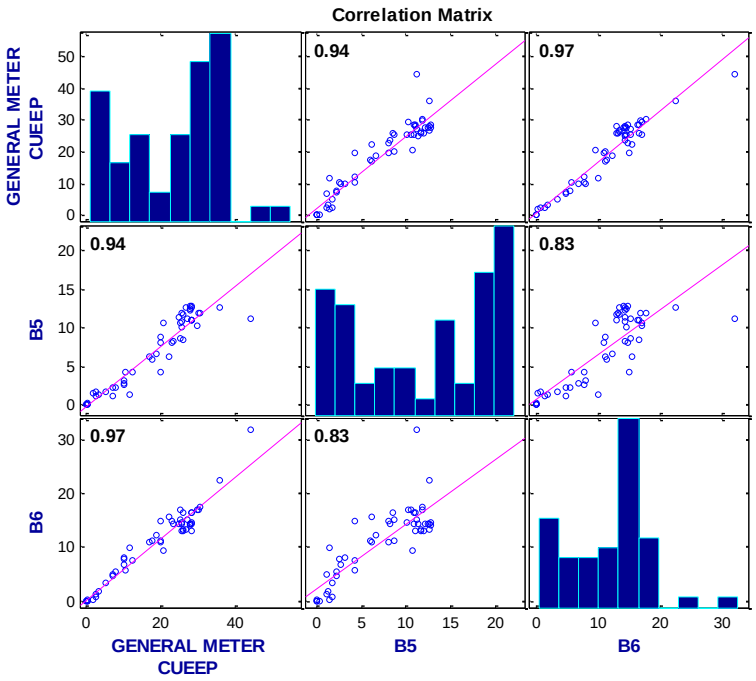

Figure 3.16: Correlation matrix between general meter CUEEP and the associated sub-meters (B5+B6)

As illustrated in Figure 3.17, the profile of the summation of B5 and B6 meters matches that of the general meter CUEEP.

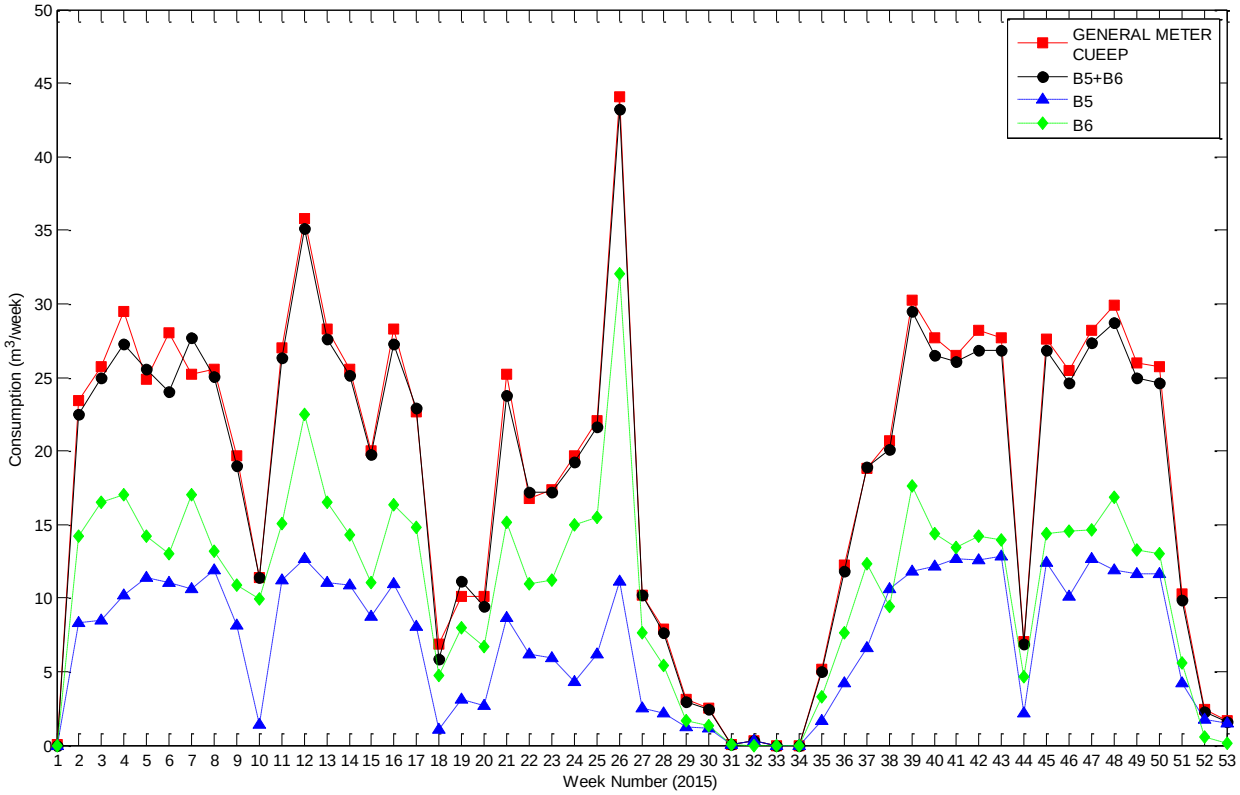

Figure 3.17: Weekly profile of the general meter CUEEP with the associated sub-meters (B5+B6)

3.5. Hourly water consumption - general meters

Analysis of the hourly water consumption of the general meters allows an identification of different critical periods. Figure 3.18 illustrates the water consumption profile per hour for the 13 general meters in 2015. We observe tow consumption profiles which correspond to business days and weekends and holidays, respectively. This distinction becomes more difficult in the low consumption periods especially in summer holidays. For each week, 5 daily peaks are identified. They correspond to the consumption from Monday to Friday. It is clear that the consumption during the week is higher than during the week-end. The maximum consumption recorded is 145 m^3/h; it corresponds to an abnormal value. The profile never drops below the threshold of 11.67 m^3/h recorded at 5 am in 25 November 2015. According to Figure 3.18, three leaks could be identified:

- Leak I - Week 12: from 16 March 2015 till 22 March 2015 where a peak consumption of 145 m^3/h occurs at 1 pm on March, 17.
- Leak II - Week 33: from 10 August 2015 till 16 August 2015 where a leak is observed
- Leak III - Week 38, 39 and 40: from 14 September 2015 till 4 October 2015 where a leak is detected.

The low consumption corresponds to holidays:

- Winter holidays (week 10): from 2 March 2015 till 8 March 2015. The maximum consumption is 55.68 m^3/h (6 March at 1 pm) while the minimum consumption is 25.06 m^3/h (2 March at 5 am).
- Spring holidays (weeks 18 and 19): from 27 April 2015 till 10 May 2015. During this period, the signal connection is lost starting from the 3rd of May at 4 pm and the missed consumption values are filled by interpolation. The minimum consumption measured during this period is 25.44 m^3/h on May 3rd at 6 am.
- Summer holidays (weeks 30 till 35): from 20 July 2015 till 30 August 2015. During this period a leak is detected on August 10th at 3 pm. The profile consumption drops to 15.79 m^3/h on 24 August at 3 am.
- Christmas holidays (weeks 52 and 53): starting from 21 December 2015 till the end of the year. The maximum consumption during this period is 40.65 m^3/h at 2 pm on 22nd of December. The consumption is least (12.61 m^3/h) at 5 am on December 31st.

In addition to these holidays, there are 11 bank holidays in 2015. The maximum consumption during the holiday and the rest of the week are shown in Table 1.2. It is remarkable that during a holiday week or in the summer, the consumption during the bank holiday cannot be clearly identified from the others due to the low water consumption the whole week.

Table 3.1: Analysis of water Comparison in holidays

Holidays	**Maximum consumption (m^3/h)**	
	During the holiday	**During the rest of the week**
New Year's day: 1 January	41.10	44.32
Easter Monday: 6 April	46.01	73.21
Labor day: 1 May	42.33	75.5
World War II Victory day: 8 May	Signal lost	
Ascension day: 14 May	Signal lost	
Whit Monday: 25 May	46.01	79.86
Bastille day: 14 July	33.53	47.63
Assumption day: 15 August	27.65	36.63
All Saint's day: 1 November	48.13	70.09
Armistice day: 11 November	58.81	77.90
Christmas Day: 25 November	26.84	40.65

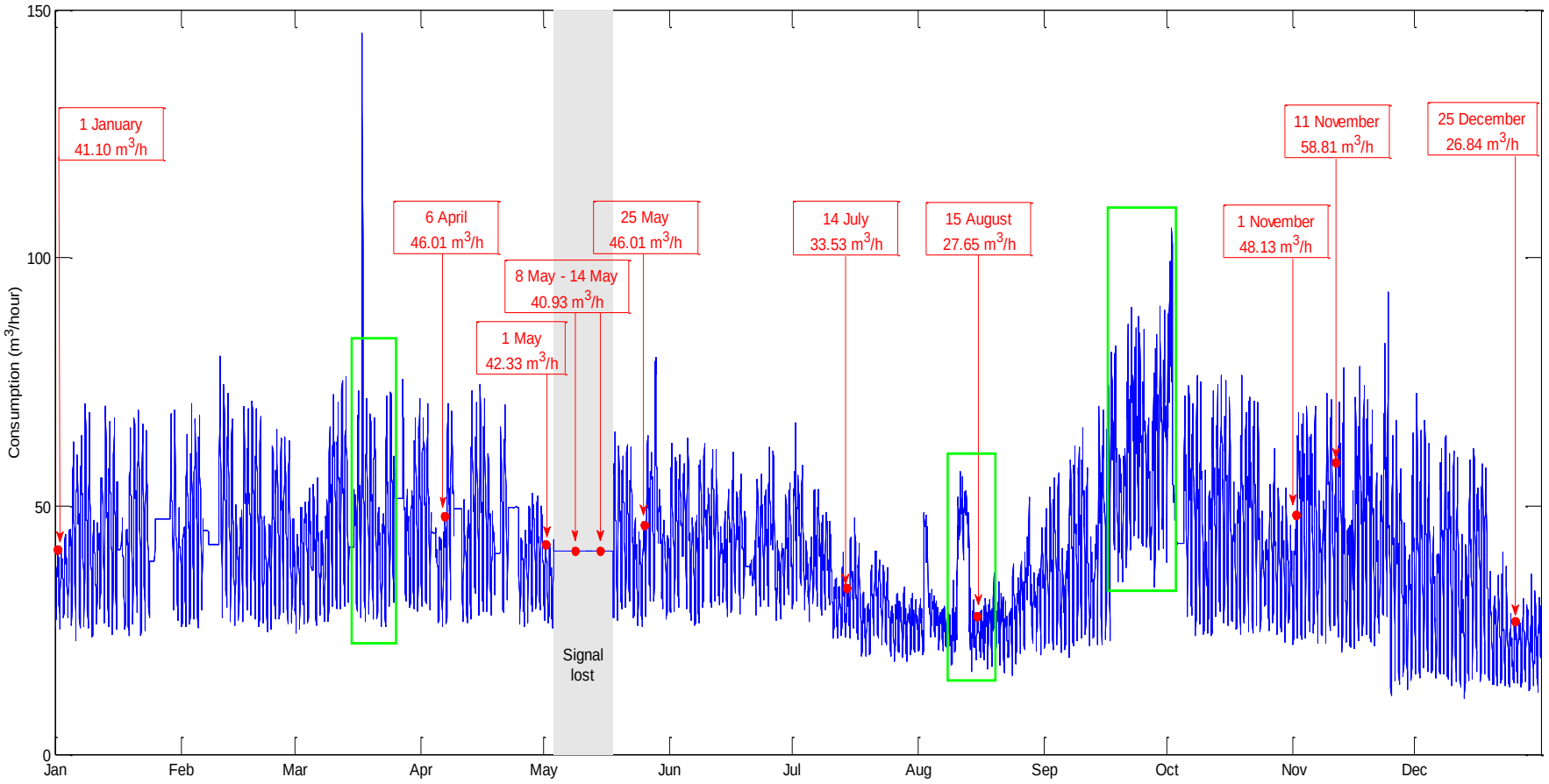

Figure 3.18: Hourly water consumption profile of the 13 general meters in 2015

3.5.1. Analysis of leak I

Figure 3.19 shows the weekly consumption measured by the 3 general meters CITE SCIENTIFIQUE, 4CANTONS and ECL. We observe a peak consumption of 145 m^3/h during the week 12.

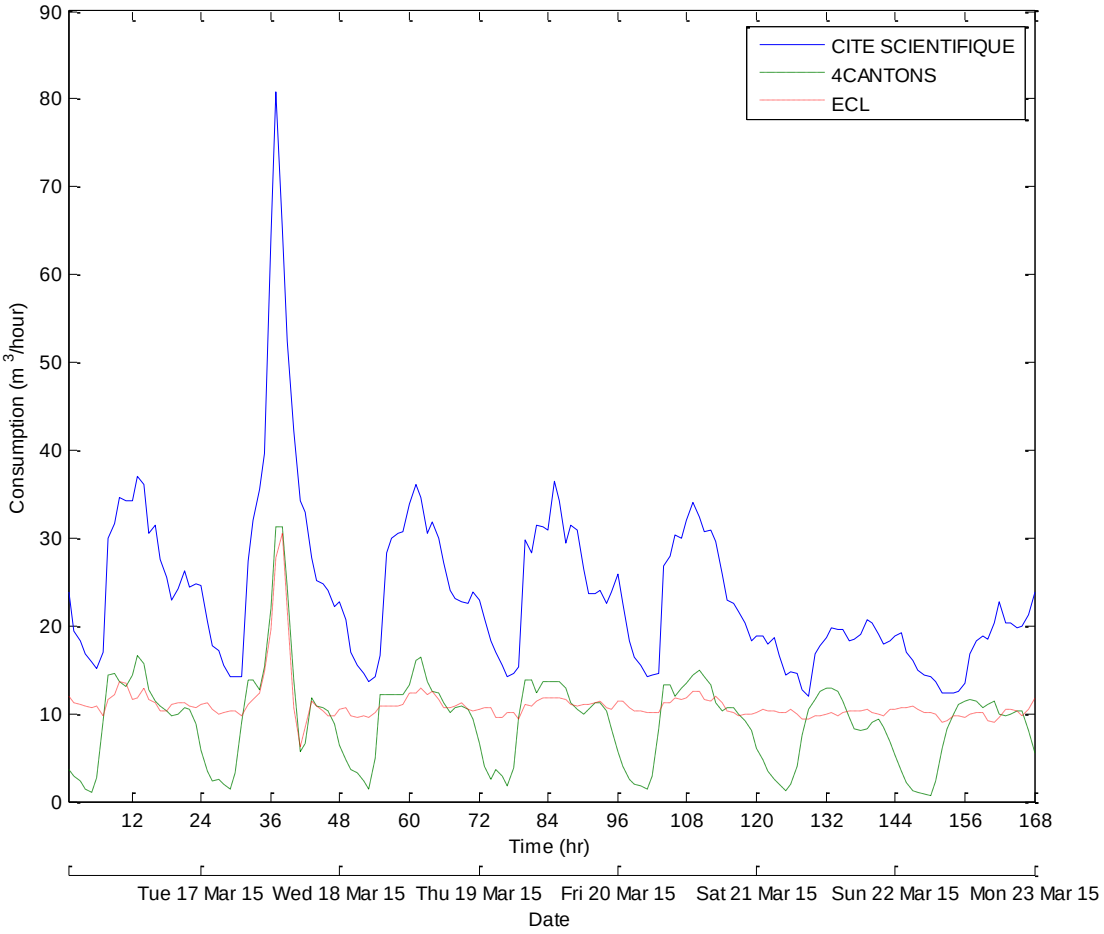

Figure 3.19: Evolution of the hourly consumption of CITE, 4CANTONS and ECL meters during week 12

The distinction of the water consumption measured through CITE SCIENTIFIQUE between business days and weekends and holidays is clear. During working days, the first peak consumption recorded by the CITE SCIENTIFIQUE occurs at midday and the second at 9 pm. During the weekend, the first peak disappears and the consumption profile during the day tends to be related to the domestic usage. Therefore, the CITE SCIENTIFIQUE meter seems to measure: i) the volume consumed by the university restaurants, ii) part the consumption of the university buildings and iii) the water used by the students' residences.

For 4CANTONS and ECL general meters, it is more difficult to distinguish the consumption between working days and weekends. The general meter 4CANTONS seems to account the volume used by the students' residences. Concerning the ECL meter, it is difficult to separate the consumption during the day from the volume consumed during the night.

The peak consumption that occurred at noon of the 17th of March is accounted by these 3 meters. This abnormal consumption can be explained by a burst during the renovation of the library (see Figure 3.20).

Figure 3.20: Burst pipe in the construction site of the new library (17 March 2015)

The hourly profile for the remaining two general meters BACHELARD and M5 is shown in Figure 3.21. Concerning the BACHELARD meter, three peaks are observed at 8:00 am, 1:00 pm and 9:00 pm. This profile corresponds to the water consumption of the students' residence.

The profile of M5 meter shows a clear distinction of the consumption between working days and weekends. During the weekend of the first critical period, the consumption seems to be constant (0.6 m^3/h). It corresponds probably to a leakage.

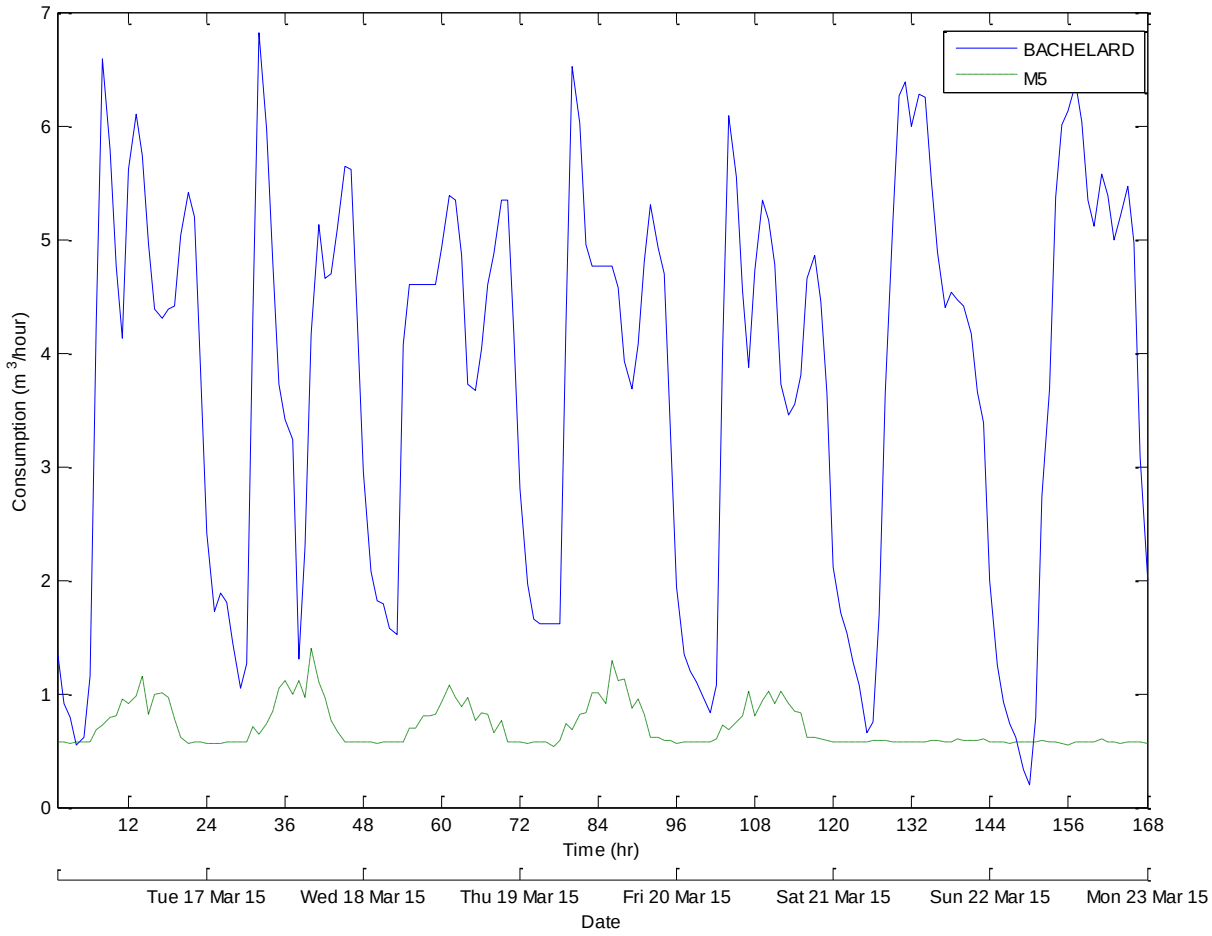

Figure 3.21: Evolution of the hourly consumption of BACHELARD and M5 meters during week 12

3.5.2. Analysis of leak II

During the summer period, a leak has been detected August, 10 at 5:00 pm. The comparison between the consumption profiles illustrated in Figure 3.22 and Figure 3.23 shows that this leak affects the general meters CITE SCIENTIFIQUE, 4CANTONS and ECL. This leak was due to another burst pipe during the renovation of the Library. Comparing the night flow before and during this period, the leak is estimated to be equal to 20 m^3/h. During this period, the ECL meter shows two peaks during the day: at 8:00 am and at midnight.

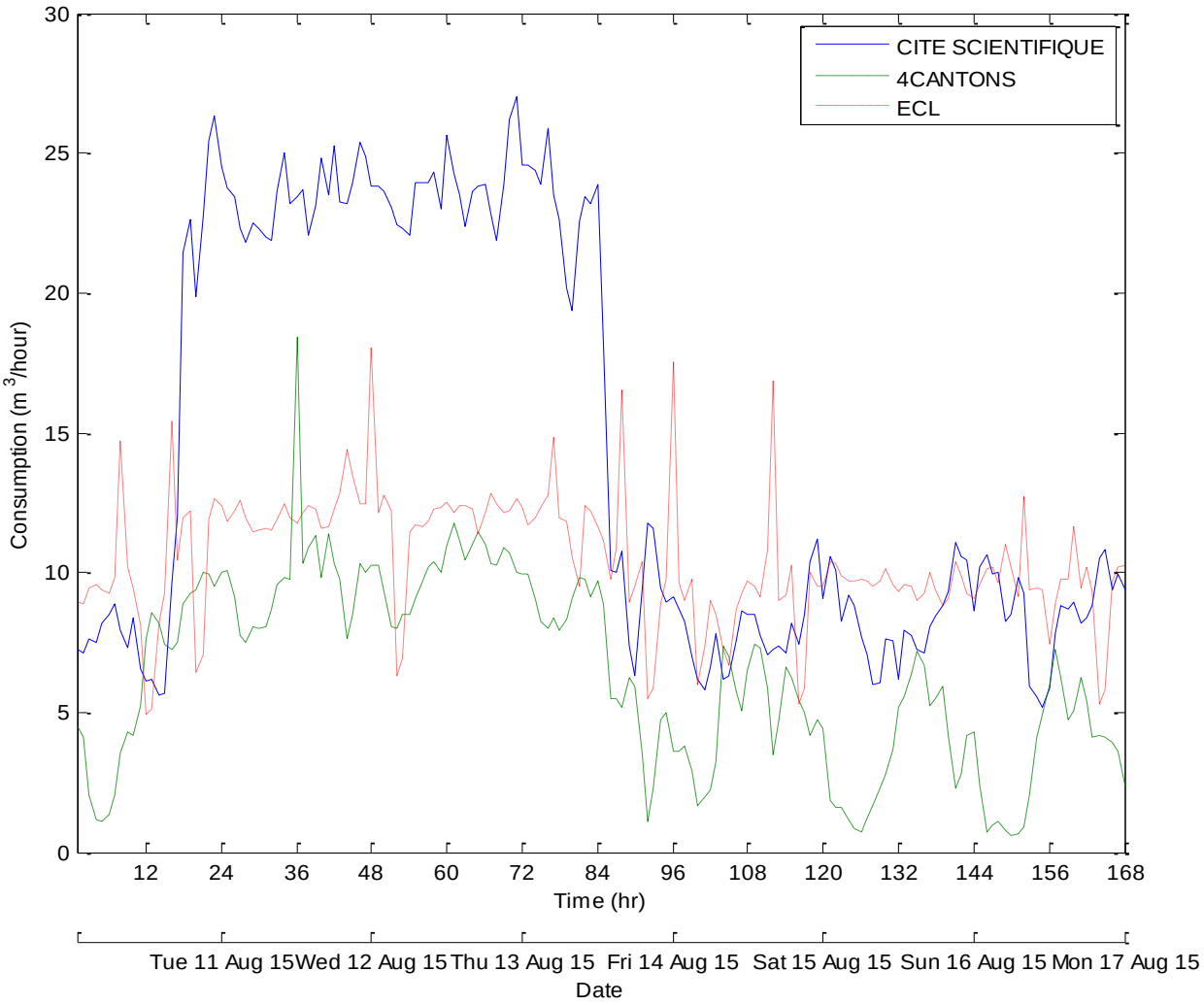

Figure 3.22: Evolution of the hourly consumption of CITE, 4CANTONS and ECL meters during week 33

The profile of M5 general meter illustrated in Figure 3.23 proves the hypothesis of the leak deduced from the critical period I. A constant flow of 0.6 m^3/h is observed during the summer.

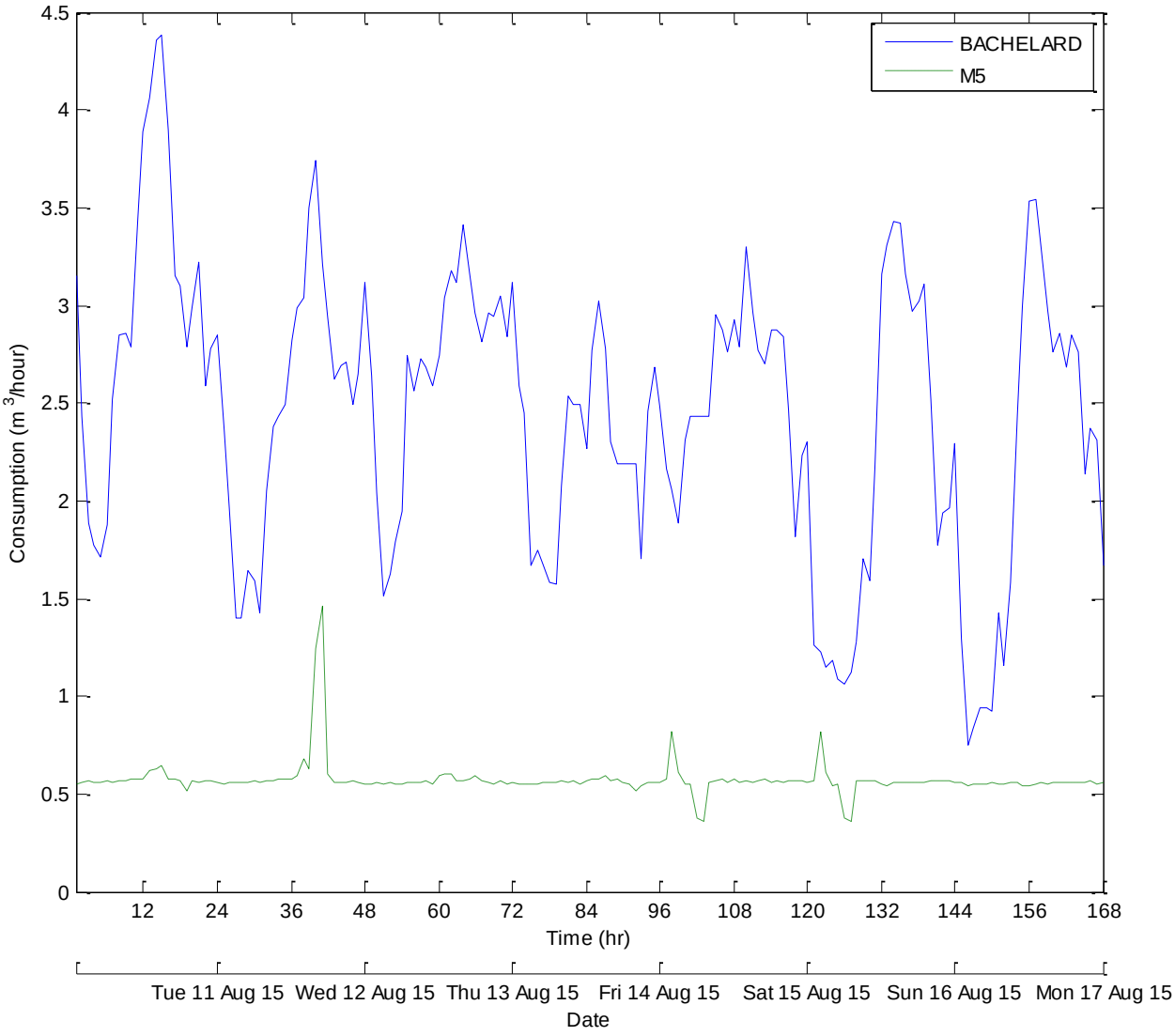

Figure 3.23: Evolution of the hourly consumption of BACHELARD and M5 meters during week 33

3.5.3. Leak III

The hourly consumption of the three general meters CITE SCIENTIFIQUE, 4CANTONS and ECL during the weeks 38 - 40 is shown in Figure 3.24. The sudden increase in the water consumption observed September, 17 at 4:00 am indicates a leak which affects the ECL and 4CANTONS meters. Comparing the night flow before and during the leak, the volume of water loss is estimated to 12 m^3/h. Since this leak affects the ECL and 4CANTONS meters, it is localized in the South West of the campus.

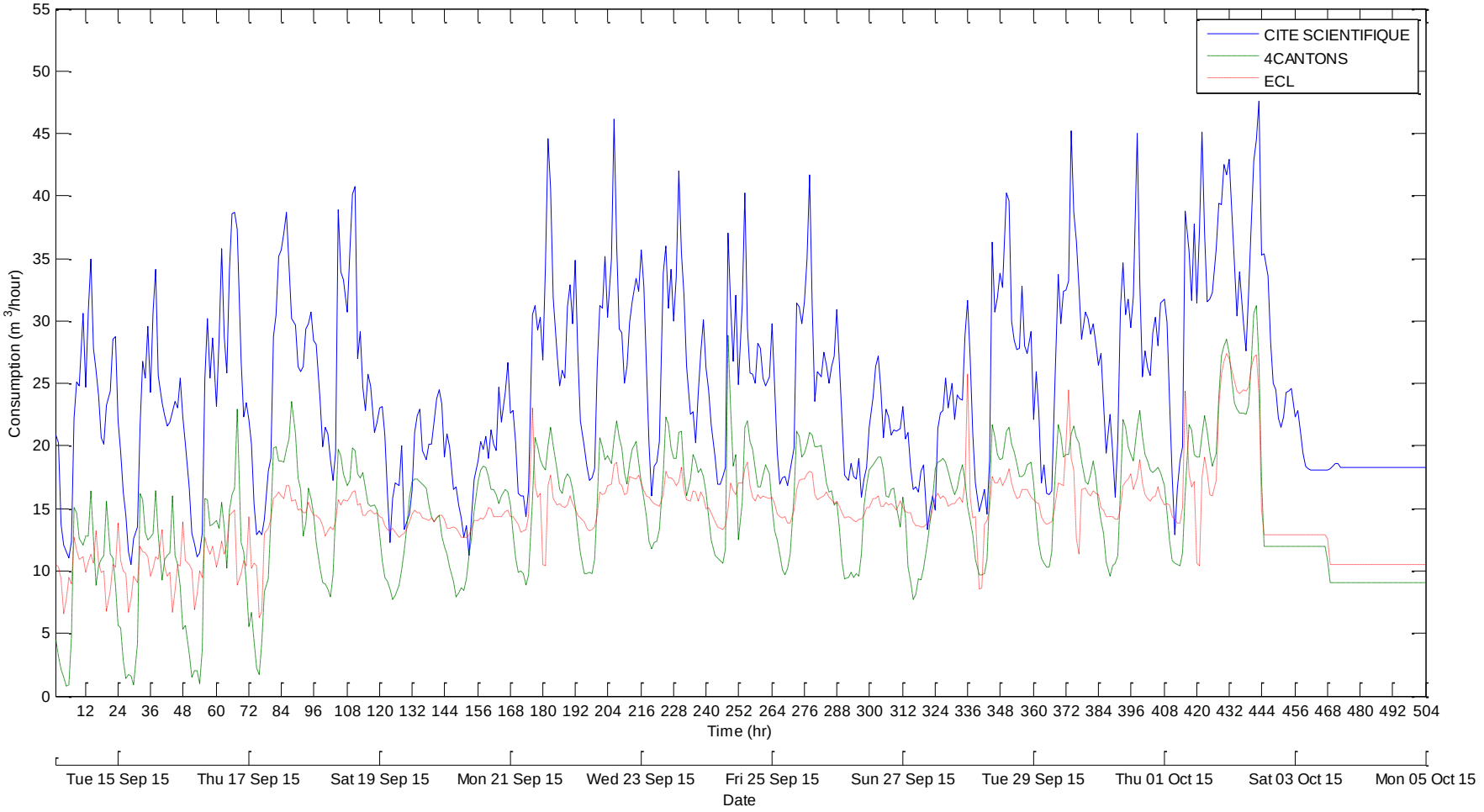

Figure 3.24: Evolution of the hourly consumption of CITE, 4CANTONS and ECL meters during weeks 38 till 40

3.5.4. Summary of water consumption data - General meters

Table 3.2: Summary data from the statistical analysis of the principal meters in the looped part

General Meters	Consumption Profile	Associated Sub-meters	Minimum Consumption	Maximum Consumption
CITE SCIENTIFIQUE	Clear distinction between working days and weekends or holidays	Campus Buildings Restaurants Residences	1.41 m^3/h (24 Dec) The background leakage is due to the night consumption of the students' residences.	80.9 m^3/h at midday (abnormal consumption) 47.6 m^3/h (2 October: 10 am)
ECL	Low distinction between working and non-working days	Campus Buildings Residences	4.91 m^3/h (10 August: 11 am)	30.5 m^3/h at midday (abnormal consumption) 27 m^3/h (24 November: 11 am)
4CANTONS	Medium distinction between working and non-working days	Campus Buildings Restaurants Residences	0.09 m^3/h (29 December: 5 am)	31.2 m^3/h at midday (abnormal consumption) 22 m^3/h (23 November: 3 pm)
BACHELARD	No distinction between working and non-working days but important consumption at the morning and at night	Bachelard Students' Residence	0.07 m^3/h (26 September: 3 am) Night consumption due to the occupancy of the residences by the students.	10.5 m^3/h (29 December: 2 pm)
M5	Clear distinction between working days and weekends or holidays	Mathematics buildings: M2, M3_LIFL, M3, M4_CRI, M5	0.3 m^3/h (25 August: 2 am) Probably a leak	2.59 m^3/h (2 July: 2 pm)

Table 3.3: Summary data from the statistical analysis of the principal meters in the disconnected part

General Meters	**Consumption Profile**	**Associated Sub-meters**	**Minimum Consumption**	**Maximum Consumption**
CUUEP	Clear distinction between working days and weekends or holidays	B5 and B6	0 (No Leak)	3.3 m^3/h (22 September: 10 am)
LML	Clear distinction between working days and weekends or holidays	M6 building with the laboratory	0.01 m^3/h	0.5 m^3/h in the morning (abnormal consumption) 27 m^3/h (2 June: 4 am)
HALLE VALLIN	Clear distinction between working days and weekends or holidays	Sport hall VALLIN	0 (No Leak)	0.4 m^3/h (31 January: 1 pm)
DELTEC ICARE	Clear distinction between working days and weekends or holidays	Parking DELTEC	0 (No Leak)	0.9 m^3/h (28 May: 12 pm)

3.6. Hourly water consumption - Sub-meters

According to the annual consumption, 11 buildings of LILLE1 have significant consumption. These buildings are: P5 and P5_BIS (Physics sector), POLYTECH, IUT, C6 and C9 (Chemistry sector), SN1, SN1_SERRES and SN3 (Biology sector), SH3 (Social Science sector) and A3. In addition to these 11 buildings, we identify also the Chemistry School ENCSL (C7), the restaurant PARISELLE and the building G of Residence BOUCHER. The hourly analysis is conducted for March 2015 including the winter holiday week (i.e. from 2 to 8 March). For each sub-meter, the background flow rates during business day and weekend and holidays are identified. This background flow is then classified as a leakage or legitimate night consumption.

- **Buildings P5 and P5_BIS (CERLA)**

Figure 3.25 and Figure 3.26 illustrate the hourly consumption in March 2015 for the buildings P5 and P5_BIS (CERLA), respectively. We observe that the winter holiday consumption is lower than that of working days. The minimum night consumption is null in winter holiday. This minimum flow varies in the weekend from 0.01 m^3/h to 0.25 m^3/h. During working days, the night consumption was equal to 0.3 m^3/h in March, 10 and then increased to 0.72 m^3/h March, 27. This night consumption is due to cooling machines. The maximum consumption of 3.9 m^3/h occurs at 2:00 pm March, 26.

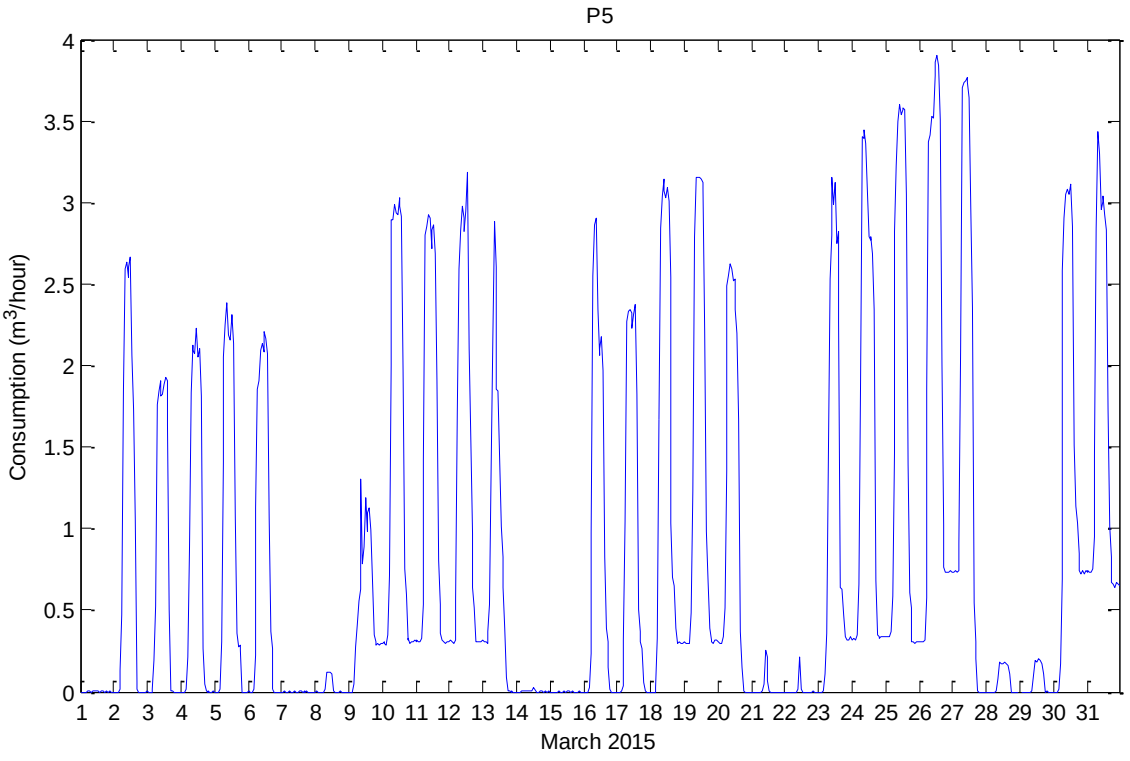

Figure 3.25: Hourly consumption of P5 - March 2015

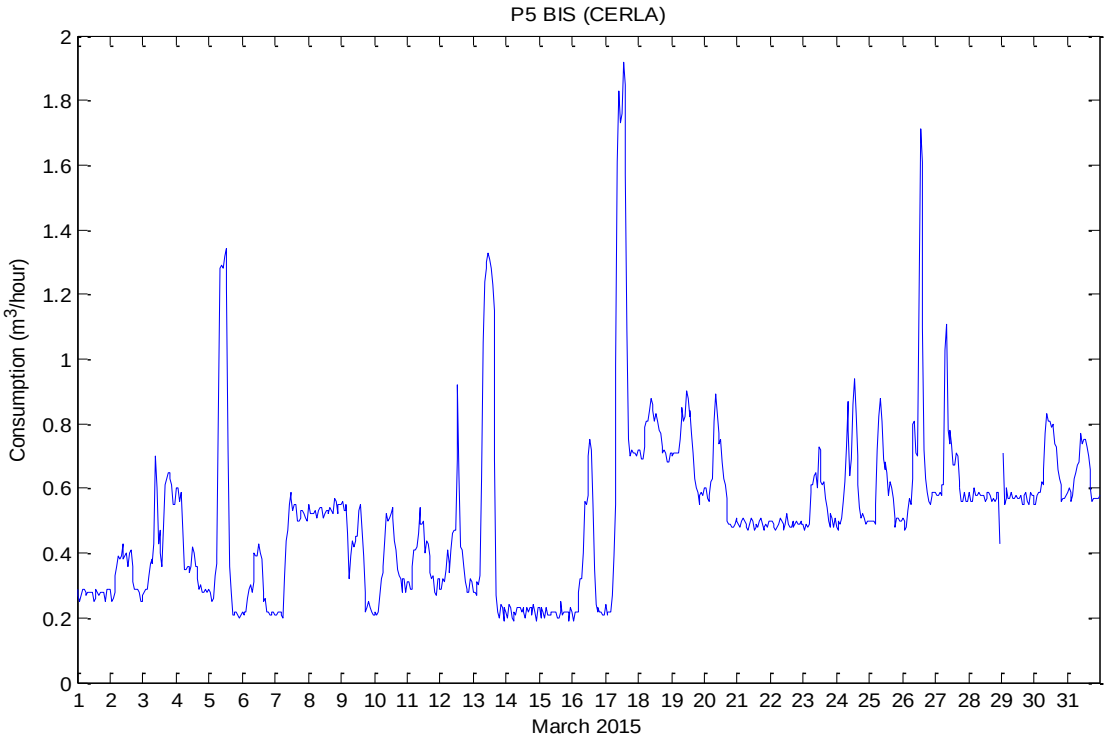

Figure 3.26: Hourly consumption of P5 BIS (CERLA) - March 2015

The hourly consumption of P5 BIS (CERLA) includes noise. The water consumption never dropped to zero. The night consumption increased from 0.2 m^3/h in March 15 to 0.56 m^3/h from March 28. This consumption could result from research facilities or leakage. A maximum consumption of 1.92 m^3/h occurs at 2:00 pm on March, 17.

- **POLYTECH**

The hourly consumption of POLYTECH (Figure 3.27) indicates a clear distinction between working days and weekends. The water consumption during the winter holidays (1st week) is half of that during working days. We observe three peaks: at 9:00 am, at noon and at 2:00 pm. We observe water consumption on Saturdays; the minimum consumption (0.01 m^3/h) is recorded on Sunday.

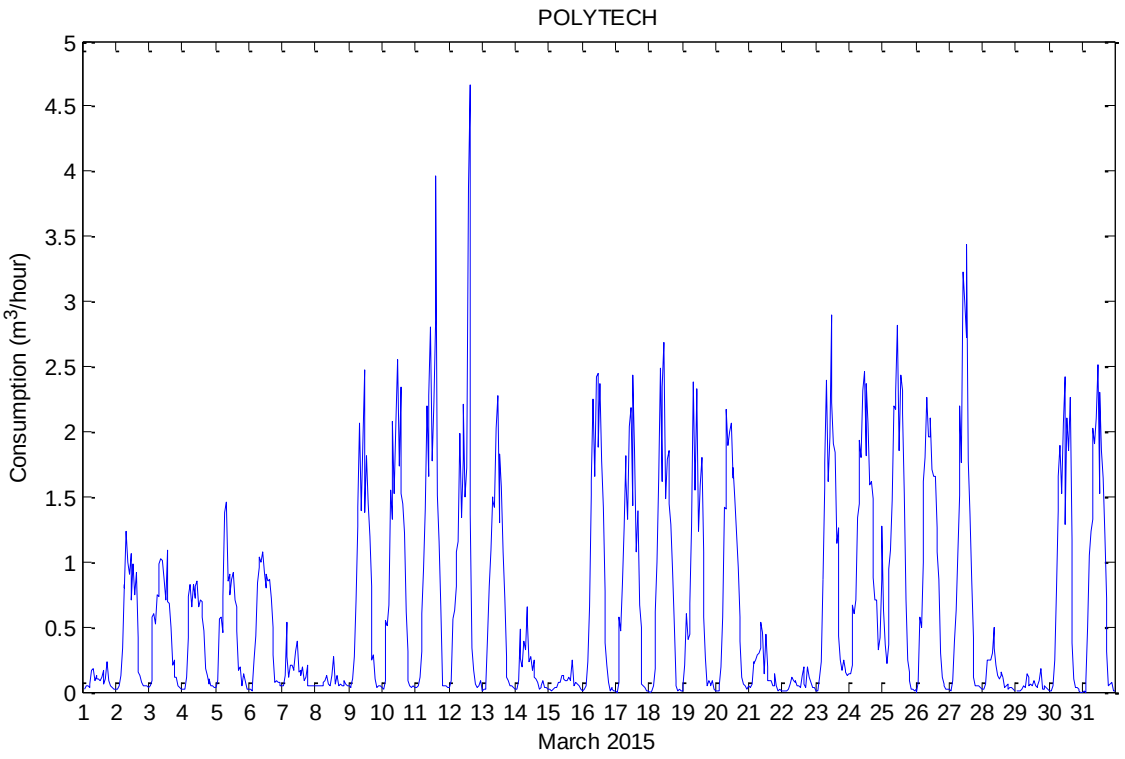

Figure 3.27: Hourly consumption of POLYTECH - March 2015

- **IUT**

Concerning the institute IUT, we observed a repeated hourly consumption during working days (Figure 3.28). The peak occurs between 10:00 am and 12:00 pm; it reaches 2.44 m^3/h at 10:00 am on March, 25. The consumption during the winter holiday is about 25% of that of working days. The minimum flow never drops below 0.2 m^3/h. This volume is probably due to a background leakage. It is equivalent to a water loss from 8 flush toilets.

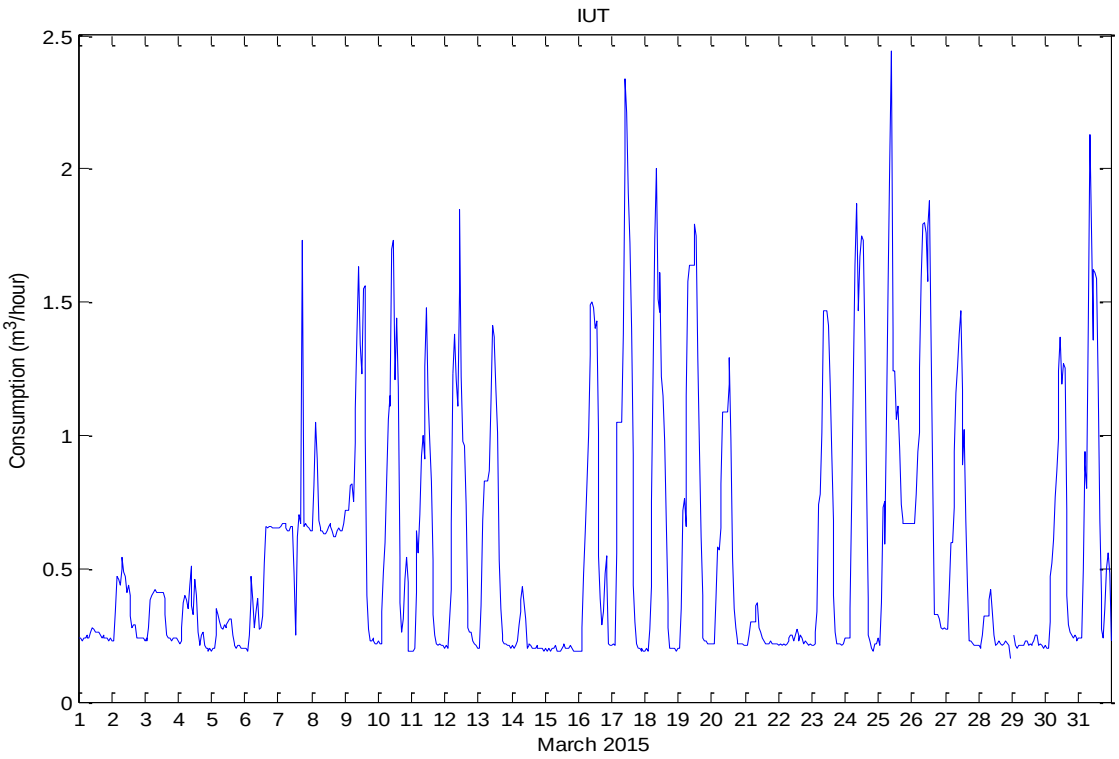

Figure 3.28: Hourly consumption of the IUT - March 2015

- **C6**

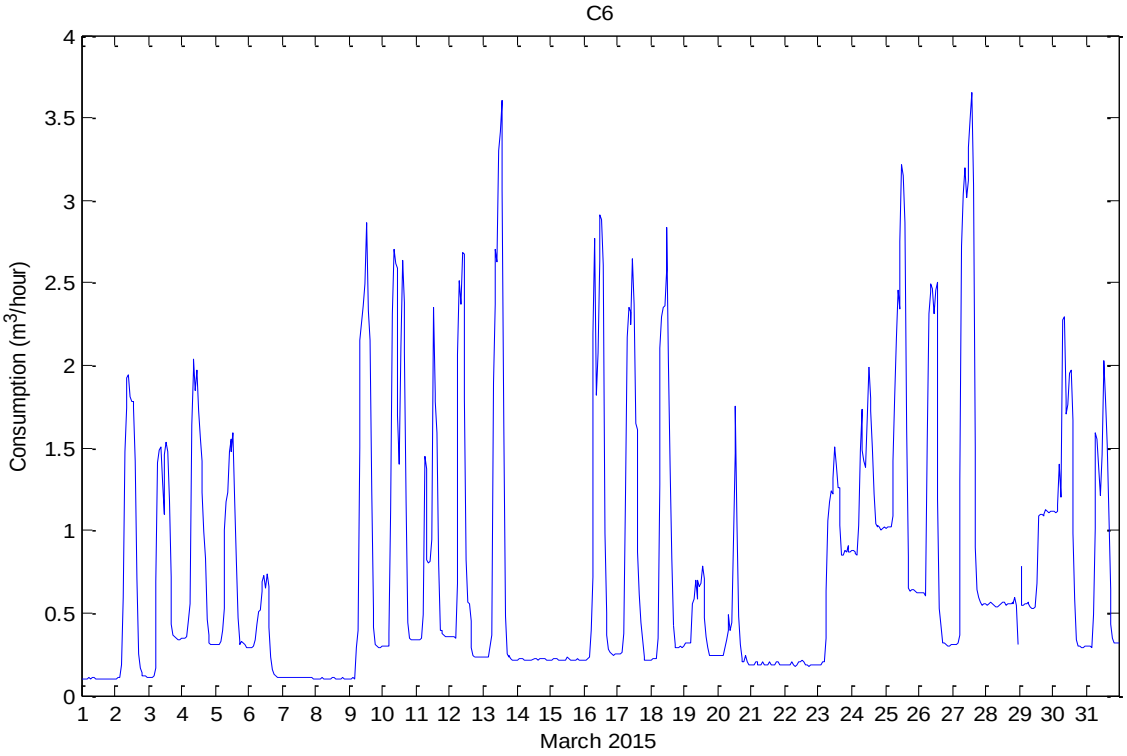

Figure 3.29: Hourly consumption of building C6 - March 2015

C6 is in the Chemistry sector. The water consumption of this building during March 2015 is depicted in Figure 3.29. The consumption during the winter holidays is due to research facilities. The distinction between the water consumption during the working days and weekend is very clear. During the non-working days, the consumption seems to be uniform and equal to 0.21 m^3/h. The minimum flow increases during the working days; it reaches 1 m^3/h 25 March, 25 at midnight.

- **C9**

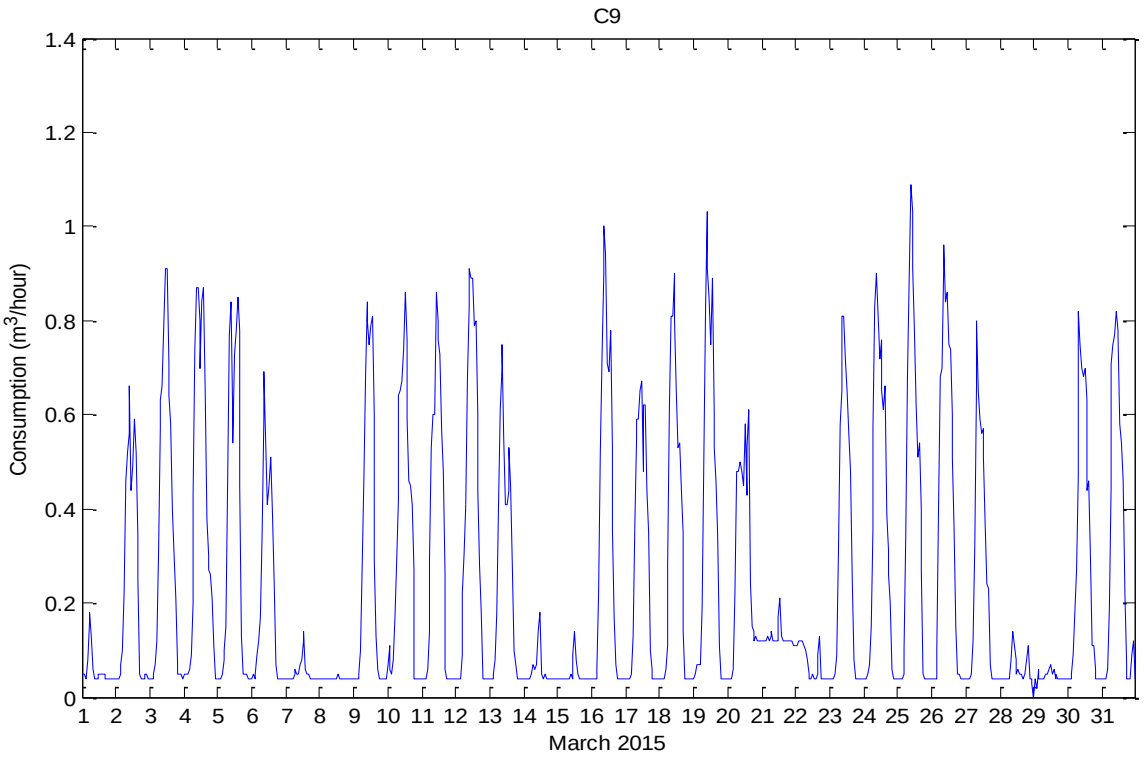

Figure 3.30: Hourly consumption of building C9 - March 2015

The chemistry sector also includes building C9 characterized by high water consumption. The consumption of this building during holidays is similar to that of working days. A minimum night flow of 0.04 m^3/h occurs during the weekdays between 8:00 pm and 4:00 am and. It could result from leakage inside the building.

- **SN1 and SN1_SERRES**

Buildings SN1 and its extension SN1_SERRES have the same water consumption profile. Figure 3.31 and Figure 3.32 represent the hourly consumption in March 2015. The holidays' consumption is about 50% of that of working days. The peak consumption during working days occurs at midday. The SN1 and SN1_SERRES peak consumptions are equal to 6.02 m^3/h and 4.28 m^3/h, respectively. The night flow is null during the working days and the weekends.

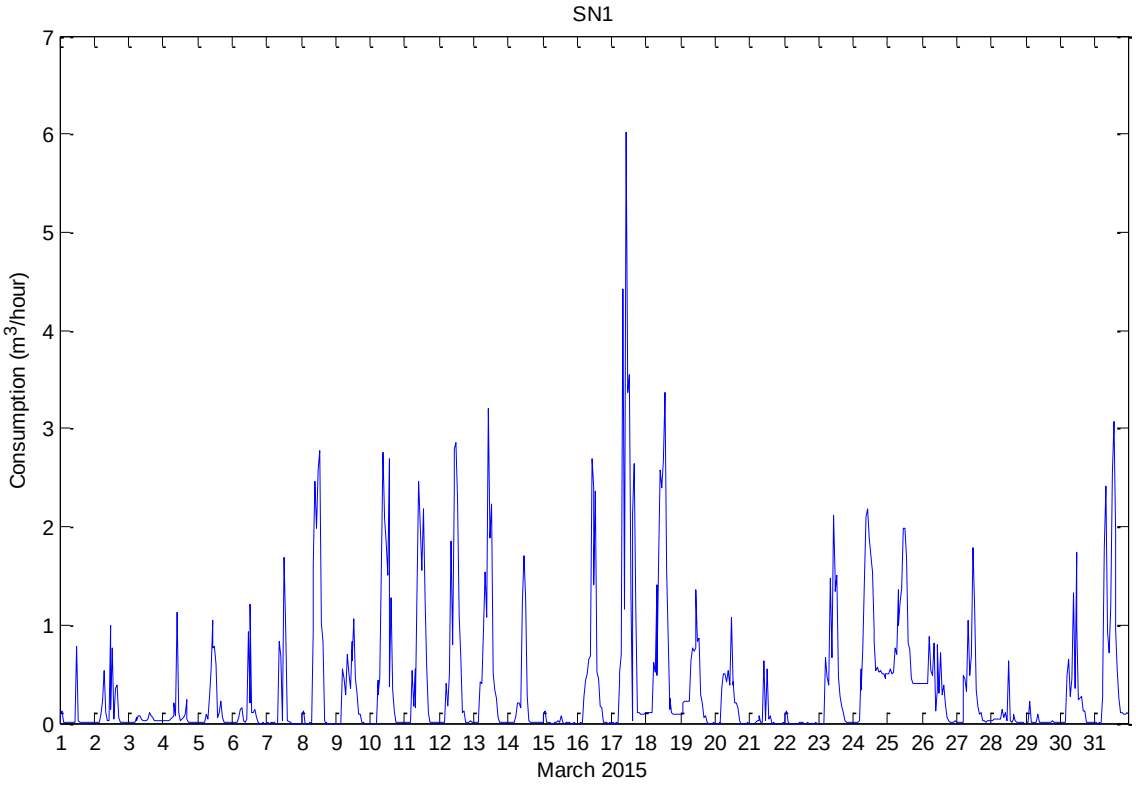

Figure 3.31: Hourly profile consumption of building SN1 - March 2015

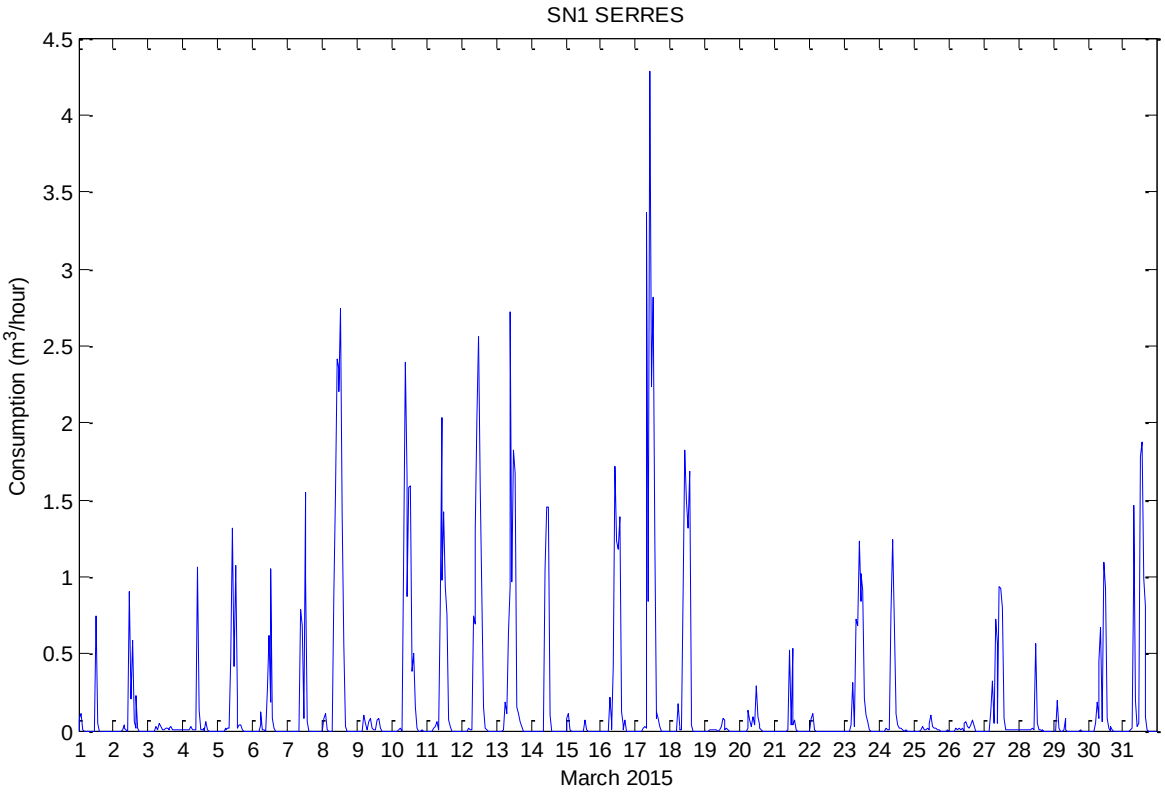

Figure 3.32: Hourly consumption of building SN1 SERRES - March 2015

- **SN3**

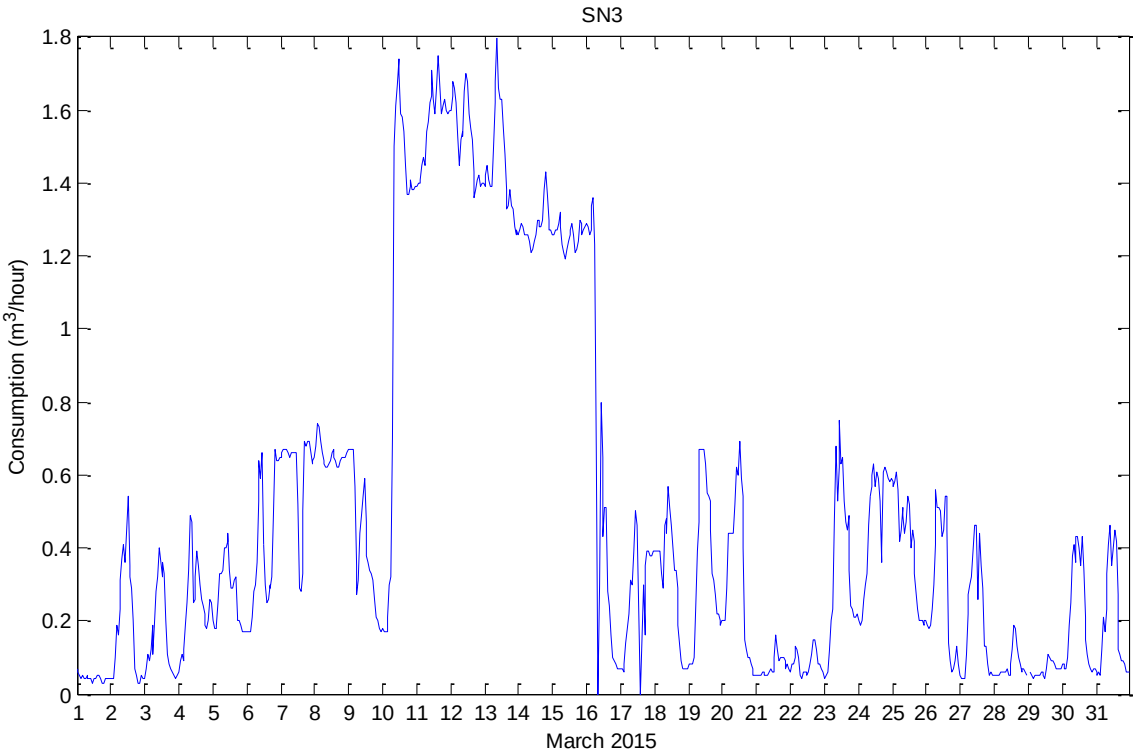

Figure 3.33: Hourly consumption of building SN3 during March 2015

The hourly consumption of the SN3 (Figure 3.33) in March 2015 shows a suspected leak on March, 10 at 10:00 am. This leak is estimated to 1 m^3/h. The water consumption presents a similar profile between the winter holidays and working days. The night flow never drops below 0.04 m^3/h. This can be explained either by a background leakage inside the building or a legitimate consumption by research facilities.

- **SH3**

SH3 is in the Social Science sector of the campus. Compared to other buildings in this sector, SH3 has the highest consumption (1 340 m^3 in 2015). The hourly consumption in March 2015 is shown in Figure 3.34. We note a clear distinction between the consumption during the holidays and working days. During the winter holidays, the consumption is reduced to the 1/3rd of that of working days. During working days, a peak is observed at 11:00 pm. It reaches 0.9 m^3/h on March, 10 at 11:00 pm. The night flow during the working days and weekends is null.

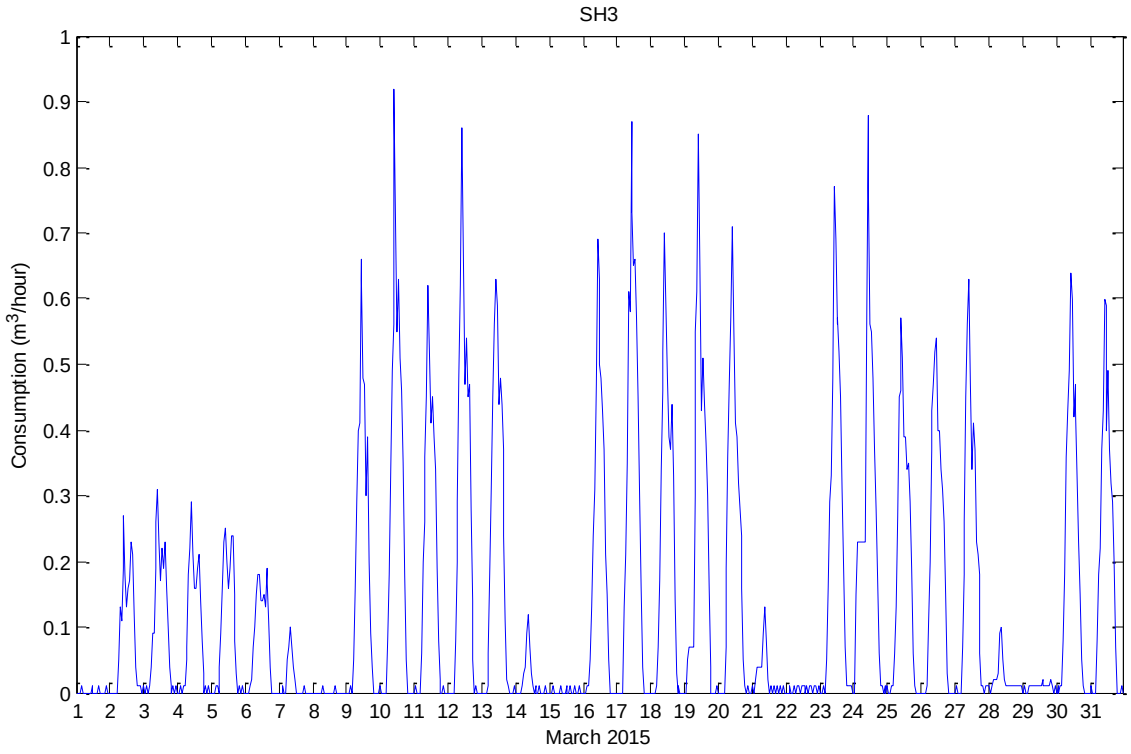

Figure 3.34: Hourly consumption of building SH3 - March 2015

- **A3**

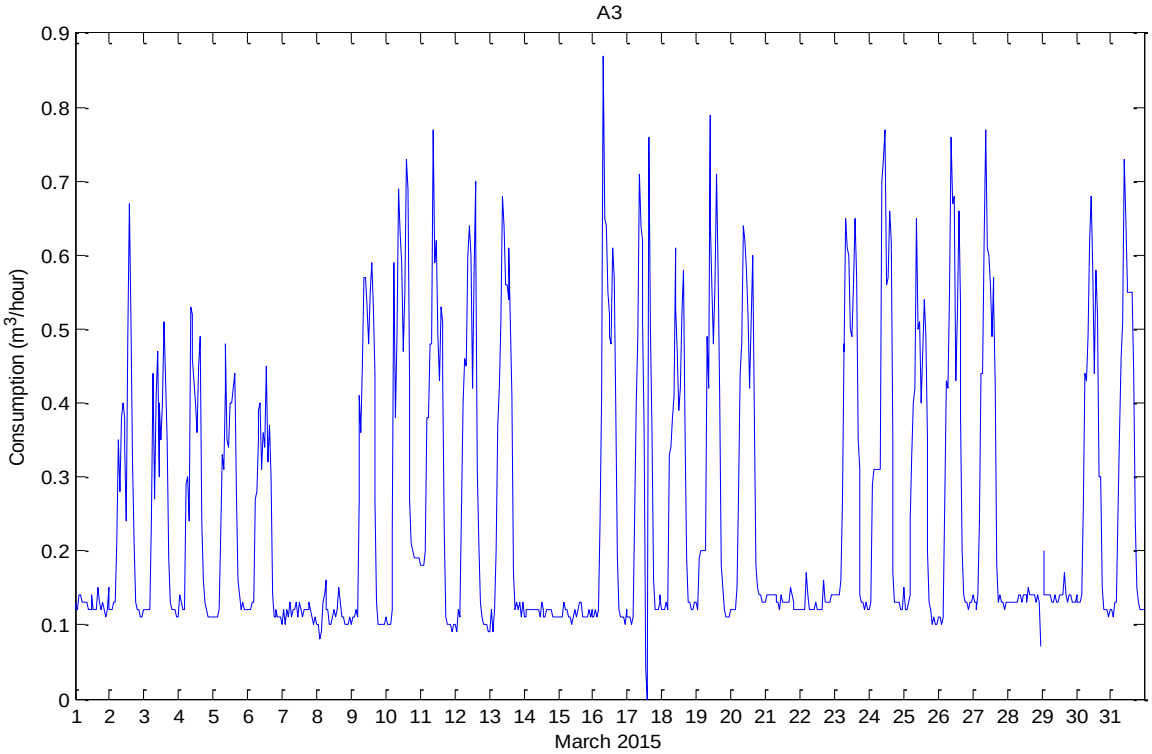

Figure 3.35: Hourly profile consumption of building A3 - March 2015

A3 is used by administration. Figure 3.35 shows the hourly consumption of this building in March 2015. We do not observe difference between the water consumption during working days and holidays. The daily consumption profile shows two peaks: around 10:00 am and at 3:00 pm. The minimum consumption either in business days or holidays is equal to 0.12 m^3/h. In this building, there is a part dedicated for the security of the campus. The security agents work there even during the night. If we consider that flush toilets use 10 liters of water per flush, the night flow of 0.12 m^3/h will correspond to 12 flushes per hour.

- **ENSCL (C7)**

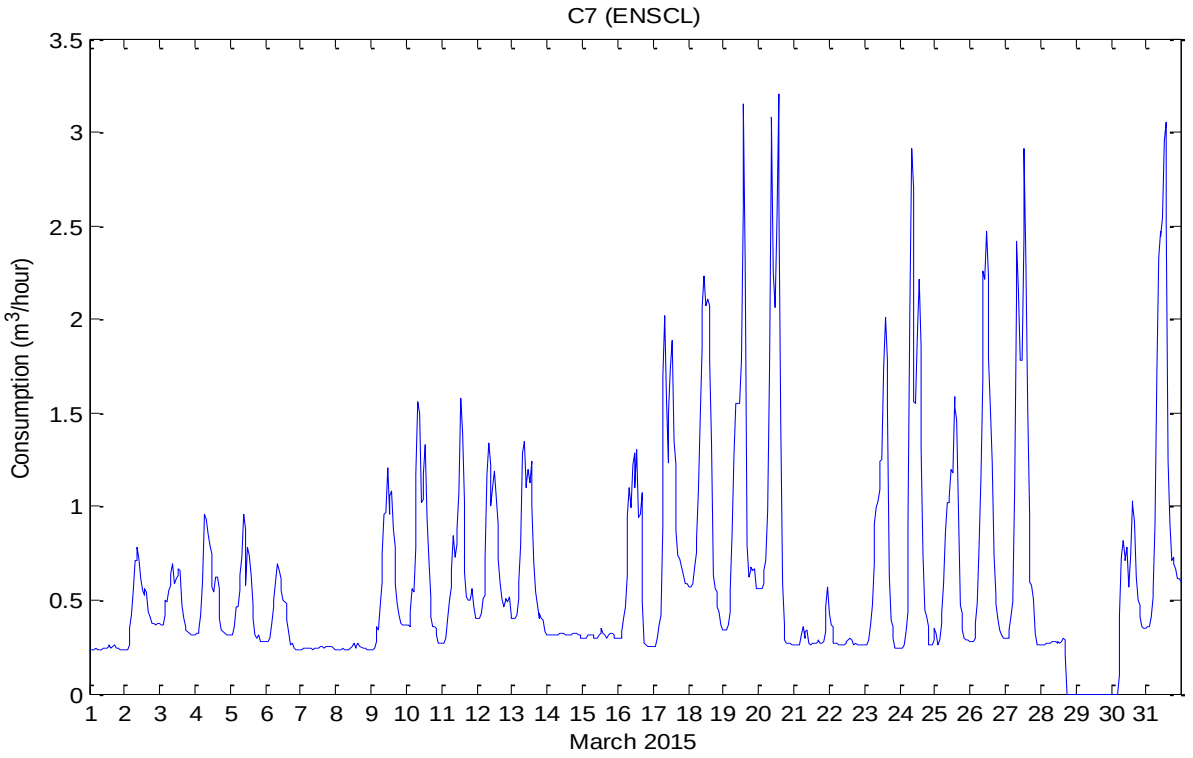

Figure 3.36: Hourly profile consumption of the sub-meter C7 during March 2015

The water consumption of the chemistry school ENSCL (C7 building) represents 2% of the total consumption in 2015. The profile of the water consumption (Figure 3.36) shows a difference between working days and holidays. Two peaks are identified during the day: at 9:00 pm and at 2:00 pm. The minimum consumption (0.3 m^3/h) is due to research facilities. As shown in Figure 3.36, this minimum flow tends to be null on Sunday 29 March proving that this building is free of any leakage.

- **PARISELLE Restaurant**

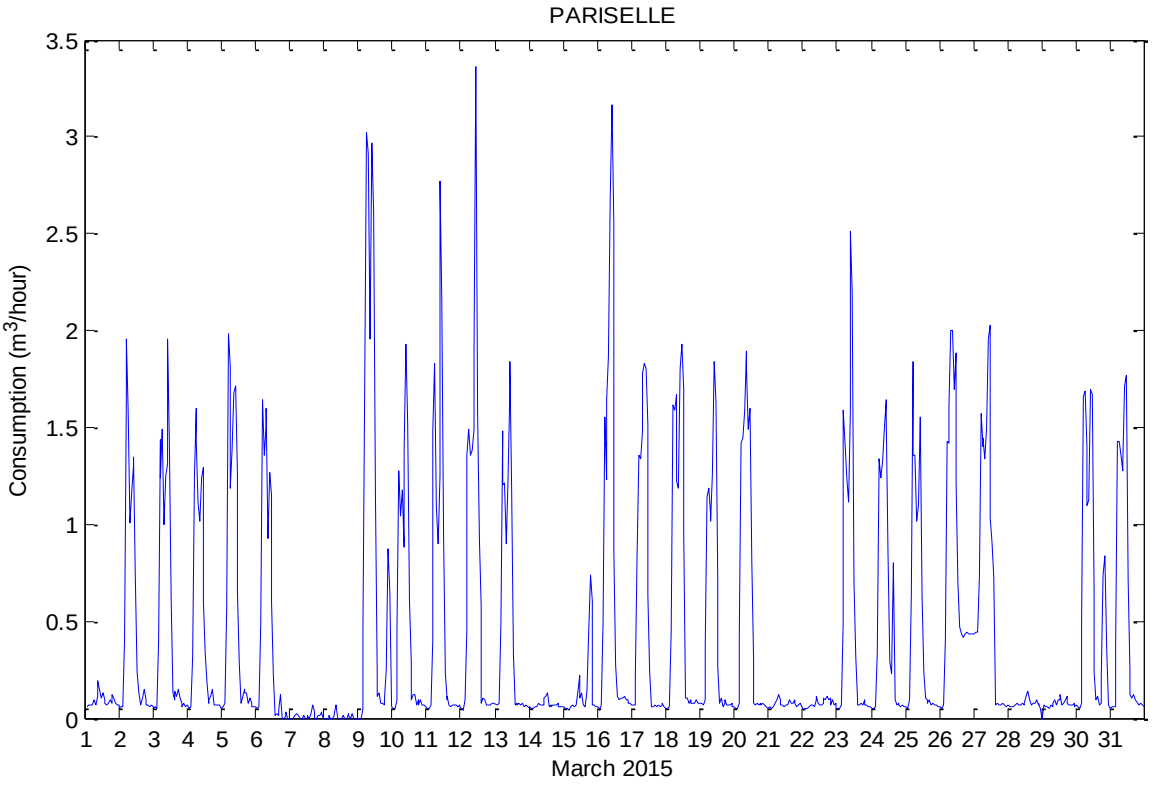

Figure 3.37: Hourly profile consumption of the sub-meter PARISELLE during March 2015

The restaurant PARISELLE consumed in 2015 more water than the two other restaurants in the campus (BARROIS and SULLY). The hourly profile (Figure 3.37) shows two peaks during working days: around 8:00 am and at noon. These peaks describe the activity of the restaurant. We observe that this restaurant used water in the first week of the month which was a holiday week. In fact, during the winter or spring holidays, one restaurant of the three remains opened for researchers, administrators and international students. A minimum night flow of 0.5 m^3/h is observed in working days and holidays. This can be explained by a leakage and probably from the dishwashing machines.

- **BOUCHER Residence**

BOUCHER is one of the four CROUS students' residences. In 2015, this residence consumed more than the other 3 residences. The water consumption in this residence is measured by two sub-meters: G that measures the consumption of 3 buildings (F, G and H) and the sub-meter J that measures the volume of water consumed by buildings I and J. Figure 3.38 shows the hourly consumption of building G in March 2016. We cannot distinguish the consumption during working days from that during holidays or weekends. The profile shows a domestic usage with 3 peaks per day: around 8:00 am when the students prepare themselves before leaving to faculties, at midday which is the break time and around 8:00 pm when the students

take their showers and use washing machines. The minimum night flow recorded at 3:00 pm on 26 March 2015 was equal to 0.18 m^3/h. This volume corresponds to 18 flushes per hour admitting that the flush toilets use 10 liters of water per flush.

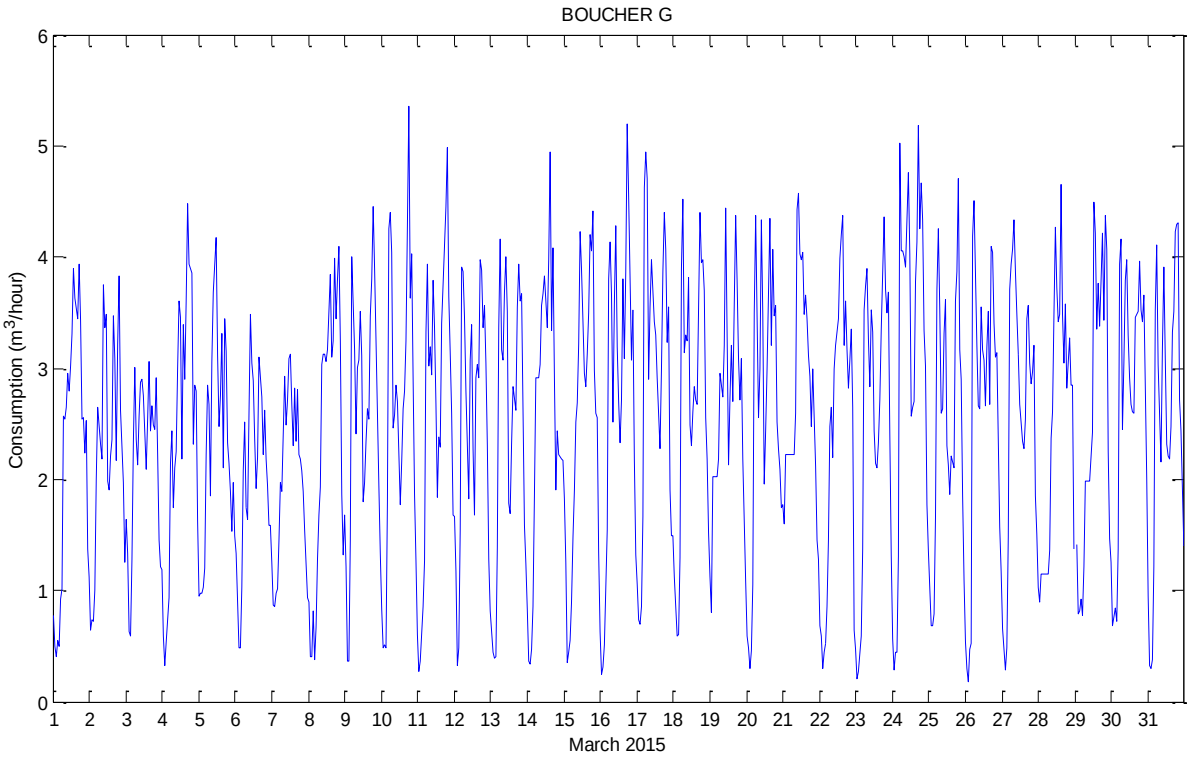

Figure 3.38: Hourly profile consumption of the meter G of BOUCHER residence during March 2015

3.6.1. Minimum night flow

In order to estimate the background leakage in the buildings of the campus, the Minimum Night Flow (MNF) is computed between 2:00 am and 6:00 am in August 2015 when the majority of the campus' buildings are closed. Figure 3.39 represents the distribution of the average of the MNF recorded in August 2015. It can be shown that the average MNF for the students' residences reaches 0.5 m^3/h. This consumption is related to the presence of international students in the Campus. The volume of 0.5 m^3/h is equivalent to 50 toilet flushes per hour.

Some research buildings such as C6, P5_BIS (CERLA), SN3 and SN4 continue to work in summer, their MNF varies between 0.05 and 0.1 m^3/h.

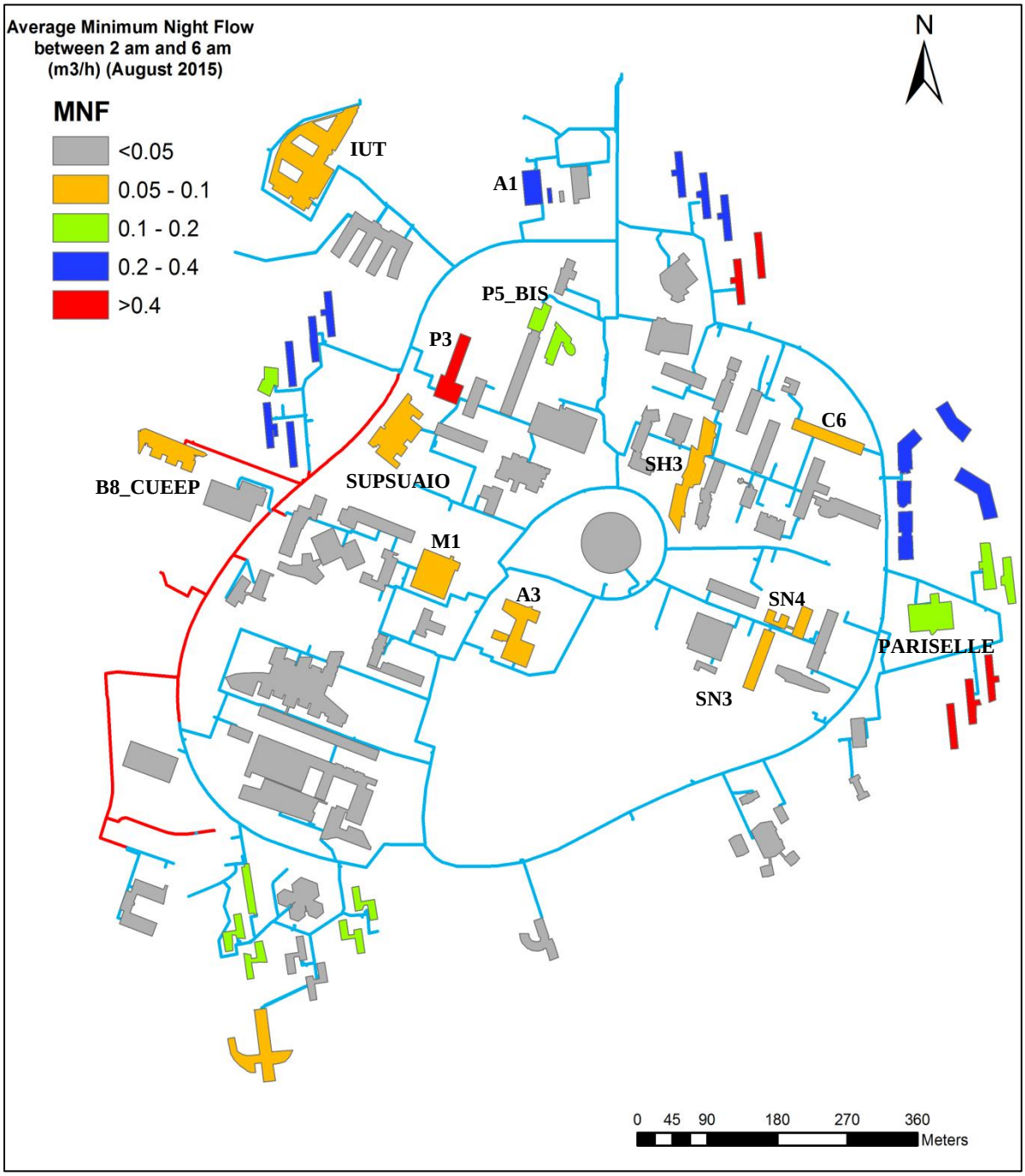

Figure 3.39: Minimum night flow in August 2015

According Figure 3.39, a leakage probably occurs in building P3 where the MNF reaches 0.5 m^3/h. The background leakage occurs also in restaurant PARISELLE (MNF = 0.11 m^3/h), in SUPSUAIO (MNF = 0.06 m^3/h), B8 CUEEP (MNF = 0.06 m^3/h), IUT (MNF= 0.09 m^3/h), SH3 (MNF = 0.09 m^3/h) and M1 (MNF= 0.06 m^3/h). The MNF of the heating center A1 recorded a critical average value of 0.4 m^3/h. The Analysis of the hourly consumption of A1 shows a continuous flow of 10 m^3/h between August, 27 at 10:00 pm and August, 28 at 9:00 am.

3.7. Clustering

The k-Means algorithm is used to establish building clustering according to their consumption profile. Since the k-Means algorithm is a distance based method (Euclidean distance), all input features are normalized. The algorithm starts with initial seeds of clustering. The data are then compared with each seed by means of the Euclidean distance and are assigned to the closet cluster seed. The method is then repeated until convergence. The most important challenge for k-Means is that the number of clusters has to be specified first. Kaufman et al. (2009) proposed the Silhoutte plot method. The Silhouette analysis provides a succinct representation of how close each point in one cluster is points in the neighboring clusters. Kailing et al. (2004) suggested measuring the quality of clustering outcome and compare it to the reference clustering:

$$Q_k(C) = \sum_{C_i \in C} \frac{|C_i|}{|O|} \cdot \left(1 - entropy_k\left(C_i\right)\right) \tag{3.1}$$

where O represents the set of data objects, k is the reference clustering of O, C is the clustering to evaluate, and $entropy_k(Ci)$ the entropy of cluster C_i with respect to k. The quality score is close to 1 if the clustering results match the reference clustering or 0 if all clusters are completely mixed or all points are predicted to be noise (Ay et al., 2014).

The percentage measured during two years from the early morning till the late night as well as the hourly consumption, the average water usage by working days and holidays and the overall consumption were used to group the meter IDs related to the university buildings into a 12 clusters that have similar consumption profile. The reference clusters refers to classification of according to their use into 8 categories: administration, teaching, research, teaching and research, catering, student residences, sport and services. The quality score for 12 clusters is 0.52 showing that a reasonable structure has been found.

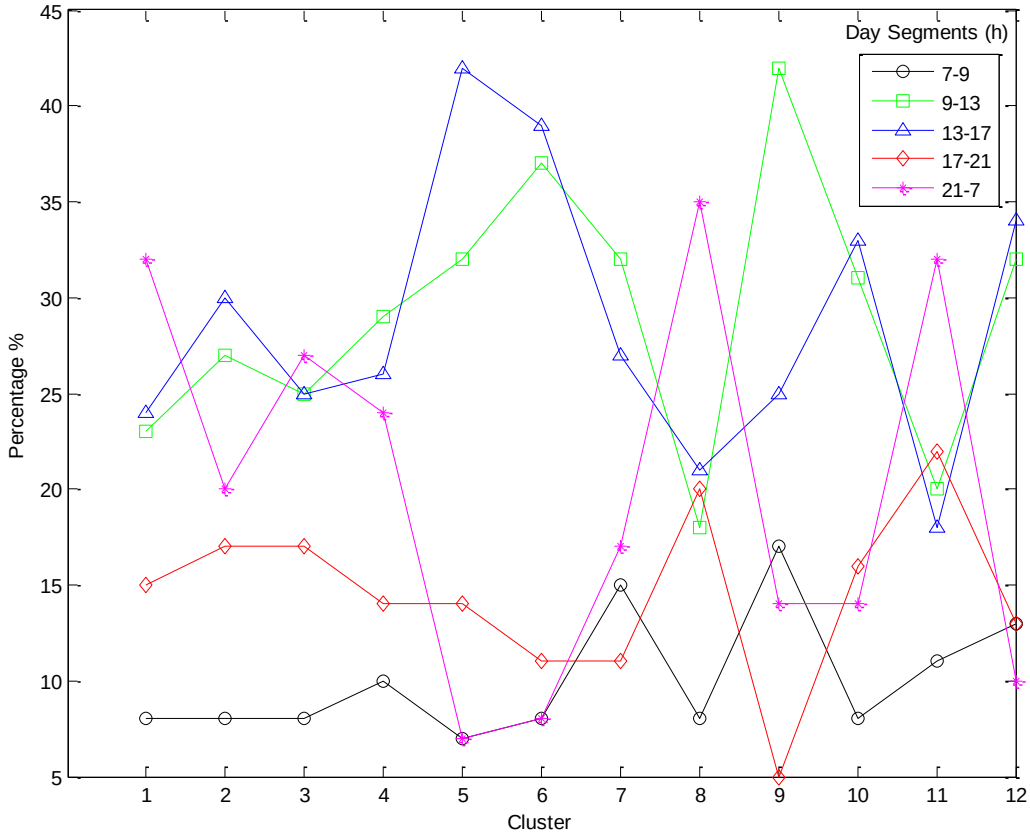

Figure 3.40: Percentage of water usage per day segment for each cluster

Figure 3.40 shows the clustering result. We observe that clusters can be regrouped into 4 main categories:

- I: Morning usage for clusters 7 and 9. The first group contains meter ID with a high morning usage of water especially between 7 am and 9 am. These two clusters contain certainly the restaurants of the campus which are highly active in the morning and the midday.
- II: Morning and afternoon usage for clusters 2, 5, 6, 10 and 12. The second group represents buildings used in teaching, administration and services which consume water during the working hours between 9 am and 5 pm.
- III: Night usage for clusters 1, 8 and 11. These clusters represent definitely the student residences and the buildings for sport and research which are highly active during the night.
- IV: Day and night usage for clusters 3 and 4. The last collection is made of clusters with a more equally distributed usage of water from 9 am till 7 am on the next day. These clusters represent mainly the buildings for teaching as well as for research regarding the late evening and early morning water usage. It may comprise the biology and chemistry research buildings which contain some machines that need water and stay turned on even in the night.

3.8. Conclusion

The flow data collected from the 93 automatic meter readers deployed in SunRise Smart Water demo site provide potentially useful information for detecting the leaks. In this chapter, a descriptive analysis has been presented in order to study the behavior of the water consumption at the scale of a building and a sector. A platform has been developed to aggregate easily the water consumption on different time scales: yearly, monthly, weekly, daily, hourly and intra-hourly. It helps to compute directly the minimum night flow, calculate the water balance and identify the performance of the network. This platform accelerates the data transformation process and it is suitable for any projects dealing with massive time-based or telemetry data.

In a complex meshed water network, the identification of the sub-meters that are related to the appropriate bulk meter is a big challenge. The correlation analysis of the weekly consumption profile discussed in this chapter has allowed linking the "child" meter IDs to the appropriate "parent" water meter. This analysis helps the water utilities to take the decisions to close permanently the appropriate valve to subdivide the meshed network into District Meter Areas (DMAs).

The analysis of the hourly water consumption profile has proved that the flow change method can be used to spot the leakage. Three critical periods in 2015 corresponding to "possible" leaks have been identified in this chapter.

The calculation of the Minimum Night Flow (MNF) inside the buildings during a period of low water demand has permitted to determine if the building is free of water leakage or not. This analysis of the MNF approach can be used to compute a threshold value for each building. Therefore, the leakage can be detected automatically online by comparing the actual MNF with the computed threshold.

In this chapter, a clustering method has also been presented. The k-means algorithms evaluated using the entropy scorer has been applied to cluster together the AMRs based on similar behaviors in terms of water usage. This clustering method is able to categorize, without any prior knowledge, the type of usage of the building depending on the water consumption. It can also be a useful method for the water companies to create customized tailored contract offers for the customers based on different behaviors in water usage.

In the next two chapters, the focus will be on the leak detection methods. The water balance will be computed to calculate the level of the water loss. In addition, a set of advanced statistical and artificial intelligence measurements-based techniques will be developed, discussed and evaluated according to its capabilities to detect the possible leaks identified in this chapter.

Chapter 4

Leak Detection Using the Water Balance Method

This chapter presents the application of the water balance method for the detection of water leakage in SunRise Demo Site. The water balance set up at regular intervals quantifies the amount of water that is being lost. This method allows understanding the magnitude, sources, the cost and the key components of Non-Revenue Water (NRW). Two techniques are used: i) the top-down method and ii) the bottom-up real loss assessment. The chapter presents the development of an Active Leakage Control (ALC) strategy for the detection of water leakage and the application of this strategy to SunRise Demo Site.

4.1. Water Balance Method

The water balance method aims to account the volume of water lost in a water distribution networks during a defined period of time. It allows identifying the components that contribute to water loss in a standardized format. An abbreviation of the water balance terminology provided by IWA is described in Table 4.1. The apparent losses include: i) the unauthorized consumption due to water theft and illegal connections and ii) meters inaccuracies. The real losses include: i) the leakage on transmission and distribution mains, ii) the leakage and overflows at utility's storage tanks and iii) the leakage on service connections up to point of customer metering. The water balance calculation depends on the accuracy and quality of data used in the computation.

Table 4.1: IWA water balance terminology (abbreviation)

System input volume, W_I	Authorized consumption,W_C	Billed authorized consumption, W_{BC}
		Unbilled authorized consumption, W_{UC}
	Water losses,W_L	Apparent losses, W_{AL}
		Real losses, W_{RL}

In order to calculate the water balance, the IWA proposed two methods: i) the top-down annual water balance and ii) the bottom-up real loss assessment.

4.1.1. Top-down annual water balance

This method aims to compute the overall annual real losses. The top-down approach requires the collect of data from the bulk (general meter) and customer sub-meters for the period of at least one year. The bulk meters installed at the upstream of the water distribution network or at the main entrance of a district zone measure the amount of water supplied to the system W_I. The billed authorized consumption W_{BC} is determined from the sub-meters that count the water consumed by the customers. The estimated unbilled authorized consumption W_{UC} includes: i) unmetered households, ii) fire services and iii) water used for operational purposes such as cleaning and flushing.
Once the system input volume and the authorized consumption have been calculated, the water losses W_L are therefore deduced. The real losses W_{RL} are then derived by subtracting the apparent losses W_{AL} from the overall water losses W_L. In order to estimate the apparent losses, Thornton et al. (2008) recommends using 0.25% of the total input volume as an initial approach. According to the IWA, the apparent losses are estimated to 5% of the billed metered consumption for developing countries. For developed countries, they are estimated between 1.5 to 2%.

The top-down water balance is performed on an annual basis. In order to develop an appropriate water loss strategy and limit the runtime of new leaks, this approach has to be combined with a bottom-up analysis based on night flow measurement.

4.1.2. Bottom-up approach

The bottom-up approach is used to verify the results of the real loss volumes obtained from the top-down assessment. The bottom-up method is based on the calculation of the minimum night flow (MNF) that occurs generally between 2:00 am and 4:00 am. The MNF has to be computed when exceptional night use (i.e. for irrigation or used for special machines) is least in order to obtain reliable results.

4.2. Water balance - SunRise water system

The annual supply volume in the campus is calculated from the data collected by the 13 general meters. In 2015, the supply volume W_I is equal to 363 180 m^3. The total water consumption of the buildings in the campus is measured by a set of 80 AMRs. According to data collected, the billed authorized consumption W_{BC} is equal to 212 320 m^3. Figure 4.1 shows the water supply and the water consumption in 2015 based on a daily scale. This Figure 4.1 as well as Figure 4.2 show the three leaks described in Chapter 3. Table 4.2 details the periods of leaks occurred between January and October 2015 in addition to the type, the duration and the location of the

bursts. According to Figure 4.2, a decrease of the NRW volume is observed during in May 2015. This decrease is due to the loss of the connection in the telemetry system.

According to the NRW evolution shown in Figure 4.2, two periods can be identified: from the beginning of 2015 till the end of October and from November till the end of the year. They correspond to the periods before and after the adopted active leakage strategy, respectively.

Table 4.2: Periods of leaks detected between January and October 2015

Onset	**Type**	**Duration**	**Location**
17 March 2015	Leak	1 day	Burst pipe - construction of the new library
11 August 2015	Leak	3 days	Burst pipe - construction of the new library
17 September 2015	Progressive Leak	17 days	Unreported leak near the 'Ecole Centrale'

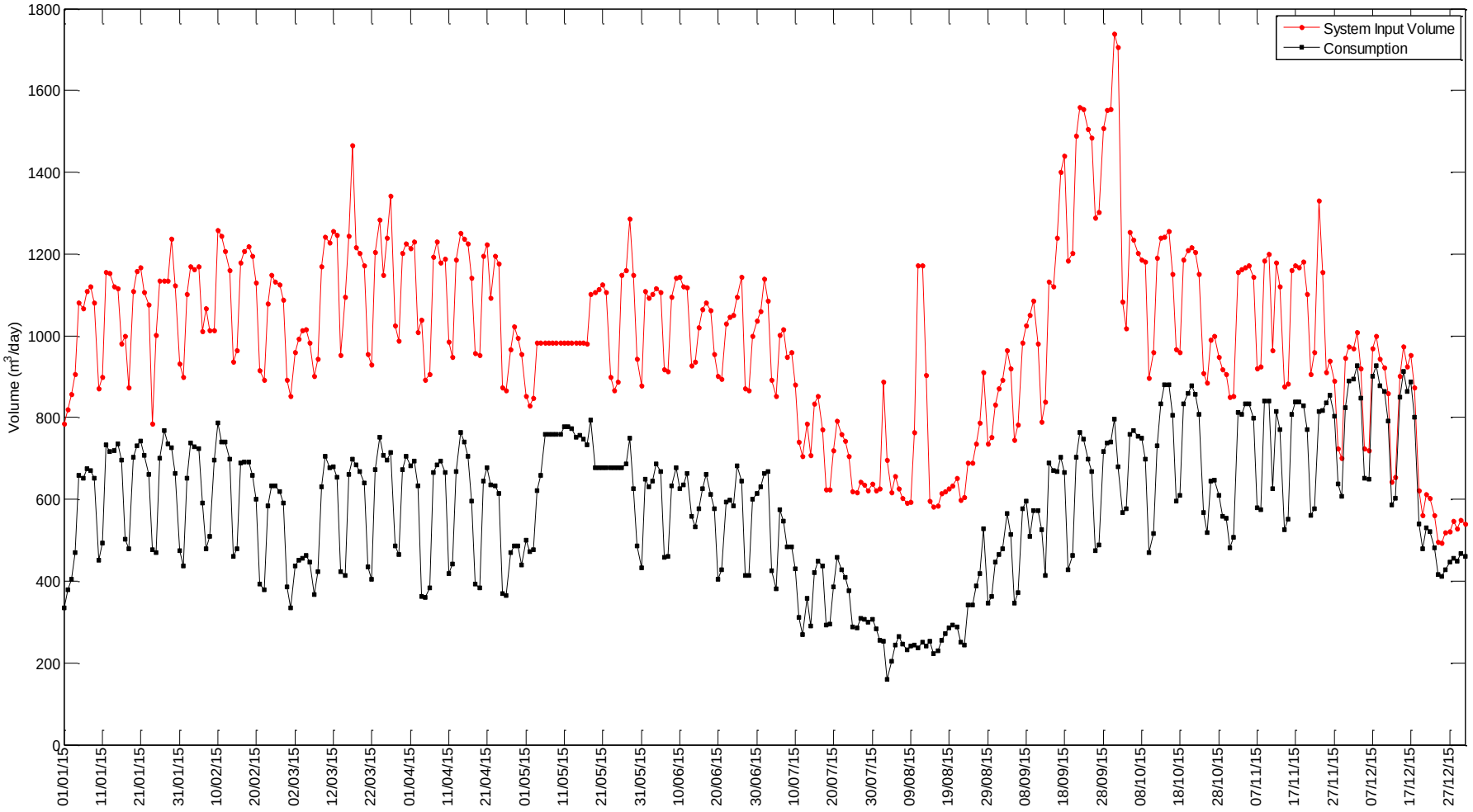

Figure 4.1: Comparison between the water supply and the buildings consumption - 2015

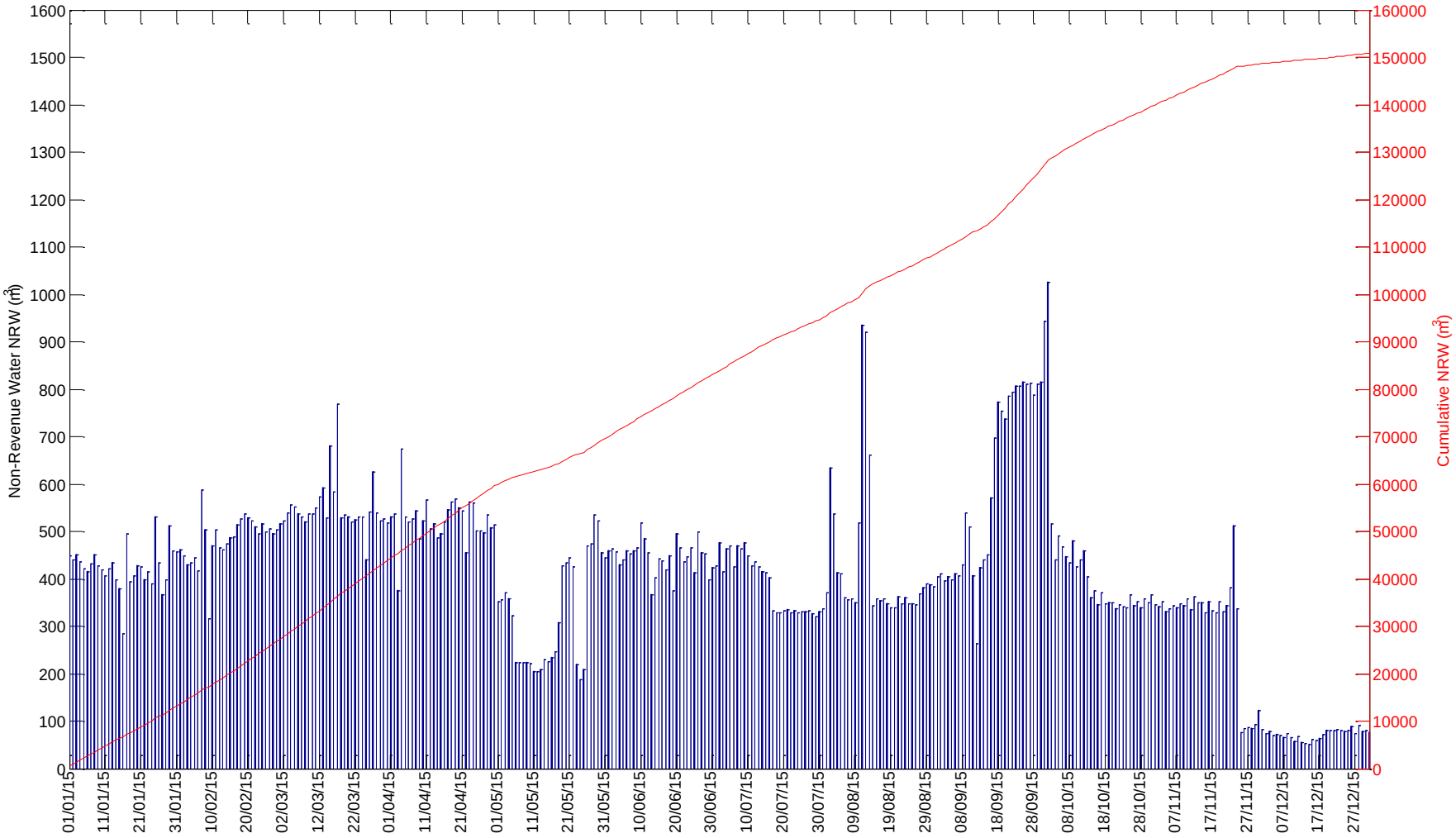

Figure 4.2: Non-Revenue Water NRW (m^3) - 2015

4.2.1. NRW January - October 2015

From January to October 2015, the distributed volume W_I is equal to 308 962 m^3, whereas the billed consumed volume W_{BC} is 169 370 m^3. The Linear Consumption Index (LCI) during this period is then equal to 37.7, which corresponds to urban network (Fantozzi et al., 2010). The efficiency of the system is equal to 55 %. Therefore, half of the water produced is lost. In order to calculate the authorized consumption, we have considered the following:

- The consumption of new student residence REEFLEX was not telemetered until 13 October 2015. The manual reading of the meter installed at the entry of the residence shows an index of **10 953 m^3**. This index corresponds to the consumption of the building starting from its occupancy until the installation of the telemetry.
- The sub-meter MDE was also not telemetered. The historical values show that this building dedicated for the service consumed an average of 45 m^3/month. Therefore, the unbilled consumption from January till October is equal to **450 m^3**.
- The telemetry of the sub-meter C3 was not working starting from the beginning of the year. Based on the historical mean value of 170 m^3/month, this building consumed a volume of **1 700 m^3** during this period.
- The telemetry of the building C6 stopped from 15 September 2015. It is estimated that this building consumed until the end of October a volume of **800 m^3**.
- Two buildings were under construction during this period. The first construction site is for the renovation of the library and the second one for the construction of the new building CISIT. The water used in these working sites was unbilled. It is estimated that these sites consumed from January till October 2015 a total volume of **10 000 m^3**.

Taking into account these volumes, the authorized consumption W_C from January till October 2015 is equal to 19 3273 m^3.

The apparent losses comprising the unauthorized consumption due to illegal connections and meters inaccuracies are estimated as 2% of the billed metered consumption, i.e. 3 388 m^3.

Table 4.3: Water balance from January till October 2015 included

<table>
<tr><td rowspan="4">System input volume
W_I = 308 962 m^3</td><td rowspan="2">Authorized consumption
W_C = 193 273 m^3</td><td>Billed authorized consumption
W_{BC} = 169 370 m^3</td><td>Revenue Water
RW = 169 370 m^3 (55%)</td></tr>
<tr><td>Unbilled authorized consumption
W_{UC} = 23 903 m^3</td><td rowspan="3">Non-Revenue Water
NRW = 139 592 m^3 (45 %)</td></tr>
<tr><td rowspan="2">Water losses
W_L = 115 689 m^3</td><td>Apparent losses
W_{AL} = 3 388 m^3</td></tr>
<tr><td>Real losses
W_{RL} = 112 301 m^3 (36%)</td></tr>
</table>

From January to October 2015, the calculated real losses W_{RL} are equal to 112 301 m^3 (see Table 4.3). The water losses present therefore 36%.

In order to classify the network performance, the European countries especially France use the approach suggested by "Federation Nationale des Collectivites Concedantes et Regies (FNCCR)" in 2003. For the 3 different network types (rural, intermediate, and urban), the performance in managing losses is assigned to one of the following four classifications in Table 4.4: worrying, mediocre, almost satisfactory, or satisfactory according to the Linear Losses Index (LLI) in m^3/km/day.

Table 4.4: Performance classification according to FNCCR proposal

LCI m^3/km/day	**Network Type**	**FNCCR Network classification according to its LLI**			
		Worrying	**Mediocre**	**Almost satisfactory**	**Satisfactory**
LCI < 10	Rural	LLI > 5	3 < LLI < 5	2 < LLI < 3	LLI < 2
10 < LCI < 30	Intermediate	LLI > 11	8 < LLI < 11	6 < LLI < 8	LLI < 6
LCI > 30	Urban	LLI > 16	13 < LLI < 16	10 < LLI < 13	LLI < 10

The LLI for the SunRise water system for the period January-October 2015 is equal to 25. Knowing that the network is considered as urban, the significant value of LLI let the network be classified as worrying. An active leakage strategy is necessary with analyzing the level and the nature of the water loss and the leakage reduction efforts has to be highly intensified.

In order to crosscheck the real loss volumes obtained from the top-down water balance, a bottom-up assessment was conducted. The Minimum Night Flow (MNF) was computed for the general meters during the month of August 2015 when the demand is low in the campus. The MNF corresponds to the minimum value between 2:00 am and 6:00 am. As shown in Figure 4.3, the minimum night in August 2015 is equal to 15 m^3/h which is equivalent to a volume of 109 440 m^3 between January and October 2015 (304 days). This value is close to losses W_{RL} calculated using the water audit (112 301 m^3).

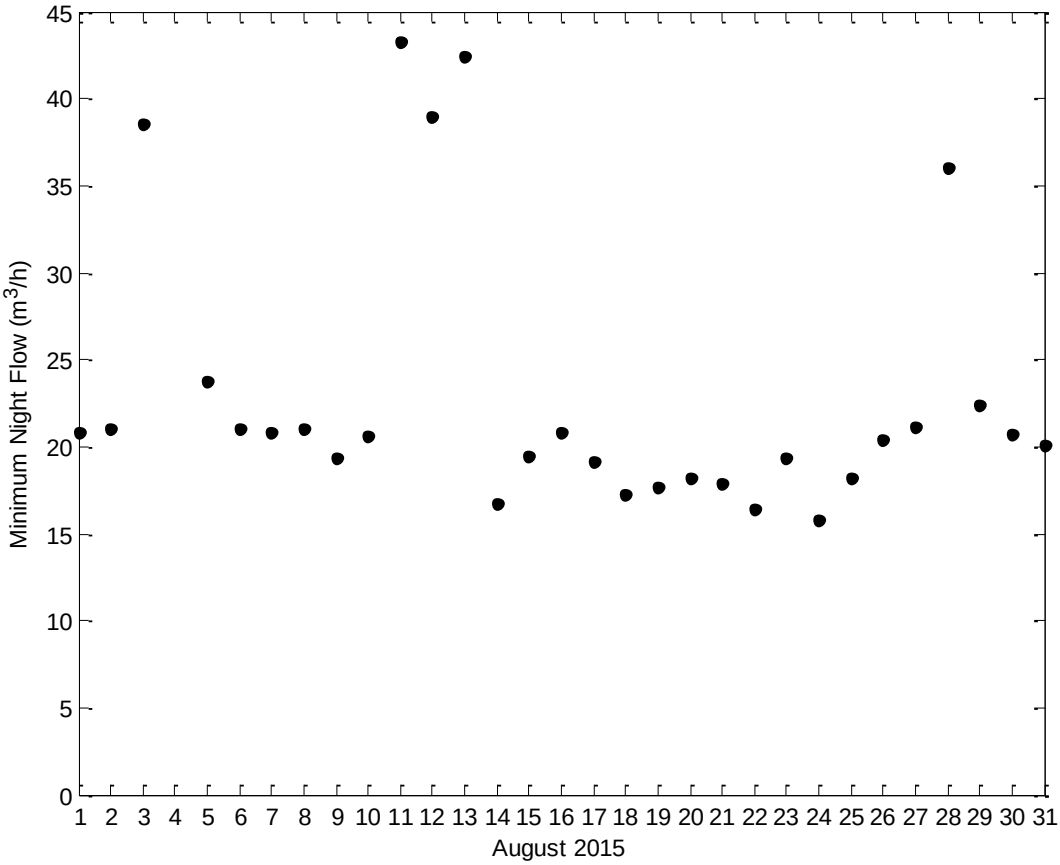

Figure 4.3: Minimum Night Flow computed from the general meters during August 2015

4.3. Active Leakage Control (ALC)

Since the water losses in SunRise water system during the period January - October 2015 is very high, an Active Leakage Control (ALC) is necessary to reduce water losses and enhance water supply capability (GIZ, 2011). The ALC aims at detecting and repairing hidden leaks. The ALC includes 4 main steps (Mutikanga, 2013): i) quantification of leakage, ii) monitoring, iii) leak detection and localization, and iv) network management.

The active leakage control strategy applied to the SunRise water system starts with the flow monitoring after quantifying the real losses using the water balance method. The inflow is monitored continuously especially during minimum night flow conditions and is compared to a previously measured reference value. During the period January - October 2015, the minimum night flows computed from the general meters CITE SCIENTIFIQUE, ECL and M5 promote the hypothesis of suspicious unreported leaks in three areas.

In order to pinpoint the leaks, a sounding survey was necessary for the suspicious areas. The discharge of water from a leakage generates acoustic waves or oscillations. The main purpose of the sounding surveys is to listen these noises directly at valves or hydrants using simple

mechanical sticks or electronically amplified sticks with a microphone and a headset. Figure 4.4 shows two operators tracking noises with the electronic sticks.

Figure 4.4: Leak detection operators with their electronically amplified sticks

The sounding surveys detected 25 hidden leaks in the networks and valves. The leak repairs consist replacing the broken pipes and the leaking valves. In addition, to prevent the water theft, many hydrants were placed underground offering a higher level of safety.

Figure 4.5: Leak repairs in front of the building M1

Figure 4.6: Leak repairs in front of the engineering school ECL

Figure 4.5 and Figure 4.6 show the leak repairs in front of the building M1 and the engineering school ECL.

The leakage did not concern only the pipes but also valves. Figure 4.7 illustrates a leaking valve as well as the new valve installed.

Figure 4.7: Leaking valve before and after leak repairs

Figure 4.8 shows the distribution of leaks detected using the active leakage control as well as the historical leaks.

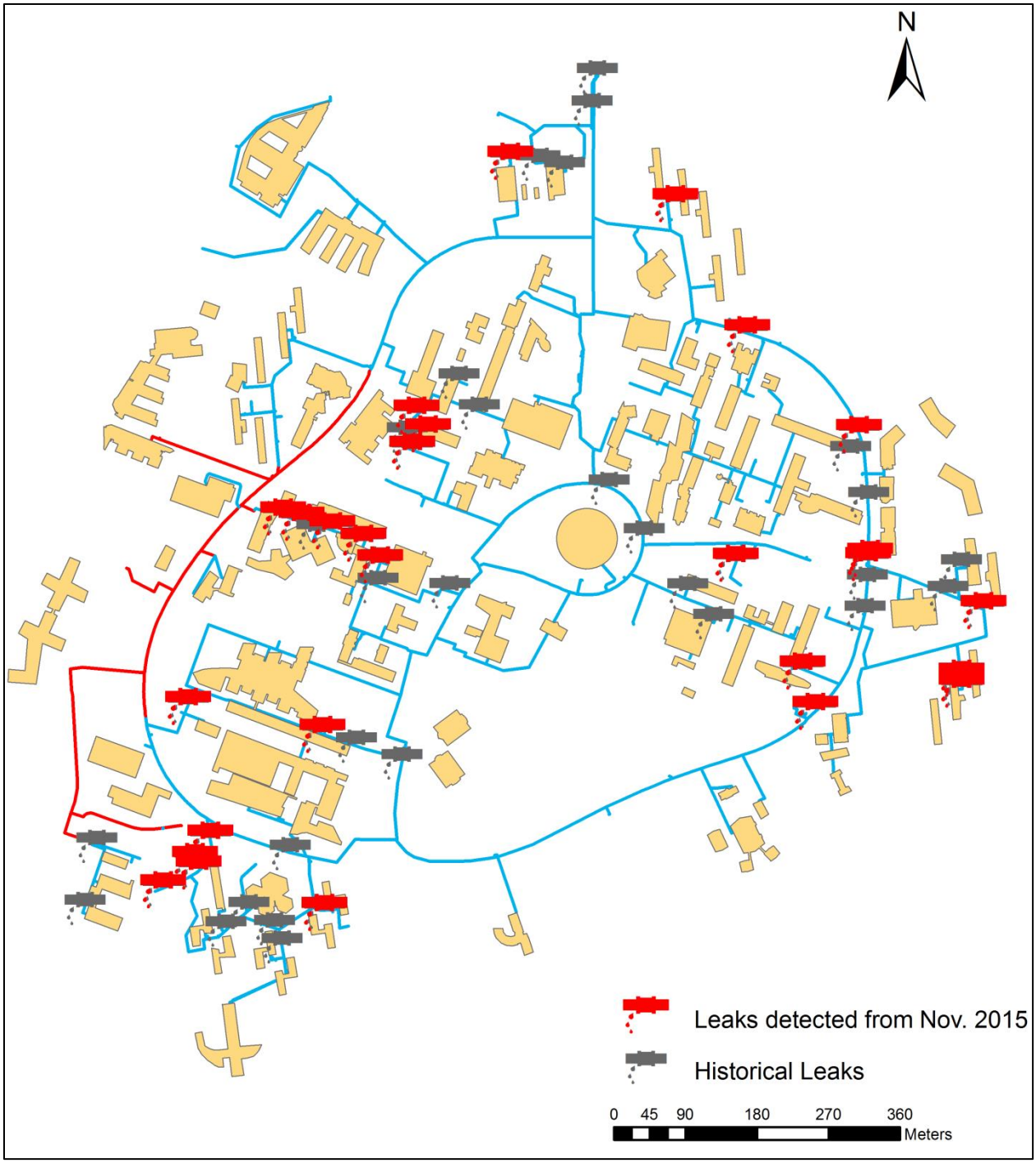

Figure 4.8: Leaks in the Campus water network since 2011

4.4. Results of the Active Leakage Control (ALC)

The Active Leakage Control (ALC) strategy applied to SunRise water system was very efficient in reducing the water losses. The NRW dropped from 400 m^3 at the end of October 2015 to 32 m^3 at the end of April 2016. Actually, the water balance is automatically calculated in real time The Non-Revenue Water during in April 2016 is depicted in Figure 4.9. The NRW in April 12 and 25 exceeds the regular values; a leak alarm was generated. The leak was detected and repaired.

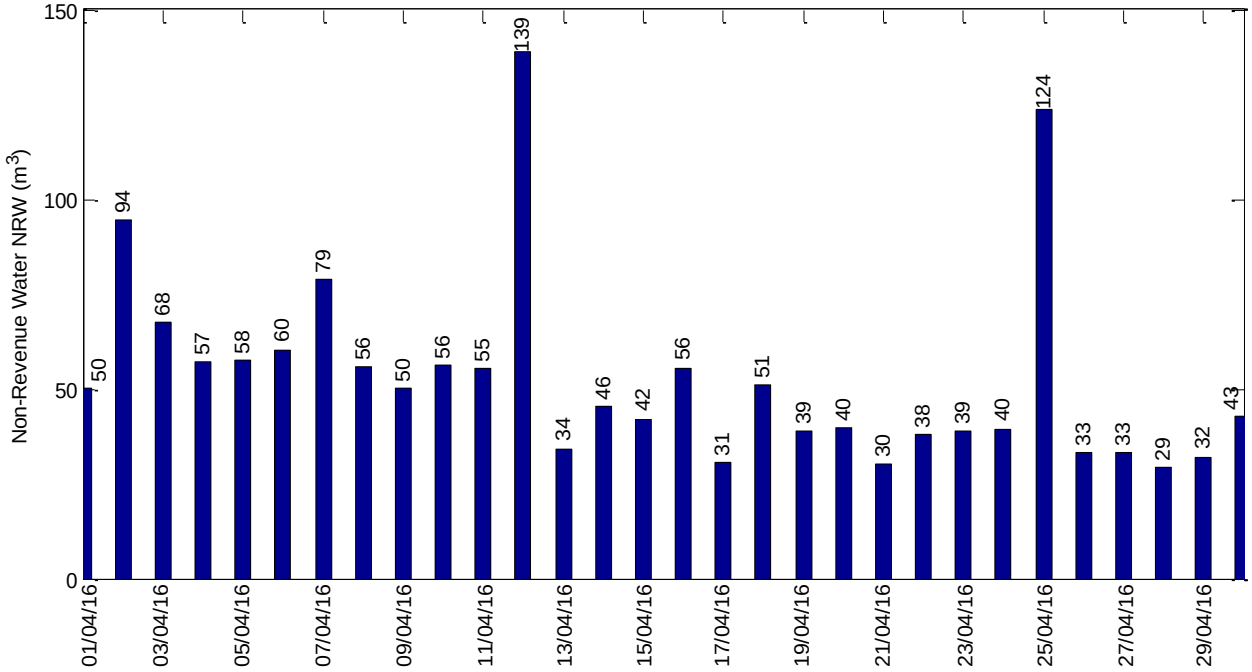

Figure 4.9: Non-Revenue Water (NRW) during April 2016

A simple comparison between the NRW in 2015 and 2016 shows the results of the ALC adopted for the demo site. Figure 4.10 shows a comparison of the NRW computed for the first 5 months in 2015 and in 2016. For instance, the NRW drops from 10 000 m^3 in May 2015 to less than 1000 m^3 in May 2016. Comparing these 5 months of the two years 2015 and 2016, the water loss decreased from 43% to 7%.

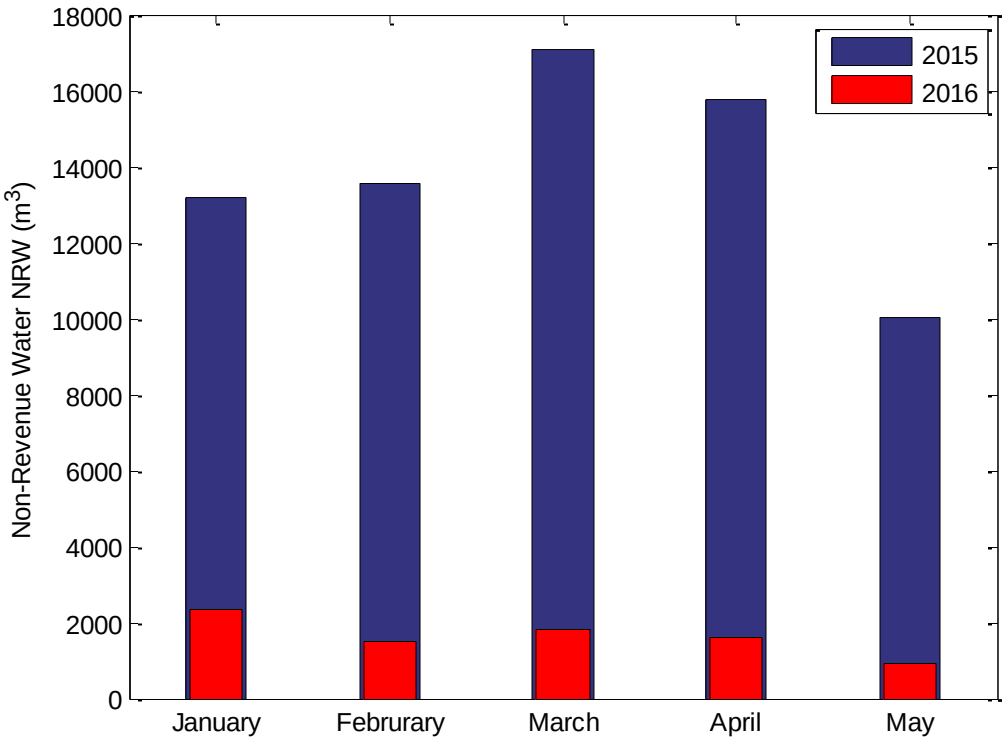

Figure 4.10: Comparison of NRW between January-May 2015 and 2015

The comparison between the system input volume and the volume of water consumed from 01/10/2015 till the end of May 2016 is shown in Figure 4.11. Figure 4.12 illustrates also the volume of Non-Revenue Water computed from the first of October 2015 till 31/05/2016.

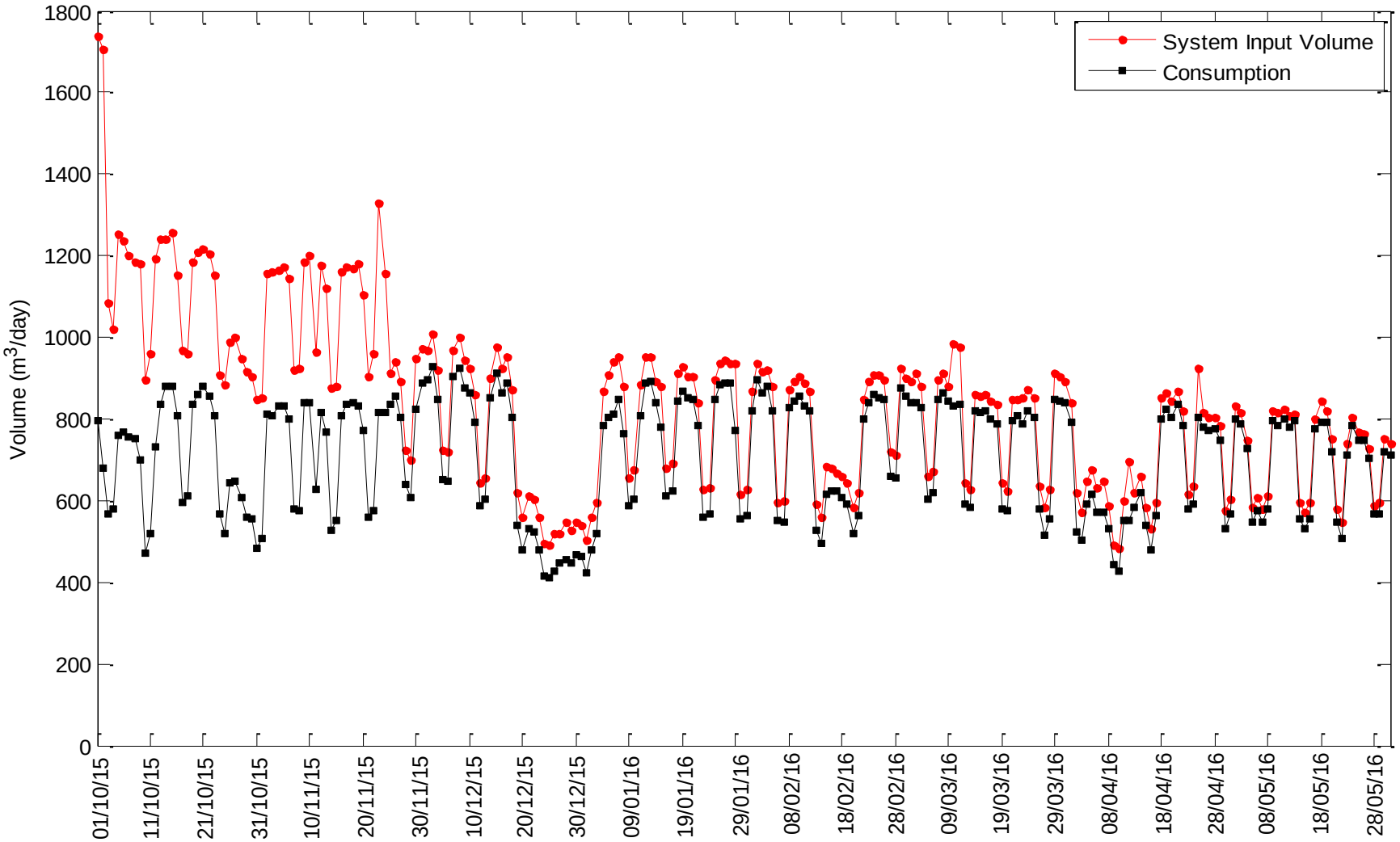

Figure 4.11: Comparison between the system input volume and the consumption of the sub-meters starting from 01/10/2015

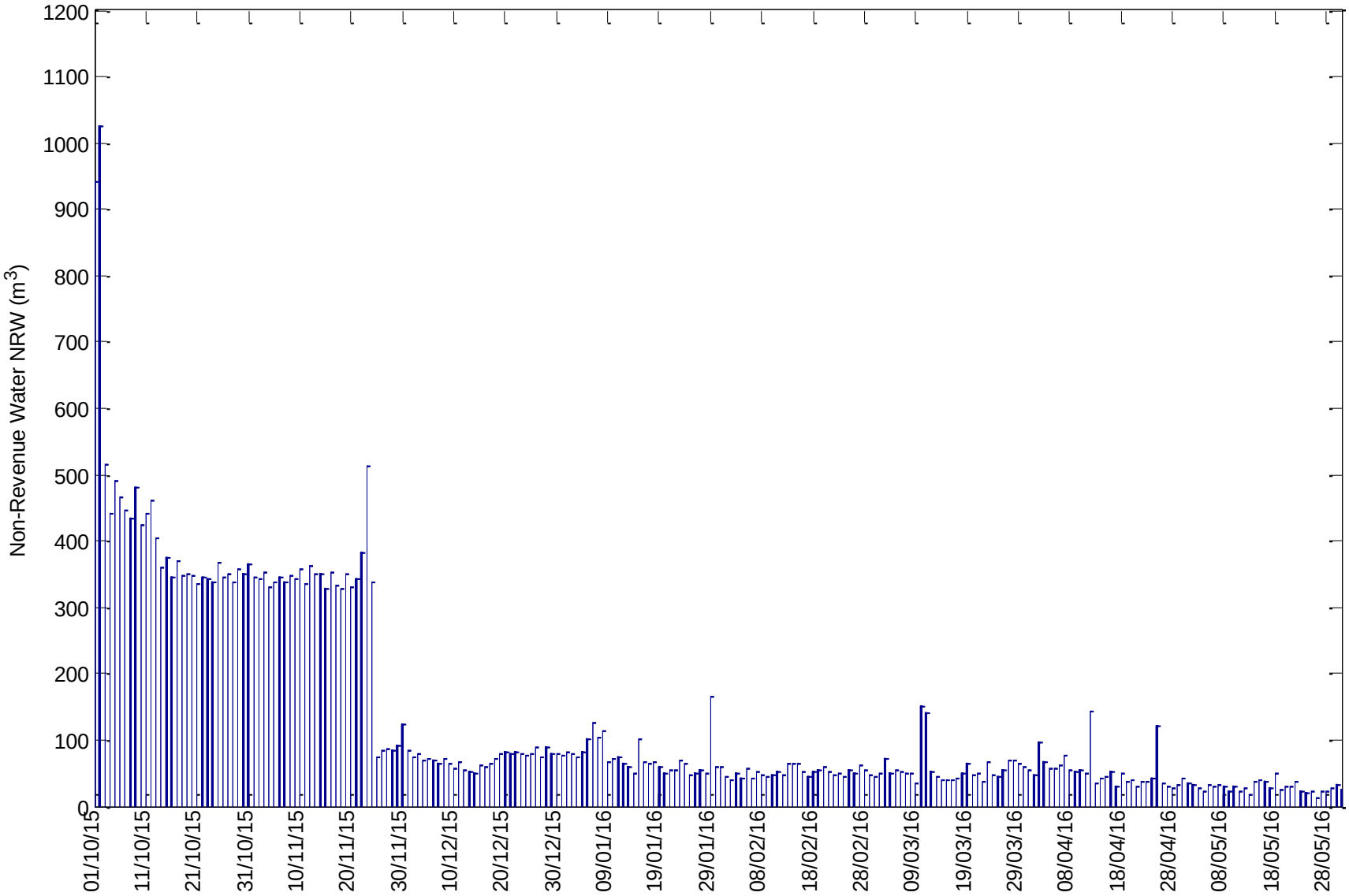

Figure 4.12: Non-Revenue Water NRW (m^3) from 01/10/2015

4.5. Conclusion

The water balance method constitutes a first step for an effective water loss management strategy. However, the computation of the level of the Non-Revenue Water (NRW) depends on the accuracy of the data collected from the production meters and sub-meters.

The calculation of the water balance by the two approaches: top-up and bottom-down assessments has led to a quantification of the water losses in the water distribution network of SunRise demo site. The results of the NRW proved the necessity of an Active leakage Control (ALC) program. The application of the ALC to SunRise network allowed the reduction of the NRW from 43% (January - May 2015) to 7% (January - May 2016).

The challenge is to maintain or even reduce water leakage in the Campus by developing new leak detection methods. The following chapter will present the use of advanced methods on the detection of water leakage in the Scientific Campus.

Chapter 5

Leak Detection Using Advanced Methods

This chapter presents the use of advanced methods for the detection of water leakage in SunRise Demo Site. These methods concern (i) the Comparison of Flow Pattern Distribution CFPD approach, (ii) The statistical approach, which is based on the Probability Density Functions of water consumption for each building, (iii) The traditional Minimum Night Flow (MNF), and (iv) the Threshold Water Consumption Profile (TWCP). Each method will be presented and then applied on SunRise Demo Site.

5.1. Comparison of Flow Pattern Distribution (CFPD)

The CFPD is a data-driven method that compares the flow datasets in order to identify and justify the changes in the water consumption (Van Thienen, 2013; 2013; 2014). The CFPD method includes 4 steps (Figure 5.1):

- Ensure that the datasets vectors to be compared have the same length covering the same period of time.
- Organize each dataset in ascending order from the smallest magnitude to the largest one.
- Plot the two comparable periods, with the reference dataset on the horizontal x-axis.
- Determine a linear best fit with a slope *a* and intercept *b*.

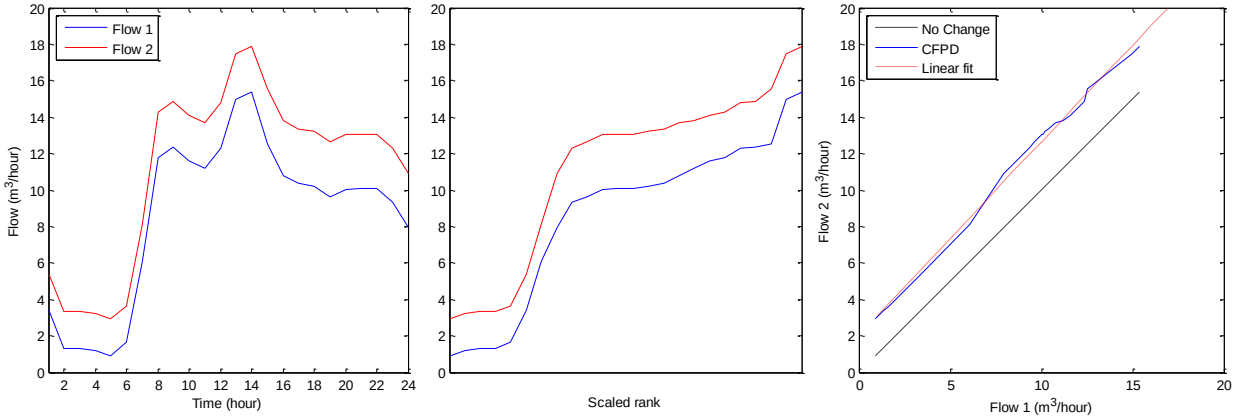

Figure 5.1: The CFPD steps demonstrated with baseline flow (flow 1) and an increased leakage (flow 2)

The linear fit for the points is of the form y = ax + b. The slope *a* and intercept *b* are used to identify changes from the baseline, where a = 1 and b = 0. If we are comparing two similar datasets, the result of the CFPD will be a straight line. An inconsistent change occurs when the two curves have similar shapes but separated by an offset of a constant value corresponding generally to a constant amount of leakage. The intercept *b* is equal to this offset. An inconsistent change can be related to new leaks, abnormal usage of water, repair of leaks, and operational works such as cleaning the network. However, a consistent change occurs when the two curves have the same shape but one curve is scaled by a factor corresponding to the slope *a*. A consistent change can be interpreted as change in population, warm period, holidays, etc. The distinction between the consistent and inconsistent change according the slope *a* and intercept *b* is summarized in Table 5.1.

Table 5.1: Consistent and inconsistent changes (factors a and b) (Van Thienen, 2013)

	No inconsistent change b=0	Inconsistent change b≠0
No consistent change a=1	No change in demand	Increase in leakage or increase in demand not following established pattern
Consistent change a≠1	Increase in demand following established pattern	Combination of increase in demand following established pattern and increase not following the pattern and/or increase in leakage

The output of the CFPD method is two antysimmetric matrixes, one for the slope *a* and the other for the intercept *b*. The matrixes *a* and *b* values contain a blue to white to red color map according to their deviation from 1 and from 0 respectively, where small deviation has blue color close to white and larger deviations has a red color.

5.1.1. CFPD methodology at water supply zone scale

The CFPD method will be tested to analyze its efficiency to detect the leaks from the flow pattern of the total supply zone. The dataset is the water consumption computed from the general meters in 2015. Following the descriptive analysis (see Chapter 3), three leaks have been identified in the weekly flow pattern of the general meters. Two bursts occurred in March 17 (week 12) and in August 11 (week 33), respectively. A third leak has been detected in September, 17 during 17 days (week 38 to 40). These three events with different anomalies are used to analyze the performances of the CFPD method. The data was first checked to see if there had been any meter faults. The measurements in May 2015 (weeks 18 to 22) were excluded from this study due to a telemetry problem. A VBA scripts coupled with a MATLAB code have been developed to compute the matrixes used in the CFPD method. The interface of the developed algorithm is shown in Figure 5.2. The script can take into consideration a block analysis based on the comparison of the flow pattern by weeks and can refine also the calculation to identify the changes at the daily scale. The script works for any measurement step. In our case, the flow is measured each hour.

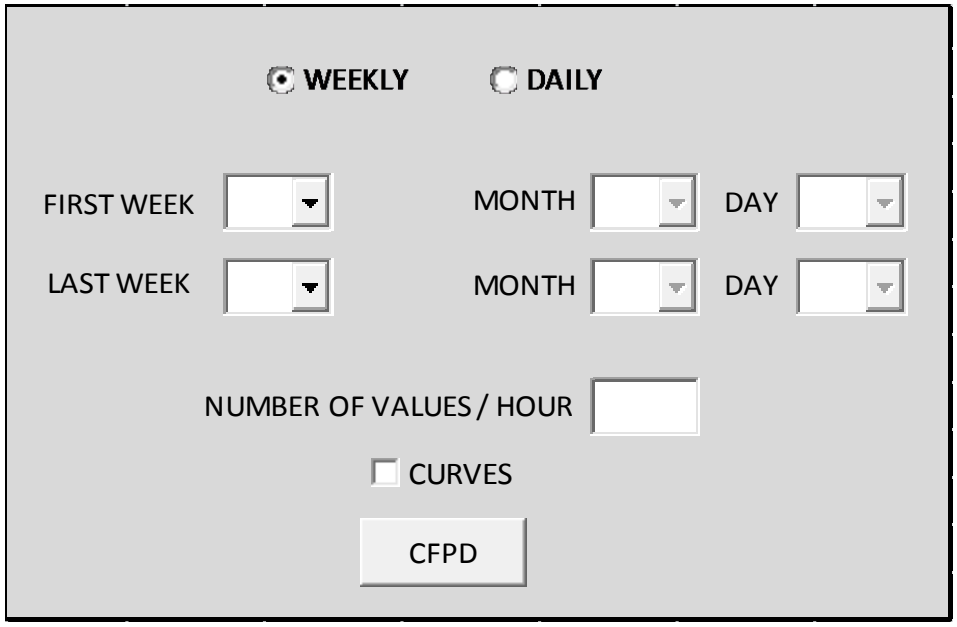

Figure 5.2: Interface of the CFPD method

The dataset is divided into two parts: the first part includes the water consumption from week 1 till week 17 and the second part from week 23 till the end of the year.

5.1.1.1. CFPD for the first period (weeks 1 to 17)

Figure 5.3 shows the comparison of the flow pattern from early 2015 to the end of April 2015.

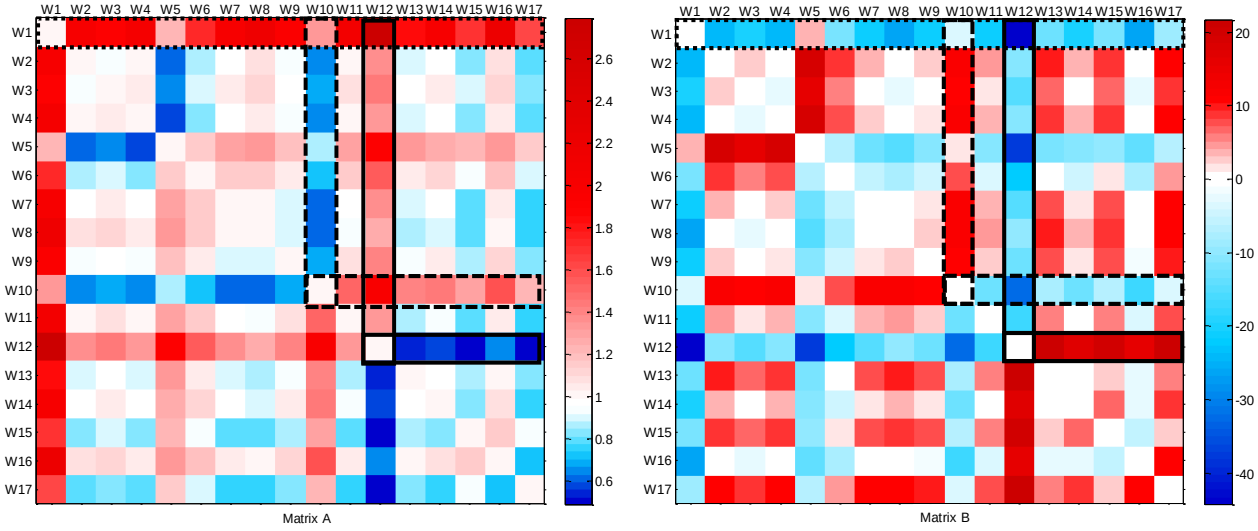

Figure 5.3: Slope matrix (A) and intercept matrix (B) for CFPD block analysis of the total water supply dataset from week 1 to week 17 in 2015

This matrix A shows consistent increases comparing the 1st week of 2015 to other weeks. This increase corresponds to the holiday period in the first week of the year. From the slope a, the water consumption during the working weeks seems to be scaled by a factor varying from 1.3 to 2.8. The consistent decrease in week 5 is related to the telemetry problem from 26 till 29 January 2015. In parallel, the decrease in the slope *a* in week 10 corresponds to the winter holidays. During these holidays, the campus seems to consume approximately half of the volume consumed in the ordinary weeks (a=0.5). A last interesting feature can be deduced from Figure 5.3 concerning the week 12. A simultaneous anomaly in the *A* and *B* matrixes with opposite signs is shown. This result of the slope (a>1) and the intercept (b<0) is relative to the burst during high consumption hours. It corresponds to the first burst in March, 17. Figure 5.4 illustrates the CFPD plot combining the flow patterns for March 16 – March 17 and March 16 – March 18, respectively. The comparison between the flow of March 17 and March 16 shows that the CFPD plot was similar to the baseline and then starts to deviate. This indicates a burst during the high consumption hours. Once the leak was repaired, the CFPD plot combining the flows of March 18 and March 16 has returned to the baseline.

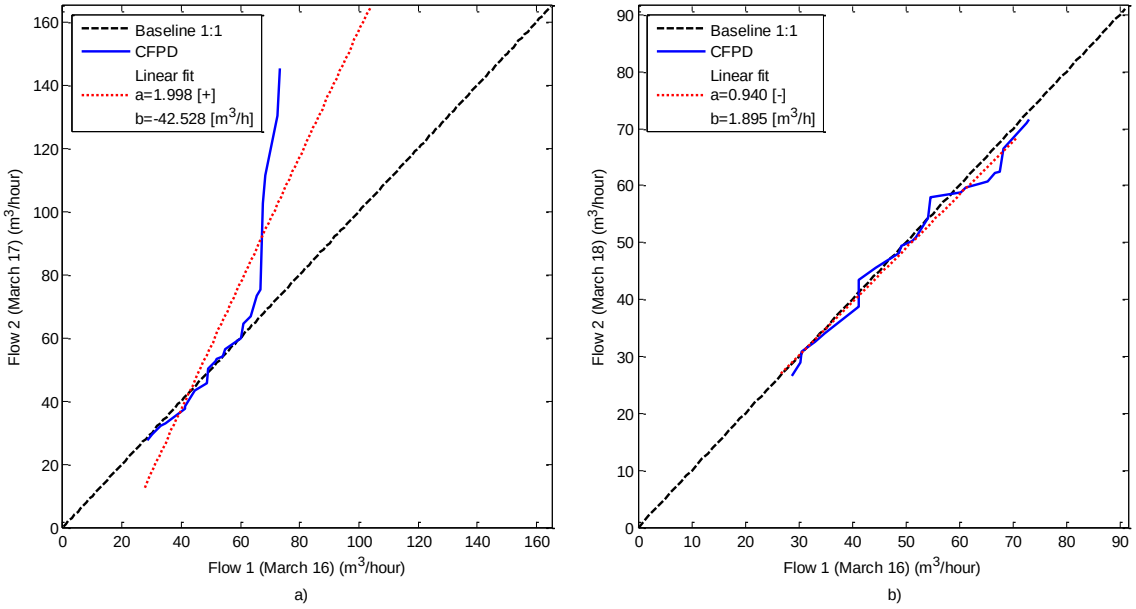

Figure 5.4: CPFD plot combining flow patterns: a) May 16 - May 17 and b) May 16 - May18

5.1.1.2. CFPD for the second period (weeks 23 to 52)

The second period includes the flow patterns of week 23 (June 2015) till the end of the year. Figure 5.5 and Figure 5.6 show the matrix A and the matrix B, respectively. We observe:

- A consistent decrease from weeks 32 to 35 with a particularity to the week 33. This decrease which coincides with the inconsistent increase is related to the summer holidays during August.
- During the week 33 in the summer, the slope of the CFPD increases (a>1) and the intercept b is lower than 1. This change in opposite ways corresponds to the burst in August 11th.
- From weeks 32 to 51, an inconsistent decrease (b<0) is very clear. It corresponds to the leak repairs. The flow measured by the general meters decreases following the active leakage control strategy. However two singularities are observed during this period, the first in week 39 and the second in week 44.
- In the week 39, there is no significant change in the consistent matrix. For the inconsistent matrix, the comparison between the water consumption in week 39 with the flow in the weeks during the summer shows a similar behavior. Starting from the week 36, an inconsistent increase of 15 m^3/h is observed; at the same time, the slope *a* tends to be close to 1. This can be explained by a leakage at the rate of 15 m^3/h. The CFPD method allows the detection of the third leak, but it misses the starting date of the leakage. The leaks started September 17th but the CFPD detects it on September 21.
- A small inconsistent increase in week 44 is observed. During this week, operating processes were conducted to repair the leaks and to clean the network.
- The consistent and inconsistent decreases in the week 52 explain the decrease in the water consumption during the Christmas holidays.

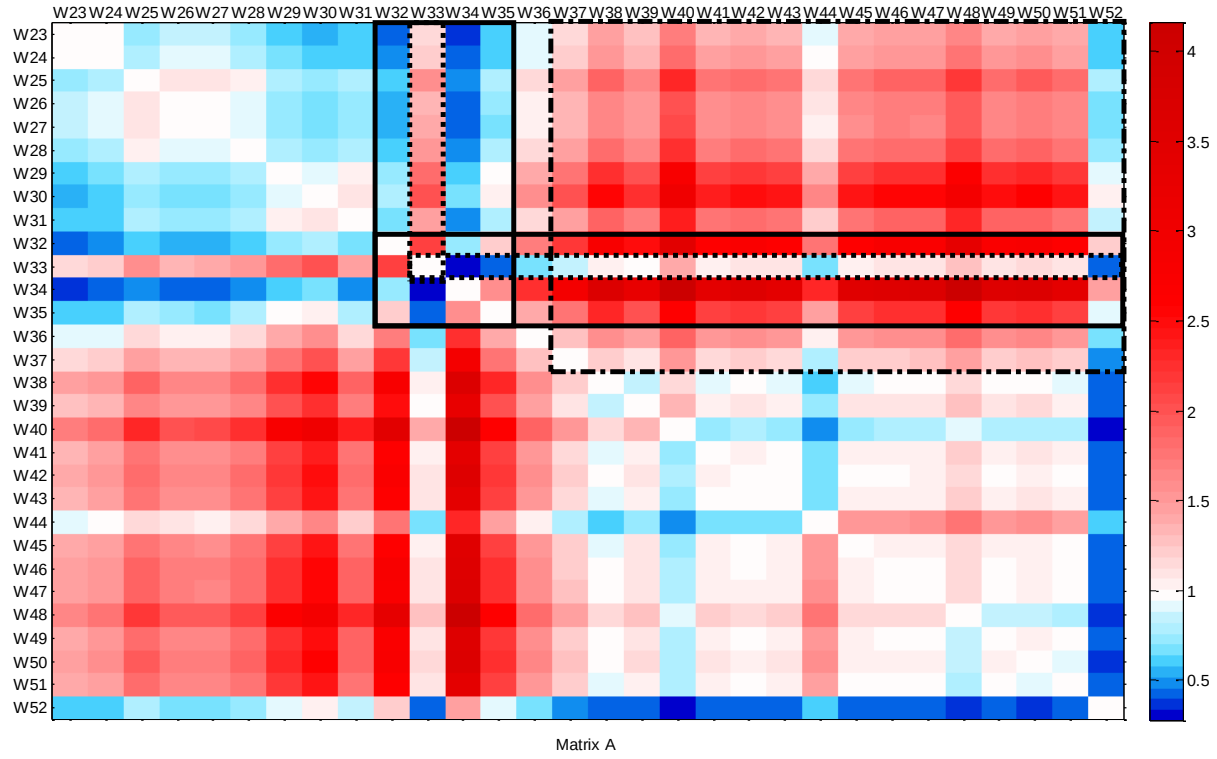

Figure 5.5: Slope matrix (A) for CFPD block analysis of the total water supply dataset from week 23 to week 52 in 2015

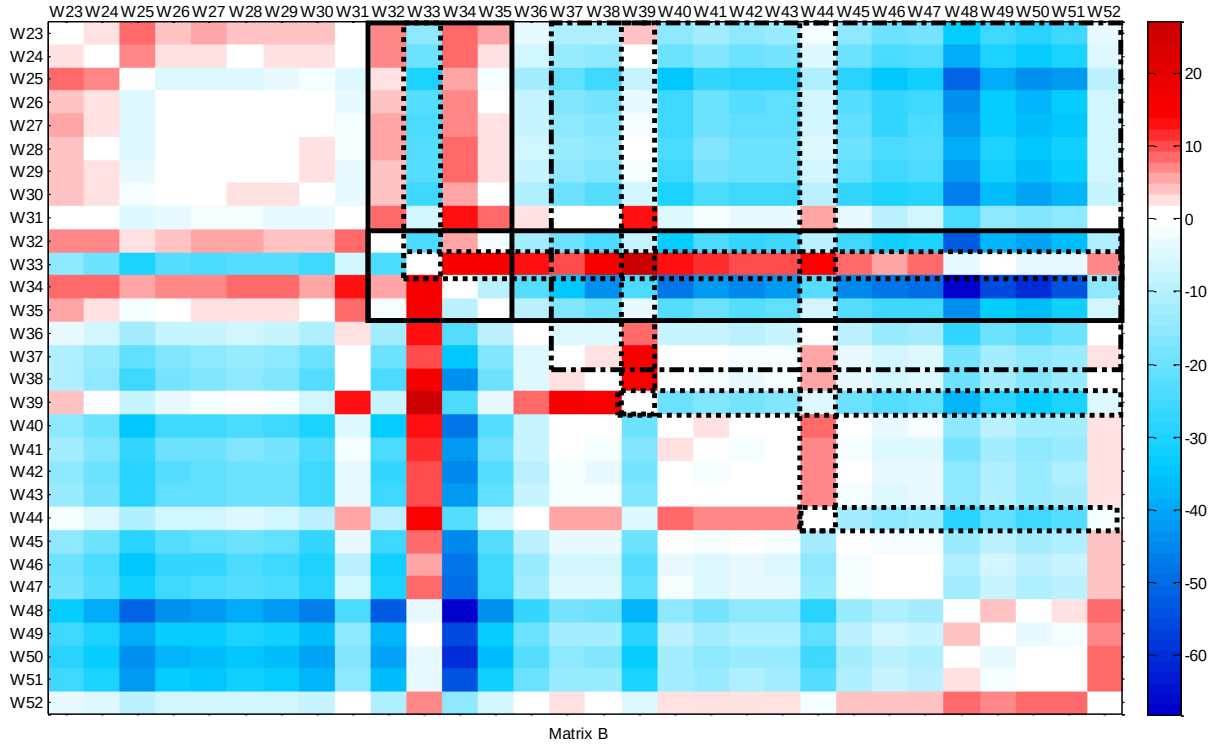

Figure 5.6: Intercept matrix (B) for CFPD block analysis of the total water supply dataset from week 23 to week 52 in 2015

5.1.2. Application of the CFPD method at buildings scale (Sub-meters)

Previous researches showed the capacity of the CPFD method for identifying the consistent and inconsistent changes at a DMA and water supply zone scale (Van Thienen, 2013; 2014). In the following example, we will discuss the performances of this method at a scale of building (building P2 from the Physics sector). A leak occurred in this building in May 2014. The first step of calculation consists checking the data for any meter faults that might cause inconsistent changes. Figure 5.7 shows the results of the CFPD block analysis from early 2014 to the first week of April 2014. The comparison between the week 1 and the other weeks shows a decrease in the water consumption of this building during the first week of the year, which corresponds to the New Year holidays.

The first interesting feature is the consistent decrease observed in the week 9 (dark blue color). This decrease is related to the winter holidays during this week. The water consumption seems to be reduced to the half compared to working weeks. The factor *a* varies from 0.5 to 0.6.

A second feature is the inconsistent decrease observed in the week 11 (b=-13 l/h). Between March 10 and March 16, the building consumed water less than usually.

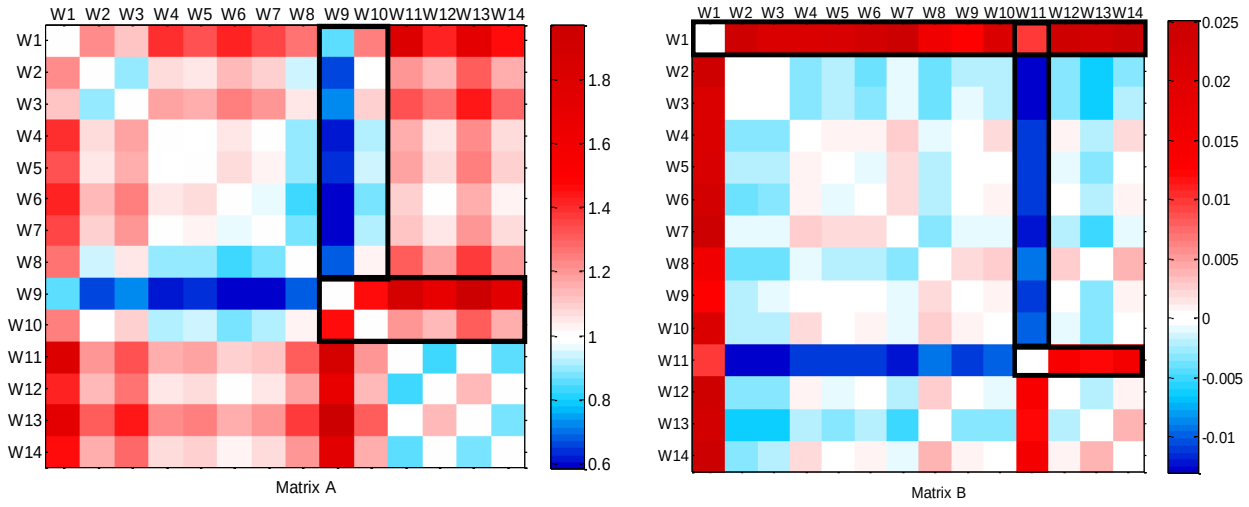

Figure 5.7: Slope matrix (A) and intercept matrix (B) for CFPD block analysis of P2 dataset from week 1 to week 14 in 2014

The results of the CFPD block analysis from week 15 till week 28 (July 13th) are depicted in Figure 5.8.

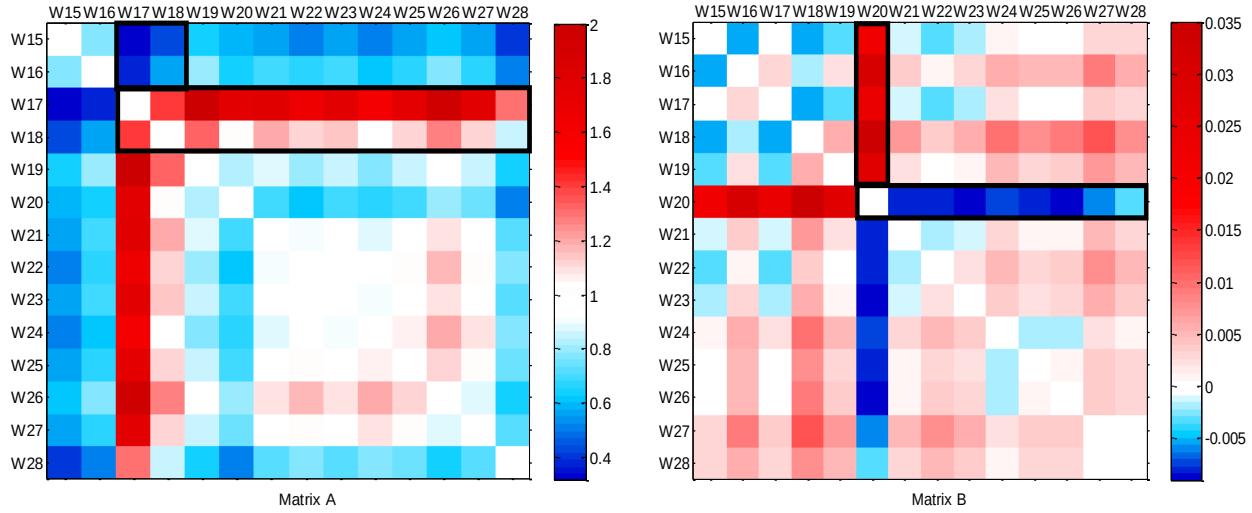

Figure 5.8: Slope matrix (A) and intercept matrix (B) for CFPD block analysis of P2 dataset from week 15 to week 28 in 2014

As shown in the matrix A, the consumption in the spring holidays (weeks 17 and 18) is very highlighted by a consistent decrease. The matrix B shows an inconsistent leak observed in week 20, which corresponds probably to a leakage. The CFPD daily analysis of P2 from March 12 to March 25, 2014 is computed in order to determine the starting date of leakage. The matrix B (Figure 5.9) shows a leakage of 100 l/h May, 18, 2014. However, according to the leak calendar of the building P2, this leak started May 17, and fixed May, 19 in the morning.

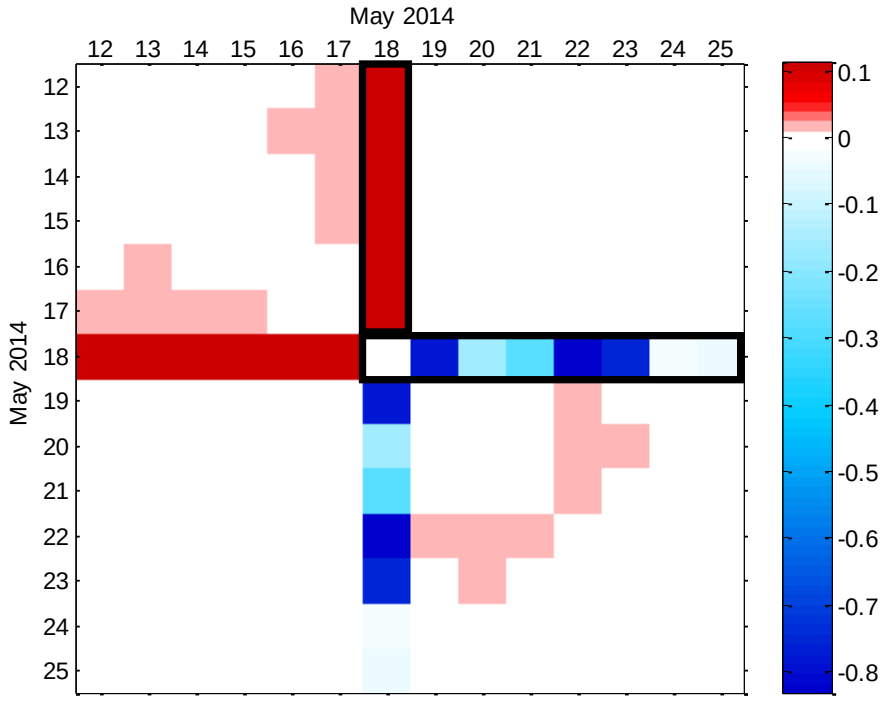

Figure 5.9: Intercept matrix (B) for CFPD daily analysis of P2 dataset in May 2014

5.2. Probability Density Function PDF

The Cumulative Distribution Function (CDF) describes the probability that a random variable *X* takes a value less than or equal to *x*:

$$F(x) = P(X < x) \tag{5.1}$$

The probability that the variable *X* takes a value more than *x* is calculated using the following formula:

$$P(X > x) = 1 - P(X < x) = 1 - F(x) \tag{5.2}$$

Based on this definition, the historical daily water consumptions are used to determine the CDF for each meter. The result function describes the cumulative frequency of the observed value and the corresponding density function that determines the probability of occurrence of a variable. Any anomaly in the water consumption could be recognized by its lower probability of occurrence. A lower and an upper bound are computed. The lower bound matches the leak probability of 0% and the upper limit corresponds to a leak probability of 100%. If any consumption value exceeds the upper bound, an alarm will be generated.

The built function has to be free from any abnormal event in the past; a pre-processing step is therefore conducted to perform data cleaning. The anomalies in time series are identified using Chebyshev's inequality (Saw et al., 1984). This theorem guarantees that in any probability distribution, the majority of the values are close to the mean value. For $\lambda > 1$; the statement defines that no more than $1/\lambda^2$ of the distribution values can be more than λ standard deviations away from the mean. If X is a random value with mean μ and variance $\sigma^2 < \infty$, then for $\lambda > 1$,

$$P\left(|X - \mu| \geq \lambda\sigma\right) \leq \frac{1}{\lambda^2} \tag{5.3}$$

The main steps of the PDF approach are summarized in Figure 5.10.

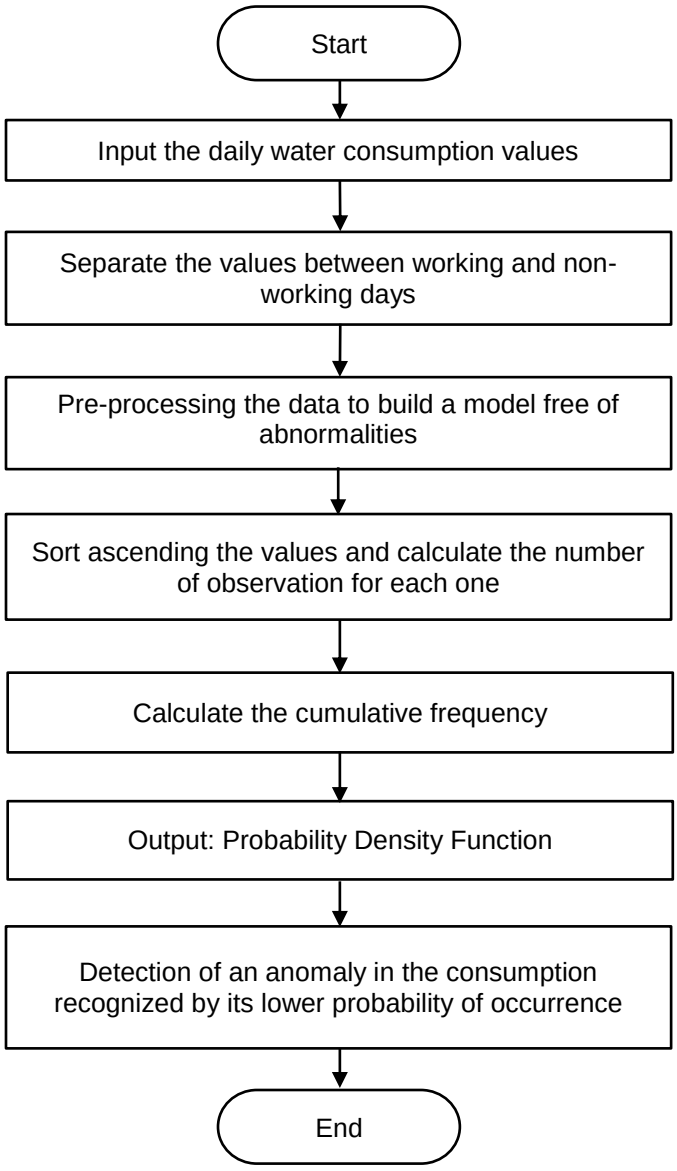

Figure 5.10: Flow chart of the Probability Density Function (PDF) Method

The daily water consumption values from January 1st 2014 to May 30, 2016 (i.e. 851 values per AMR) are used as an input for the PDF methodology. These values are separated between working days from one hand and the weekends and holidays from the other hand. The data are filtered according to Chebyshev's inequality with λ equal to 2. For each category, a cumulative distribution function and the corresponding probability density function are determined for each building. A lower and an upper limit are consequently extracted for each meterID. The lower bound corresponds to zero leak risk probability, while the upper limit corresponds to 100% leak probability. This method is applied at the sub-meter scale and at the bulk meter level.

Figure 5.11 and Figure 5.12 illustrate the CDF and PDF functions of the water consumption of a teaching and research chemistry building C6 in working days as well as weekends and

holidays, respectively. During a working day, the daily water consumption of this building varies between 12 m^3/day and 37 m^3/day. For this building, water consumption higher than 42 m^3/day has a probability of 10%. During the weekends and holidays, the lower limit passes from 2 m^3/day to 0 m^3/day and the upper bound drops from 52 m^3/h to 35 m^3/h. C6 building tends to consume 5 m^3/day during the non-working days. This consumption is due to research facilities.

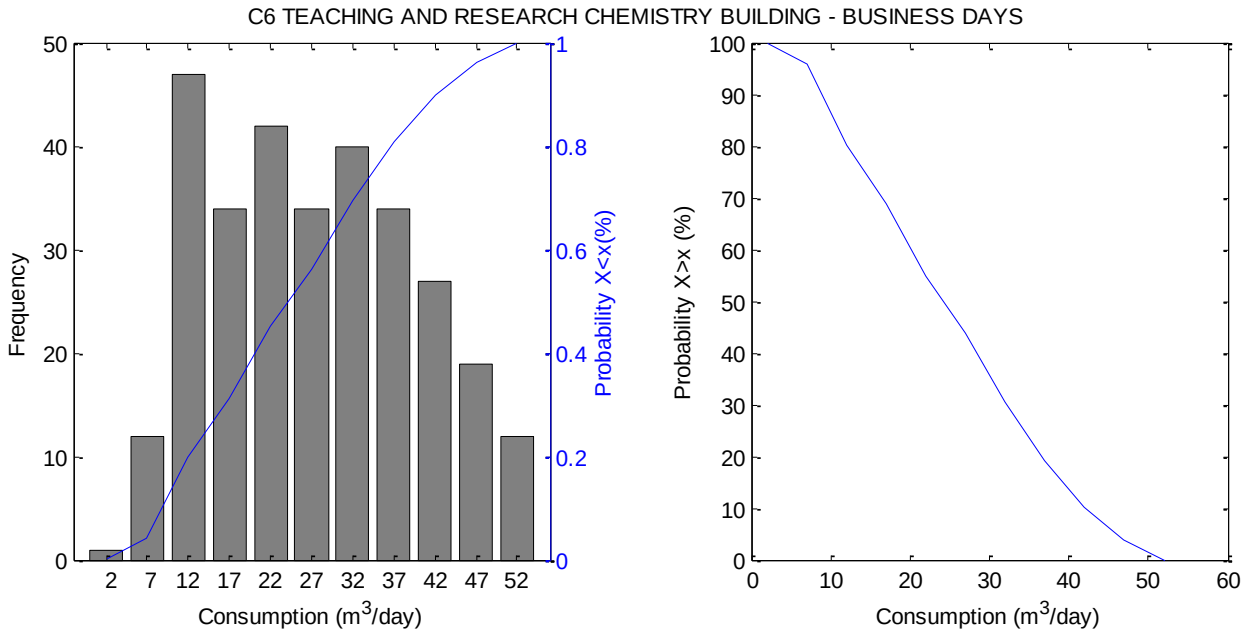

Figure 5.11: CDF and PDF functions for water consumption of building C6 - working days

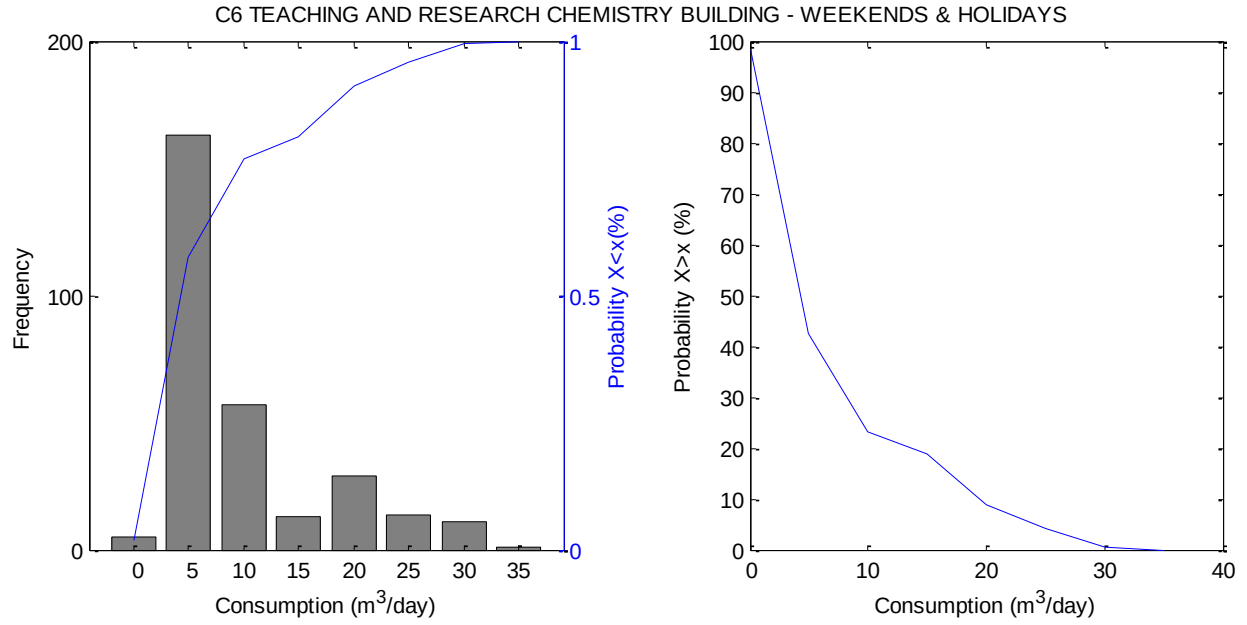

Figure 5.12: CDF and PDF functions for the water consumption of building C6 - weekends and holidays

The output of the PDF methodology applied to water consumption of building SN1 (biology sector) is shown in Figure 5.13 and Figure 5.14. During the working days, this building consumes between 5 m^3/day and 25 m^3/day. Any daily water consumption higher than 45 m^3/day has a risk probability of leak of 100%. During the holidays, the upper limit drops to 35 m^3/day ; the building tends to consume about 5 m^3/day due to the research activity.

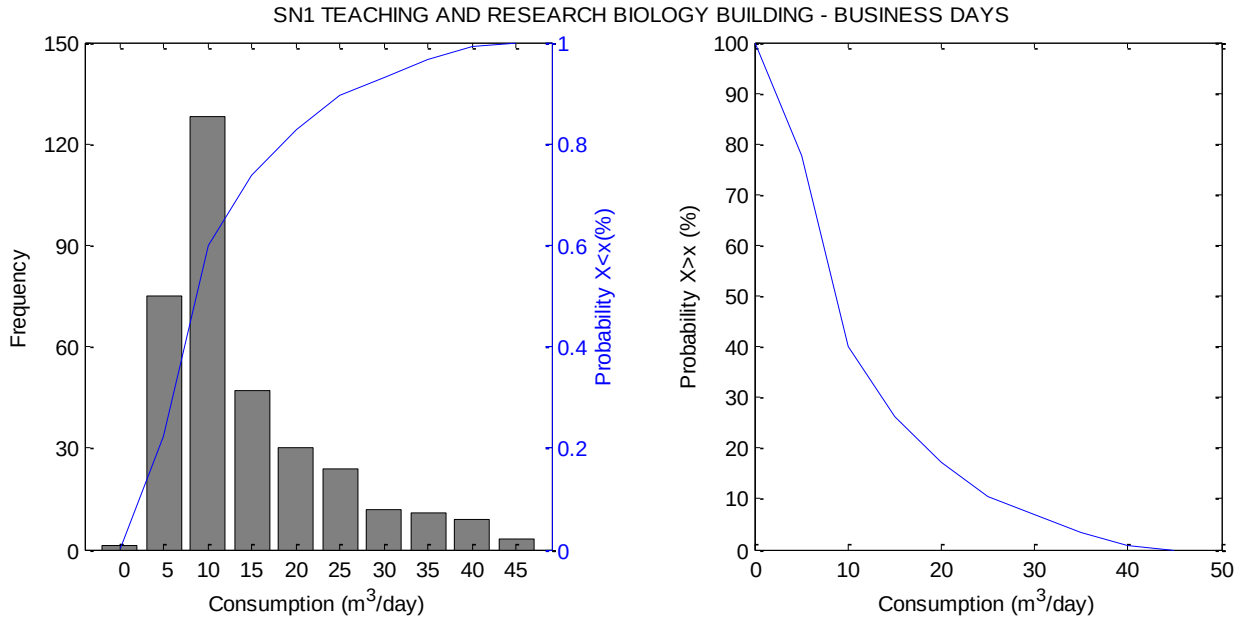

Figure 5.13: CDF and PDF functions of the water consumption of building SN1 - working days

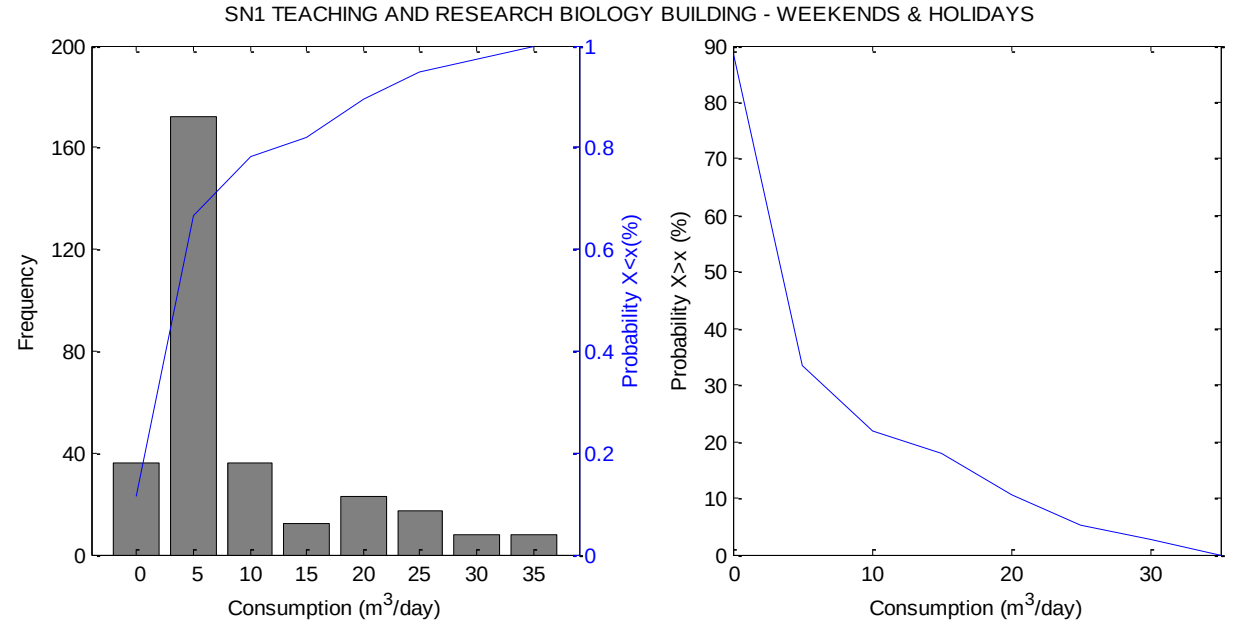

Figure 5.14: CDF and PDF functions of the water consumption of building SN1 - weekends and holidays

The PDF methodology is also applied at the scale of a general or a bulk meter. Figure 5.15 and Figure 5.16 show the CDF and PDF functions of the water consumption of the principal meter BACHELARD. This bulk meter measures the water consumption of 6 residential buildings. The water consumption in working and non-working days ranges between 80 m^3/day and 100 m^3/day. The upper limit does not change between working days and the holidays; it is about 110 m^3/day. This is due to the use of residences all over the year.

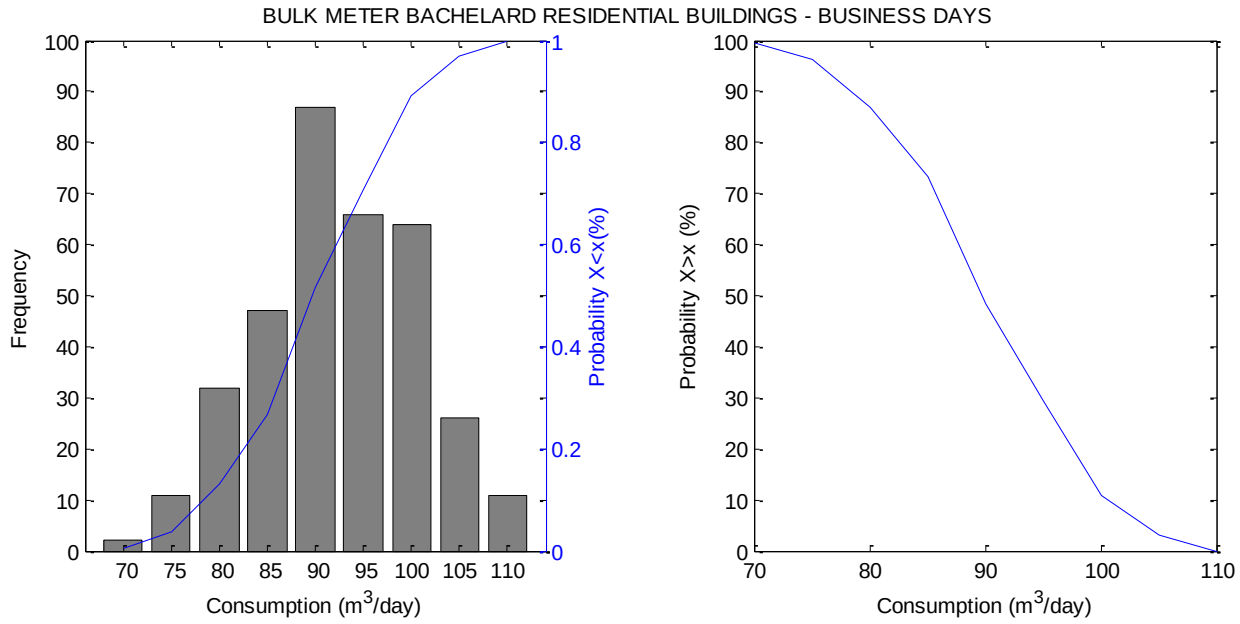

Figure 5.15: CDF and PDF functions of the flow - BACHELARD bulk - working business days

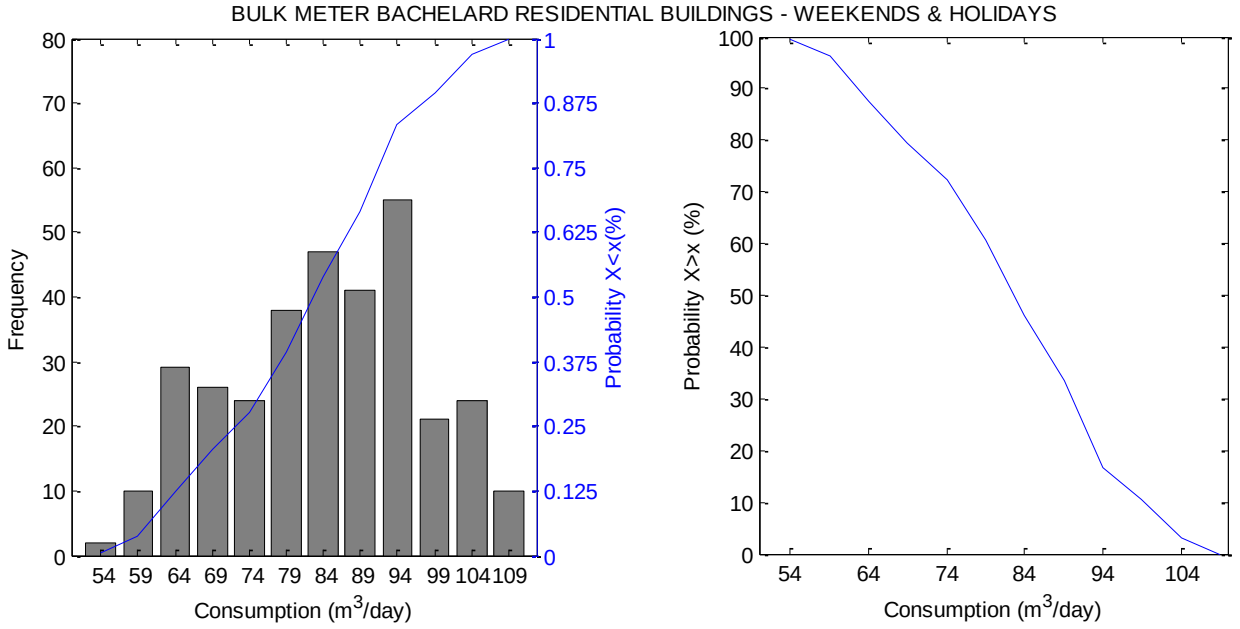

Figure 5.16: CDF and PDF functions of the flow - BACHELARD bulk - weekends and holidays

5.2.1. Discussion

The PDF methodology is applied at the scale of the bulk meters and the sub-meters. The main outputs of this method are the lower and upper limits for working and non-working days. Any future consumption will be compared to the upper limit to identify leakage. This approach was tested to evaluate its efficiency to detect the leakage in SunRise demo site.

Figure 5.17 shows the distribution of the daily water consumption of building P2 from January, 1, 2014 to the end of August 2014. Two upper limits were determined by the PDF method: for working days and weekends and holidays. Once the consumption exceeds these limits, an abnormal event is detected. Each point surpassing its appropriate limit is labeled by the corresponding date. According to Figure 5.17, the leak during the weekend of 17 and 18 May 2014 is clearly detected by this method. An abnormal event occurs also April, 22, which is a non-working day during the spring holidays. This abnormal event can be explained by an excessive usage of water or negligence.

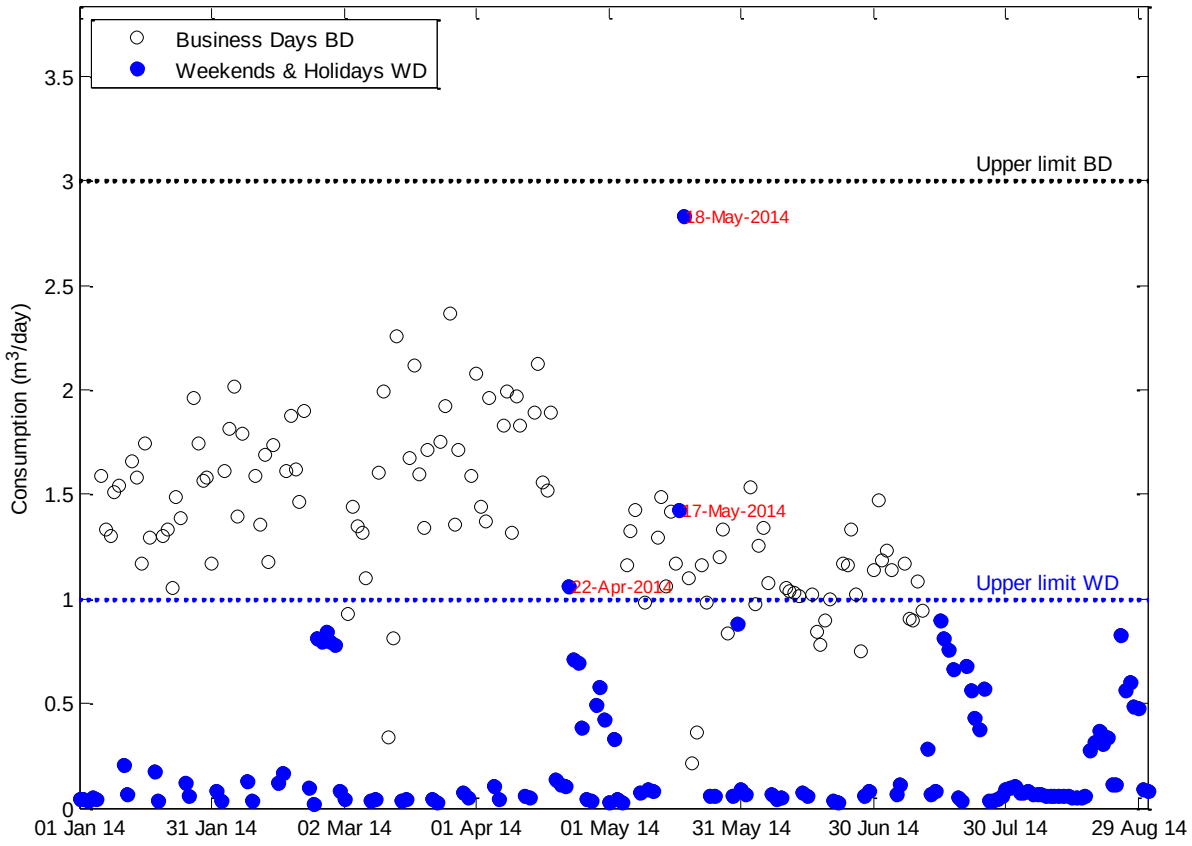

Figure 5.17: Leak detection in P2 building by the PDF approach

Figure 5.18 shows the data of 1 building SN1 from January 1st 2016 to end of June 2016. The upper limits are 45 m^3/day and 35 m^3/day for working and non-working days, respectively. As shown in Figure 5.18, a leak started June 13 until June 17. After this period, the consumption returns under the upper limits.

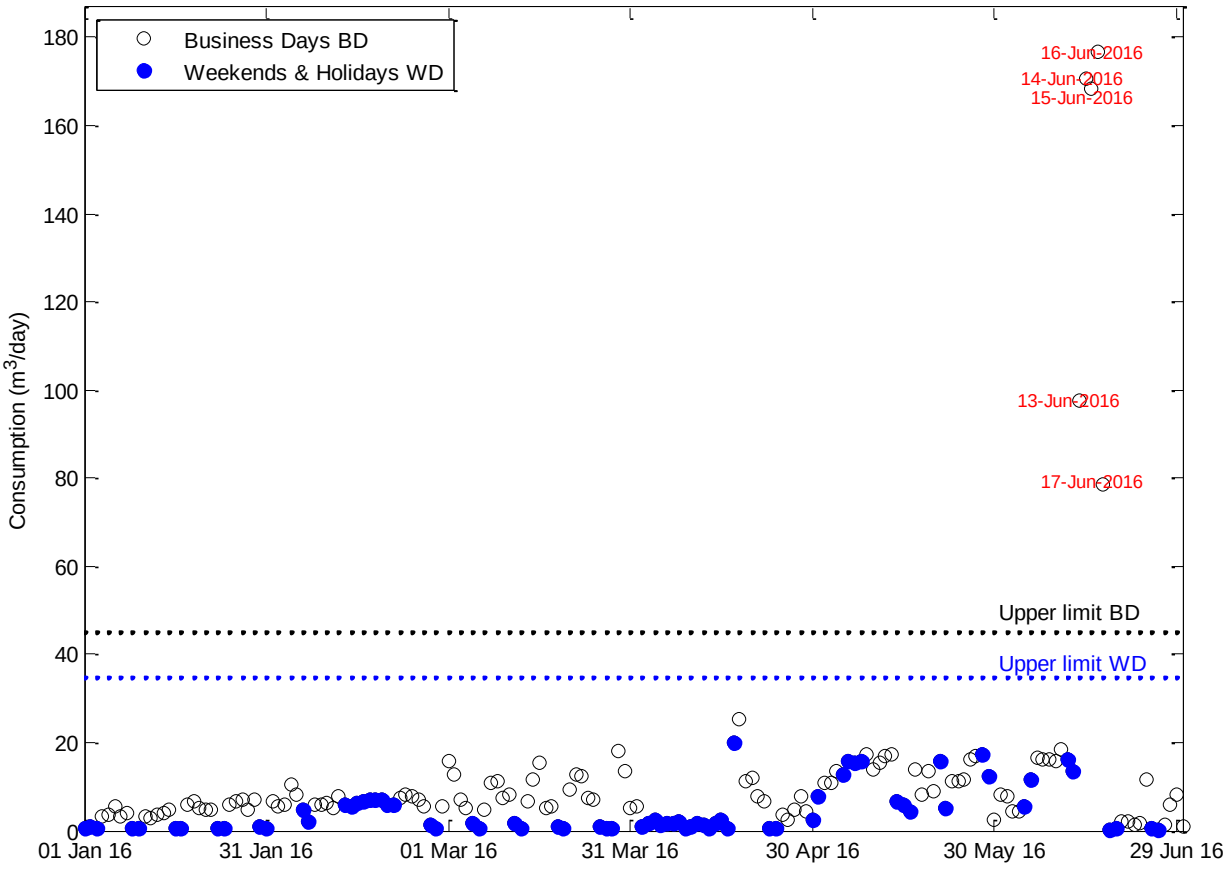

Figure 5.18: Leak detection in SN1 building by the PDF approach

The PDF methodology is also applied at a bulk meter. Figure 5.19 shows the ability of the PDF approach to identify three leaks in 2015. The upper consumption limits of all the general meters are 1 344 m^3/day for working days and 1 039 m^3/day for holidays and weekends.

The first two abnormalities occur February 7, 2015 (1 067 m^3) and March 15, 2015 (1 095 m^3). These two days are weekends. These abnormalities could be considered as an excessive water usage.

The method was able to detect the burst occurs March 17th, 2015. The consumption of this working day exceeds the upper limit. Furthermore, the second leak of August 11 and 12, 2015 was identified by this approach.

The PDF methodology was capable to detect the onset of the third burst during 2015. This unreported leak started September 17th, 2015 and was repaired October 1st. During this period, the water consumption exceeded the limit for both working and non-working days.

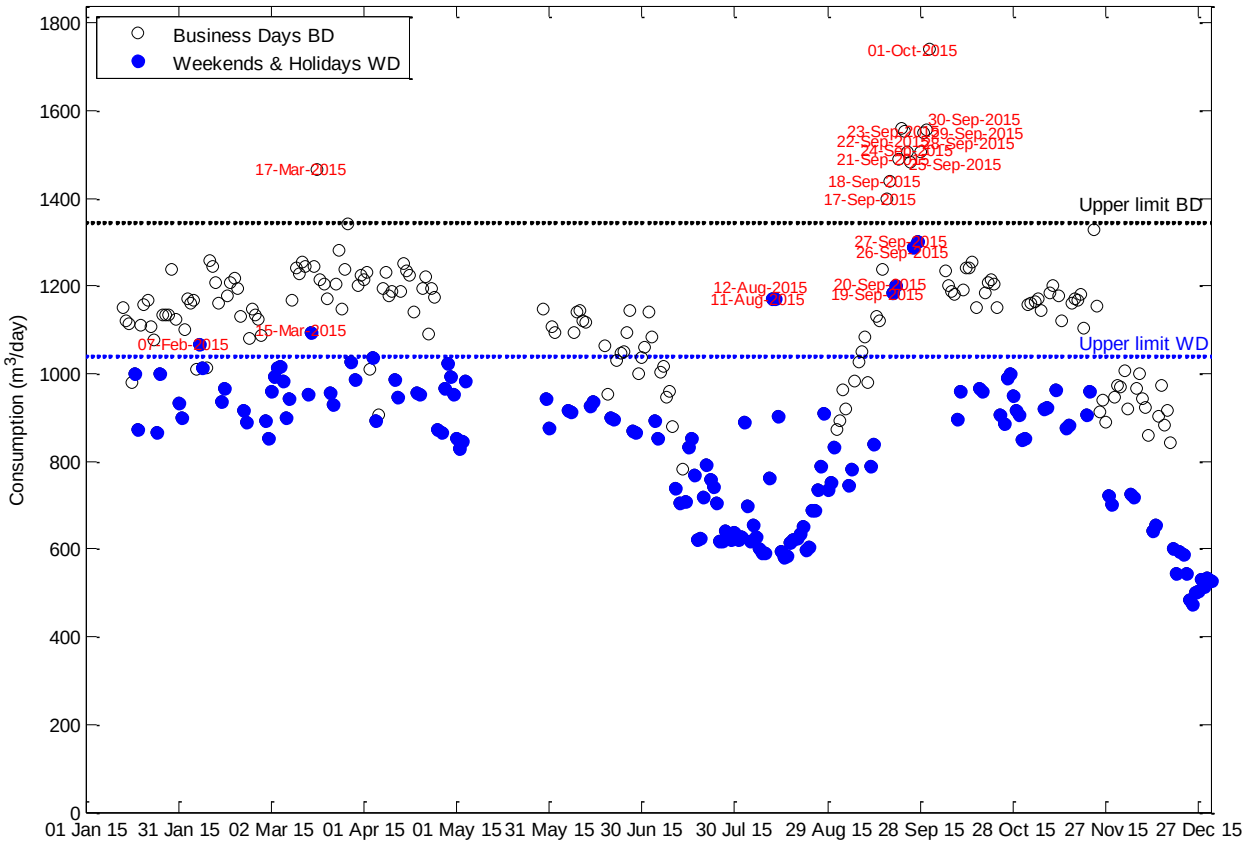

Figure 5.19: Leak detection from the data of the main bulk meter by the PDF approach

5.3. Minimum Night Flow (MNF) approach

The Minimum Night Flow (MNF) approach is a common method for leak detection. The MNF is measured between 2:00 am and 4:00 am when customer demand is least, network pressures are high and leakage is dominant in a District Metered Area (DMA) (Thornton et al., 2008). A DMA is created by subdividing the water distribution network into discrete zones by the closure of valves, in which the volume of water entering and leaving the zone is metered (Morrison, 2010). In residential buildings, the maximum decrease of the night flow was observed from 3:00 am to 4:00 am (Tabesh et al., 2009). A leak alarm is generated when the MNF between 1:00 am and 5:00 am exceeds a threshold set by water utilities. The threshold depends on the age and length of pipes, the number of connections and the pressure (Alkasseh et al., 2013). Several studies developed some methods based on the observation of the minimum night flow (García et al., 2006). For instance, Cheung et al. (2010) used the results of the MNF in order to validate the leakage estimated by a calibrated hydraulic model. Buchberger et al. (2004) proposed a method to assume minimum and maximum rates of leakage based on sequential statistical analyses computed from continuous measurements of the flow especially the night flows. However, this method was not tested in the field. The previous studies have used the MNF approach to estimate the water loss rather than detecting the leakage. In order to detect leakage using the minimum

night flows, the real time monitoring requires a threshold. A leak alarm will be generated if the night flows exceed that limit. In order to detect the leakage in real time, a method has been developed using the minimum night flow approach. It is based on defining a threshold by computing repeatedly the mean and standard deviation of the extracted night flows. The future night consumptions can be compared to the dynamic threshold in order to detect any abnormality.

5.3.1. Methodology

The first step consists in extracting the daily minimum night flow. In order to avoid the false values due to a dysfunction of the sensor, the night flow is computed as at 5% of the measured values over the restricted time series between 2:00 am and 5:00 am. It provides a value that is above 5% of the points and below 95% of the remaining points instead of taking the exact minimum value over the defined time series. Once the MNF has been extracted, the Moving Average MA and Moving Standard Deviation MSD are computed taking into account a lag indicating the number of previous data points used to calculate these two parameters. The new MNF value has to be compared to a threshold which is the mean plus a factor α multiplying the standard deviation. If the new MNF is lower than this limit, the response will be equal to 0 and the process of computing the MA and the MSD is repeated over the data series. If it exceeds the threshold, the response will be equal to 1 and the new MA and MSD will be equal to the last parameters found in normal state. The steps of this method are summarized in the flow chart of Figure 5.20.

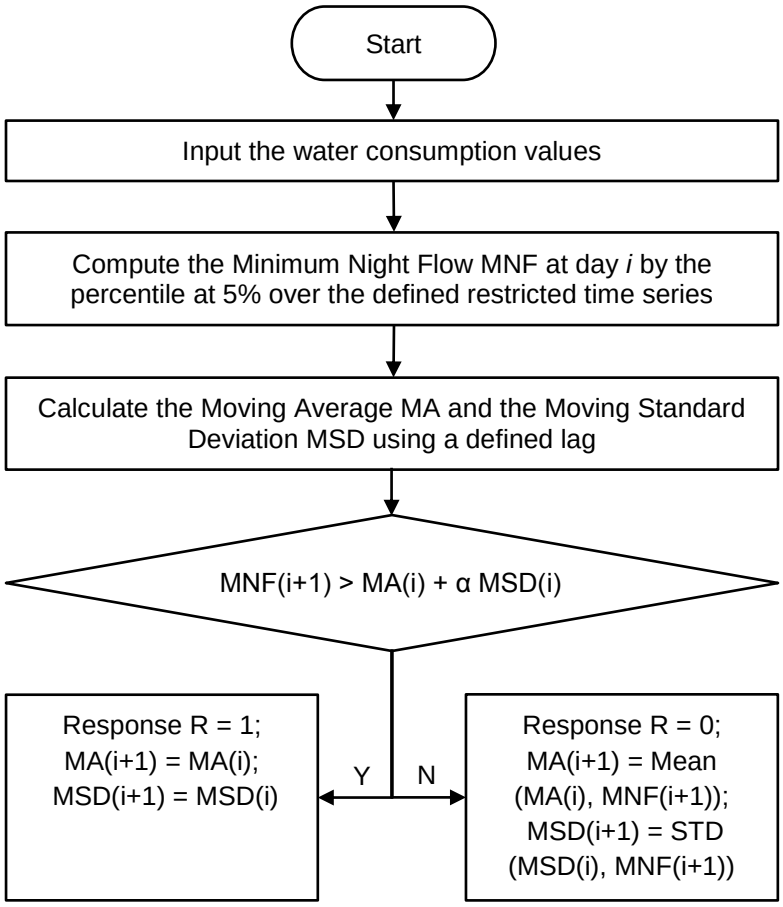

Figure 5.20: Flow chart of MNF methodology

5.3.1.1. The α-factor

The defined threshold is set to the moving average plus a factor α multiplying the moving standard deviation. Based on Chebyshev's inequality (Saw et al., 1984), if X is a random variable that follows any probability distribution with a mean μ and standard deviation σ, then for any real number $\alpha > 0$,

$$P\left(\left|X-\mu\right| \geq \alpha\sigma\right) \leq \frac{1}{\alpha^2} \tag{5.4}$$

Under this statement, a minimum of 89% of values must lie within 3 standard deviations and 75% within two standard deviations. Table 5.2 shows for different values of α, the minimum percentage of values within α standard deviations.

Table 5.2: Percentage of values according to the factor α

α	Minimum % within α standard deviations of mean
1	0.00%
2	75.00%
3	88.89%
4	93.75%
5	96.00%
6	97.22%
7	97.96%
8	98.44%
9	98.77%
10	99.00%

The factor α is determined based on the confusion matrix (contingency table) which is one of the basic statistical quality metrics for detection performance assessment. The strategy consists in relying on recorded data in the period January 1st 2015 – April, 30 2016 to superimpose the real leaks detected during this period. These leaks are summarized in Table 5.3.

Table 5.3: Leaks detected between January 2015 and April 2016

Onset	**Type**	**Duration**	**Location**
17 March 2015	Leak	1 day	Burst pipe in the construction site of the new library
11 August 2015	Leak	3 days	Burst pipe in the construction site of the new library
17 September 2015	Progressive Leak	17 days	Unreported leak near the 'Ecole Centrale'
27 February 2016	Operational purposes	1 day	Maintenance of the water network
11 March 2016	Operational purposes	1 day	Maintenance of the water network

The MNF steps were repeated for different values of α. For each value of α corresponds a confusion matrix. The suspected leaks reported by the method are classified as follows:

- True Positive (TP): An actual leak is detected. The method reported a leak and it was verified by the operators.
- False Negative (FN): An actual leak is not detected. The water loss continues until the leak is detected during a survey.
- False Positive (FP): The method generates a false alarm.
- True Negative (TN): There is no leak generated by the method and verified by the field team.

The Table 5.4 shows the components of the confusion (2x2) matrix as well as the common performance metrics: sensitivity, specificity, accuracy, fall-out, miss rate, precision, false omission rate, false discovery rate and negative predictive value.

Table 5.4: Confusion matrix and common performance metrics

<table>
<tr><th></th><th>Positive Prediction</th><th>Negative Prediction</th><th colspan="2"></th></tr>
<tr><td>Positive Class</td><td>True Positive
TP</td><td>False Negative
FN</td><td>Sensitivity, Recall, True Positive Rate,
$TPR = \frac{TP}{TP + FN}$</td><td>Miss Rate, False Negative Rate,
$FNR = \frac{FN}{TP + FN}$</td></tr>
<tr><td>Negative Class</td><td>False Positive
FP</td><td>True Negative
TN</td><td>Fall-out, False Positive Rate,
$FPR = \frac{FP}{FP + TN}$</td><td>Specificity, True Negative Rate,
$TNR = \frac{TN}{FP + TN}$</td></tr>
<tr><td></td><td>Precision, Positive Predicted Value,
$PPV = \frac{TP}{TP + FP}$</td><td>False Omission Rate,
$FOR = \frac{FN}{FN + TN}$</td><td colspan="2" rowspan="2">Accuracy,
$ACC = \frac{TP + TN}{TP + TN + FP + FN}$</td></tr>
<tr><td></td><td>False Discovery Rate,
$FDR = \frac{FP}{TP + FP}$</td><td>Negative Predictive Value,
$NPV = \frac{TN}{FN + TN}$</td></tr>
</table>

5.3.2. Results

This method is applied to the night flow of bulk meters of the network for the period starting from January, 1st 2016. The data set is filtered from any false values due to a dysfunction of the sensor or the telemetry system. A MATLAB script has been created in order to automate this approach. To calculate the first MA and the first MSD, a lag of 15 points is taken into consideration. For different values of α, we get the response which is 0 in case of normal state and 1 in case of a leak. For every threshold, a comparison is conducted with the leak calendar shown in Table 5.3 to evaluate the detection performance. Noting that the positive class corresponds to a leak. All the results for different values of α are described in Table 5.5. The sensitivity measures the proportion of leaks that are correctly identified. In parallel, the specificity measures the percentages of no-leaks that are properly recognized.

Table 5.5: Performance metrics for different values of α

Metrics \ α	2	3	3.5	4	4.5	5	5.5	6	6.5	7
Sensitivity TPR	95%	90%	90%	90%	90%	90%	90%	90%	90%	90%
Specificity SPC	51%	90%	93%	95%	96%	97%	98%	98%	99%	99%
Accuracy ACC	53%	90%	93%	95%	95%	97%	97%	98%	98%	98%
False Negative Rate FNR - miss rate	5%	10%	10%	10%	10%	10%	10%	10%	10%	10%
False Positive Rate FPR - fall out	49%	10%	7%	5%	4%	3%	2%	2%	1%	1%
Precision	9%	31%	39%	47%	50%	62%	67%	69%	75%	75%
Negative Predictive Value NPV	100%	99%	99%	99%	99%	100%	100%	100%	100%	100%
False Omission Rate, FOR	0%	1%	1%	1%	1%	0%	0%	0%	0%	0%
False Discovery Rate, FDR	91%	69%	61%	53%	50%	38%	33%	31%	25%	25%

As shown in Table 5.5, for α equal to 2 (threshold MA+2MSD), the proposed method detected 95% of t leaks. However, 49% of the responses correspond to false alarms. Starting from α equal to 3.5, the percentage of false alarms decreases to 7% and reach 1% for α equal to 6.5. The sensitivity starts to converge to 90% from α equal to 3. A factor $\alpha = 5$ seems to be an optimal value where the accuracy of the method reaches 97% and the percentage of false alarms drops to 3%.

Figure 5.21 shows the results of this method when applied to all the principal meters for $\alpha = 3$. It is clear that when the new extracted MNF exceeds the defined limit, the response is equal to 1 and an alarm (red rectangle) appears on the calendar to indicate the corresponding day as shown in Figure 5.22. The response for $\alpha = 5$ are depicted in Figure 5.23 and Figure 5.24, respectively. Figure 5.25 and Figure 5.26 summarize the results obtained for $\alpha = 7$.

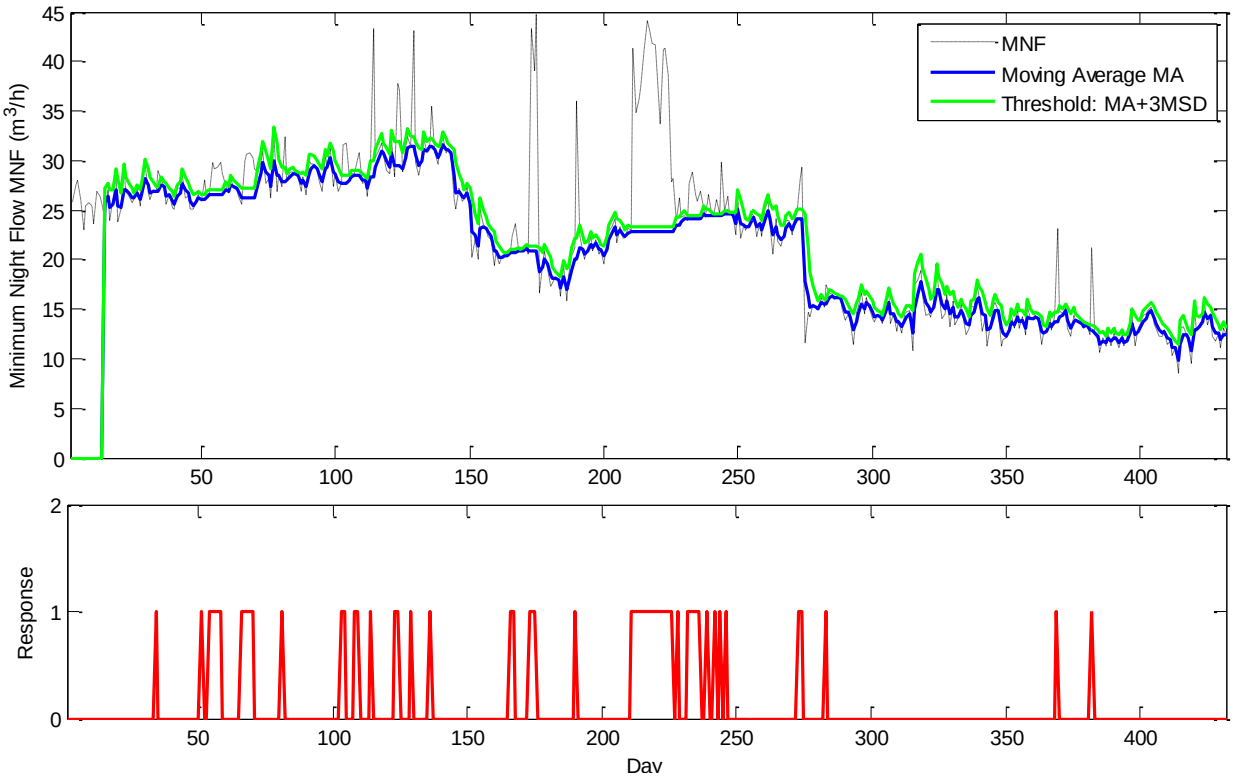

Figure 5.21: MNF methodology applied to all bulk meters and the appropriate response for $\alpha = 3$

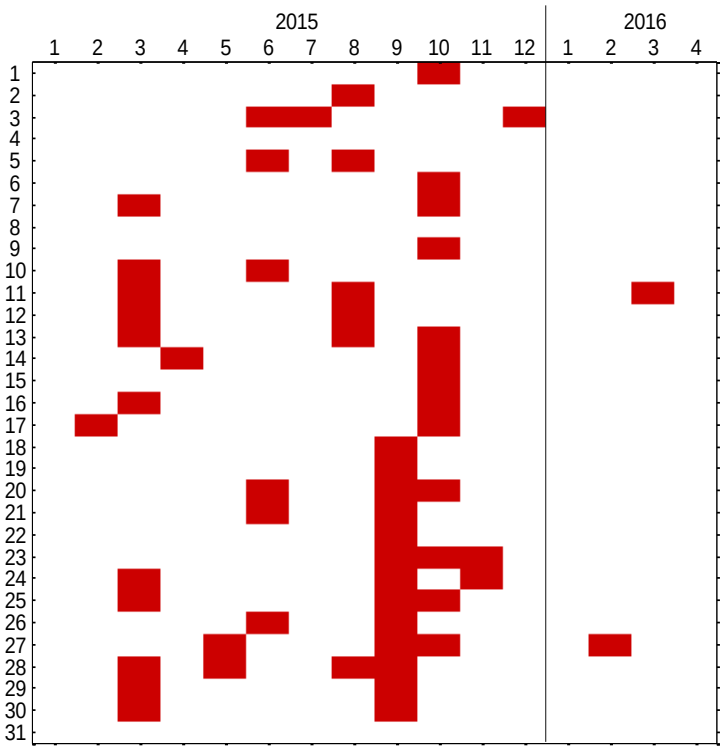

Figure 5.22: Calendar of leaks detected by the MNF method for $\alpha = 3$

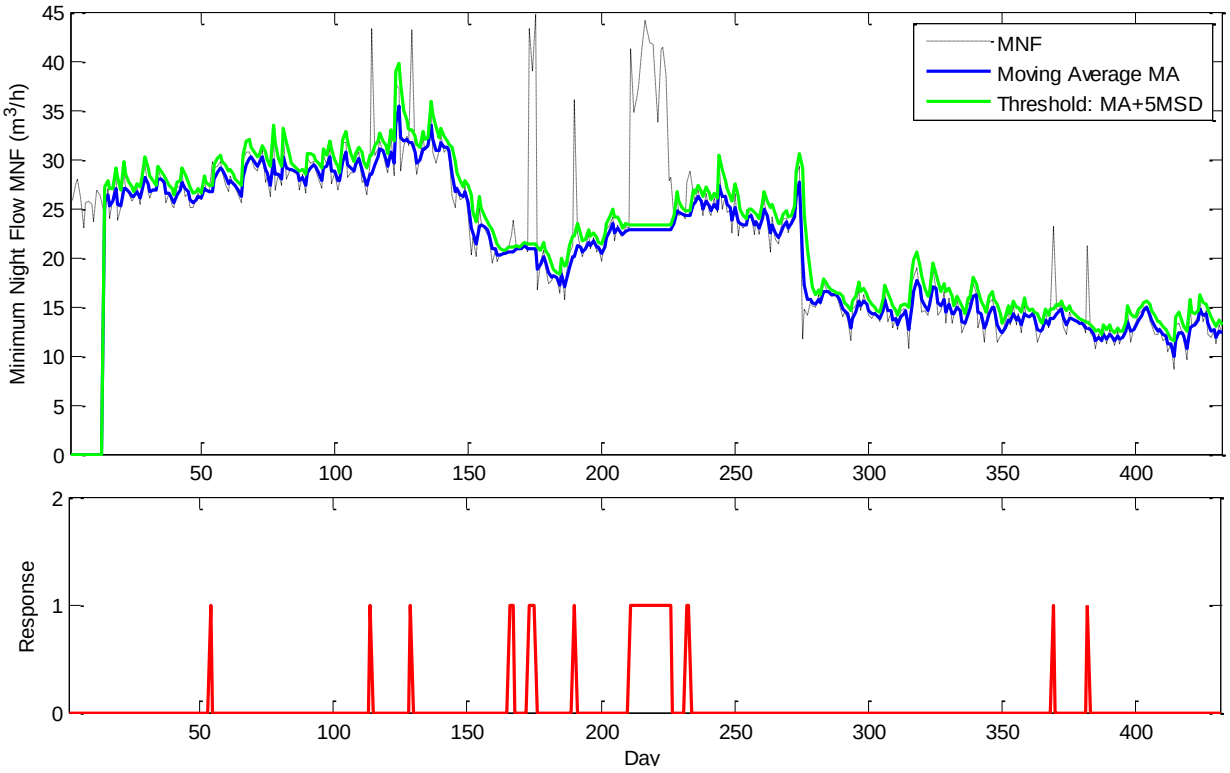

Figure 5.23: MNF methodology applied to all bulk meters and the appropriate response for $\alpha = 5$

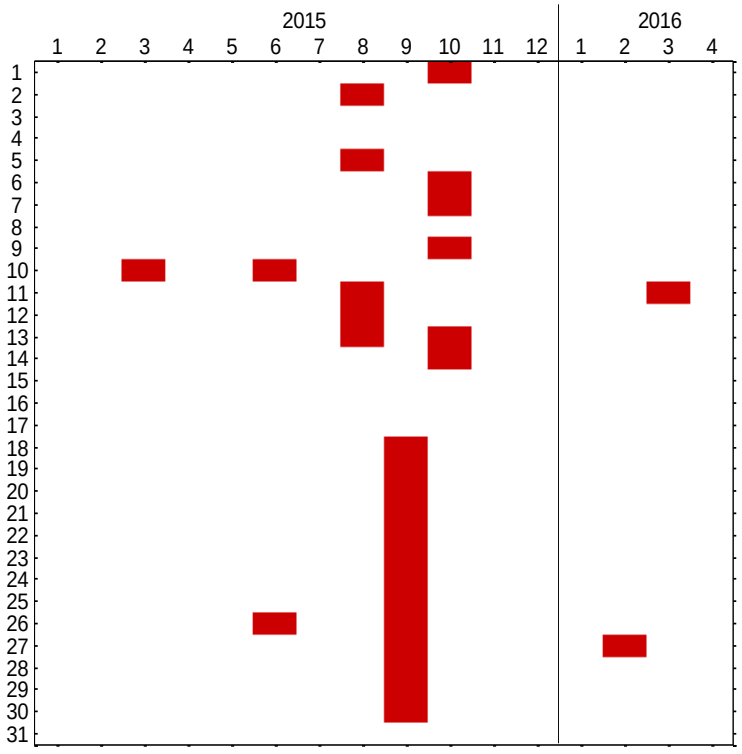

Figure 5.24: Calendar of leaks detected by the MNF method for $\alpha = 5$

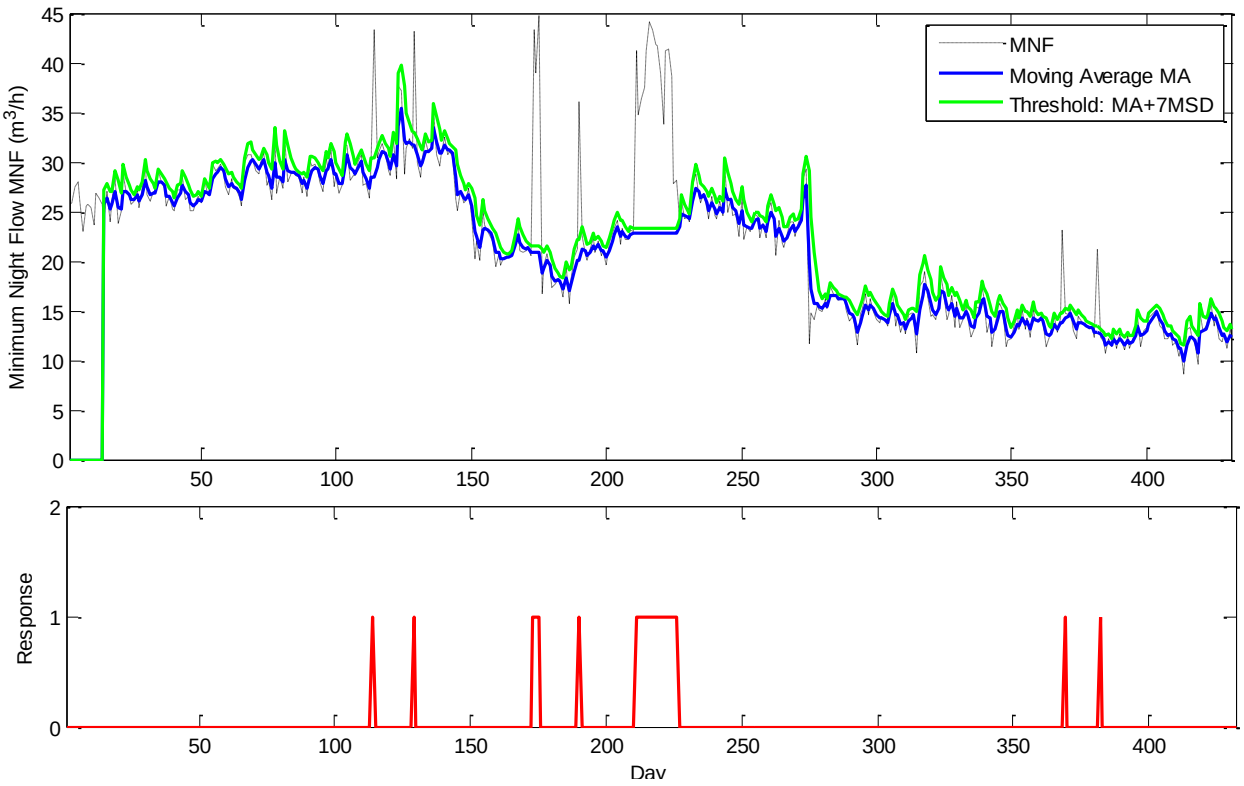

Figure 5.25: MNF methodology applied to all bulk meters and the appropriate response for $\alpha = 7$

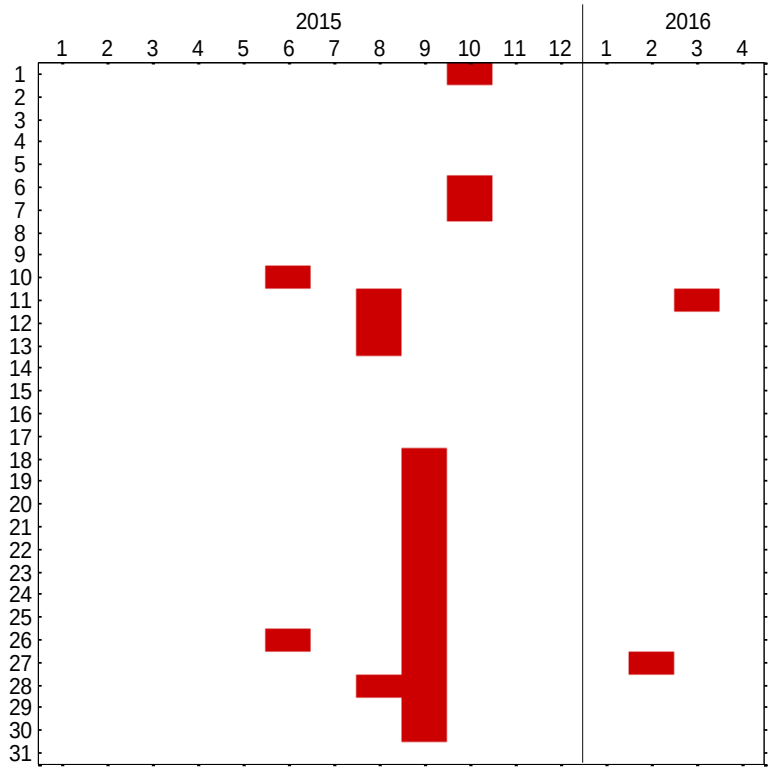

Figure 5.26: Calendar of leaks detected by the MNF method for a threshold of $\alpha = 7$

5.3.2.1. Discussion

The automated MNF methodology with thresholds of standards deviations of the mean (α = 3, 5 and 7) has allowed the detection of the two leaks in August and September 2015. For α = 3, 10% of the responses were classified as false alarms. As shown in Figure 5.22, a leak alarm was generated from 10 to 14 March 2015, where we did not observe any leakage. The leak alarm can be explained by the fact that this period came after the winter holidays. Figure 5.26 illustrates the flow measured through all the general meters one week before and one week after this holiday (From 23/02/2015 till 14/03/2015).

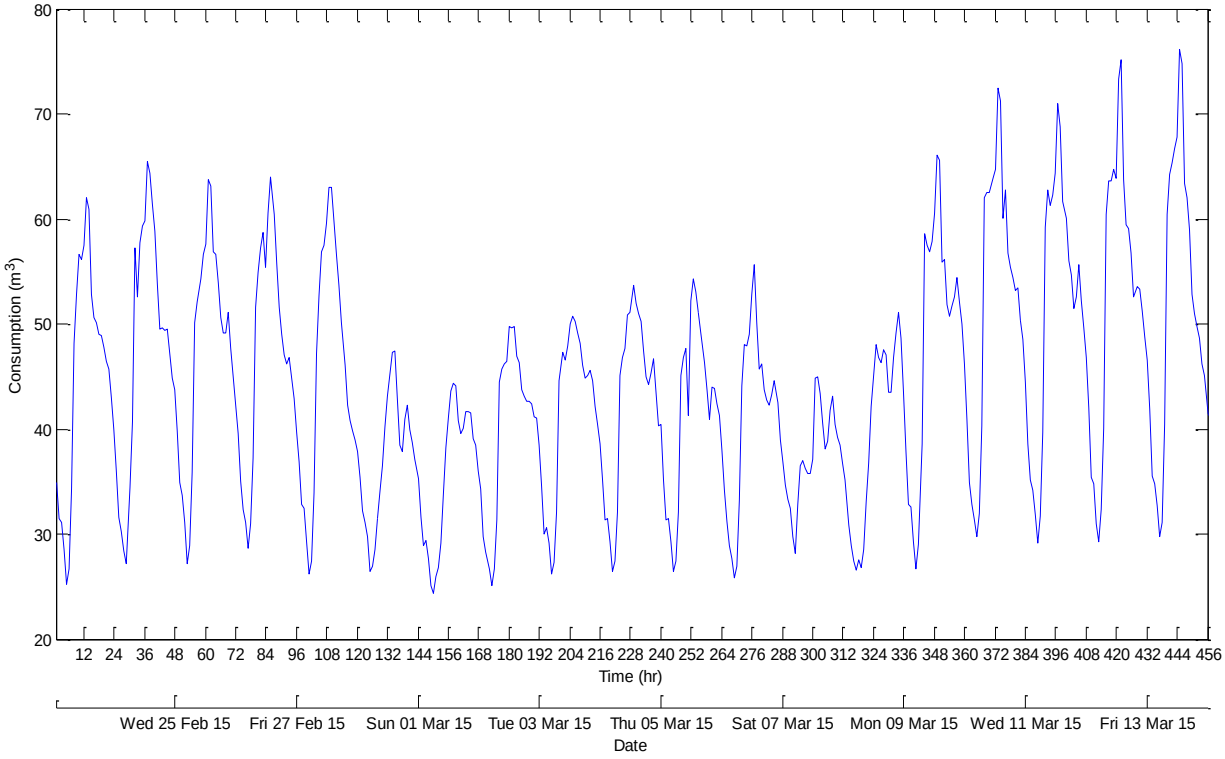

Figure 5.27: Hourly water consumption profile of all the general meters from 23/02/2015 till 14/03/2015

During these holidays (from 2 March 2015 till 8 March 2015), due to the non-activity of the university buildings, we had a decrease in water consumption. The minimum night flows show a drop comparing to the values recorded in working days. The calculation of the moving average took into consideration this decrease of the minimum night flow during this period and the threshold is therefore reduced. After the holidays, the new MNF is then compared to the limit influenced by the decrease in the MNF during holidays and the method generates consequently false alarms. Such false alarms are reduced starting from α = 3.5. By adopting a limit set to 5 standard deviations of the mean, the method is 97% accurate and was able to correctly identify 90% of leaks. The undetected leaks (10%) can be explained by:

- The pipe burst in March 17 occurred during the day and was repaired immediately.
- The onset of the third leak starting from 17th of September was not reported by the method. The response started to be equal to 1 and generated consequently a leak alarm

from September 18. In fact, the leak occurred at 4:00 am of September 17. During this day, the MNF extracted was the percentile at 5% of the measured values between 2:00 am and 5:00 am. The MNF computed for the 17th of September occurred certainly between 2:00 am and 4:00 am. The method then spotted the leak the next day when all the night flow values over the restricted time series increased by the water loss rate.

5.4. Threshold Water Consumption Profile

In order to improve the current state of leak detection in quasi real time, the Threshold Water Consumption Profile (TWCP) method is developed. The TWCP method consists in building a model from the historical values. The raw data is statistically analyzed to set a threshold based on its history. A distinction between the water consumption during working days and holidays is necessary. The water consumption values measured by the AMRs are then compared to the limit to detect any consumption anomaly or leakage. A pre-processing step is applied to filter the model from any abnormal event in the past. The model is based on the computation of the mean and the standard deviation of the hourly consumption data over the week. A corresponding simplified model is calculated based on the variation of the consumption over the day between morning, midday, afternoon and night. The threshold is then defined by the obtained mean plus a factor α multiplying the standard deviation. All the steps of the TWCP method are summarized in Figure 5.28.

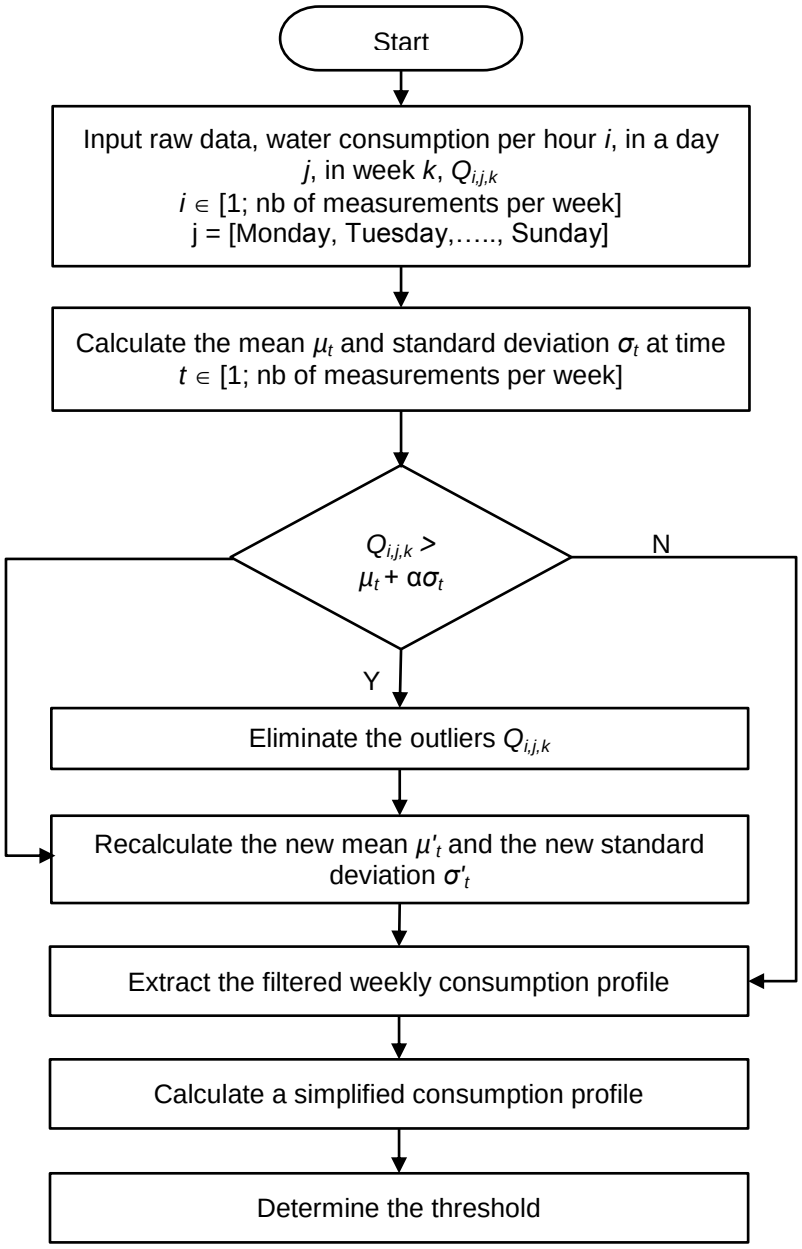

Figure 5.28: Flow chart of TWCP methodology

The factor α is determined by training of the historical data. An anomaly is reported if the real time data exceeds the threshold. A leak alarm is generated when the anomaly persists for four consecutive hours considering the same range of the leak detection from MNF method.

5.4.1. Detection performance assessment

The factor α is calculated based on the confusion matrix (contingency table) which is one of the basic statistical quality metrics for performance assessment. The strategy consists in relying on recorded data to superimpose a variety of abnormal behaviors similar to real known faults.

In our case study, 17 472 values collected for 2 years (2013 and 2014) represent the raw data. The input signal is the sum of the water consumption in the chemistry sector including 10 buildings including working days and holidays. Since leak patterns are well characterized, some artificial leaks were designed by adding an abrupt and progressive leak to the realistic signal as described in Table 5.6. The signal retrieved after introducing the artificial anomalies to the raw data depicted in Figure 5.29 represents the input data for the application of the TWCP method. The reliability of this method is evaluated by comparing results of the TWCP to simulated leaks.

Table 5.6: Calendar of artificial leak addition

Artificial leak	**Type**	**Onset**	**Duration (days)**	**Leak Rate**
A	Progressive	19/04/2013	12	$0.2\, m^3 / day$
B	Abrupt	01/06/2013	10	$1\ m^3 / hour$
C	Abrupt	10/09/2013	10	$2\ m^3 / hour$
D	Abrupt	24/11/2013	8	$3\ m^3 / hour$
E	Abrupt	20/01/2014	11	$4\ m^3 / hour$
F	Progressive	10/04/2014	15	$0.1\ m^3 / day$
G	Abrupt	20/08/2014	12	$1.5\ m^3 / hour$
H	Progressive	15/09/2014	15	$0.3\ m^3 / day$

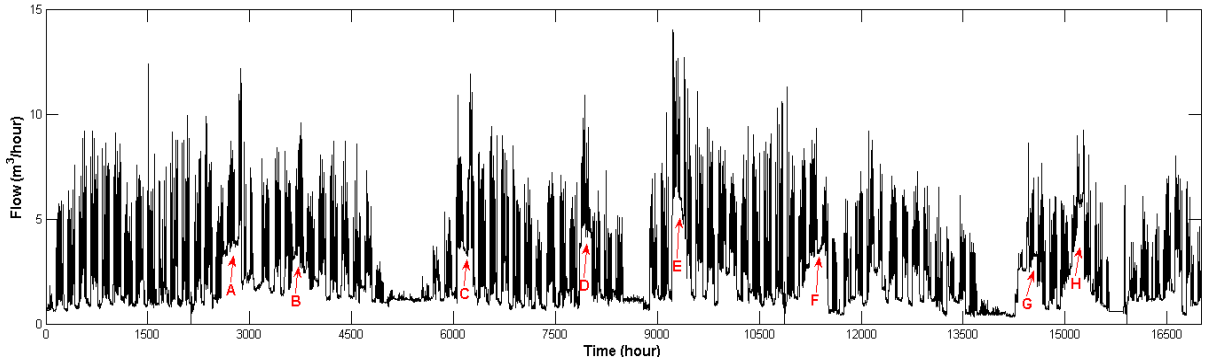

Figure 5.29: Artificial leak addition

The TWCP steps were repeated by changing the value of α. For each value of α corresponds a confusion matrix. The suspected leaks reported by the method were classified as follows:

- True Positive (TP): An actual leak is detected. The method reported a leak and it was verified by the operators.
- False Negative (FN): An actual leak is not detected. The water loss will continue in this case until the leak is detected during a survey.
- False Positive (FP): The method generates a false alarm.
- True Negative (TN): There is no leak generated by the method and verified by the field team.

5.4.2. ROC curve

The Receiver Operating Characteristics (ROC) curve is a useful tool for visualizing, organizing and selecting classifiers based on their performance (Fawcett, 2006). This technique has been widely used for medical diagnostic testing (Subtil et al., 2015) and to differentiate the hit rates from the false alarm in a signal.

The ROC curve is a two-dimensional graph in which the true positive rate (TPR) or the sensitivity is plotted in function of the false positive rate (FPR) or (1-Specificity).

The sensitivity of a classifier in calculated as following:

$$Sensitivity = TPR = \frac{TP}{TP + FN} \tag{5.5}$$

The specificity of a classifier is estimated as:

$$Specificit\,y = 1 - FPR = \frac{TN}{FP + FN} \tag{5.6}$$

The lower left point (0, 0) of the ROC space represents the strategy of never issuing a positive classification. The opposite strategy of unconditionally issuing positive classifications is represented by the upper right point of the curve (1, 1). The (0, 1) point is the perfect classification, representing 100% sensitivity (no false negatives) and 100% specificity (100%) specificity (no false positives). The best possible prediction method would yield close to this point. A completely random guess is represented by the diagonal line (y=x); it can be expected to get half the positives and half the negatives correct.

The ROC curve is used in this work to choose the optimal value of the factor α and calculate consequently the threshold. As shown in Figure 5.30, the perfect classification occurs for α = 2.2 and the threshold is consequently equal to $\mu'_t + 2.2\sigma'_t$. Based on Chebyshev's inequality (Saw et al., 1984), 75% of the values must lie within two standard deviations of the mean. The results of the ROC curve shows that for α = 2, the sensitivity and the specificity are equal to 91% and 87% respectively. Therefore, it is possible to define the threshold using the present statistical laws by multiplying the standard deviation by α = 2. However, the optimal threshold found following the ROC curve analysis is defined by α = 2.2.

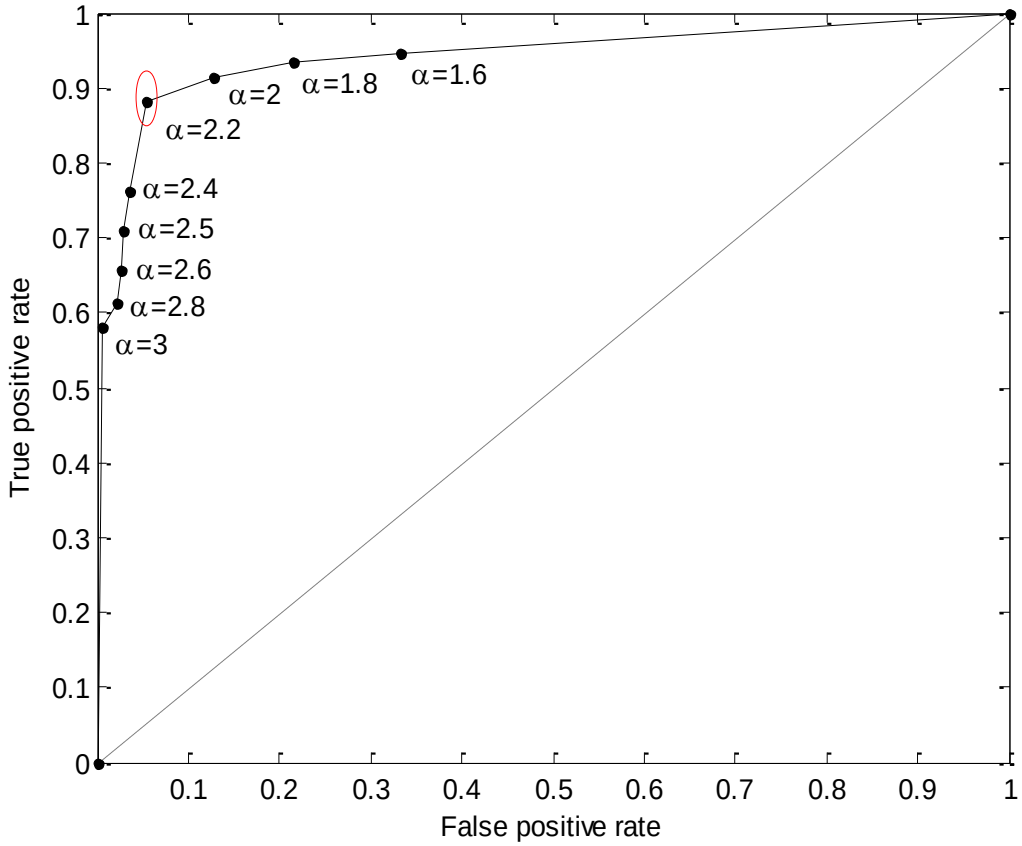

Figure 5.30: ROC curve for different values of α for the TWCP method

5.4.3. Discussion

The TWCP method has been applied in Lille Demo Site at District Metered Areas (DMAs) and for buildings. The water consumption data are compared to the threshold $\mu'_t + 2.2\sigma'_t$ derived from the analysis of the ROC curve. A leak alarm is generated when the anomaly persists for four consecutive hours.

Figure 5.31 shows a leak detected inside a building in the physic sector between May 17 and 19, 2014. The water consumption exceeds clearly the threshold during that weekend. The onset of this leak is detected clearly on May 17 at midday. An abnormal consumption is also reported on May, 13 2014 at 3 pm. This event is not considered as a leak because the anomaly has disappeared the next hour.

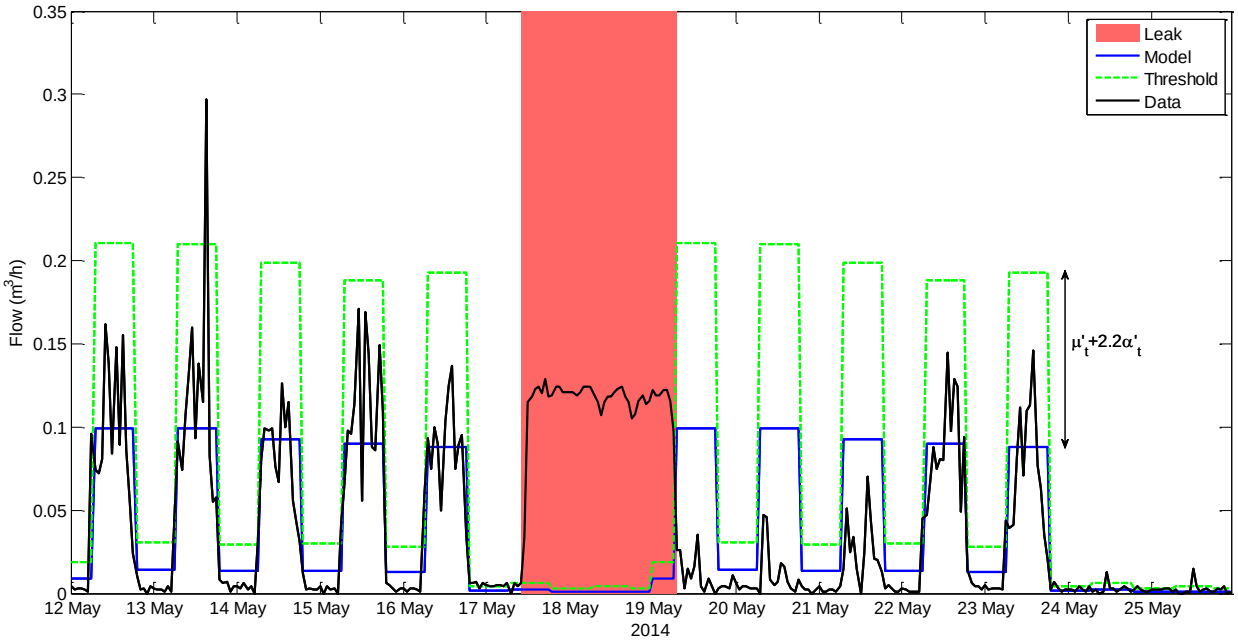

Figure 5.31: TWCP evaluation process for a physic building (leak alarm on May 17, 2014)

Besides the application of the method on the building level, the TWCP method has been applied on the data collected from all the bulk meters in the demo site representing the overall consumption of the campus. The Figure 5.33 shows a leak detected in the midday of September 17, 2015. This leak was impossible to be detected using the MNF approach due to its occurrence in the morning.

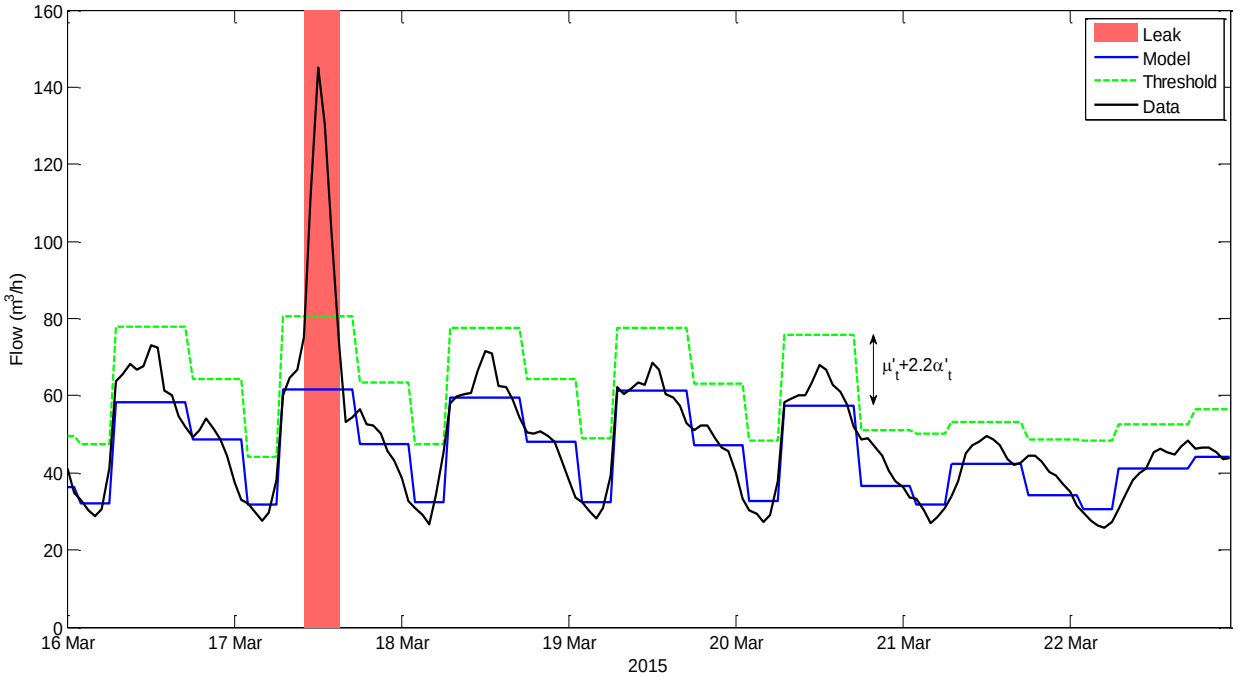

Figure 5.32: Leak detected on March 17, 2015 using the TWCP approach applied on the data of all principal meters

The Figure 5.33 demonstrates the ability of the TWCP approach to detect the leakage starting on September 17, 2015. This method was capable to identify the onset of the leakage that started at 4 pm in the morning.

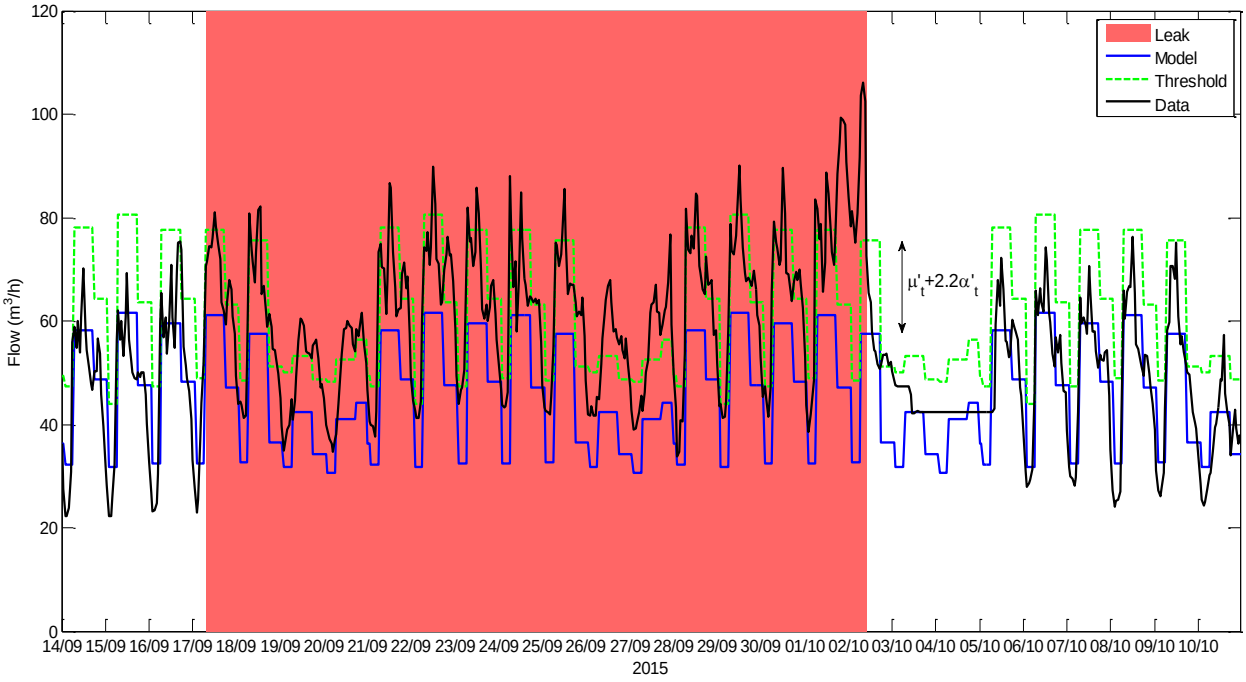

Figure 5.33: Leak detected starting from September 17, 2015 using the TWCP approach applied on the data of all principal meters

5.5. Conclusion

The real time measurements collected from the hydraulic sensors in the smart water networks need to be coupled with appropriate data analysis methodologies to detect immediately the leakage. In this chapter, we have applied available approaches, developed advanced methods and tested their efficiencies:

- The Comparison of Flow Pattern Distribution (CFPD) is a data driven method that compares flow pattern to detect leakage and manage the water demand. It is useful at the scale of a DMA or water supply data set. It has been successfully demonstrated that the CFPD method can be applied to customer or sub-meter data. The application of this method at SunRise Demo site showed its capacity to detect three leaks in the campus. It showed also the capacity of this method to spot the leak in the building of Physics and to highlight the effect of the holidays on the water consumption. However, this method did not allow determining the onset of the leakage. In addition, it is a retrospective analysis method and requires human judgment. In order to detect in real-time new leakage, Van Thienen et al. (2016) developed Cuboid for automated feature recognition in CFPD analyses of supply area flow data.
- The Probability Density Functions (PDF) of the water consumption data have allowed to define an upper limit during working and non-working days at the daily scale. The boundaries are determined based on historical values filtered from any anomalies. This methodology is very useful to: i) describe the daily behavior in terms of water usage and ii) take the appropriate decisions by comparing the actual daily consumption with the modeled one. It has been demonstrated that this method be applied at the scale of a building and a sector.
- The traditional MNF method consists of monitoring the flow in the early morning. Till now, this method depends on the human judgment and on a manual interpretation of the data. The proposed improvement of this traditional method based on the moving average and moving standard deviation of the computed MNF has permitted to automate this process. The developed method is cost effective and can be easily implemented in any project. It allows a rapid response to the leakage but only detected during the night.
- In order to detect the leakage in near real time, a new method has been developed: Threshold Water Consumption Profile (TWCP). This statistical approach is based on the historical hourly consumption data to build a free of leak model for the business days and for the holidays and weekends. A threshold is defined based on the mean and the standard deviation of the measurements and optimized using a leak detection performance assessment. This method was able to detect the onset of the leakage at the scale of the building and the sector. It is simply to be implemented and can be used for online event detection.

Conclusion

This work concerns the application of both the conventional methods and the smart technology on the detection of the water leakage, which constitutes one of the major water challenges. Indeed, in some cities the water leakage could attain around 50% of the water supply.

This research is conducted within the SunRise Smart City project, which aims at turning the Scientific Campus of the University of Lille1 into a large scale demonstrator of the Smart and Sustainable City. This campus stands for a town of around 25000 inhabitants. It is also conducted within the European Project SmartWater4Europe, which consists in the construction of 4 European demonstrators of the Smart Water System.

The smart monitoring of the Scientific campus included the installation of AMR at the supply sections as well as in the buildings, which allow to access to the water consumption at hourly time-step. The monitoring included also the installation of 5 pressure sensors and an acoustic system. Thanks to this monitoring, we collected a huge amount of data concerning the water system. Since the water system of the scientific campus is around 60 years old, it suffers from serious deterioration, which resulted in multitude of leakage events. These events constitute an interesting base for the analysis of the efficiency of the methods proposed for the detection of water leakage as well as for the development of new methods.

The descriptive analysis presented in this thesis is very efficient in predicting the behavior of the AMRs in terms of water consumption. It has been demonstrated that a simply correlation analysis is efficient in predicting the corresponding meters that are related to the bulk meter in a highly meshed network. Therefore, the division of the meshed network into specified DMAs is possible just by closing the appropriate valves. The analysis of the flow change of the water consumption allowed the identification of possible leaks. Additionally, to the descriptive analysis, the k-means algorithm applied to the water consumption data and evaluated using the entropy scorer was able to cluster the AMRs based on similar behaviors in the water usage. Clustering is useful: i) to categorize, without any prior knowledge, the type of usage of the building depending on the water consumption and ii) to reinforce the ability of the water utilities to define customized offers for the customers based on specific behaviors in water usage.

The water balance calculation using the top down and bottom up approaches allowed the estimation of the NRW level. The application of the proposed Active Leakage Control (ALC) strategy has reduced the NRW rate from 43% (January – May 2015) to 7 % (January – May 2016). The water audit coupled with the ALC strategy has proved its efficiency to provide an overall overview of the water losses and to detect the high level of leakage in the DMAs.

For a rapid detection of abnormal events, a set of advanced methods has been developed. Their performances have been evaluated using the collected data.

The Comparison of Flow Pattern Distribution (CFPD) data driven method allowed the detection of leaks in the campus at both the scale of a building or a sector. However, this method is limited in identifying the onset of leakage.

The MNF monitoring is largely used by water utilities to detect water losses. This method uses a manual interpretation of the data. A methodology based on moving the average and the standard deviation of the computed MNF allowed the automation of this traditional approach. It is possible now to use the improved method online to detect the night abnormal events.

In order to improve the identification of the leakage in near real time, two statistical approaches have been developed. They are based on the time series historical data to build a model free of any leaks and determine an appropriate threshold. The actual consumption is then compared with the defined threshold and the decision is automatically taken in case of any anomaly. These two methods have been successfully applied on data collected from a building as well as from a sector. The developed methods are able to detect the leaks based on the empirical observation of the pattern without the necessity of a hydraulic based simulation model of the WDS.

A platform was developed for the integration of methods used and developed in this work. This platform allows the use and the combination of conventional and advanced methods for leakage detection. In the future, it will be interesting to develop an expert system, which allows combining these methods for an efficient detection of the water leakage as well as water flow. The platform should also be enhanced by numerical modeling and advanced visualization tools such as augmented reality, which will improve the users' awareness as well as the asset management.

References

Adachi, S., Takahashi, S., Kurisu, H., and Tadokoro, H. (2014). Estimating Area Leakage in Water Networks Based on Hydraulic Model and Asset Information. *Procedia Engineering*, 89, 278-285. doi: http://dx.doi.org/10.1016/j.proeng.2014.11.188.

Alkasseh, J. A., Adlan, M., Abustan, I., Aziz, H., and Hanif, A. (2013). Applying Minimum Night Flow to Estimate Water Loss Using Statistical Modeling: A Case Study in Kinta Valley, Malaysia. *Water Resources Management,* 27(5), 1439-1455. doi: 10.1007/s11269-012-0247-2.

Allen, M., Preis, A., Iqbal, M., Srirangarajan, S., Lim, H. B., Girod, L., and Whittle, A. J. (2011). Real-time in-network distribution system monitoring to improve operational efficiency. *Journal American Water Works Association (AWWA),* 103(7), 63-75.

Ariaratnam, S. T., and Chandrasekaran, M. (2010). Development of an Innovative Free-Swimming Device for Detection of Leaks in Oil and Gas Pipelines. *Construction Research Congress* 588-596.

AWWA. (2005). Computer modeling of water distribution system - Manual of water supply practices, M32 (2nd ed.). *Denver*: *American Water Works Association*.

Ay, M., and Kisi, O. (2014). Modelling of chemical oxygen demand by using ANNs, ANFIS and k-means clustering techniques. *Journal of Hydrology*, 511, 279-289. doi: http://dx.doi.org/10.1016/j.jhydrol.2014.01.054.

Ayala–Cabrera, D., Herrera, M., Izquierdo, J., Ocaña–Levario, S., and Pérez–García, R. (2013). GPR-Based Water Leak Models in Water Distribution Systems. *Sensors*, 13(12), 15912-15936.

Barry, M. G., Purcell, M. E., and Eck, B. J. (2014). Using Smart Water Meters in (Near) Real-Time on the IWIDGET System. *Proccedings of the 11th International Conference on Hydroinformatics*, New York City, USA

Beuker, T., Brockhaus, S., Ahlbrink, R., and McGee, M. (2009). Addressing challenging environments–advanced in-line inspection solutions for gas pipelines. *Proceedings of the 24th World Gas Conference*, Argentina

Blindu, I. (2004). Outil d'aide au diagnostic du réseau d'eau potable pour la ville de Chisinau par analyse spatiale et temporelle des dysfonctionnements hydrauliques. *PhD thesis*, Ecole Nationale Supérieure des Mines de Saint-Etienne.

Boulos, P. F., and Wiley, A. N. (2013). Can We Make Water Systems Smarter? *Opflow*, 39(3), 20-22.

Boyle, T., Giurco, D., Mukheibir, P., Liu, A., Moy, C., White, S., and Stewart, R. (2013). Intelligent Metering for Urban Water: A Review. *Water*, 5(3), 1052.

Brennan, M. J., Gao, Y., and Joseph, P. F. (2007). On the relationship between time and frequency domain methods in time delay estimation for leak detection in water distribution pipes. *Journal of Sound and Vibration*, 304(1–2), 213-223. doi: http://dx.doi.org/10.1016/j.jsv.2007.02.023.

Brothers, K., Eng, P., and Force, I. W. L. T. (2001). Using the IWA Performance Indicators and Noise Mapping for NRW Reductions in Halifax, Nova Scotia, Canada. *Proceedings of the Water Loss Specialist Conference, International Water Association*, Brno, Czech Republic

Brunone, B., and Ferrante, M. (2004). Pressure waves as a tool for leak detection in closed conduits. *Urban Water Journal*, 1(2), 145-155. doi: 10.1080/15730620420000271073.

Buchberger, S. G., and Nadimpalli, G. (2004). Leak Estimation in Water Distribution Systems by Statistical Analysis of Flow Readings. *Journal of Water Resources Planning and Management*, 130(4), 321-329. doi: 10.1061/(ASCE)0733-9496(2004)130:4(321).

Burn, S., DeSilva, D., Eiswirth, M., Hunaidi, O., Speers, A., and Thornton, J. (1999). Pipe leakage–future challenges and Solutions. *Pipes Wagga Wagga*, Australia

Burrows, R., Crowder, G. S., and Zhang, J. (2000). Utilisation of network modelling in the operational management of water distribution systems. *Urban Water*, 2(2), 83-95. doi: http://dx.doi.org/10.1016/S1462-0758(00)00046-7.

Cahn, A. (2013). Shaping the Architecture of Smart Water Networks. *Water & Sewerage Journal 3*, 13-15.

Calcatelli, A., Bergoglio, M., and Mari, D. (2007). Leak detection, calibrations and reference flows: Practical example. *Vacuum*, 81(11–12), 1538-1544. doi: http://dx.doi.org/10.1016/j.vacuum.2007.04.019.

Candelieri, A., and Archetti, F. (2014). Identifying Typical Urban Water Demand Patterns for a Reliable Short-term Forecasting – The Icewater Project Approach. *Procedia Engineering*, 89, 1004-1012. doi: http://dx.doi.org/10.1016/j.proeng.2014.11.218.

Caputo, A. C., and Pelagagge, P. M. (2002). An inverse approach for piping networks monitoring. *Journal of Loss Prevention in the Process Industries*, 15(6), 497-505. doi: http://dx.doi.org/10.1016/S0950-4230(02)00036-0.

Chapman, H. (2012). Development of a Successful Internal Leak Detection and Pipeline Condition Assessment Technology for Large Diameter Pipes. *Proceedings of the 6th Annual WIOA NSW Water Industry Engineers & Operators Conference*, Tamworth, Australia, 27-29 March.

Charlton, M., and Mulligan, M. (2001). Efficient detection of mains water leaks using ground-penetrating radar (GPR). *Proceedings of Subsurface and Sensing Technologies and Applications III*, San Diego, CA, 30 July – 1 August.

Chastain-Howley, A. (2005). Transmission main leakage: how to reduce the risk of a catastrophic failure. *Proceedings of IWA Special Conference Leakage 2005*, Halifax, Nova Scota, Canada, September.

Cheung, P. B., Girol, G. V., Abe, N., and Propato, M. (2010). Night flow analysis and modeling for leakage estimation in a water distribution system (pp. 509-513): Taylor & Francis Group, London.

Chourabi, H., Taewoo, N., Walker, S., Gil-Garcia, J. R., Mellouli, S., Nahon, K., Pardo, T. A., and Scholl, H. J. (2012). Understanding Smart Cities: An Integrative Framework. *Proccedings of the 45th Hawaii International Conference on System Science (HICSS)*, Maui, HI, USA, 4-7 January.

Christodoulou, S., Agathokleous, A., Kranioti, S., Xanthos, S., and Gagatsis, A. (2012). Wireless Sensors for Leak Detection and Automatic Meter Reading (AMR) *NIREAS-IWRC/D5.15.1*. Nicosia, Cyprus.

Colombo, A. F., Lee, P., and Karney, B. W. (2009). A selective literature review of transient-based leak detection methods. *Journal of Hydro-environment Research*, 2(4), 212-227. doi: http://dx.doi.org/10.1016/j.jher.2009.02.003.

Crocco, L., Prisco, G., Soldovieri, F., and Cassidy, N. J. (2009). Early-stage leaking pipes GPR monitoring via microwave tomographic inversion. *Journal of Applied Geophysics*, 67(4), 270-277. doi: http://dx.doi.org/10.1016/j.jappgeo.2008.09.006.

De Silva, D., Mashford, J., and Burn, S. (2011). Computer aided leak location and sizing in pipe networks. *Queensland*: *Technical Report No. 17, Urban Water Security Research Alliance*.

Depuru, S. S. S. R., Wang, L., and Devabhaktuni, V. (2011). Smart meters for power grid: Challenges, issues, advantages and status. *Renewable and Sustainable Energy Reviews*, 15(6), 2736-2742. doi: http://dx.doi.org/10.1016/j.rser.2011.02.039.

Dong, L., Carnalla, S., and Shinozuka, M. (2011). Experimental and Analytical Study of Detecting Leakage of Water Pipes Using Ground-Penetrating Radar. *Proceedings of the 9th International Workshop on Remote Sensing for Disaster Response*, Standford, CA, USA, 15–16 September.

Fahmy, M., and Moselhi, O. (2009). Detecting and locating leaks in underground water mains using thermography. *Proceedings of the 26th International Symposium on Automation and Robotic in Construction (ISARC)*, Austin, Texas, U.S.

Fang, X., Misra, S., Xue, G., and Yang, D. (2012). Smart grid—The new and improved power grid: A survey. *Communications Surveys & Tutorials, IEEE*, 14(4), 944-980.

Fanner, P. V., Sturm, R., Thornton, J., Liemberger, R., Davis, S. E., and Hoogerwerf, T. (2007). Leakage management technologies. *Denver, Colorado*: *American Water Works Association (AWWA) Research Foundation*.

Fantozzi, M., Lambert, A. O., and Liemberger, R. (2010). Some examples of European water loss targets, and the law of unintended consequences. *Proceedings of IWA Conference Water Loss*, Sao Paulo, Brazil, 6 - 9 June.

Fantozzi, M., Popescu, I., Farnham, T., Archetti, F., Mogre, P., Tsouchnika, E., Chiesa, C., Tsertou, A., Gama, M. C., and Bimpas, M. (2014). ICT for Efficient Water Resources Management: The ICeWater Energy Management and Control Approach. *Procedia Engineering*, 70, 633-640. doi: http://dx.doi.org/10.1016/j.proeng.2014.02.069.

Farley, M. (2001). Leakage Management and Control - A Best Practice Training Manual. *Geneva, Switzerland*: *World Health Organisation*.

Farley, M., Wyeth, G., Ghazali, Z., Istandar, A., Singh, S., Dijk, N., Raksakulthai, V., and Kirkwood, E. (2008). The Manager's Non-Revenue Water Handbook - A Guide to Understanding Water Losses. *Bangkok, Thailand*: *Ranhill Utilities Berhad and the United States Agency for International Development (USAID)*.

Fawcett, T. (2006). An introduction to ROC analysis. *Pattern Recognition Letters*, 27(8), 861-874. doi: http://dx.doi.org/10.1016/j.patrec.2005.10.010.

Ferrante, M., and Brunone, B. (2003a). Pipe system diagnosis and leak detection by unsteady-state tests. 1. Harmonic analysis. *Advances in Water Resources*, 26(1), 95-105. doi: http://dx.doi.org/10.1016/S0309-1708(02)00101-X.

Ferrante, M., and Brunone, B. (2003b). Pipe system diagnosis and leak detection by unsteady-state tests. 2. Wavelet analysis. *Advances in Water Resources*, 26(1), 107-116. doi: http://dx.doi.org/10.1016/S0309-1708(02)00102-1.

Frings, J., and Walk, T. (2010). Pipeline Leak Detection using Distributed Fiber Optic Sensing. *3R international· Special-Edition*, 2, 57-61.

Fuchs, H. V., and Riehle, R. (1991). Ten years of experience with leak detection by acoustic signal analysis. *Applied Acoustics*, 33(1), 1-19. doi: http://dx.doi.org/10.1016/0003-682X(91)90062-J.

García, V. J., Cabrera, E., and Cabrera Jr, E. (2006). The minimum night flow method revisited. *Proceedings of the 8th Annual Water Distribution Systems Analysis Symposium. Cincinnati, USA*

Ge, N., and Peng, G. (2008). A Novel Leakage Detection and Localization Method Based on Infrared Thermography. *Proceedings of the 7th JFPS International Symposium on Fluid Power*, Toyama, Japan, September 15-18.

Geiger, G. (2006). State-of-the-art in leak detection and localization. *Oil Gas European Magazine*, 32(4), 193-218.

Ghazali, M. F. (2012). Leak detection using instantaneous frequency analysis. *PhD thesis*, University of Sheffield, UK.

Ghazali, M. F., Beck, S. B. M., Shucksmith, J. D., Boxall, J. B., and Staszewski, W. J. (2012). Comparative study of instantaneous frequency based methods for leak detection in pipeline networks. *Mechanical Systems and Signal Processing*, 29(0), 187-200. doi: http://dx.doi.org/10.1016/j.ymssp.2011.10.011.

Giugni, M., Fontana, N., Portolano, D., and Romanelli, D. (2008). A DMA Design for "Napoli Est" Water Distribution System. *Proceedings of the 13th IWRA World Water Congress*, Montpellier, France, 1-4 September.

Giustolisi, O., Savic, D., and Kapelan, Z. (2008). Pressure-Driven Demand and Leakage Simulation for Water Distribution Networks. *Journal of Hydraulic Engineering*, 134(5), 626-635. doi: 10.1061/(ASCE)0733-9429(2008)134:5(626).

GIZ. (2011). Guidelines for water loss reduction - A Focus on pressure management.: Internationale Zusammenarbeit (GIZ) GmbH (Germany), VAG Armaturen GmbH (Germany), the Institute for Ecopreneurship (IEC) at the University of Applied Sciences Northwestern Switzerland (FHNW) and the Karlsruhe Institute of Technology (KIT, Germany)

Gong, J., Lambert, M., Simpson, A., and Zecchin, A. (2012). Single-Event Leak Detection in Pipeline Using First Three Resonant Responses. *Journal of Hydraulic Engineering,* 139(6), 645-655. doi: 10.1061/(ASCE)HY.1943-7900.0000720.

Grise, S., Idolyantes, E., Brinton, E., Booth, B., and Zeiler, M. (2001). Water utilities. ArcGIS™ data models. *Environmental Systems Research Institute*.

GrowingBlue. (2011). Water. Economics. Life (pp. 34).

Günther, M., Camhy, D., Steffelbauer, D., Neumayer, M., and Fuchs-Hanusch, D. (2015). Showcasing a Smart Water Network Based on an Experimental Water Distribution System. *Procedia Engineering,* 119, 450-457. doi: http://dx.doi.org/10.1016/j.proeng.2015.08.857.

Hamilton, S., and Charalambous, B. (2013). Leak Detection: Technology and Implementation: *IWA Publishing, London, UK*.

Han, D. M., and Lim, J. H. (2010). Smart home energy management system using IEEE 802.15.4 and zigbee. *IEEE Transactions on Consumer Electronics,* 56(3), 1403-1410. doi: 10.1109/TCE.2010.5606276.

Ho, C.-I., Lin, M.-D., and Lo, S.-L. (2010). Use of a GIS-based hybrid artificial neural network to prioritize the order of pipe replacement in a water distribution network. *Environmental Monitoring and Assessment,* 166(1-4), 177-189. doi: 10.1007/s10661-009-0994-6.

Hunaidi, O. (1999). Leak detection methods for plastic water distribution pipes: *American Water Works Association*.

Hunaidi, O. (2000). Detecting leaks in water-distribution pipes. *Construction Technology Update,* 40, 6.

Hunaidi, O., and Chu, W. T. (1999). Acoustical characteristics of leak signals in plastic water distribution pipes. *Applied Acoustics,* 58(3), 235-254.

Hunaidi, O., and Giamou, P. (1998). Ground-penetrating radar for detection of leaks in buried plastic water distribution pipes. *Proceedings of the 7th International Conference on Ground-Penetrating Radar,* Lawrence, Kansas

Hunaidi, O., and Wang, A. (2006). A new system for locating leaks in urban water distribution pipes. *Management of Environmental Quality: An International Journal,* 17(4), 450-466.

Hunaidi, O., Wang, A., Bracken, M., Gambino, T., and Fricke, C. (2004). Acoustic methods for locating leaks in municipal water pipe networks. *Proceedings of the International Conference on Water Demand Management*, Dead Sea, Jordan, 30 May - 3 June.

Inaudi, D., Belli, R., and Walder, R. (2008). Detection and localization of micro-leakages using distributed fiber optic sensing. *Proceedings of the 7th International Pipeline Conference, IPC*, Calgary, Alberta, Canada, 29th September - 3rd October.

Irons, L. M., Boxall, J., Speight, V., Holden, B., and Tam, B. (2015). Data driven analysis of customer flow meter data. *Procedia Engineering*, 119, 834-843. doi: http://dx.doi.org/10.1016/j.proeng.2015.08.947.

Jafar, R., Shahrour, I., and Juran, I. (2010). Application of Artificial Neural Networks (ANN) to model the failure of urban water mains. *Mathematical and Computer Modelling*, 51(9–10), 1170-1180. doi: http://dx.doi.org/10.1016/j.mcm.2009.12.033.

Jones, C., Mergelas, B., Laven, K., and Bond, A. (2006). Pinpointing Exfiltration in Large Diameter Pressurized Wastewater Pipelines with the Sahara Tethered System. *Pipelines 2006*, 1-8: American Society of Civil Engineers.

Kailing, K., Kriegel, H.-P., Pryakhin, A., and Schubert, M. (2004). Clustering Multi-Represented Objects with Noise. *Proceedings of the 8th Pacific-Asia Conference on Knowledge Discovery and Data Mining (PAKDD)*, Sydney, Australia

Kaufman, L., and Rousseeuw, P. J. (2009). Finding groups in data: an introduction to cluster analysis (Vol. 344): *John Wiley & Sons*.

Khomsi, D., Walters, G., Thorley, A., and Ouazar, D. (1996). Reliability Tester for Water-Distribution Networks. *Journal of Computing in Civil Engineering*, 10(1), 10-19. doi: 10.1061/(ASCE)0887-3801(1996)10:1(10).

Kingdom, B., Liemberger, R., and Marin, P. (2006). The Challenge of Reducing Non-Revenue (NRW) Water in Developing Countries. How the Private Sector can Help: A Look at Performance-Based Service Contracting. *Water Supply and Sanitation (WSS) Sector Board Discussion Paper N. 8. Washington DC. The World Bank*.

Lambert, V., and Hirner, W. (2002). Losses from water supply systems: standard terminology and recommended performance measures. *Voda i sanitarna tehnika*, 32(1), 29-38.

Lansey, K., El-Shorbagy, W., Ahmed, I., Araujo, J., and Haan, C. (2001). Calibration Assessment and Data Collection for Water Distribution Networks. *Journal of Hydraulic Engineering*, 127(4), 270-279. doi: 10.1061/(ASCE)0733-9429(2001)127:4(270).

Li, L., Xiaoguang, H., and Weicun, Z. (2009). Design of an ARM-based power meter having WIFI wireless communication module. *Proceedings of the 4th IEEE Conference on Industrial Electronics and Applications*, Xi'an, China, 25-27 May.

Li, W., Ling, W., Liu, S., Zhao, J., Liu, R., Chen, Q., Qiang, Z., and Qu, J. (2011). Development of systems for detection, early warning, and control of pipeline leakage in drinking water distribution: A case study. *Journal of Environmental Sciences*, 23(11), 1816-1822. doi: http://dx.doi.org/10.1016/S1001-0742(10)60577-3.

Licciardi, S. V. (1998). Quantification and location of leaks by internal inspection. *Tunnelling and Underground Space Technology*, 13, Supplement 2(0), 5-15. doi: http://dx.doi.org/10.1016/S0886-7798(98)00089-3.

Lin, M., Wu, Y., and Ian, W. (2008). Wireless sensor network: Water distribution monitoring system. *Radio and Wireless Symposium, IEEE*, 22-24 January.

Liu, Z., and Kleiner, Y. (2013). State of the art review of inspection technologies for condition assessment of water pipes. *Measurement*, 46(1), 1-15.

MacDonald, G., and Yates, C. (2005). DMA Design and Implementation, a North American Context. *Proceedings of IWA Special Conference Leakage 2005*, Halifax, Nova Scotia, Canada, September.

Makar, J., Desnoyers, R., and McDonald, S. (2001). Failure modes and mechanisms in gray cast iron pipe. *Underground Infrastructure Research; Municipal, Industrial and Environmental Applications*, 10-13.

Mamo, T. G., Juran, I., and Shahrour, I. (2014). Virtual DMA Municipal Water Supply Pipeline Leak Detection and Classification Using Advance Pattern Recognizer Multi-Class SVM. *Journal of Pattern Recognition Research,* 1, 25-42.

Martínez-Rodríguez, J., Montalvo, I., Izquierdo, J., and Pérez-García, R. (2011). Reliability and Tolerance Comparison in Water Supply Networks. *Water Resources Management,* 25(5), 1437-1448. doi: 10.1007/s11269-010-9753-2.

Mashford, J., De Silva, D., Burn, S., and Marney, D. (2012). Leak Detection in Simulated Water Pipe Networks using SVM. *Applied Artificial Intelligence,* 26(5), 429-444. doi: 10.1080/08839514.2012.670974.

May, J. (1994). Leakage, Pressure and Control. *Proceedings of BICS International Conference on Leakage Control Investigation in underground Assets*, London

McNabb, J. K. (2012). Vulnerabilities of wireless water meter networks. *Journal of the New England Water Works Association,* 126(1), 31.

Meniconi, S., Brunone, B., and Ferrante, M. (2010). In-Line Pipe Device Checking by Short-Period Analysis of Transient Tests. *Journal of Hydraulic Engineering,* 137(7), 713-722. doi: 10.1061/(ASCE)HY.1943-7900.0000309.

Mergelas, B., and Henrich, G. (2005). Leak locating method for precommissioned transmission pipelines: North American case studies. *Proceedings of IWA Special Conference Leakage 2005,* Halifax, Nova Scotia, Canada, September.

Misiūnas, D. (2005). Failure Monitoring and Asset Condition Asssessment in Water Supply Systems. *Doctoral Dissertation in Industrial Automation*, Lund University.

Misiūnas, D., Lee, P., Lambert, M., Simpson, A., and Vitkovsky, J. P. (2007). Leak location in single pipelines using transient reflections. *Australian Journal of Water Resources,* 11(1), 53.

Misiūnas, D., Vítkovský, J., Olsson, G., Simpson, A., and Lambert, M. (2005). Pipeline Break Detection Using Pressure Transient Monitoring. *Journal of Water Resources Planning and Management,* 131(4), 316-325. doi: 10.1061/(ASCE)0733-9496(2005)131:4(316).

Morrison, J. (2010). Managing leakage by District Metered Access: a practical approach. *Water 21*, 44-46.

Mounce, S. R., Boxall, J., and Machell, J. (2009). Development and verification of an online artificial intelligence system for detection of bursts and other abnormal flows. *Journal of Water Resources Planning and Management,* 136(3), 309-318.

Mounce, S. R., Boxall, J. B., and Machell, J. (2010). Development and Verification of an Online Artificial Intelligence System for Detection of Bursts and Other Abnormal Flows. *Journal of Water Resources Planning and Management,* 136(3), 309-318. doi: 10.1061/(ASCE)WR.1943-5452.0000030.

Mounce, S. R., Khan, A., Wood, A. S., Day, A. J., Widdop, P. D., and Machell, J. (2003). Sensor-fusion of hydraulic data for burst detection and location in a treated water distribution system. *Information Fusion,* 4(3), 217-229. doi: http://dx.doi.org/10.1016/S1566-2535(03)00034-4.

Mounce, S. R., and Machell, J. (2006). Burst detection using hydraulic data from water distribution systems with artificial neural networks. *Urban Water Journal,* 3(1), 21-31. doi: 10.1080/15730620600578538.

Mounce, S. R., Mounce, R. B., Jackson, T., Austin, J., and Boxall, J. B. (2014). Pattern matching and associative artificial neural networks for water distribution system time series data analysis. *Journal of Hydroinformatics,* 16(3), 617-632.

Mueller, F. J. (2013). Recent Developments in Pipeline Condition Assessment Using Inline Technologies. Abu Dhabi: Pure Technologies Ltd.

Mutikanga, H. E., Sharma, S. K., Vairavamoorthy, K. . (2013). Methods and Tools for Managing Losses in Water Distribution Systems. *Journal of Water Resources Planning and Management,* 139(2), 166-174. doi: doi:10.1061/(ASCE)WR.1943-5452.0000245.

Newell, R. D., and Greenwood, B. (2006). Mass balance leak detect, can it work for you? *ENTELEC*.

Nikjoofar, A., and Zarghami, M. (2013). Water Distribution Networks Designing by the Multiobjective Genetic Algorithm and Game Theory. *Metaheuristics in Water, Geotechnical and Transport Engineering*, 99-119. doi: http://dx.doi.org/10.1016/B978-0-12-398296-4.00005-2.

Nikles, M., Vogel, B. H., Briffod, F., Grosswig, S., Sauser, F., Luebbecke, S., Bals, A., and Pfeiffer, T. (2004). Leakage detection using fiber optics distributed temperature monitoring. *Proceedings of the 11th SPIE Annual International Symposium on Smart Structures and Materials*, San Diego, California, USA, 14-18 March.

Noran, P., and Obenauf, P. (2010). Asset Management of a Failing 36" Ductile Iron Sewage Force Main. *Pipelines 2010*, 566-576: American Society of Civil Engineers.

Oliveira, F., Ross, T., Trovato, A., Chandrasekaran, M., and Leal, F. (2011). Smartball: A New Pipeline Leak detection Sytsem and its Survey of Two Petrobras/Transpetro Pipelines Field Tests. *Proceedings of Rio Pipeline Conference & Exposition*, Rio de Janeiro, Brazil, September 20-22.

Ormsbee, L. E., and Lingireddy, S. (1997). Calibrating hydraulic network models. *American Water Works Association. Journal*, 89(2), 42.

Oven, S. (2014). Leak Detection in Pipelines by the use of State and Parameter Estimation. *Master Thesis*, Norwegian University of Science and Technology.

Owojaiye, G., and Sun, Y. (2013). Focal design issues affecting the deployment of wireless sensor networks for pipeline monitoring. *Ad Hoc Networks,* 11(3), 1237-1253.

Pilcher, R. (2003). Leak detection practices and techniques: a practical approach. *Water 21,* 44-45.

Pure-Technologies. (2011). SmartBall® Inspection Report of North Beach Force Main. Columbia, Maryland, USA.

Rajani, B., and Kleiner, Y. (2001). Comprehensive review of structural deterioration of water mains: physically based models. *Urban Water,* 3(3), 151-164. doi: http://dx.doi.org/10.1016/S1462-0758(01)00032-2.

Rajani, B., and Kleiner, Y. (2013). External and Internal Corrosion of Large-Diameter Cast Iron Mains. *Journal of Infrastructure Systems,* 19(4), 486-495. doi: doi:10.1061/(ASCE)IS.1943-555X.0000135.

Rajani, B., and Tesfamariam, S. (2004). Uncoupled axial, flexural, and circumferential pipe–soil interaction analyses of partially supported jointed water mains. *Canadian Geotechnical Journal,* 41(6), 997-1010. doi: 10.1139/t04-048.

Ribeiro, R., Loureiro, D., Barateiro, J., Smith, J. R., Rebelo, M., Kossieris, P., Gerakopoulou, P., Makropoulos, C., Vieira, P., and Mansfield, L. (2015). Framework for Technical Evaluation of Decision Support Systems Based on Water Smart Metering: The iWIDGET Case. *Procedia Engineering,* 119, 1348-1355. doi: http://dx.doi.org/10.1016/j.proeng.2015.08.976.

Rothwell, S. (2013). Alabama City Uses Leak Detection Survey on Large-Diameter Pipes. *Trenchless TECHNOLOGY, 22,* 36-37.

Russell, D. (2005). Pigging in pipeline pre-commissioning. *Pigging Products and Services Association,* 9.

Sadeghioon, A. M., Metje, N., Chapman, D. N., and Anthony, C. J. (2014). SmartPipes: Smart Wireless Sensor Networks for Leak Detection in Water Pipelines. *Journal of Sensor and Actuator Networks,* 3(1), 64-78.

Savic, D. A., Kapelan, Z. S., and Jonkergouw, P. M. R. (2009). Quo vadis water distribution model calibration? *Urban Water Journal,* 6(1), 3-22. doi: 10.1080/15730620802613380.

Saw, J. G., Yang, M. C. K., and Mo, T. C. (1984). Chebyshev Inequality with Estimated Mean and Variance. *The American Statistician,* 38(2), 130-132. doi: 10.1080/00031305.1984.10483182.

Sehgal, A. (2005). AMR offers multiple benefits. *Pipeline and gas technology. Itron Inc. Spokane, Washington.*

Silipo, R., and Winters, P. (2013). Big data, Smart Energy, and Predictive Analytics.

Stafford, M., Williams, N., and Britain, G. (1996). Pipeline leak detection study. *London UK*: *Technical Report Bechtel Limited for the Health and Safety Executive*.

Stoianov, I., Nachman, L., Madden, S., and Tokmouline, T. (2007). PIPENET: A Wireless Sensor Network for Pipeline Monitoring. *Proceedings of the 6th international conference on Information processing in sensor networks*, Cambridge, Massachusetts, USA

Sturman, J., Ho, G. E., and Mathew, K. (2004). Water Auditing and Water Conservation: *IWA Publishing*.

Subtil, F., and Rabilloud, M. (2015). An enhancement of ROC curves made them clinically relevant for diagnostic-test comparison and optimal-threshold determination. *Journal of clinical epidemiology*, 68(7), 752-759.

SWAN. (2012). The Value of Online Water Network Monitoring.

Tabesh, M., Yekta, A. H. A., and Burrows, R. (2008). An Integrated Model to Evaluate Losses in Water Distribution Systems. *Water Resources Management*, 23(3), 477-492. doi: 10.1007/s11269-008-9284-2.

Tabesh, M., Yekta, A. H. A., and Burrows, R. (2009). An Integrated Model to Evaluate Losses in Water Distribution Systems. *Water Resources Management*, 23(3), 477-492. doi: 10.1007/s11269-008-9284-2.

Thornton, J., Sturm, R., and Kunkel, G. (2008). Water loss control: *McGraw Hill Professional, Second Edition*.

Torres, L. (2014). Location of leaks in pipelines using parameter identification tools. *Proceedings of the 8th International Federation of Automatic Control (IFAC) Symposium SAFEPROCESS*, Mexico City, Mexico, August.

Van Thienen, P. (2013). A method for quantitative discrimination in flow pattern evolution of water distribution supply areas with interpretation in terms of demand and leakage. *Journal of Hydroinformatics*, 15(1), 86-102.

Van Thienen, P., and Montiel, F. (2014). Flow Analysis And Leak Detection With The CFPD Method In The Paris Drinking Water Distribution System. *Proceedings of the 11th International Conference on Hydroinformatics HIC* New York City, USA

Van Thienen, P., Pieterse-Quirijns, I., Vreeburg, J., Vangeel, K., and Kapelan, Z. (2013). Applications of discriminative flow pattern analysis using the CFPD method. *Water Science & Technology: Water Supply*, 13(4), 906-913.

Van Thienen, P., and Vertommen, I. (2016). Automated feature recognition in CFPD analyses of DMA or supply area flow data. *Journal of Hydroinformatics*, 18(3), 514-530. doi: 10.2166/hydro.2015.056.

Vítkovský, J. P., Simpson, A., and Lambert, M. (2000). Leak Detection and Calibration Using Transients and Genetic Algorithms. *Journal of Water Resources Planning and Management*, 126(4), 262-265. doi: 10.1061/(ASCE)0733-9496(2000)126:4(262).

Walker, D., Creaco, E., Vamvakeridou-Lyroudia, L., Farmani, R., Kapelan, Z., and Savić, D. (2015). Forecasting Domestic Water Consumption from Smart Meter Readings Using Statistical Methods and Artificial Neural Networks. *Procedia Engineering*, 119, 1419-1428. doi: http://dx.doi.org/10.1016/j.proeng.2015.08.1002.

Whittle, A. J., Allen, M., Preis, A., and Iqbal, M. (2013). Sensor networks for monitoring and control of water distribution systems. *Proceedings of the 6th International Conference on Structural Health Monitoring of Intelligent Infrastructure* Hong Kong, 9-11 December.

Whittle, A. J., Girod, L., Preis, A., Allen, M., Lim, H. B., Iqbal, M., Srirangarajan, S., Fu, C., Wong, K. J., and Goldsmith, D. (2010). WATERWISE@ SG: A testbed for continuous monitoring of the water distribution system in Singapore. *Proceedings of the 12th Proceedings of Water Distribution Systems Analysis Conference (WDSA 2010)*, Tucson, AZ, USA, Sept. 12-15.

Winncy, D., and Scott, Y. (2008). Post-Earthquake Pipeline Leak Detection Technologies. *Smart Sensors and Sensing Technology*, 20, 265-283. doi: 10.1007/978-3-540-79590-2_18.

Wu, Z., Sage, P., and Turtle, D. (2009). Pressure-Dependent Leak Detection Model and Its Application to a District Water System. *Journal of Water Resources Planning and Management*, 136(1), 116-128. doi: 10.1061/(ASCE)0733-9496(2010)136:1(116).

Wu, Z. Y., Walski, T., Mankowski, R., Herrin, G., Gurrieri, R., and Tryby, M. (2002). Calibrating water distribution model via genetic algorithms. *AWWA IM Tech Conference*, Kansas City, Missouri, USA, April 16-19.

Yaacoub, E. (2014). On real-time smart meter reading using OFDMA-based random access. *Proceedings of the 17th IEEE Mediterranean Electrotechnical Conference MELECON* 13-16 April 2014.

Yaminighaeshi, H. (2009). Probability of failure analysis and condition assessment of cast iron pipes due to internal and external corrosion in water distribution systems. *PhD thesis in Civil Engineering*, University of British Columbia.

Yazdani, A., and Jeffrey, P. (2011). Complex network analysis of water distribution systems. *Chaos: An Interdisciplinary Journal of Nonlinear Science*, 21(1), 016111.

Zhang, J. (1997). Designing a Cost-Effective and Reliable Pipeline Leak-Detection System. *Pipes and Pipelines International*, 42(1), 20-26.

Zhang, J., and Di Mauro, E. (1998). Implementing a Reliable Leak Detection System on a Crude Oil Pipeline. *Advances in Pipeline Technology*, Dubai, UAE

Zhang, J., and Twomey, M. (2000). Statistical Pipeline Leak Detection Techniques for All Operating Conditions. *Proceedings of the 26th Environmental Symposium & Exhibition*, California, USA

Appendix A Attributes of Water Meters

Sites		ID		Meter Number	Serial Number
General Meters	Looped network	CITE SCIENTIFIQUE	CITE_1	D13UI037551	3911149270007
			CITE_2	D13UI037558	3911149270008
			CITE_3	D13UI037557	3911149270010
			CITE_4	D13UI037552	3911149270009
			CITE_5	D13UI037550	3911149270011
		BACHELARD		D13UI032678	3911144410015
		M5		D12UG052982	3911144410017
		ECL		D12XK118838	3911144410014
		4CANTONS		D10UI000002	3911144410020
	Branched	CUEEP		D02TD100036	3911144350012
		DELTEC_ICARE		D06AD040523	3911144350013
		HALL_VALLIN		D04PE021587	3911144350016
		LML (M6)		C14SE007722	3911144410019
Lille 1	Mathematics	M1		D08FE017733	SREA0000641
		M2		D07UD353317	SREA0000686
		M3	M3	D08FE0117693	SREA0000669
			M3_LIFL	D07UD353319	SREA0000668
		M4_CRI		D08UD367194	SREA0000687
		M5		D08AE032252	SREA0000638
	Physics	P1		D07UD353312	SREA0000670
		P2		D08AE041518	SREA0000671
		P3		D08FE032447	SREA0000684
		P4		D02PC000684	SREA0000683
		P5		D11XG051771	SREA0000681
		P5_BIS (CERLA)		D08UG038159	SREA0000685
	Chemistry	C1		D07AD354190	SREA0000680
		C3		D02PE048698	SREA0000633
		C4		D08AE041521	SREA0000673
		C5		D02PE051562	SREA0000636
		C6		D01PE0722367	SREA0000639
		C8		D08AE041543	SREA0000642
		C9		D08AE041548	SREA0000643
		C11		D08AE032252	SREA0000635
		TP_C16		D08AE037564	SREA0000679

	Biology	SN1	D08AD373680	SREA0000674
		SN1_SERRES	D08AE041493	SREA0000673
		SN2	D08AE032253	SREA0000644
		SN3	D08AE032282	SREA0000645
		SN4	D08AD373683	SREA0000647
		SN5	D08AE041522	SREA0000646
		SN6	D07AD128395	SREA0000648
	Social Science	SH1	D08AB004856	SREA0000634
		SH2	D08AE041523	SREA0000691
		SH3	D08XG042206	SREA0000690
		UFR_GEOGRAPHIE	-	SREA0000649
	Sport	COSEC	D08AD367742	SREA0000675
		COSEC_ADMIN	D02AB010039	SREA0000661
		CLUBHOUSE	D08AB004814	SREA0000660
		GREMEAUX	D08AB004721	SREA0000651
		V2	D08FE032439	SREA0000659
		VALLIN	D08AE041541	SREA0000672
	Engineering Schools	Polytech EPU_A_B_C	D08UH059441	SREA0000650
		Polytech EPU_D	D08UG044108	SREA0000665
		Polytech EPU_D_ECL	D08UG044098	SREA0000662
	Institutes	IUT	D08UG038149	SREA0000656
		B5	D08AE037557	SREA0000663
		B6	D08AE037546	SREA0000664
		B8_CUEEP	D08AE041550	SREA0000688
	Administration	A3	D08UD367193	SREA0000689
		A7_PCET	D07LA038971	SREA0000653
		SUDES	D08UD367195	SREA0000712
		SUPSUAIO	D08AE041506	SREA0000678
	Service	A1	D08FE032426	SREA0000654
		A2	D02PE048699	SREA0000655
		A10	D08AB004962	SREA0000652
		A16 (CAS 2)	D08LA571132	SREA0000658
		BU (Learning Center)	D08FE017686	SREA0000657
		ESPACE_CULTURE	D08LA519999	SREA0000666
		MDE	D08AB008032W	SREA0000712
Reeflex		REEFLEX	C14JG001687	SREA0000713
		CRECHE_REEFLEX	D14UD092750	SREA0000714

CROUS	Students' Residence	Bachelard	L	D09UG206019	SREA0000694
			N	D08UH059439	SREA0000695
			PYTHAGORE	D08UI019113	SREA0000696
		Boucher	G	D09UH209294	SREA0000697
			J	D09UH166602	SREA0000698
		Camus	R	D10UG068958	SREA0000705
			S	D10XG075513	SREA0000706
			U	D10XG067230	SREA0000707
			W	D10XG064759	SREA0000708
		Galois	A_B	D09UG206021	SREA0000699
			D_C	D09UG210844	SREA0000700
	Restaurants	BARROIS		D09AE190909	SREA0000702
		PARISELLE		D09UG210845	SREA0000703
		SULLY		D09UH209293	SREA0000704
ENSCL		C7 (Chemistry)		D08AE037565	SREA0000640
Ecole Centrale	Engineering Schools	ECL	ECL_C	D10UG050481	SREA0000710
			ECL_FOSSE	D08AE037549	SREA0000667
			FONDERIE	D08XG042205	SREA0000711
			INCENDIE	D09UH275909	SREA0000693
		C_D_DEVINCI		D08UI019112	SREA0000701
Others		BONDUELLE		D09AB009854	SREA0000709
		CLINIQUE		D09FE206807	SREA0000692

Appendix B Noise Level Measurements

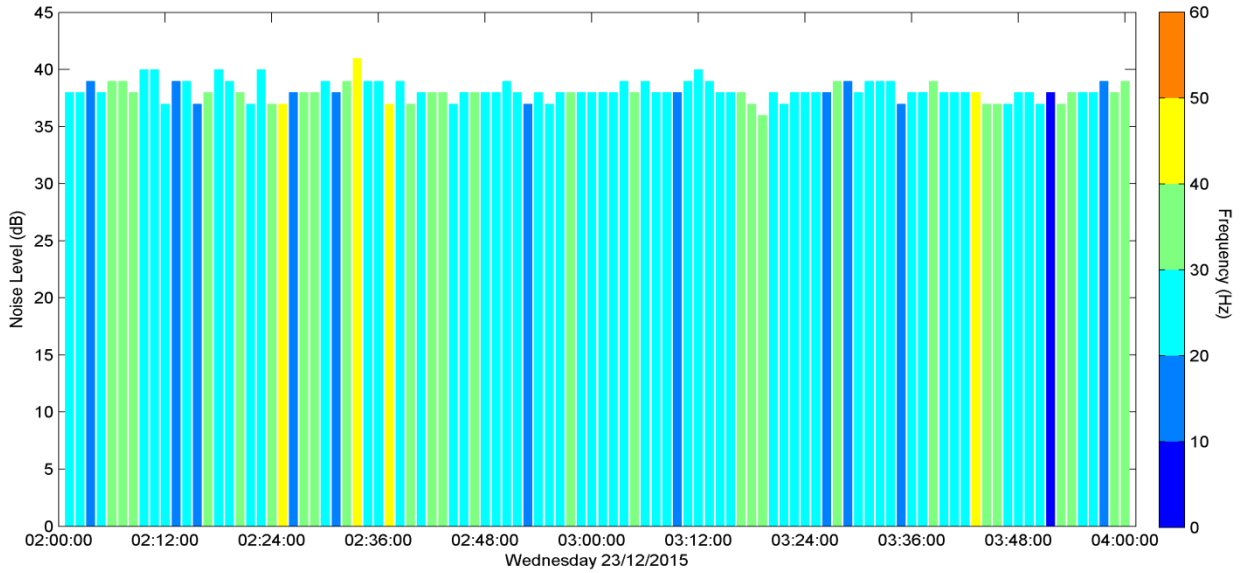

Figure B.1: Noise level measured in the early morning of Wednesday 23/12/2015

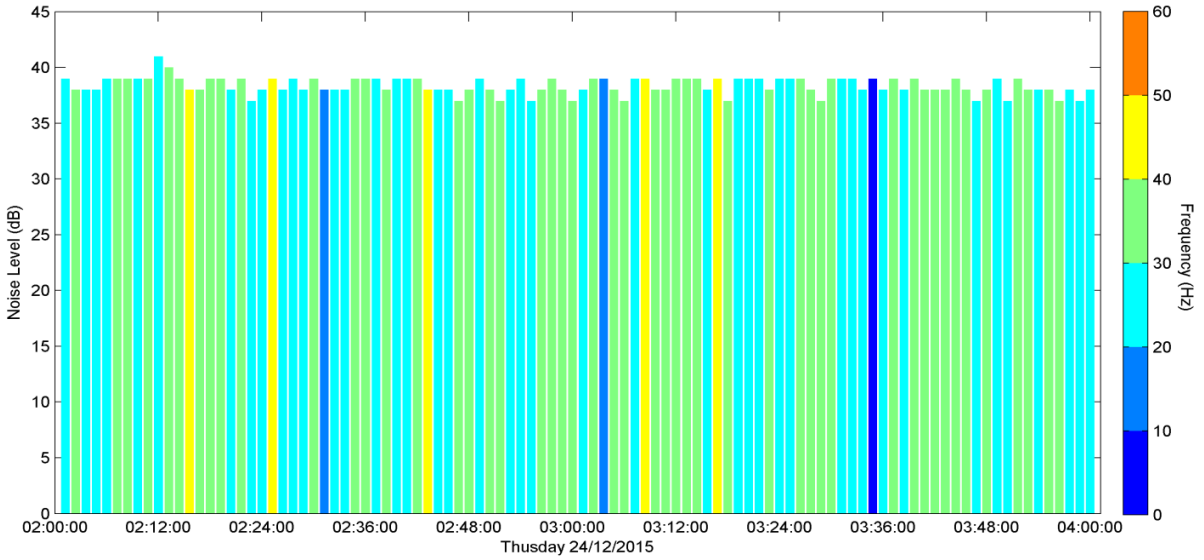

Figure B.2: Noise level measured in the early morning of Thursday 24/12/2015

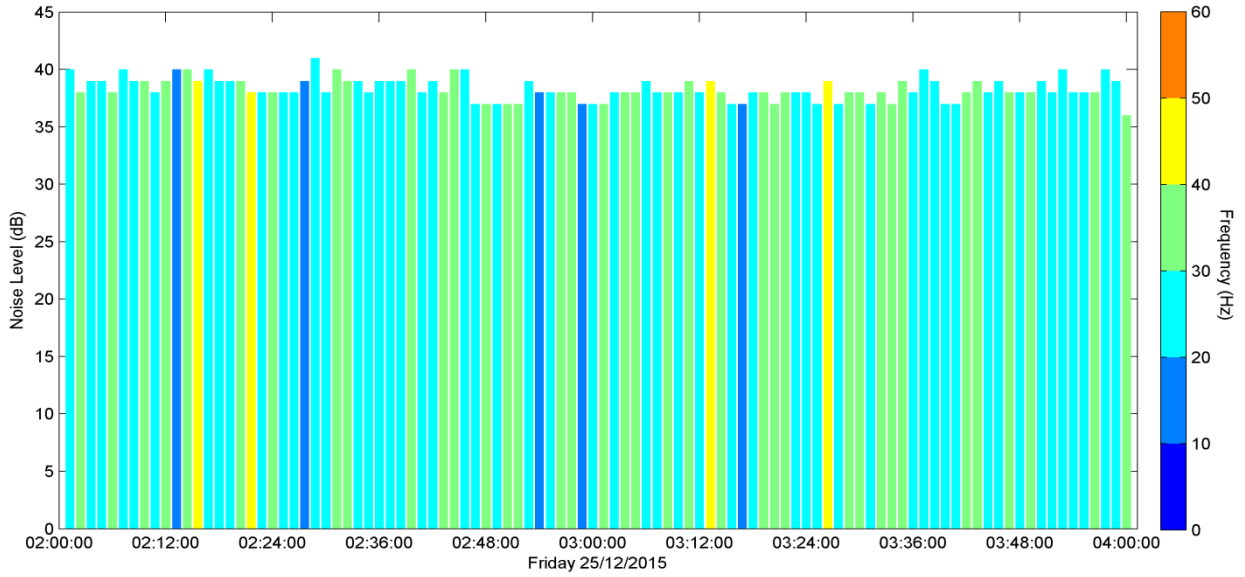

Figure B.3: Noise level measured in the early morning of Friday 25/12/2015

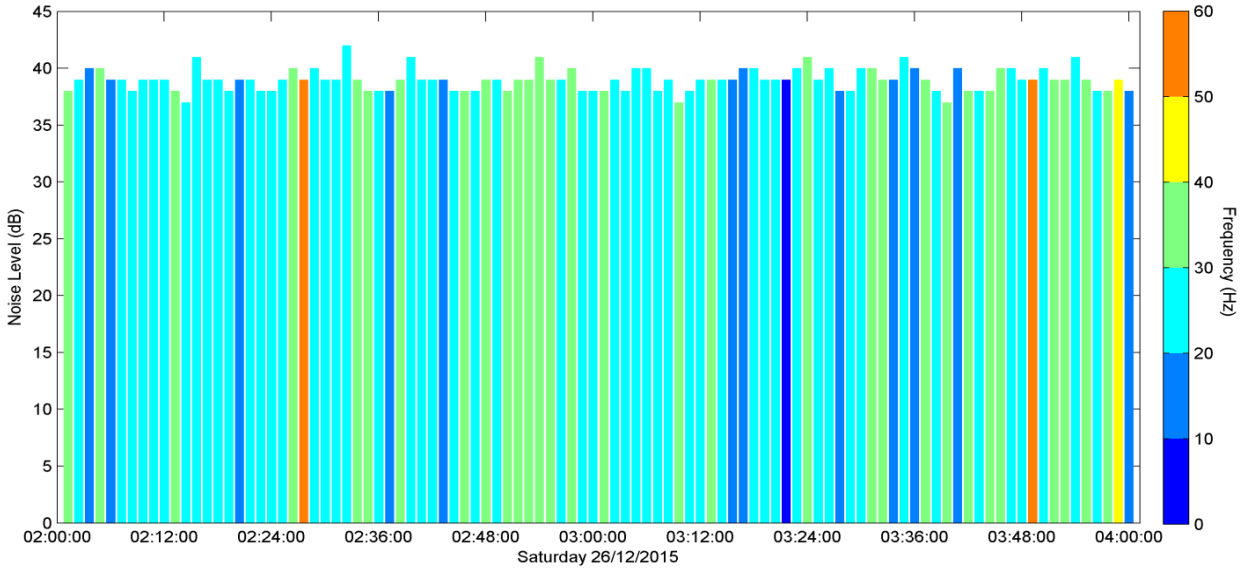

Figure B.4: Noise level measured in the early morning of Saturday 26/12/2015

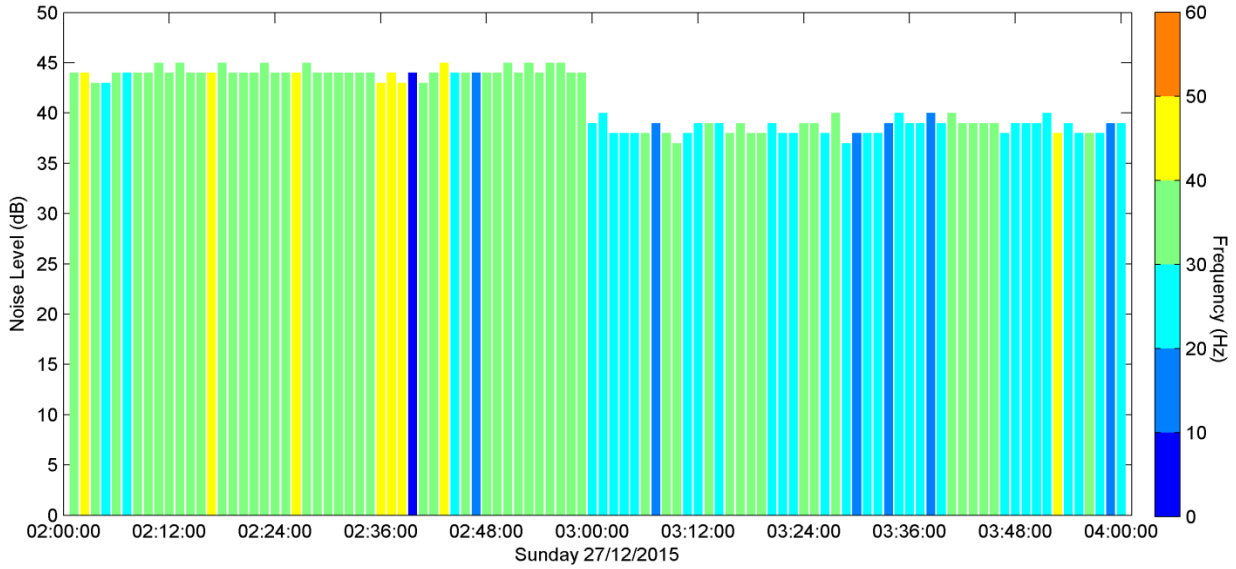

Figure B.5: Noise level measured in the early morning of Sunday 27/12/2015

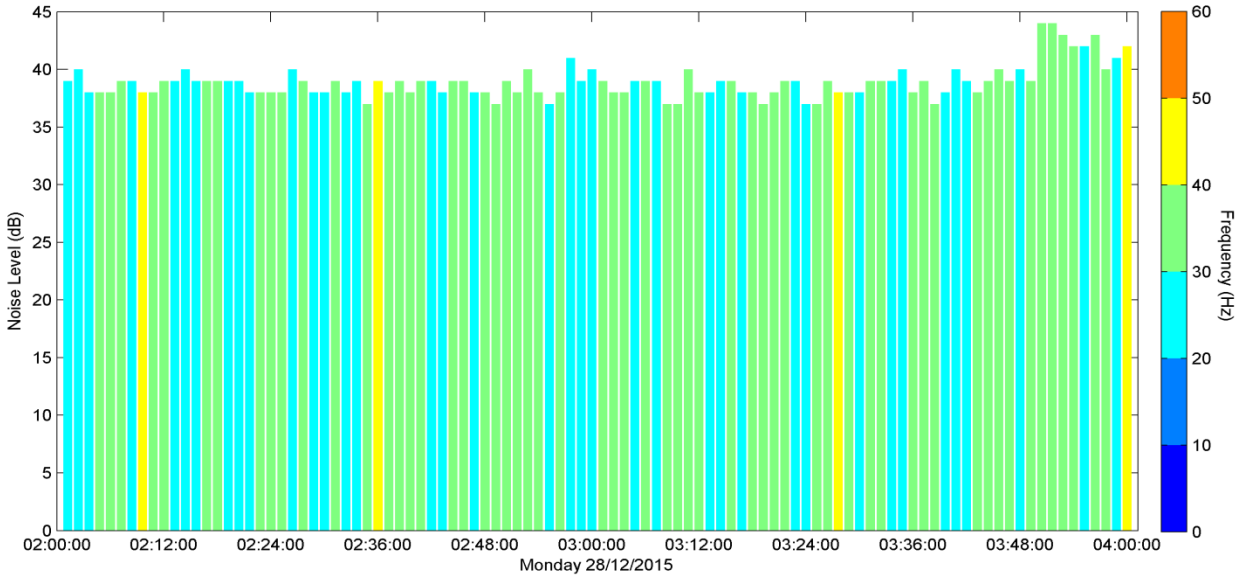

Figure B.6: Noise level measured in the early morning of Monday 28/12/2015

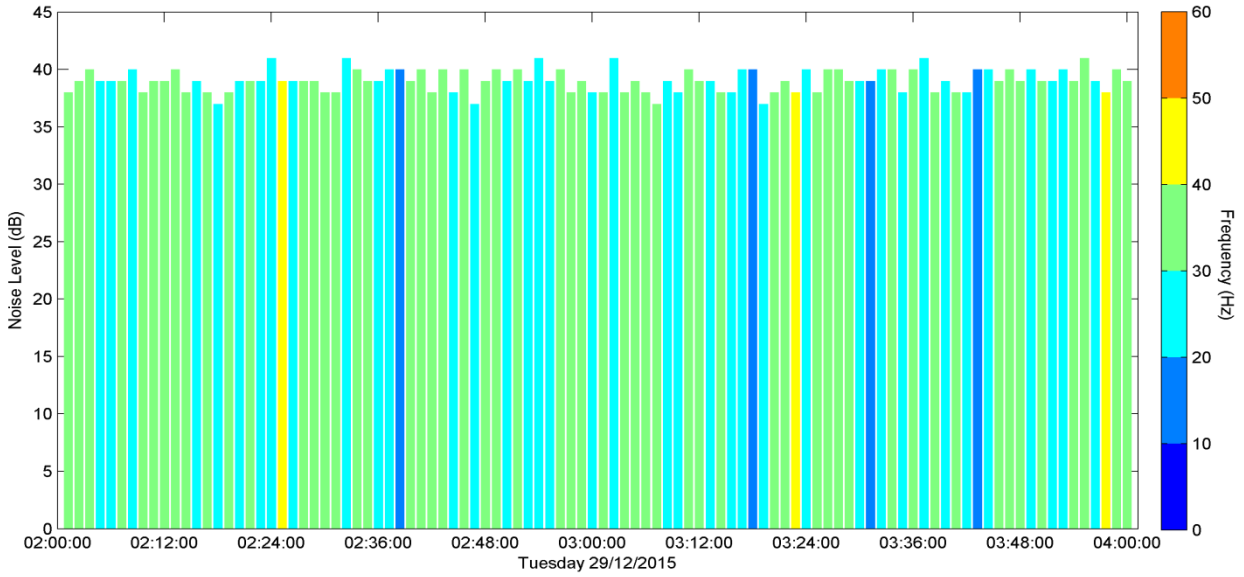

Figure B.7: Noise level measured in the early morning of Tuesday 29/12/2015

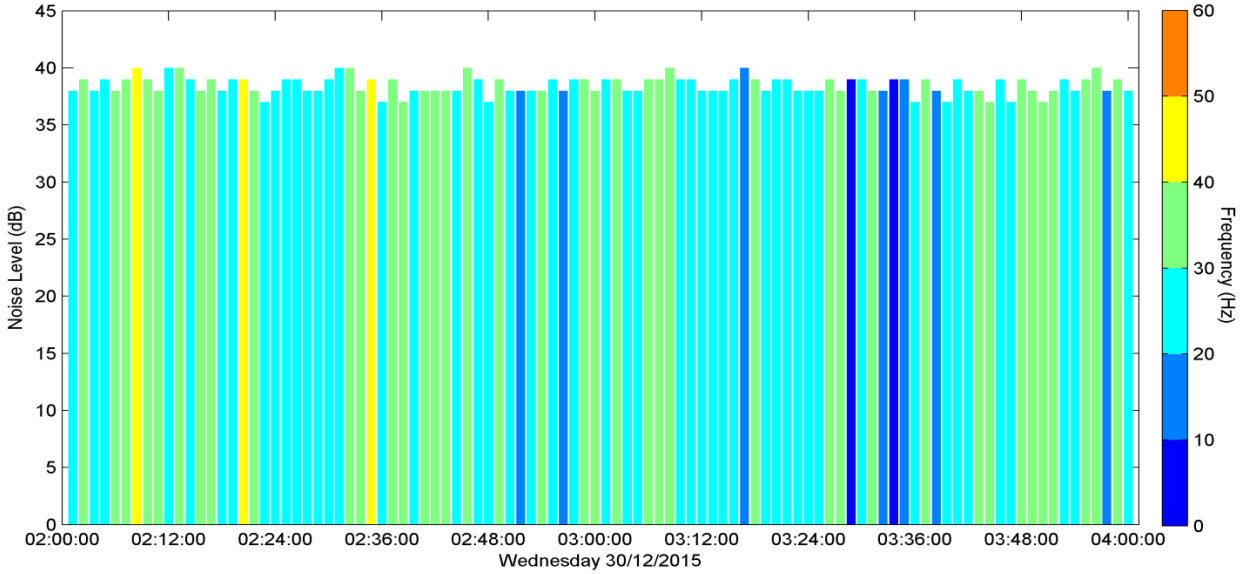

Figure B.8: Noise level measured in the early morning of Wednesday 30/12/2015